HAL
archives-ouvertes.fr

Two studies on conformal and strongly coupled quantum field theories in d > 2 dimensions

Matthijs Hogervorst

▶ **To cite this version:**

Matthijs Hogervorst. Two studies on conformal and strongly coupled quantum field theories in d > 2 dimensions. High Energy Physics - Theory [hep-th]. ENS Paris - Ecole Normale Supérieure de Paris, 2015. English. <tel-01171444>

HAL Id: tel-01171444

https://tel.archives-ouvertes.fr/tel-01171444

Submitted on 3 Jul 2015

HAL is a multi-disciplinary open access archive for the deposit and dissemination of scientific research documents, whether they are published or not. The documents may come from teaching and research institutions in France or abroad, or from public or private research centers.

L'archive ouverte pluridisciplinaire **HAL**, est destinée au dépôt et à la diffusion de documents scientifiques de niveau recherche, publiés ou non, émanant des établissements d'enseignement et de recherche français ou étrangers, des laboratoires publics ou privés.

Two studies on conformal and strongly coupled quantum field theories in $d > 2$ dimensions

Deux essais sur les théories quantiques des champs conformes et fortement couplées en $d > 2$ dimensions

Matthijs Hogervorst

Département de Physique
École normale supérieure

École normale supérieure
École Doctorale 564: Physique en Île-de-France

2015

Two studies on conformal and strongly coupled quantum field theories in $d > 2$ dimensions

Deux essais sur les théories quantiques des champs conformes et fortement couplées en $d > 2$ dimensions

Matthijs Hogervorst

Thèse de doctorat de l'École normale supérieure, Paris
École Doctorale 564 : Physique en Île-de-France

Soutenue le 29 juin 2015 devant le jury composé de :

Miguel Costa	examinateur
Giuseppe Mussardo	rapporteur
Hugh Osborn	examinateur
Vyacheslav Rychkov	directeur de thèse
Marco Serone	rapporteur
Jan Troost	examinateur
Jean-Bernard Zuber	président du jury

Abstract

This thesis investigates two aspects of Conformal Field Theories (CFTs) in d dimensions. Its first part is devoted to conformal blocks, special functions that arise in the partial wave expansion of CFT four-point functions. We prove that these conformal blocks admit an expansion in terms of polar coordinates and show that the expansion coefficients are determined by recursion relations. Conformal blocks are naturally defined on the complex plane: we study their restriction to the real line, and show that they obey a fourth-order differential equation there. This ODE can be used to efficiently compute conformal blocks and their derivatives in general d. Several applications to the conformal bootstrap program are mentioned. The second half of this thesis investigates RG flows that are defined by perturbing a CFT by a number of relevant operators. We study such flows using the Truncated Conformal Space Approach (TCSA) of Yurov and Zamolodchikov, a numerical method that allows for controlled computations in strongly coupled QFTs. Two different RG flows are considered: the free scalar field deformed by a mass term, and ϕ^4 theory. The former is used as a benchmark, in order to compare numerical TCSA results to exact predictions. TCSA results for ϕ^4 theory display spontaneous $\mathbb{Z}_2$ symmetry breaking at strong coupling: we study the spectrum of this theory both in the $\mathbb{Z}_2$-broken and preserved phase, and we compare the critical exponents governing the phase transition to known values. In a separate chapter, we show how truncation errors can be reduced by adding suitable counterterms to the bare TCSA action, following earlier work in $d = 2$ dimensions.

Résumé

Cette thèse examine deux aspects des théories conformes des champs (TCC) en d dimensions. Sa première partie est dédiée aux blocs conformes, des fonctions spéciales qui contribuent au développement en ondes partielles des fonctions à quatre points dans les TCC. On montre que ces blocs admettent un développement en coordonnées polaires dont les coefficients se calculent par une récurrence. Les blocs conformes sont naturellement définis sur le plan complexe : on considère alors leur restriction à l'axe réel, afin de montrer qu'ils obéissent à une équation différentielle sur ce domaine, ce qui mène à un algorithme efficace pour calculer les blocs conformes et leurs dérivées pour tout d. Quelques applications au programme de bootstrap sont développées. La seconde partie de cette thèse examine les perturbations d'une TCC par des opérateurs pertinents. On étudie de tels flots du groupe de renormalisation en utilisant la Méthode de Troncature Conforme (MTC) de Yurov et Zamolodchikov, une méthode numérique qui permet de faire des calculs non-perturbatifs en théorie quantique des champs. Deux théories différentes sont considérées : le boson libre avec un terme de masse, et la théorie ϕ^4. Pour le dernier cas, les résultats de la MTC mettent en évidence la brisure de symétrie $\mathbb{Z}_2$. Finalement, on développe une méthode pour réduire les erreurs de troncature en ajoutant des contre-termes à l'action "nue" de la MTC, suivant des travaux antérieurs en $d = 2$ dimensions.

Contents

Introduction

A practical goal of theoretical physics, and quantum field theory in particular, is to make quantitative predictions about experimentally accessible systems such as metals or liquids. This is both a vast and complicated pursuit. Part of the complication originates in the large hierarchies of scales that are involved: in ferromagnets, we try for example to understand long-range order by modelling spins interacting over distances of $a \sim 10^{-10}$ cm.

Conceptually, problems like the above can be understood using the renormalization group (RG). It asserts that we should describe phenomena at a characteristic distance L by an effective Hamiltonian, the parameters of which depend on L. At very short distances $L \sim a$, we consider that the Hamiltonian in question is described by a set of couplings $g_i(a)$ that control local interactions. The same physical system can be described at a slightly different scale $L = a + \delta L$ (with $\delta L \ll a$) using a Hamiltonian of the same form, but with different couplings $g_i(L) \neq g_i(a)$. By gradually increasing L, we can eventually construct an effective Hamiltonian that controls physics at macroscopic distances.

A special role in this framework is played by scale-invariant theories. Physically, such theories describe critical points, characterized by a diverging coherence length ξ. At the same time, the additional scale invariance constrains the form such theories can take. It turns out that scale invariance is generically enhanced to *conformal* invariance,[1] which is even more restrictive.

Conformal bootstrap

This opens up a new way of studying critical phenomena: rather than constructing critical theories as endpoints of RG flows, we may use conformal symmetry as a guiding principle. Consider for example the Ising phase transition in three dimensions (or any other system in the same universality class). The order parameter of a ferromagnet is its magnetization m, which can be up or down: any description of this theory must have a $\mathbb{Z}_2$ symmetry that flips the sign of m. It is then an interesting problem to classify all interacting three-dimensional

1. In two dimensions, this has been proven under mild assumptions [1, 2]. The general case is not yet understood at the same level of rigor, see e.g. [3–5]. A physical argument is given in [6].

quantum field theories that (a) are conformally invariant, (b) unitary and (c) have a global $\mathbb{Z}_2$ symmetry. If the requirements (a)—(c) single out a unique theory, the latter *must* describe the critical point of the 3d Ising model. In particular, we may hope that such a strategy could be used to predict critical exponents and other universal quantities. [2]

We can therefore focus our attention to the problem of classifying all Conformal Field Theories (CFTs) in d dimensions. This seems like a daunting task, but it can be attacked systematically by considering the local observables of a CFT, i.e. the correlation functions of its local operators $\mathcal{O}_i(x)$. It may for example be shown that all two-point functions $\langle \mathcal{O}_i(x)\mathcal{O}_j(y)\rangle$ are completely determined by the scaling dimensions Δ_i of the operators in question. Three-point functions are almost as constrained as two-point functions: the three-point function $\langle \mathcal{O}_i(x_1)\mathcal{O}_j(x_2)\mathcal{O}_k(x_3)\rangle$ is fixed by conformal symmetry up to a constant of proportionality c_{ijk}.

Surprisingly, it turns out that the data $\mathscr{T} = \{\Delta_i, c_{ijk}\}$ completely specify *all* correlation functions in a CFT. This follows from the fact that CFT correlation functions admit partial wave expansions: for the four-point function of four scalars $\phi_i(x_i)$, this expansion takes the form

$$\langle \phi_1(x_1)\phi_2(x_2)\phi_3(x_3)\phi_4(x_4)\rangle \;\sim\; \sum_i c_{12i}c_{34i}\, G_{\mathcal{O}_i}(u,v)\,.$$

The notation $\sim$ means that we have omitted various unimportant x-dependent factors on the right hand side, and u and v are two conformally invariant cross ratios:

$$u = \frac{|x_{12}|^2|x_{34}|^2}{|x_{13}|^2|x_{24}|^2}, \quad v = \frac{|x_{14}|^2|x_{23}|^2}{|x_{13}|^2|x_{24}|^2}\,,$$

writing $x_{ij} = x_i - x_j$. The above sum runs over all operators $\mathcal{O}_i$ in the theory. [3] The function $G_{\mathcal{O}_i}(u,v)$ therefore encodes the contribution of the operator $\mathcal{O}_i$ to the four-point function $\langle \phi_1\phi_2\phi_3\phi_4\rangle$: it is known as a *conformal partial wave* or a *conformal block*. These conformal blocks are fixed by conformal invariance, and they are *universal*, in the sense that they do not depend on the theory under consideration.

Although the above expansion is convergent, it ultimately arises from a short-distance limit and holds only in a domain $\mathcal{D}$ where $|x_1 - x_2|$ and $|x_3 - x_4|$ are sufficiently small (in a sense that can be made precise). There is some arbitrariness to this: we could obtain a similar expansion in a domain $\mathcal{D}'$ where $|x_2 - x_3|$ and $|x_1 - x_4|$ are both small. It turns out that the intersection $\mathcal{D} \cap \mathcal{D}'$ of these domains is non-empty: imposing that both expansions agree on this intersection, we find a consistency condition

$$\sum_i c_{12i}c_{34i}\, G_{\mathcal{O}_i}(u,v) \;\sim\; \sum_i c_{32i}c_{14i}\, G_{\mathcal{O}_i}(v,u)$$

2. A more precise formulation of this problem has been succesfully investigated in Refs. [7–9].

3. Technically, over all *primary* local operators, which transform homogeneously under conformal transformations.

that involves both the spectrum $\{\mathcal{O}_i\}$ and the constants $\{c_{ijk}\}$ appearing in the three-point functions of the theory. There are infinitely many equations of this form, one for every four-point function $\langle\phi_1\phi_2\phi_3\phi_4\rangle$: the full set of equations is known as the *bootstrap system* of the theory.

Clearly, if a particular choice $\mathscr{T}$ of CFT data is to describe a consistent CFT, it must satisfy the bootstrap system. The converse also holds: if $\mathscr{T}$ solves a bootstrap system, it gives rise to a set of correlation functions consistent with conformal invariance. This way, classifying CFTs reduces to a well-defined but non-trivial problem, namely solving an infinite set of functional equations. This bottom-up approach to studying CFTs is known as the *bootstrap program*, and it goes back to the work of Ferrara, Gatto and Grillo [10] and Polyakov [11] in the 1970s.

The above ideas were soon applied to two-dimensional conformal field theories [12, 13], where they led to a solution of many experimentally relevant critical systems. A crucial ingredient there was the representation theory of the conformal group, which is infinite-dimensional in two dimensions. In $d > 2$ dimensions, significant progress on the bootstrap program was first made by Rattazzi, Rychkov, Tonni and Vichi in 2008 [14]. Their approach relied on closed-form expressions for the conformal blocks $G_{\mathcal{O}_i}(u, v)$, that were found several years before by Dolan and Osborn [15, 16]. [4] Such closed-form expressions exist for operators $\mathcal{O}_i$ of any dimension Δ and Lorentz spin ℓ in $d = 2$ and $d = 4$ dimensions, but have not (yet?) been found in $d = 3$. Still, the bootstrap program has been applied to the 3d Ising model [7] without knowing exact formulas for the conformal blocks, making clever use of recursion relations that hold in general d [20].

It appears that advances in conformal block technology and progress in the conformal bootstrap go hand in hand. In the first half of this thesis, we therefore concentrate on developing new methods to compute these special functions. In chapter 2, we develop a new way to represent conformal blocks, as a series expansion in terms of polar coordinates. We focus on two sets of coordinates. The first one, labeled by $z \in \mathbb{C}$, has been used earlier by Dolan and Osborn. The second one, denoted by $\rho \in \mathbb{C}$, was used in Ref. [21] in a different context. We show that conformal blocks in the ρ coordinate have improved convergence properties, in a way that will be made precise.

Chapter 3 has a different goal, namely to streamline the actual computations used in conformal bootstrap applications. We focus on the 'diagonal' (where $z = \bar{z}$ or $\rho = \bar{\rho}$) and show that conformal blocks restricted to this domain obey a fourth-order differential equation (third-order for scalars). We then use Frobenius' method to develop an efficient algorithm for computing conformal blocks and their derivatives directly, avoiding the recursion relations used in Ref. [7].

4. The study of conformal blocks was initiated by Ferrara, Gatto and Grillo [17–19] and Polyakov [11].

Two appendices provide additional material: appendix A contains a proof that coefficients in the ρ series expansion are bounded, and appendix B contains recursion relations on the diagonal $z = \bar{z}$, following Frobenius' method.

Non-critical RG flows and TCSA

The conformal bootstrap allows to make predictions about CFTs, which correspond to fixed points of the RG flow. Critical theories are however isolated points in the infinite-dimensional 'landscape' of RG flows: [5] all other theories lie on some RG trajectory and have a finite correlation length.

How can we then study such non-critical theories? In a limited number of cases, it is possible to do renormalization group calculations analytically. This is notably the case when the theory in question is close to a free theory, and all couplings g_i are small. For such a theory, the flow of the couplings can be computed in perturbation theory. More generally, we can think of an RG flow as a deformation of a CFT:

$$\mathcal{A} = \mathcal{A}_{\text{CFT}} + \sum_i g_i \int \mathrm{d}^d x \, \mathcal{O}_i(x) \,,$$

where the $\mathcal{O}_i$ are conformal operators of dimension Δ_i. For this to describe a non-trivial RG flow, we require that the perturbing operators $\mathcal{O}_i$ are relevant (meaning that $\Delta_i < d$). Turning on the couplings g_i clearly breaks conformal invariance. Following the RG flow, the couplings g_i grow at a rate that is controlled by the scaling dimensions Δ_i:

$$g_i(L) \;\sim\; L^{d-\Delta_i} \,.$$

Consequently, the theory becomes non-perturbative at some scale L_*, even if all couplings g_i are tiny at short distances.

There is no simple way to obtain quantitative results beyond this intermediate scale L_*. Let us mention at least one well-known method for doing computations at strong coupling, which regulates the theory by putting it on a discrete lattice [22]. This scheme, known as *lattice quantum field theory*, has proved very succesful in various theories, including QCD. Its range of applicability is however limited by the computational resources that it requires.

Above, we considered RG flows as perturbations of CFTs. In that context, it is natural to ask whether the conformal symmetry of the short-distance theory can be used to simplify computations in the resulting RG flow. The answer is affirmative: Yurov and Al. Zamolodchikov proposed such a scheme, which works in two-dimensional theories and makes full use of the broken conformal symmetry [23]. Their method is known as the *Truncated Conformal*

5. Some special CFTs (such as $\mathcal{N} = 4$ super-Yang-Mills) are described by a finite-dimensional manifold of conformal fixed points.

Space Approach (TCSA), and it puts the theory on the cylinder $\mathbb{R} \times S^1$. The key idea behind the TCSA is that CFTs have a Hamiltonian formulation on this geometry. After truncating the Hilbert space to some maximum energy Λ, the Hamiltonian becomes a finite matrix that can be diagonalized numerically. The radius R of the cylinder plays the role of RG scale: when R is small, the flow is close to the UV, and by increasing R we approach the IR.

Following the seminal work of Yurov and Zamolodchikov, the TCSA has been very succesful, especially in checking predictions in the realm of integrable RG flows (see e.g. Refs. [24–26]). This begs the question to which extent the TCSA can be generalized to more than two dimensions: the second half of this thesis is devoted to answering this question. In chapter 4, we start by describing a generalization that puts the theory on the d-dimensional cylinder $\mathbb{R} \times S^{d-1}$. Then we specialize to a particular CFT, the free massless scalar boson: since this theory exists in any d, it forms a suitable starting point for investigations into d-dimensional RG flows. In chapter 5 we consider a simple RG flow, the free boson with a mass term $\frac{1}{2}m^2\phi^2$. We explain how to do exact computations in this theory on the cylinder, and compare the resulting predictions to numerical TCSA results.

Chapter 6 is more technical in nature: it is devoted to understanding the limit where the cutoff Λ is taken to infinity. We explain how the TCSA Hamiltonian can be 'improved' in order to reduce truncation errors. In chapter 7 the TCSA is applied to ϕ^4 theory. This theory is supposed to have the same phase structure as the Ising model: depending on the ϕ^2 coupling, it can be in a $\mathbb{Z}_2$ preserving (paramagnetic) or broken (ferromagnetic) phase. We observe this phase structure in TCSA computations, which we do in $d = 2.5$ for technical reasons. For a critical value of the ϕ^2 coupling, the theory should flow to a CFT, specifically the critical Ising model; as a consistency check of the method, we compare TCSA predictions for critical exponents in this theory to their actual values.

Appendix C provides details on how some computations in the free scalar CFT were done. In appendix D, some details on TCSA renormalization are given.

Pedagogical remarks

Some familiarity with statistical field theory [27–30] and the renormalization group [31–33] will be useful, but not strictly necessary. No prior knowledge of conformal field theory is required: in chapter 1, the necessary formalism is developed.

Citations to published work

Most of the material in this thesis has been taken from three papers. Chapter 2 is based on:

M. Hogervorst and S. Rychkov, "Radial Coordinates for Conformal Blocks," *Phys.Rev.* **D87** (2013) 106004, arXiv:1303.1111 [hep-th].

Chapter 3 is based on:

M. Hogervorst, H. Osborn, and S. Rychkov, "Diagonal Limit for Conformal Blocks in d Dimensions," *JHEP* **1308** (2013) 014, arXiv:1305.1321 [hep-th].

Finally, chapters 4-7 are based on:

M. Hogervorst, S. Rychkov, and B. C. van Rees, "Truncated Conformal Space Approach in d Dimensions: A Cheap Alternative to Lattice Field Theory?," *Phys.Rev.* **D91** (2015) 025005, arXiv:1409.1581 [hep-th].

Résumé substantiel

Une des applications de la théorie quantique des champs (TQC) se trouve dans le domaine des phénomènes critiques. Un exemple connu est fourni par les aimants : certains matériaux perdent leur aimantation quand la température augmente au-delà de la température de Curie, qui dépend du matériau en question. En revanche, la physique au voisinage de ce point est indépendante du matériau. Il existe alors un certain nombre de quantités *universelles*, partagées par tous les matériaux qui réalisent la même transition de phase. Cette universalité est expliquée par la théorie du groupe de renormalisation [34].

Comment peut-on alors prédire ces quantités universelles ? On remarque que les théories critiques sont invariantes sous les transformations d'échelle (voire toutes les transformations conformes) : les classes d'universalité des transitions de phases sont ainsi en correspondance avec les théories conformes des champs (TCC). Le but du *programme de bootstrap* est d'abord de classifier les TCC, afin d'en extraire les quantités observables (comme les exposants critiques). Ce programme est basé sur le fait que les fonctions à quatre points en TCC se calculent de deux façons différentes :

$$\sum_i c_{12i}c_{34i}\, G_{\mathcal{O}_i}(u,v) \;\sim\; \sum_i c_{32i}c_{14i}\, G_{\mathcal{O}_i}(v,u)\,,$$

où la somme porte sur tous les opérateurs $\mathcal{O}_i$ (avec spin ℓ_i et dimension d'échelle Δ_i) de la théorie en question, et les c_{ijk} sont des coefficients qui s'observent dans les fonctions à trois points $\langle \mathcal{O}_i\mathcal{O}_j\mathcal{O}_k\rangle$. Toute la « cinématique » de cette équation est contenue dans les *blocs conformes* $G_{\mathcal{O}}(u,v)$, qui dépendent uniquement des deux rapports anharmoniques u et v et des propriétés conformes de l'opérateur $\mathcal{O}$.

Ces blocs conformes sont l'objet d'étude de la première partie de cette thèse. En chapitre 2, on montre que ces blocs admettent un développement de la forme

$$G_{\mathcal{O}}(r,\theta) = \sum_{n=0}^{\infty}\sum_j C_{n,j}\, r^{\Delta_{\mathcal{O}}+n}\, \mathrm{Geg}_j^{(\nu)}(\cos\theta)\,,$$

où on utilise des coordonnées polaires $\{r,\theta\}$ au lieu de u et v, et $\mathrm{Geg}_j^{(\nu)}$ sont les polynômes de Gegenbauer en d dimensions. Si la théorie en question est unitaire, les $C_{n,j}$ sont automatiquement positifs. Ensuite, on montre que ce développement converge uniformement sur tout compact du disque unité, et que dans un jeu de coordonnées bien choisi (qui définit une coordonnée radiale "ρ"), les coefficients $C_{n,j}$ sont bornés pour tout $\Delta_{\mathcal{O}}$. Finalement, on établit des récurrences qui déterminent les $C_{n,j}$ à partir de $C_{0,\ell}$.

Dans le chapitre 3, on étudie la restriction de ces blocs conformes à la "diagonale" $\theta = 0$. En nous appuyant sur les équations de Casimir du groupe conforme (celle de 2$^{\mathrm{e}}$ et de 4$^{\mathrm{e}}$ ordre), on montre qu'ils obéissent à des équations différentielles de la forme $D_x\, f_{\Delta,\ell}(x) = 0$, où D_x est un opérateur différentiel d'ordre quatre. Ici x est soit la coordonnée z de Dolan

et Osborn [15, 16], soit $x = |\rho|$ pour la coordonnée radiale ρ mentionnée auparavant. La méthode de Frobenius permet d'établir un développement convergeant pour $x \in [0, 1)$:

$$f_{\Delta,\ell}(x) = x^{\Delta} \sum_{n=0}^{\infty} c_n \, x^n \,,$$

ce qui permet de calculer f et ses dérivées efficacement sur la diagonale.

La deuxième partie de cette thèse est dédiée à la Méthode de Troncature Conforme (MTC) de Yurov et Al. Zamolodchikov [23]. La première étape de cette méthode consiste à quantifier une théorie conforme sur la sphère S_R^{d-1} de rayon R, perturbée par un opérateur pertinent $\mathcal{V}$. Le hamiltonien de ce système est donné par

$$H = H_{\mathrm{TCC}} \; + g \int_{S_R^{d-1}} \mathcal{V} \,,$$

où g est une constante de couplage. Les états dans l'espace de Hilbert de la TCC sont en correspondance avec les opérateurs locaux $\mathcal{O}(x)$. La seconde étape de la MTC consiste à tronquer cet espace d'Hilbert, c'est-à-dire de garder seulement les opérateurs de dimension $\Delta \leqslant \Delta_{\max}$ dans le spectre de la TCC. Physiquement, l'opérateur $\mathcal{V}$ engendre un flot du groupe de renormalisation ; on peut montrer que le rayon R joue le rôle d'échelle dans ce flot.

La MTC a été utilisée uniquement en $d = 2$ auparavant, notamment pour le cas où la théorie conforme en question est un modèle minimal de Virasoro $\mathcal{M}(p, q)$. On étudie dans cette thèse sa généralisation à $d > 2$ dimensions : plus spécifiquement, on considère deux flots différents qui partent de la théorie du champ scalaire libre ϕ (avec une masse nulle). Dans un premier temps – au chapitre 5 – on considère la perturbation massive en $d = 3$, donnée par le terme $\frac{1}{2}m^2\phi^2$. Le spectre du boson massif sur $\mathbb{R} \times S_R^{d-1}$ peut être calculé analytiquement, ce qui permet de comparer les résultats numériques de la MTC à des résultats analytiques. On conclut que les prédictions numériques sont en bon accord avec le spectre analytique, bien au-delà du régime perturbatif.

Le chapitre 6 est dédié à une analyse des erreurs induites par la troncature de la MTC, c'est-à-dire par la présence d'une énergie de coupure $\Lambda = \Delta_{\max}/R$. On montre que la dépendance des observables (ici : les valeurs propres E_n du hamiltonien) avec Λ est une loi de puissance : $E_n(\Lambda) \sim c + c'/\Lambda^{\alpha} + \ldots$, où $c, c', \ldots$ sont des constantes. Pour les théories étudiées dans cette thèse, la limite continue $\Lambda \to \infty$ est finie. On développe dans ce chapitre une méthode qui permet de réduire les erreurs de troncature, c'est-à-dire d'améliorer le taux de convergence quand $\Lambda \to \infty$, basée sur des travaux antérieurs pour la MTC et $d = 2$ (voir [35]).

Finalement, on étudie le flot engendré par $\frac{1}{2}m^2\phi^2 + \lambda\phi^4$, autrement dit la théorie de Landau-Ginzburg. Afin de ne pas introduire des divergences de courte distance, on travaille en $d = 2.5$ dimensions. Cette théorie exhibe une transition de phase : plus précisément, il

existe une valeur critique m_*^2 telle que la symétrie $\mathbb{Z}_2$ est préservée pour $m^2 > m_*^2$, mais brisée spontanément pour $m^2 < m_*^2$. Ce phénomène est reproduit par la MTC : les résultats numériques mettent en évidence que le spectre est doublement dégénéré. Finalement, on remarque que cette théorie est censée décrire la transition de phase du modèle d'Ising. En effet, les exposants critiques prédits par la MTC sont en accord avec leurs valeurs prédites par le bootstrap et le groupe de renormalisation.

Conventions and special functions

Conventions

All computations in this thesis are done in Euclidean signature and using the Einstein summation convention. The Ricci scalar is denoted by $\mathcal{R}$. S^{d-1} is the unit sphere of dimension $d-1$; it is naturally embedded in $\mathbb{R}^d$ as follows:

$$S^{d-1} = \{x^\mu \in \mathbb{R}^d \mid |x|^2 = 1\}. \tag{0.1}$$

The shorthand notation S_d denotes its volume:

$$\mathrm{S}_d = \mathrm{Vol}(S^{d-1}) = \frac{2\pi^{d/2}}{\Gamma(d/2)}. \tag{0.2}$$

The scaling dimension of the free, massless boson $[\phi]$ in $d > 2$ dimensions is given by $\nu \equiv (d-2)/2$.

Special functions

We briefly review the special functions used in this manuscript. More details can be found in Refs. [36–38]. The *Pochhammer symbol* $(x)_n$ is defined as

$$(x)_n \equiv \frac{\Gamma(x+n)}{\Gamma(x)}\,. \tag{0.3}$$

If n is a positive integer,

$$(x)_n = (x+n-1)\cdots(x+1)x, \qquad n \in \mathbb{N}_{>0}\,. \tag{0.4}$$

The *hypergeometric function* ${}_2F_1(a,b;c;z)$ can be defined as a series expansion around $z=0$:

$${}_2F_1(a,b;c;z) \equiv {}_2F_1\left[\begin{matrix} a,\, b \\ c \end{matrix};z\right] \equiv \sum_{n=0}^{\infty} \frac{(a)_n (b)_n}{(c)_n}\frac{z^n}{n!}\,, \qquad |z|<1\,. \tag{0.5}$$

Generalized hypergeometric functions ${}_pF_q\left(a_1,\ldots,a_p;b_1,\ldots,b_q;z\right)$ are defined similarly. The *Gegenbauer polynomials* $\mathrm{Geg}_n^{(\alpha)}(z)$ are defined as follows:

$$\frac{1}{(1-2zt+t^2)^\alpha} \equiv \sum_{n=0}^{\infty} t^n\, \mathrm{Geg}_n^{(\alpha)}(z). \tag{0.6}$$

As a consequence, $\mathrm{Geg}_n^{(\alpha)}(x)$ is an even (odd) polynomial of degree n in z when n is even (odd):

$$\mathrm{Geg}_n^{(\alpha)}(-z) = (-1)^n\, \mathrm{Geg}_n^{(\alpha)}(z). \tag{0.7}$$

Useful closed-form expressions for even (odd) n are given by

$$\mathrm{Geg}_{2n}^{(\alpha)}(z) = (-1)^n \frac{(\alpha)_n}{n!}\, {}_2F_1\left[\begin{matrix} -n,\, n+\alpha \\ 1/2 \end{matrix};z^2\right] \tag{0.8a}$$

$$\frac{\mathrm{Geg}_{2n+1}^{(\alpha)}(z)}{z} = (-1)^n \frac{2\alpha(\alpha+1)_n}{n!}\, {}_2F_1\left[\begin{matrix} -n,\, n+\alpha+1 \\ 3/2 \end{matrix};z^2\right]. \tag{0.8b}$$

Chapter 1

Elements of conformal field theory

This thesis uses the tools of conformal field theory heavily. In order to make this manuscript reasonably self-contained, we have chosen to collect the necessary results about CFTs in $d > 2$ dimensions. Readers familiar with the subject may skip this chapter, because no new material is presented.

We have organized this introductory chapter as follows: in sections 1.1 and 1.2, we describe the conformal group in $d > 2$ dimensions and its Lie algebra. Section 1.3 concerns the representation theory of the conformal group, in particular the transformation laws for tensor operators. Closely related are constraints that conformal invariance puts on correlation functions, which are natural observables in CFTs; these are described in section 1.4. Sections 1.5 and 1.6 introduce radial quantization, a method that is at the heart of the Truncated Conformal Space Approach. Finally, sections 1.7 and 1.8 are intended as a brief introduction to the conformal bootstrap program.

Because of the scope of the subject, we do not aim to give a comprehensive account of the CFT literature. In particular, we do not discuss the relation of conformal invariance to critical phenomena in statistical physics — we point the reader to Ref. [31] for details. Furthermore, there are many pedagogical texts available focusing on different aspects of conformal invariance, including [39–42, 28, 43, 44, 6]. Applications of conformal invariance in two dimensions to string theory are discussed in many textbooks on the subject, including [45–48]. An introduction to the bootstrap program is given in the dissertation [49]. Finally we point the reader to various sets of lecture notes, focusing either on CFTs [50–54] or on the AdS/CFT-correspondence [55].

1.1 Conformal group

Conformal transformations $x \to x'$ in d-dimensional Euclidean space are defined by the requirement that the line element $\mathrm{d}s^2 = \delta_{\mu\nu}\,\mathrm{d}x^\mu \mathrm{d}x^\nu$ transforms as

$$\mathrm{d}s^2 \;\to\; \mathrm{d}s'^2 = \delta_{\mu\nu}\,\mathrm{d}x'^\mu \mathrm{d}x'^\nu \;\overset{\text{must be}}{=}\; \Omega(x)^2 \mathrm{d}s^2 \tag{1.1}$$

for some function $\Omega(x) > 0$. Such transformations clearly form a group: if $x \to x'$ and $x' \to x''$ are two conformal transformations, then the composition $x \to x''$ is conformal as well.

Our goal in this section is to classify this group. We start by remarking that Eq. (1.1) is equivalent to

$$\frac{\partial x'^\mu}{\partial x^\alpha}\frac{\partial x'^\nu}{\partial x^\beta}\,\delta_{\mu\nu} = \Omega(x)^2\,\delta_{\alpha\beta}\,. \tag{1.2}$$

From this equation, it follows that the Jacobian of any conformal transformation $x \to x'$ can be decomposed as

$$\frac{\partial x'^\mu}{\partial x^\nu} = \Omega(x)\Lambda^\mu{}_\nu(x)\,, \tag{1.3}$$

where the matrix $\Lambda^\mu{}_\nu(x)$ is orthogonal at every point x:

$$\delta_{\mu\nu}\,\Lambda^\mu{}_\rho(x)\Lambda^\nu{}_\sigma(x) = \delta_{\rho\sigma}. \tag{1.4}$$

Conversely, any transformation $x \to x'$ whose Jacobian is of the form (1.3) is conformal. Rigid transformations of the form

$$x \;\to\; x' = \mathcal{R}\cdot x + a, \qquad {}^t\mathcal{R} = \mathcal{R}^{-1} \tag{1.5}$$

are obvious examples of conformal transformations, with a conformal factor $\Omega(x) = 1$. Dilatations

$$x \;\to\; x' = \lambda x, \qquad \lambda > 0 \tag{1.6}$$

are conformal transformations as well, satisfying $\Omega(x) = \lambda$. A more involved example of a conformal transformation is given by the *inversion*

$$\mathrm{I} \;:\; x^\mu \;\to\; x'^\mu = \frac{x^\mu}{x^2}\,. \tag{1.7}$$

It is an easy exercise to show that the inversion satisfies Eq. (1.3) with

$$\Omega(x) = \frac{1}{x^2}, \qquad \Lambda^\mu{}_\nu(x) = \delta^\mu_\nu - 2\frac{x^\mu x_\nu}{x^2} =: \mathcal{I}^\mu{}_\nu(x). \tag{1.8}$$

Notice however that $\det \mathcal{I} = -1$, meaning that the inversion cannot be continuously connected to the unit element of the conformal group. By composing an inversion with a translation $x^\mu \to x^\mu + a^\mu$ and a second inversion, one obtains a *special conformal transformation* (SCT):

$$x^\mu \;\to\; x'^\mu = \frac{x^\mu + a^\mu x^2}{1 + 2a\cdot x + a^2x^2}\,, \tag{1.9}$$

which has the scale factor

$$\Omega(x) = \frac{1}{1 + 2a \cdot x + a^2 x^2}. \tag{1.10}$$

Such SCTs are part of identity component of the conformal group, as may be seen by taking the limit $a^\mu \to 0$.

The above transformations generate the full conformal group: to be precise (see theorem 1.9 of [42]), any conformal transformation in $d > 2$ dimensions is a composition of translations, rotations, dilatations and SCTs. By counting parameters, it follows that the conformal group has dimension $\frac{1}{2}(d+1)(d+2)$.

The case $d = 2$ is special, as can be seen by parametrizing the $\{x^1, x^2\}$-plane by a complex coordinate $z = x^1 + ix^2$. The Euclidean metric in this coordinate is $\mathrm{d}s^2 = \mathrm{d}z\,\mathrm{d}\bar{z}$, which means that any analytic transformation

$$z \;\mapsto\; w(z)\,, \qquad \bar{z} \;\mapsto\; \bar{w}(\bar{z}) \tag{1.11}$$

is conformal. This implies that the 2d conformal group is infinite-dimensional. The analog of the $d > 2$ conformal group is isomorphic to $SL(2, \mathbb{C})$: this is a six-dimensional subgroup of the full conformal group in two dimensions.

1.2 Conformal algebra

We will now discuss infinitesimal conformal transformations $x^\mu \to x'^\mu = x^\mu + \alpha^\mu(x)$. The requirement that $x \to x'$ is conformal is equivalent to

$$\partial_\mu \alpha_\nu(x) + \partial_\nu \alpha_\mu(x) = \frac{2}{d}(\partial \cdot \alpha)\delta_{\mu\nu}\,, \tag{1.12}$$

as follows from Eq. (1.2). It is a textbook exercise [39] to classify the solutions to Eq. (1.12) in $d > 2$ dimensions; the results are shown in the table below. As foreseen, all infinitesimal transformations can be derived from the finite transformations discussed in Sec. (1.1):

type	$\alpha^\mu(x)$
translations	ϵ^μ
rotations	$\omega^\mu{}_\nu x^\nu \qquad [\omega_{\mu\nu} = -\omega_{\nu\mu}]$
dilatations	ϵx^μ
SCTs	$x^2\epsilon^\mu - 2(\epsilon \cdot x)x^\mu$

The Lie algebra of the conformal group can easily be found using this result. Let us define the action of a group element $g : x \mapsto (gx) = x'$ on an arbitrary function $\Psi : \mathbb{R}^d \to \mathbb{C}$ as follows:

$$\Psi(x) \;\to\; (T_g\Psi)(x) = \Psi(g^{-1}x)\,. \tag{1.13}$$

This forms a representation of the conformal group: to see this, it is sufficient to check that $T_g(T_h\Psi) = T_{gh}\Psi$. Consider now a group element g close to the identity: as such, it acts infinitesimally on coordinates, and we may write $(gx)^\mu = x^\mu + \alpha_g^\mu(x)$. On the other hand, we may expand $T_g = \mathbb{1} - i\omega_g{}^I G_I$, where the G_I are group generators and the infinitesimal numbers $\omega_g{}^I$ parametrize g. Hence the action of the generators G_I is fixed:

$$(T_g\Psi)(x) = \Psi(x) - \alpha^\mu(x)\partial_\mu\Psi(x) \quad \Rightarrow \quad \omega_g{}^I G_I\Psi(x) = -\alpha_g^\mu(x)\partial_\mu\Psi(x)\,. \tag{1.14}$$

Working this out for all generators, we find:

$(gx)^\mu$	T_g	generator(s)
$x^\mu + \epsilon^\mu$	$\mathbb{1} - i\epsilon^\mu P_\mu$	$P_\mu = -i\partial_\mu$
$x^\mu + \omega^\mu{}_\nu x^\nu \quad [\omega_{\mu\nu} = -\omega_{\nu\mu}]$	$\mathbb{1} - \frac{i}{2}\omega^{\mu\nu}M_{\mu\nu}$	$M_{\mu\nu} = i(x_\mu\partial_\nu - x_\nu\partial_\mu)$
$x^\mu + \epsilon x^\mu$	$\mathbb{1} + i\epsilon D$	$D = ix\cdot\partial$
$x^\mu + x^2\epsilon^\mu - 2(\epsilon\cdot x)x^\mu$	$\mathbb{1} - i\epsilon^\mu K_\mu$	$K_\mu = -i\left(x^2\partial_\mu - 2x_\mu\, x\cdot\partial\right)$.

The non-vanishing commutators between the generators are:

$$[M_{\mu\nu}, M_{\rho\sigma}] = i\left(-\delta_{\mu\rho}M_{\nu\sigma} + \delta_{\mu\sigma}M_{\nu\rho} + \delta_{\nu\rho}M_{\mu\sigma} - \delta_{\nu\sigma}M_{\mu\rho}\right), \tag{1.15a}$$

$$[M_{\mu\nu}, X_\rho] = -i\delta_{\mu\rho}X_\nu + i\delta_{\nu\rho}X_\mu, \qquad [X_\mu = P_\mu \text{ or } K_\mu] \tag{1.15b}$$

$$[K_\mu, P_\nu] = 2i\left(\delta_{\mu\nu}D + M_{\mu\nu}\right), \tag{1.15c}$$

$$[D, P_\mu] = -iP_\mu, \tag{1.15d}$$

$$[D, K_\mu] = iK_\mu. \tag{1.15e}$$

Eq. (1.15a) is the familiar Lie algebra of $SO(d)$, whereas Eq. (1.15b) shows that K_μ and P_μ transform as vectors under rotations. It is useful to think of the conformal algebra as being graded by iD. With respect to this grading, P_μ (resp. K_μ) acts as a raising (resp. lowering) operator, as can be seen from the last two commutators.

Casimir operators [1]

We now turn our attention to the Casimir operators of the conformal algebra. To construct these Casimirs, we first revisit the isomorphism between the conformal group in d dimensions and and the Lorentz group in $d+2$ dimensions, $SO(d+1,1)$. To establish this isomorphism, let us consider a set of generators $L_{AB} = -L_{BA}$ $(A, B = 0, 1, \ldots, d+1)$ defined as follows:

$$L_{0\,\mu} = X_\mu^+, \quad L_{0\,d+1} = D, \quad L_{\mu\nu} = M_{\mu\nu}, \quad L_{\mu\,d+1} = X_\mu^-\,, \tag{1.16}$$

1. This section is included to provide a complete derivation of the Casimir eigenvalues of the conformal group and is not essential to the rest of the text.

where $X_\mu^\pm \equiv \frac{1}{2}(P_\mu \pm K_\mu)$. In matrix form, L_{AB} has the following structure:

$$L_{AB} = \begin{pmatrix} 0 & X_\mu^+ & D \\ & M_{\mu\nu} & X_\mu^- \\ & & 0 \end{pmatrix} \tag{1.17}$$

We now claim the generators L_{AB} satisfy the $SO(d+1,1)$ commutation relations:

$$[L_{AB}, L_{CD}] = i\left(-\eta_{AC}L_{BD} + \eta_{AD}L_{BC} + \eta_{BC}L_{AD} - \eta_{BD}L_{AC}\right) , \tag{1.18}$$

where $\eta_{AB} = \text{diag}(-1, \underbrace{1, \ldots, 1}_{\text{d+1}})$ is the Minkowski metric in $d+2$ dimensions. This may be readily checked using the commutators (1.15) and

$$[D, X_\mu^\pm] = -iX_\mu^\mp, \tag{1.19a}$$
$$[X_\mu^\pm, X_\nu^\pm] = \pm iM_{\mu\nu}, \tag{1.19b}$$
$$[X_\mu^\pm, X_\nu^\mp] = \pm i\delta_{\mu\nu}D, \tag{1.19c}$$
$$[M_{\mu\nu}, X_\rho^\pm] = -i\delta_{\mu\rho}X_\nu^\pm + i\delta_{\nu\rho}X_\mu^\pm. \tag{1.19d}$$

The commutator (1.18) establishes that the conformal group is isomorphic to $SO(d+1,1)$.

With the isomorphism (1.16) in place, we can use some basic facts about the group theory of $SO(d+1,1)$ [56] to study the Casimirs of the conformal algebra. We recall that the number of Casimirs of a given Lie algebra equals its rank, which is r for $SO(2r)$ and $SO(2r+1)$. Schematically, these Casimirs are of the form $\mathscr{C}_k \sim \text{tr } L^k$ for $k = 2, 4, \ldots$. For $SO(2r)$, one of the Casimir operators is given by $\epsilon^{\mu_1\cdots\mu_{2r}}L_{\mu_1\mu_2}\cdots L_{\mu_{2r-1}\mu_{2r}}$, where ϵ is the Levi-Civita symbol in $2r$ dimensions.

For $d = 2$ and $d = 3$, there are thus two independent Casimirs, $\mathscr{C}_2$ and $\mathscr{C}_4$. The goal of the rest of this section is to express these Casimirs in terms of the generators $\{D, P_\mu, K_\mu, M_{\mu\nu}\}$. Any extra Casimirs that exist in $d \geqslant 4$ dimensions do not play a role in this thesis. [2]

The quadratic Casimir is given by

$$\begin{aligned} \mathscr{C}_2 &\equiv -\tfrac{1}{2}\text{tr}\, L^2 = \tfrac{1}{2}L_{AB}L^{AB} \\ &= \tfrac{1}{2}M_{\mu\nu}M^{\mu\nu} + iD(iD - d) - P\cdot K. \end{aligned} \tag{1.20}$$

The first term in Eq. (1.20) is of course the quadratic Casimir of the subgroup $SO(d)$, which we denote by

$$\mathcal{C}_2 \equiv \tfrac{1}{2}M_{\mu\nu}M^{\mu\nu}. \tag{1.21}$$

It's not hard to check that $[\mathscr{C}_2, G_I] = 0$ for all generators G_I of the conformal algebra.

2. The cubic Casimir of the conformal group is discussed e.g. in [40, 57].

The next Casimir is quartic in the $SO(d+1,1)$ generators:

$$\mathscr{C}_4 \equiv \tfrac{1}{2}\mathrm{tr}\, L^4 = \tfrac{1}{2} L_{AB} L^{BC} L_{CD} L^{DA}. \tag{1.22}$$

A straightforward but tedious calculation shows that

$$\begin{aligned}\mathscr{C}_4 = &-D^2(iD-d)^2 + \tfrac{1}{2}d(d-1)iD(iD-d) + \mathcal{C}_4 - \mathcal{C}_2 \\ &+ \tfrac{1}{2}\left(P^2K^2 + P^\mu P^\nu K_\mu K_\nu\right) - \tfrac{1}{2}(3d^2-d+2)P\cdot K \\ &+ 2\left(D^2 P\cdot K + P^\mu M_{\mu\nu} M^{\nu\rho} K_\rho - D P^\mu M_{\mu\nu} K^\nu\right) \\ &+ (3d+1)iDP\cdot K - (3d-1)iP^\mu M_{\mu\nu} K^\nu. \end{aligned} \tag{1.23}$$

The term $\mathcal{C}_4$ represents another $SO(d)$ Casimir operator, namely

$$\mathcal{C}_4 \equiv \tfrac{1}{2} M_{\mu\nu} M^{\nu\rho} M_{\rho\sigma} M^{\sigma\mu}\,, \tag{1.24}$$

which is independent from $\mathcal{C}_2$ for $d > 3$. Again, it may be verified that all commutators $[\mathscr{C}_4, G_I]$ vanish.

1.3 Local operators

In the previous sections, we have described the conformal group and its algebra. We will now pass to CFTs: field theories that are invariant under conformal transformations. In what follows, a CFT will be regarded as a set of *local operators* $\{\mathcal{O}_i\}$ together with their Euclidean correlation functions $\langle \mathcal{O}_1(x_1)\cdots\mathcal{O}_n(x_n)\rangle$.

By assumption, all local operators can be organized in representations of the conformal group. A subset of the $\{\mathcal{O}_i\}$ transforms homogeneously under conformal transformations; such operators are called *primary*.[3] To be precise, we recall that any conformal transformation $x^\mu \to (gx)^\mu = x'^\mu$ is characterized by scale factor $\Omega_g(x)$ and an orthogonal matrix $\Lambda_g(x)$, cf. Eq. (1.3). A primary operator $\mathcal{O}$ then transforms as [58–62, 39]

$$\begin{aligned} x^\mu &\to (gx)^\mu = x'^\mu \\ \mathcal{O}(x) &\to \mathcal{O}'(x') = \Omega_g(x)^{-\Delta}\, D[\Lambda_g(x)]\, \mathcal{O}(x)\,, \end{aligned} \tag{1.25}$$

where $D[\Lambda_g(x)]$ is a matrix that acts on the indices of $\mathcal{O}(x)$. Under a dilatation $x \to \lambda x$, the above transformation law reduces to

$$\mathcal{O}(x) \to \mathcal{O}'(\lambda x) = \lambda^{-\Delta}\, \mathcal{O}(x). \tag{1.26}$$

The number Δ is also known as the *scaling dimension* of $\mathcal{O}$, and sometimes denoted as $[\mathcal{O}] = \Delta$. Similarly, under a rotation $x \to \mathcal{R}\cdot x$, a primary $\mathcal{O}$ transforms as

$$\mathcal{O}(x) \to \mathcal{O}'(\mathcal{R}\cdot x) = D[\mathcal{R}]\, \mathcal{O}(x) \tag{1.27}$$

3. In the 2d CFT literature, such operators are called *quasi-primary*.

which requires that the matrix $D[\mathcal{R}]$ forms a representation of $SO(d)$. In conclusion, the transformation law (1.25) is completely determined by the dimension Δ and the $SO(d)$ quantum numbers of $\mathcal{O}$.

For now, we want to find the action of the generators G_I on primary operators $\{\mathcal{O}\}$. In principle, this can be done analogously to the computation in Sec. 1.2, but using the transformation law $g : \mathcal{O} \mapsto \mathcal{O}'$ defined above in Eq. (1.25). This is rather tedious, and a easier method is proposed by Mack and Salam [58]. [4]

As a first step, we can restrict ourselves to the little group (the stabilizer subgroup of $x = 0$), that consists of rotations, dilatations and SCTs. For the corresponding generators, we find

$$[D, \mathcal{O}(0)] = -i\Delta\mathcal{O}(0), \qquad [K_\mu, \mathcal{O}(0)] = 0, \qquad [M_{\mu\nu}, \mathcal{O}(0)] = \mathcal{S}_{\mu\nu}\mathcal{O}(0). \tag{1.28}$$

The matrix $\mathcal{S}_{\mu\nu} = -\mathcal{S}_{\nu\mu}$ above is a generator of the $SO(d)$ algebra, and it is defined by imposing that under an infinitesimal rotation

$$\mathcal{R}^\mu{}_\nu = \delta^\mu_\nu + \omega^\mu{}_\nu + \mathrm{O}(\omega^2) \quad \text{with} \quad \omega_{\mu\nu} = -\omega_{\nu\mu} \tag{1.29}$$

the matrix $D[\mathcal{R}]$ is expanded to first order in $\omega_{\mu\nu}$ as

$$D[\mathcal{R}] = \mathbb{1} - \frac{i}{2}\omega^{\mu\nu}\mathcal{S}_{\mu\nu} + \mathrm{O}(\omega^2). \tag{1.30}$$

As with the matrix $D[\mathcal{R}]$, the generator $\mathcal{S}_{\mu\nu}$ depends on the representation of $\mathcal{O}$. Moreover, it can be shown that the property $[K_\mu, \mathcal{O}(0)] = 0$ is equivalent to $\mathcal{O}$ being a primary operator.

Next, we notice that P_μ acts as a generator of translations:

$$\mathcal{O}(x) = e^{ix\cdot P}\mathcal{O}(0)e^{-ix\cdot P} \quad \Rightarrow \quad [P_\mu, \mathcal{O}(x)] = -i\partial_\mu\mathcal{O}(x). \tag{1.31}$$

The action of a generator G at $x \neq 0$ therefore obeys

$$[G, \mathcal{O}(x)] = e^{ix\cdot P}[G', \mathcal{O}(0)]e^{-ix\cdot P}, \qquad G' = e^{-ix\cdot P}Ge^{ix\cdot P}. \tag{1.32}$$

The translated generator G' is easily calculated using a variant of the Baker-Campbell-Hausdorff formula:

$$G' = G - ix^\mu[P_\mu, G] - \frac{1}{2!}x^\mu x^\nu[P_\mu, [P_\nu, G]] + \dots. \tag{1.33}$$

Although a priori (1.33) is an infinite series, it truncates at the displayed order for all generators, and we obtain:

$$D' = D + x \cdot P\,, \tag{1.34a}$$

$$M'_{\mu\nu} = M_{\mu\nu} + x_\mu P_\nu - x_\nu P_\mu\,, \tag{1.34b}$$

$$K'_\mu = K_\mu - 2x_\mu D + 2x^\lambda M_{\lambda\mu} + x^2 P_\mu - 2x_\mu x \cdot P\,. \tag{1.34c}$$

4. See also [39] for a pedagogical treatment.

The commutators $[G, \mathcal{O}(x)]$ at $x \neq 0$ are therefore given by

$$[D, \mathcal{O}(x)] = -i(\Delta + x \cdot \partial)\, \mathcal{O}(x), \tag{1.35a}$$

$$[M_{\mu\nu}, \mathcal{O}(x)] = \{\mathcal{S}_{\mu\nu} - i(x_\mu \partial_\nu - x_\nu \partial_\mu)\}\, \mathcal{O}(x), \tag{1.35b}$$

$$[K_\mu, \mathcal{O}(x)] = \left\{2x^\kappa \mathcal{S}_{\kappa\mu} + 2i\Delta x_\mu + 2ix_\mu x \cdot \partial - ix^2 \partial_\mu\right\} \mathcal{O}(x). \tag{1.35c}$$

As a consistency check of the above result, it may be shown that

$$[[G_1, G_2], \mathcal{O}(x)] = [G_1, [G_2, \mathcal{O}(x)]] - [G_2, [G_1, \mathcal{O}(x)]] \tag{1.36}$$

for any two generators G_1, G_2, provided that

$$[\mathcal{S}_{\mu\nu}, \mathcal{S}_{\rho\sigma}]\, \mathcal{O}(0) = i\left\{\delta_{\mu\rho}\mathcal{S}_{\nu\sigma} - \delta_{\mu\sigma}\mathcal{S}_{\nu\rho} - \delta_{\nu\rho}\mathcal{S}_{\mu\sigma} + \delta_{\nu\sigma}\mathcal{S}_{\mu\rho}\right\} \mathcal{O}(0). \tag{1.37}$$

The latter is the $SO(d)$ commutator from Eq. (1.15a) with all signs reversed.

1.3.1 Tensor operators

We have seen that any $SO(d)$ representation can be extended to a representation of the conformal group. In this thesis, only a specific class of tensor operators will play a role, namely traceless symmetric tensors (TSTs) $\mathcal{O}_{\mu_1\cdots\mu_\ell}(x)$. If a TST has ℓ indices, we will refer to it as having spin ℓ. If $\mathcal{O}_{\mu_1\cdots\mu_\ell}(x)$ has dimension Δ, then it transforms under a finite conformal transformation $x^\mu \to x'^\mu$ as [63]

$$\mathcal{O}'_{\mu_1\cdots\mu_\ell}(x') = \left|\det \frac{\partial x'}{\partial x}\right|^{(\ell-\Delta)/d} \frac{\partial x^{\nu_1}}{\partial x'^{\mu_1}} \cdots \frac{\partial x^{\nu_\ell}}{\partial x'^{\mu_\ell}}\, \mathcal{O}_{\nu_1\cdots\nu_\ell}(x)\,. \tag{1.38}$$

Reinstating the scale factor $\Omega(x)$ and the orthogonal matrix $\Lambda^\mu{}_\nu$ from the Jacobian $\partial x'/\partial x$ as in equation (1.3), we can rewrite the above transformation law as

$$\mathcal{O}'_{\mu_1\cdots\mu_\ell}(x') = \Omega(x)^{-\Delta}\, \Lambda_{\mu_1}{}^{\nu_1}(x) \cdots \Lambda_{\mu_\ell}{}^{\nu_\ell}(x)\, \mathcal{O}_{\nu_1\cdots\nu_\ell}(x)\,, \tag{1.39}$$

where $\Lambda_\mu{}^\nu$ is the transpose (inverse) of $\Lambda^\mu{}_\nu$. Obviously, scalars (with $\ell = 0$) and vectors ($\ell = 1$) are particular examples of TSTs.

In what follows, we will require the Casimir eigenvalue of $\mathcal{C}_2$ and $\mathcal{C}_4$ for the spin-ℓ representation. Let us start by remarking that the spin generator $\mathcal{S}_{\alpha\beta}$ is given by

$$(\mathcal{S}_{\alpha\beta})_{\mu_1\cdots\mu_\ell}{}^{\nu_1\cdots\nu_\ell} = -i\sum_{j=1}^{\ell} \delta_{\mu_1}{}^{(\nu_1} \cdots \left[\delta_{\alpha\mu_j}\delta_\beta{}^{\nu_j} - \delta_{\beta\mu_j}\delta_\alpha{}^{\nu_j}\right] \cdots \delta_{\mu_\ell}{}^{\nu_\ell)} \;-\; \text{traces in } \nu_j. \tag{1.40}$$

Using this expression, it is straightforward to compute the Casimirs:

$$\mathcal{C}_2 = \tfrac{1}{2}\mathcal{S}^{\mu\nu}\,\mathcal{S}_{\mu\nu} \qquad = \lambda_\ell\, \mathbb{1}\,, \tag{1.41a}$$

$$\mathcal{C}_4 = \tfrac{1}{2}\mathcal{S}^{\sigma\mu}\,\mathcal{S}_{\rho\sigma}\,\mathcal{S}^{\nu\rho}\,\mathcal{S}_{\mu\nu} \qquad = \left[\lambda_\ell^2 + \tfrac{1}{2}(d-2)(d-3)\lambda_\ell\right] \mathbb{1}\,, \tag{1.41b}$$

for $\lambda_\ell = \ell(\ell + d - 2)$. Here $\mathbb{1}$ is the identity operator: $\mathbb{1}_{\mu_1\cdots\mu_\ell}{}^{\nu_1\cdots\nu_\ell} = \delta_{\mu_1}{}^{\nu_1}\cdots\delta_{\mu_\ell}{}^{\nu_\ell}$.

1.3.2 Descendants

Derivatives of primary operators do not transform homogeneously under conformal transformations, as is easy to see. As an example, let us consider a scalar primary $\mathcal{O}_\Delta$ of dimension Δ, together with its derivative $V_\mu \equiv \partial_\mu \mathcal{O}_\Delta(x)$. Using the transformation law (1.25), it can easily be shown that V_μ transforms as

$$V_\mu(x) \;\to\; V'_\mu(x') = \Omega(x)^{-(\Delta+1)} \Lambda_\mu{}^\nu(x) \left[V_\nu(x) - \Delta \frac{\partial \ln \Omega(x)}{\partial x^\nu} \mathcal{O}_\Delta(x) \right]. \tag{1.42}$$

The second term is inconsistent with V_μ being a primary, although under dilatations and rotations V_μ transforms just like a vector primary of dimension $\Delta + 1$. Algebraically, V_μ can be defined as

$$V_\mu(x) \equiv i[P_\mu, \mathcal{O}_\Delta(x)]. \tag{1.43}$$

The easiest way to see that V_ρ is not primary is to remark that it is not annihilated by K_μ at $x = 0$:

$$[K_\mu, V_\rho(0)] = 2i\Delta\delta_{\mu\rho}\, \mathcal{O}_\Delta(0) \tag{1.44}$$

which is non-zero unless $\Delta = 0$.

We can slightly formalize the above idea. Any operator that is an n-th derivative of a primary $\mathcal{O}$ is called a *descendant* of $\mathcal{O}$, having *level* n. It is easy to see that any level-n descendant has scaling dimension $[\mathcal{O}] + n$. For concreteness, we display the descendants of levels $n \leqslant 3$ of a scalar primary $\mathcal{O}$ in the table below. Various traces have been subtracted in order to give all descendants a definite spin:

level	spin-0	spin-1	spin-2	spin-3
0	$\mathcal{O}$			
1		$\partial_\mu \mathcal{O}$		
2	$\partial^2 \mathcal{O}$		$\left(\partial_\mu \partial_\nu - (1/d)\delta_{\mu\nu}\partial^2\right) \mathcal{O}$	
3		$\partial_\mu \partial^2 \mathcal{O}$		$(\partial_\mu \partial_\nu \partial_\rho - \text{traces})\, \mathcal{O}$
...				

The above easily generalizes to spin-ℓ primaries, taking into account that derivatives can both raise and lower the spin: the operator $\partial^{\mu_\ell} \mathcal{O}_{\mu_1 \cdots \mu_\ell}$ has spin $\ell - 1$, for example. As a consequence, level-n descendants of a spin-ℓ primary have their spin j restricted to

$$j \in \max(\ell - n \bmod 2, \ell - n), \ldots, \ell + n\,, \tag{1.45}$$

but only half of the spins in this interval occur.

A primary operator $\mathcal{O}$ together with its descendants forms an irreducible representation of the conformal group, labeled by the dimension and spin of the primary of $\mathcal{O}$. Such a representation is also known as a *conformal family*. As a consequence of conformal invariance,

the set of local operators decomposes into conformal families: this means that every local operator can be written as a sum of primaries and descendants.

1.4 Constraints on correlation functions

We now turn to a systematic study of the constraints imposed by conformal invariance on correlation functions, in the same way that Poincaré invariance restricts correlation functions in ordinary QFTs. Formally, correlation functions must be consistent with the transformation laws from section (1.3). Consider for example a primary scalar $\mathcal{O}$ of dimension Δ. If $x^\mu \to x'^\mu$ is any conformal transformation with scale factor $\Omega(x)$, then any correlation function involving $\mathcal{O}$ must satisfy

$$\langle \mathcal{O}(x_1') \cdots \rangle = \Omega(x_1)^{-\Delta} \langle \mathcal{O}(x_1) \cdots \rangle. \tag{1.46}$$

In this section, we will work out how these transformation laws constrain two, three and four point functions.

1.4.1 Scalar correlators

Let us start by considering correlation functions of scalar primaries. As a warm-up exercise, consider the one-point function of a scalar primary $\mathcal{O}$ with $[\mathcal{O}] = \Delta$. By translation invariance, it must be constant: $\langle \mathcal{O}(x) \rangle \equiv v$. Applying a dilatation $x \to \lambda x$, we conclude that $v = \lambda^\Delta v$ for all $\lambda > 0$, which is only possible if $v = 0$ or $\Delta = 0$. An operator with $\Delta = 0$ exists: it is the unit operator $\mathbb{1}$, which by definition satisfies $\langle \mathbb{1} \rangle = 1$. All other scalars have a vanishing one-point function.

Consider now the correlator $\langle \mathcal{O}_1 \mathcal{O}_2 \rangle$ of two primaries with dimensions Δ_1, Δ_2. By translation, rotation and scale invariance, it must be of the form

$$\langle \mathcal{O}_1(x_1) \mathcal{O}_2(x_2) \rangle = \frac{b}{|x_1 - x_2|^\alpha}, \qquad \alpha = \Delta_1 + \Delta_2 \tag{1.47}$$

for some number b. To find a further constraint, we apply the inversion $x^\mu \to x'^\mu = x^\mu / x^2$. Conformal invariance then requires that

$$\frac{b}{|x_1' - x_2'|^\alpha} = b \frac{|x_1|^\alpha |x_2|^\alpha}{|x_1 - x_2|^\alpha} \overset{\text{must be}}{=} |x_1|^{2\Delta_1} |x_2|^{2\Delta_2} \frac{b}{|x_1 - x_2|^\alpha} \tag{1.48}$$

which is satisfied if $\alpha = 2\Delta_1 = 2\Delta_2$ or if $b = 0$. Consequently, the correlator $\langle \mathcal{O}_1 \mathcal{O}_2 \rangle$ vanishes unless $\Delta_1 = \Delta_2$.

Two-point functions of primaries $\mathcal{O}_i, \mathcal{O}_j$ with the same dimension Δ are therefore fixed by conformal invariance up to a coefficient b_{ij}. In reflection-positive CFTs (see section 1.6.2),

it is always possible to redefine the operators in way that makes b_{ij} diagonal, yielding

$$\langle \mathcal{O}_i(x)\mathcal{O}_j(y)\rangle = \frac{\delta_{ij}}{|x-y|^{2\Delta_i}}\,, \qquad (\Delta_i = \Delta_j). \tag{1.49}$$

Three-point functions of scalar primaries are also fixed by conformal symmetry, up to a multiplicative constant [64]:

$$\langle \mathcal{O}_1(x_1)\mathcal{O}_2(x_2)\mathcal{O}_3(x_3)\rangle = \frac{c_{123}}{|x_{12}|^{\Delta_{123}}|x_{23}|^{\Delta_{231}}|x_{13}|^{\Delta_{132}}}\,, \tag{1.50}$$

for

$$x_{ij} = x_i - x_j, \qquad \Delta_{ijk} = \Delta_i + \Delta_j - \Delta_k. \tag{1.51}$$

The proof of Eq. (1.50) is analogous to the argument used to fix the two-point function. An additional constraint comes from Bose symmetry, which requires that $\langle \mathcal{O}_1\mathcal{O}_2\mathcal{O}_3\rangle$ is invariant under exchanging any two operator insertions $\mathcal{O}_i(x_i) \leftrightarrow \mathcal{O}_j(x_j)$. Applying this to (1.50), it follows directly that c_{ijk} is symmetric in its indices i, j and k.

For $n \geqslant 4$ operator insertions, correlation functions are no longer fixed by conformal kinematics alone. This is due to the existence of *cross ratios* that are invariant under any conformal transformation. Using $n = 4$ coordinates $x_1, \ldots, x_4$, there are two such ratios:

$$u = \frac{|x_{12}|^2|x_{34}|^2}{|x_{13}|^2|x_{24}|^2}, \qquad v = \frac{|x_{14}|^2|x_{23}|^2}{|x_{13}|^2|x_{24}|^2}. \tag{1.52}$$

The most general four-point function of scalar primaries is then of the form

$$\langle \phi_1(x_1)\phi_2(x_2)\phi_3(x_3)\phi_4(x_4)\rangle = \left(\frac{|x_{24}|}{|x_{14}|}\right)^{\Delta_{12}} \left(\frac{|x_{14}|}{|x_{13}|}\right)^{\Delta_{34}} \frac{\mathcal{G}_{1234}(u,v)}{|x_{12}|^{\Delta_1+\Delta_2}|x_{34}|^{\Delta_3+\Delta_4}} \tag{1.53}$$

where $\mathcal{G}_{1234}(u,v)$ is an arbitrary function of u and v and $\Delta_{ij} = \Delta_i - \Delta_j$.

Not all functions $\mathcal{G}_{ijkl}(u,v)$ are allowed in the four-point function (1.53): we have not yet considered the constraints coming from Bose symmetry. First, let us remark that all permutations of the points $\{x_1, x_2, x_3, x_4\}$ are generated by $x_1 \leftrightarrow x_2$, $x_3 \leftrightarrow x_4$ and $x_1 \leftrightarrow x_3$. Mathematically, this is because the permutations (12) and (12)(34)(13) = (1234) together generate all 4! permutations of four points. It is therefore sufficient to consider the constraints coming from $\phi_1(x_1) \leftrightarrow \phi_2(x_2)$, $\phi_3(x_3) \leftrightarrow \phi_4(x_4)$ and $\phi_1(x_1) \leftrightarrow \phi_3(x_3)$.

Let us now consider these three permutations separately. Under the exchange $x_1 \leftrightarrow x_2$, the cross ratios transform as $u \to u/v$ and $v \to 1/v$. From Eq. (1.53), it then follows that

$$\mathcal{G}_{2134}(u/v, 1/v) = v^{\Delta_{34}/2}\,\mathcal{G}_{1234}(u,v). \tag{1.54a}$$

Similarly, for $x_3 \leftrightarrow x_4$ and $x_1 \leftrightarrow x_3$, we find

$$\mathcal{G}_{1243}(u/v, 1/v) = v^{-\Delta_{12}/2}\,\mathcal{G}_{1234}(u,v) \tag{1.54b}$$

$$\mathcal{G}_{3214}(v,u) = u^{-(\Delta_1+\Delta_2)/2} v^{(\Delta_2+\Delta_3)/2}\,\mathcal{G}_{1234}(u,v). \tag{1.54c}$$

In general, these Bose symmetry constraints involve *different* functions $\mathcal{G}_{ijkl}(u,v)$. Let us now specialize to the correlator $\langle\phi\phi\phi\phi\rangle \sim \mathcal{G}_\phi(u,v)$ of four identical scalars. In that case, the above constraints apply to a single function $\mathcal{G}_\phi(u,v)$:

$$\mathcal{G}_\phi(u/v,1/v) = \mathcal{G}_\phi(u,v)\,, \qquad \mathcal{G}_\phi(v,u) = (v/u)^{\Delta_\phi}\,\mathcal{G}_\phi(u,v). \tag{1.55}$$

Similar relations can be found for mixed correlation functions of the form $\langle\phi_1\phi_1\phi_2\phi_2\rangle$ [9].

1.4.2 Spinning correlators

The above discussion will be slightly extended here to cover certain two- and three-point functions of primary operators with spin. The formalism required to establish these results is presented in Ref. [61].

It can be shown that two-point functions of primaries with different spin or conformal dimension vanish: this generalizes the selection rule found above for scalar primaries. Explicitly, the two-point function of a tensor primary $\mathcal{O}_{\mu_1\cdots\mu_\ell}$ of spin ℓ and dimension Δ is

$$\langle\mathcal{O}_{\mu_1\cdots\mu_\ell}(x)\mathcal{O}_{\nu_1\cdots\nu_\ell}(0)\rangle = \frac{1}{|x|^{2\Delta}}\left[\mathcal{I}_{\mu_1\nu_1}(x)\cdots\mathcal{I}_{\mu_\ell\nu_\ell}(x) + \text{symm.} - \text{traces}\right] \tag{1.56}$$

where $\mathcal{I}_{\mu\nu}(x) = \delta_{\mu\nu} - 2x_\mu x_\nu/x^2$ was introduced in Eq. (1.8). The notation '+symm. − traces' means that both the μ- and ν-indices must be symmetrized and made traceless.

Three-point functions of operators with spin require extra attention. In the case of scalar (primary) three-point functions, only one x-dependent structure was consistent with conformal invariance. This is not true in general: when the operators $\mathcal{O}_i, \mathcal{O}_j, \mathcal{O}_k$ are in different $SO(d)$ representations, the correlator $\langle\mathcal{O}_i\mathcal{O}_j\mathcal{O}_k\rangle$ can also vanish or be a sum of different conformally covariant tensor structures. Constructing these correlators is non-trivial, see e.g. [65–68].

The situation simplifies if two out of the three operators (say $\mathcal{O}_i$ and $\mathcal{O}_j$) are scalars. In that case, it follows from conformal invariance that $\langle\mathcal{O}_i\mathcal{O}_j\mathcal{O}_k\rangle$ can only be non-vanishing if $\mathcal{O}_k$ is a spin-ℓ TST. Such scalar-scalar-spin ℓ correlators are of the form [14]

$$\langle\phi_1(x_1)\phi_2(x_2)\mathcal{O}_{\mu_1\cdots\mu_\ell}(x_3)\rangle = f_{\phi_1\phi_2\mathcal{O}}\,\frac{Z_{\mu_1}\cdots Z_{\mu_\ell} - \text{traces}}{|x_{12}|^{\Delta_{123}+\ell}|x_{23}|^{\Delta_{231}-\ell}|x_{13}|^{\Delta_{132}-\ell}} \tag{1.57}$$

where $f_{\phi_i\phi_j\mathcal{O}}$ is a constant and

$$Z^\mu = \frac{x_{13}^\mu}{|x_{13}|^2} - \frac{x_{23}^\mu}{|x_{23}|^2}. \tag{1.58}$$

For the scalar three-point function, we used Bose symmetry to argue that the coefficient c_{ijk} must be symmetric under exchanging any two indices. For the scalar-scalar-spin ℓ correlator (1.57), a similar argument shows that

$$f_{\phi_2\phi_1\mathcal{O}} = (-1)^\ell\, f_{\phi_1\phi_2\mathcal{O}}. \tag{1.59}$$

This immediately implies that the correlator $\langle\phi\phi\mathcal{O}\rangle$ of two identical scalars ϕ and a spin-ℓ tensor operator $\mathcal{O}$ vanishes if ℓ is odd.

1.4.3 Example: free scalar boson

One CFT that will be studied extensively in this thesis is the free, massless scalar field, which is described by the Euclidean action

$$S[\phi] = \frac{1}{2}\int \mathrm{d}^d x\, (\partial_\mu \phi)^2 \tag{1.60}$$

and satisfies the equation of motion $\partial^2\phi(x) = 0$. Correlation functions in this theory can be defined by a path integral [69]:

$$\langle \phi_1(x_1)\cdots\phi_n(x_n)\rangle = \int [\mathrm{d}\phi]\, \phi_1(x_1)\cdots\phi_n(x_n)\, e^{-S[\phi]}\,, \tag{1.61}$$

where the measure $\int[\mathrm{d}\phi]$ is normalized such that $\langle \mathbb{1}\rangle = 1$. In particular, the two-point function of ϕ is given by

$$\langle\phi(x)\phi(0)\rangle = \frac{1}{(d-2)\mathrm{S}_d}\frac{1}{|x|^{d-2}}\,, \qquad \mathrm{S}_d = \frac{2\pi^{d/2}}{\Gamma(d/2)} = \mathrm{Vol}(S^{d-1}). \tag{1.62}$$

It is customary to redefine $\phi \to \sqrt{(d-2)\mathrm{S}_d}\,\phi$, after which the two-point function becomes unit-normalized:

$$\langle\phi(x)\phi(0)\rangle = \frac{1}{|x|^{d-2}}. \tag{1.63}$$

We recall that the path integral (1.61) for the free theory is Gaussian, and correlation functions of $n > 2$ fields are given by Wick's theorem. A particular consequence is that odd correlation functions vanish, consistent with the $\mathbb{Z}_2$ symmetry $\phi \to -\phi$ of the action.

We remark that the action (1.60) is manifestly invariant under a dilatation $x \to \lambda x$, provided that ϕ has scaling dimension $\nu \equiv (d-2)/2$. In section 1.5 we will prove a stronger statement, namely that the theory is conformally invariant. An immediate consequence is that ϕ transforms as a scalar primary of dimension $[\phi] = \nu$, consistent with (1.63). A non-trivial check of conformal invariance is provided by the four-point function, which can be computed using Wick's theorem:

$$\langle\phi(x_1)\phi(x_2)\phi(x_3)\phi(x_4)\rangle = \frac{\mathcal{G}_\phi(u,v)}{|x_{12}|^{2\nu}|x_{34}|^{2\nu}}, \qquad \mathcal{G}_\phi(u,v) = 1 + u^\nu + (u/v)^\nu. \tag{1.64}$$

This correlator has the functional form required by Eq. (1.53). Additionally, it may be checked that $\mathcal{G}_\phi(u,v)$ obeys the Bose symmetry constraints from Eq. (1.55).

Wick's theorem also determines correlation functions involving composite operators. As an exercise, it may e.g. be shown that the composite operator [5] $\mathcal{O}_2 = :\phi^2:/\sqrt{2}$ is a scalar

5. The notation $:X:$ denotes normal ordering. Concretely, it means that no Wick contractions between fields in X are allowed.

primary of dimension $[\mathcal{O}_2] = 2\nu$, and that it satisfies

$$\langle \mathcal{O}_2(x)\mathcal{O}_2(0)\rangle = \frac{1}{|x|^{4\nu}}\,, \qquad \langle \phi(x_1)\phi(x_2)\mathcal{O}_2(0)\rangle = \frac{\sqrt{2}}{|x_1|^{2\nu}|x_2|^{2\nu}}\,. \tag{1.65}$$

1.5 Weyl invariance

So far, we have restricted ourselves to study conformal field theories defined on flat space. In the next sections, we will need to put CFTs (and deformations thereof) on curved spaces. Formally, such a theory is described by a Euclidean action $S[\phi; g_{\mu\nu}]$ that is a functional of a set of fields $\phi_I(x)$ and the metric $g_{\mu\nu}(x)$, turned on as a background field. Such a theory is *Weyl invariant* if it is invariant under the rescaling of the metric

$$g_{\mu\nu}(x) \;\to\; g'_{\mu\nu}(x) = \Omega(x)^2\, g_{\mu\nu}(x) \tag{1.66}$$

and the simultaneous rescaling of the ϕ_I:

$$\phi_I(x) \;\to\; \phi'_I(x) = \Omega(x)^{-\eta_I}\, \phi_I(x)\,. \tag{1.67}$$

Note that the Weyl rescaling (1.66) leaves the coordinates x^μ unchanged.

Weyl invariance reduces to conformal invariance in flat space, as defined in section 1.1. To see why this is true, consider a conformal transformation $x \to x'$ with scale factor $\Omega(x)$. We can implement such a transformation in two steps: first, we perform as Weyl rescaling, which changes the metric as

$$\delta_{\mu\nu} \;\to\; g'_{\mu\nu}(x) = \Omega(x)^2\, \delta_{\mu\nu} \tag{1.68}$$

and rescales (primary) operators according to (1.67). Next, we perform a coordinate change $x \to x'$. This changes the metric $g'_{\mu\nu}(x)$ back to the Euclidean metric $\delta_{\mu\nu}$. The fields ϕ_I transform under this diffeomorphism according to their spin:

$$\phi(x) \;\mapsto\; \phi'(x') = \phi(x)\,, \qquad V_\mu(x) \;\mapsto\; V'_\mu(x') = \frac{\partial x^\nu}{\partial x'^\mu} V_\nu(x) \tag{1.69}$$

and similarly for operators of spin $\ell > 1$. Under the combined Weyl rescaling and subsequent coordinate change, operators therefore transform as

$$\begin{aligned} \phi(x) \;&\mapsto\; \phi'(x') = \Omega(x)^{-\eta_\phi}\, \phi(x)\,, \\ V_\mu(x) \;&\mapsto\; V'_\mu(x') = \Omega(x)^{-\eta_V}\, \frac{\partial x^\nu}{\partial x'^\mu} V_\nu(x) \end{aligned} \tag{1.70}$$

etc., in agreement with the transformation law for primary operators from Eq. (1.39).

Weyl invariance can be rephrased in terms of the stress tensor $T_{\mu\nu}$, which is defined as the linear response of the theory to an arbitrary change in the metric:

$$S[g_{\mu\nu} + \delta g_{\mu\nu}] - S[g_{\mu\nu}] = \frac{1}{2}\int \sqrt{g}\, \mathrm{d}^d x\, T^{\mu\nu}(x)\delta g_{\mu\nu}(x) + \mathrm{O}(\delta g^2). \tag{1.71}$$

An infinitesimal Weyl rescaling induces a change in the metric of the form $\delta g_{\mu\nu}(x) = \rho(x) g_{\mu\nu}(x)$ for a some function $\rho(x)$, hence Weyl invariance requires that $T^{\mu}{}_{\mu} \equiv 0$. [6]

The discussion so far has been classical. Weyl symmetry however extends to correlation functions [46]. This is useful when doing computations in *conformally flat* backgrounds, which are flat up to a Weyl rescaling:

$$\mathrm{d}s^2 = \Omega^2(x)\, \delta_{\mu\nu} \mathrm{d}x^{\mu} \mathrm{d}x^{\nu}. \tag{1.72}$$

Correlation functions $\langle \cdots \rangle_{\Omega}$ on such backgrounds are related to flat-space correlation functions by Weyl invariance: if $\mathcal{O}(x)$ is for example a scalar primary of dimension Δ, then [7]

$$\langle \mathcal{O}(x_1) \cdots \rangle_{\Omega} = \Omega(x_1)^{-\Delta} \langle \mathcal{O}(x_1) \cdots \rangle_{\text{flat}} \,. \tag{1.73}$$

Example computations involving the d-sphere S^d (which is conformally flat in stereographic coordinates) are given in Refs. [75–78].

1.5.1 The free boson revisited

Let us now come back to the theory of the free, massless scalar field. Rather than proving that the flat-space theory is conformally invariant, we will show that the theory can be coupled to curvature in a way that makes it Weyl invariant. The flat-space action (1.60) can be made diffeomorphism invariant as follows:

$$S[\phi; g_{\mu\nu}] = \frac{1}{2} \int \sqrt{g}\, \mathrm{d}^d x\, g^{\mu\nu} \partial_{\mu}\phi \partial_{\nu}\phi. \tag{1.74}$$

The stress tensor of the theory (1.74) is (in the flat-space limit) given by

$$T_{\mu\nu} = -\partial_{\mu}\phi\partial_{\nu}\phi + \frac{1}{2}\delta_{\mu\nu} (\partial_{\lambda}\phi)^2 \quad \Rightarrow \quad T^{\mu}{}_{\mu} = \frac{d-2}{2} (\partial_{\lambda}\phi)^2 \,, \tag{1.75}$$

hence it fails to be traceless in $d \neq 2$. Consequently, the theory described by Eq. (1.74) is not Weyl invariant. The same conclusion can also be reached by a direct computation.

The minimally coupled theory (1.74) is however far from general: any local operator can be coupled to the curvature invariants $\mathcal{R}$ (Ricci scalar), $\mathcal{R}_{\mu\nu}$ (Ricci tensor) etc., all of which vanish in the flat-space limit. We can therefore write the Ansatz

$$S[\phi; g_{\mu\nu}] \stackrel{?}{=} \frac{1}{2} \int \sqrt{g}\, \mathrm{d}^d x \left[g^{\mu\nu} \partial_{\mu}\phi\partial_{\nu}\phi + \lambda \mathcal{R}\phi + \kappa \mathcal{R}\phi^2 + \ldots \right] \tag{1.76}$$

for a set of undetermined constants $\{\lambda, \kappa, \ldots\}$. A rather obvious constraint on these curvature terms is that they must preserve the global $\mathbb{Z}_2$ symmetry $\phi \to -\phi$; the term $\mathcal{R}\phi$ is therefore

6. In certain cases, a stress tensor with non-vanishing trace can be improved, see e.g. [2, 70].

7. An exception to this transformation law is the Weyl anomaly [71–74, 46], which implies that $\langle T_{\mu\nu}(x) \rangle_{\Omega}$ is in general non-zero on curved backgrounds in even d, although $\langle T_{\mu\nu} \rangle$ vanishes in flat space.

not allowed. A second constraint comes from imposing that physics at distances much shorter than the typical radius of curvature ρ of the metric must agree with flat-space physics. This means that only terms that are relevant (in the RG sense) may be written down. The scaling dimensions of the invariants $\mathcal{R}, \mathcal{R}_{\mu\nu}, \ldots$ can be determined by power counting: the Ricci scalar $\mathcal{R} \sim 1/\rho^2$ e.g. has dimension $[\mathcal{R}] = 2$. With some additional work, it may be shown that $\mathcal{R}\phi^2$ is the only possible curvature term that satisfies this criterion.

We therefore expect that the theory

$$S[\phi; g_{\mu\nu}] = \frac{1}{2}\int \sqrt{g}\,\mathrm{d}^d x\,\left[g^{\mu\nu}\partial_\mu\phi\partial_\nu\phi + \kappa\mathcal{R}\phi^2\right] \tag{1.77}$$

is Weyl invariant, at least for a judicious choice of κ. Adding the $\mathcal{R}\phi^2$ term modifies the stress tensor as follows:

$$T_{\mu\nu} \;\to\; T_{\mu\nu} + \kappa\,(\partial_\mu\partial_\nu - \delta_{\mu\nu}\partial^2)\phi^2 \tag{1.78}$$

in the flat-space limit [8] [73]. Consequently, the stress tensor becomes traceless if we set

$$\kappa \;\to\; \kappa_c \equiv \frac{d-2}{4(d-1)}\,. \tag{1.79}$$

Alternatively, after integration by parts and discarding a boundary term, the action (1.77) can be rewritten as

$$S[\phi; g_{\mu\nu}] = \frac{1}{2}\int \sqrt{g}\,\mathrm{d}^d x\,\phi(x)\,\widetilde{\Delta}[\kappa]\,\phi(x)\,, \qquad \widetilde{\Delta}[\kappa] \equiv -g^{\mu\nu}\nabla_\mu\nabla_\nu + \kappa\mathcal{R}. \tag{1.80}$$

If $\kappa = \kappa_c$, the differential operator $\widetilde{\Delta}[\kappa]$ transforms under a Weyl rescaling as [71]

$$\widetilde{\Delta}[\kappa_c] \;\mapsto\; \Omega(x)^{-(d+2)/2}\,\widetilde{\Delta}[\kappa_c]\,\Omega(x)^{(d-2)/2}\,, \tag{1.81}$$

which also proves that the action with $\kappa = \kappa_c$ is Weyl invariant.

1.6 Radial quantization

At this stage, we can define a quantization procedure that applies to any CFT, called *radial quantization*, which goes back to Fubini, Hanson and Jackiw [79]. This scheme sets the CFT in question on the 'cylinder' $\mathbb{R} \times S^{d-1}$, where the sphere S^{d-1} has radius R. For $d = 2$ this geometry is really a cylinder; we employ the same name for $d > 2$. The cylinder is naturally parametrized by coordinates $(t, \mathbf{n})$ where $t \in \mathbb{R}$ is a time coordinate and $\mathbf{n}^\mu$ is a unit vector on S^{d-1}, cf. figure 1.1.

Crucially, the cylinder is conformally flat [80]. In terms of the $(t, \mathbf{n})$ coordinates, the metric is given by

$$\mathrm{d}s^2_{\mathrm{cyl}} = \mathrm{d}t^2 + R^2\mathrm{d}\Omega \tag{1.82}$$

8. This means that $\mathcal{R}$ and $\mathcal{R}_{\mu\nu}$ have been set to zero.

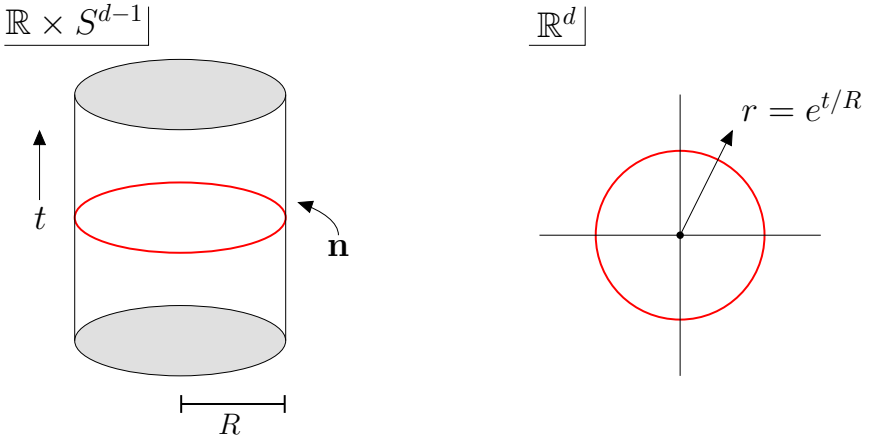

Figure 1.1: Left: the cylinder $\mathbb{R} \times S^{d-1}$ with time t running upwards. The red timeslice is isomorphic to S^{d-1} and parametrized by a unit vector $\mathbf{n}$. Right: the same geometry, mapped to flat space.

where $\mathrm{d}\Omega$ is the canonical metric on S^{d-1}. Let us now define a new 'radial' coordinate r through $t = R \ln r$, in terms of which the metric is given by

$$\mathrm{d}s^2_{\mathrm{cyl}} = \left(\frac{R}{r}\right)^2 \left[\mathrm{d}r^2 + r^2 \mathrm{d}\Omega\right] . \tag{1.83}$$

The factor inside brackets is obviously the flat-space metric on $\mathbb{R}^d$, written in radial coordinates $(r, \mathbf{n})$. Eq. (1.83) proves that the cylinder is conformally flat, with the Weyl factor given by $\Omega(r) = R/r$. Explicitly, the map between flat space and the cylinder is given by

$$x^\mu(t, \mathbf{n}) = e^{t/R}\, \mathbf{n}^\mu . \tag{1.84}$$

In principle, CFT correlation functions on the cylinder can be worked out using Weyl invariance (1.73). A dimension-Δ scalar transforms for example as [21, 59]

$$\langle \mathcal{O}(t, \mathbf{n}) \cdots \rangle_{\mathrm{cyl}} = \frac{e^{\Delta t/R}}{R^\Delta} \langle \mathcal{O}(x = e^{t/R}\, \mathbf{n}) \cdots \rangle_{\mathrm{flat}} . \tag{1.85}$$

The reader will remark that a time translation $t \to t + \tau$ on the cylinder has the same effect as rescaling $r \to e^{\tau/R}\, r$. Alternatively, the dilatation operator D displaces points along the time direction of the cylinder:

$$D = ix \cdot \frac{\partial}{\partial x} \to iR \frac{\partial}{\partial t} . \tag{1.86}$$

This observation can be used to quantize CFTs on the cylinder. As a starting point, we postulate the existence of a ground state $|0\rangle$, that by conformal invariance must satisfy

$$P_\mu |0\rangle = K_\mu |0\rangle = M_{\mu\nu} |0\rangle = D|0\rangle = 0 . \tag{1.87}$$

In the next section, we will construct the Hilbert space of the CFT. Abstractly, we can already learn something about quantum mechanics on the cylinder. In the Schrödinger

picture (on the Euclidean cylinder), states $|\psi(t)\rangle$ should evolve as

$$\frac{\partial}{\partial t}|\psi(t)\rangle = -H|\psi(t)\rangle\,, \tag{1.88}$$

hence we should identify the Hamiltonian H with the dilatation operator: [9]

$$H = iD/R. \tag{1.89}$$

Notice that the factor of $1/R$ gives H dimensions of energy, as befits a Hamiltonian; the factor of i is needed to make H self-adjoint. When dealing with local operators, it is more convenient to use the Heisenberg picture, in which any operator $\mathcal{A}$ evolves as

$$\mathcal{A}(t) = e^{Ht}\,\mathcal{A}(t=0)\,e^{-Ht}. \tag{1.90}$$

Physically, we can think of e^{-Ht} as a transfer matrix that acts on timeslices S^{d-1}. This is consistent with the fact that we are working on the Euclidean cylinder: on the Minkowski cylinder (with time coordinate $t \to it$), time evolution of operators is unitary.

1.6.1 State-operator correspondence

With the basic framework of radial quantization in place, we will now construct a complete basis of states on the cylinder. First, we remark that the $SO(d)$ generators $M_{\mu\nu}$ commute with H: the Hilbert space can therefore be organized according to two quantum numbers, energy E and spin j.

How can we define states $|E, j\rangle$ that fit this label? The key idea is to define states by inserting local operators at the origin:

$$\mathcal{O}_i(x) \;\mapsto\; |\mathcal{O}_i\rangle \equiv \lim_{x\to 0}\mathcal{O}_i(x)|0\rangle. \tag{1.91}$$

The quantum numbers of these states can easily be computed using the commutators (1.35). If $\mathcal{O}(x)$ is for example a primary of dimension $[\mathcal{O}] = \Delta$, then its energy is Δ/R:

$$\begin{aligned} H|\mathcal{O}\rangle &= [H, \mathcal{O}(0)]|0\rangle + \mathcal{O}(0)H|0\rangle \\ &= \Delta/R\,|\mathcal{O}\rangle \end{aligned} \tag{1.92a}$$

9. In local CFTs, this can be further motivated via Noether's procedure. The dilatation current in flat space is $j_\mu(x) = T_{\mu\nu}x^\nu$, hence dilatations around the origin are generated by [81, 79]

$$\int_{|x|=\text{cst.}} \mathrm{d}\sigma^\mu\, j_\mu(x)\,, \qquad \mathrm{d}\sigma^\mu = |x|^{d-2}x^\mu \mathrm{d}\mathbf{n}\,.$$

The dilatation current maps to the cylinder as $|x|^{d-2}x^\mu j_\mu(x)_{\text{flat}} = R^d\, T_{tt}(t,\mathbf{n})_{\text{cyl}}$ for $t = R\ln|x|$. In cylinder coordinates, the above dilatation charge therefore maps to

$$R\int_{S^{d-1}} T_{tt}(t,\mathbf{n})\, R^{d-1}\mathrm{d}\mathbf{n}$$

which is a familiar expression for the Hamiltonian (up to a factor of R).

where we use that $H|0\rangle \propto D|0\rangle = 0$. Similarly,

$$K_\mu|\mathcal{O}\rangle = 0\,, \tag{1.92b}$$

$$M_{\mu\nu}|\mathcal{O}\rangle = \mathcal{S}_{\mu\nu}|\mathcal{O}\rangle\,. \tag{1.92c}$$

How about descendants of the primary $\mathcal{O}$? If we insert the operator

$$\partial_\mu \mathcal{O}(x) = i[P_\mu, \mathcal{O}(x)] \tag{1.93}$$

at the origin, we obtain

$$|\partial_\mu \mathcal{O}\rangle \equiv \lim_{x\to 0} \partial_\mu \mathcal{O}(x)|0\rangle = i[P_\mu, \mathcal{O}(0)]|0\rangle = iP_\mu|\mathcal{O}\rangle. \tag{1.94}$$

This can be iterated: the state

$$P_{\mu_1}\cdots P_{\mu_n}|\mathcal{O}\rangle = (-i)^n \lim_{x\to 0} \partial_{\mu_1}\cdots\partial_{\mu_n}\mathcal{O}(x)|0\rangle \tag{1.95}$$

corresponds to a level-n descendant of $\mathcal{O}$ inserted at $x = 0$. Using the commutation relation $[H, P_\mu] = R^{-1}P_\mu$, it is easy to see that the above state has energy $(\Delta + n)/R$.

Let $\mathcal{H}$ be the vector space defined by inserting all local operators $\mathcal{O}_i$ at the origin. It may now be shown that any state $|\Psi\rangle$ is included in $\mathcal{H}$, hence $\mathcal{H}$ describes the full Hilbert space of the CFT. This property of CFTs is known as the *state-operator correspondence*; for details of the proof, we refer to [53].

1.6.2 Adjoint states and matrix elements

Although we have constructed a basis of states $|\mathcal{O}_i\rangle$, no inner product $\langle\mathcal{O}_i|\mathcal{O}_j\rangle$ has yet been specified. The goal of the current section is to define the adjoint $\langle\psi|$ to any state $|\psi\rangle$. As a starting point, we remark from Eq. (1.90) that formally the adjoint of any Heisenberg operator $\mathcal{A}(t)$ is given by

$$[\mathcal{A}(t)]^\dagger = e^{-Ht}\,\mathcal{A}^\dagger(t=0)\,e^{Ht}\,, \tag{1.96}$$

using the fact that H is self-adjoint. If $\mathcal{A} = \mathcal{A}(t=0)$ is self-adjoint, the above equation implies that $[\mathcal{A}(t)]^\dagger = \mathcal{A}(-t)$. This may look confusing, but analytically continuing to Minkowski space (with time $t' = -it$) gives back the usual rule for hermitian operators: $[\mathcal{A}(t')]^\dagger = \mathcal{A}(t')$.

Using the operator-state correspondence, this Euclidean adjoint is all we need to completely define the map $|\psi\rangle \mapsto \langle\psi|$. Recall that a basis of the Hilbert space is given by states $|\mathcal{O}_i\rangle$ that correspond to local operators:

$$|\mathcal{O}\rangle = \lim_{x\to 0} \mathcal{O}(x)|0\rangle\,. \tag{1.97}$$

The adjoint $\langle\mathcal{O}|$ to such a state can in principle be computed as

$$\langle\mathcal{O}| = \lim_{x\to 0}\langle 0|[\mathcal{O}(x)]^\dagger\,. \tag{1.98}$$

To make this concrete, let us specialize to the case where $\mathcal{O}$ is a scalar primary with $[\mathcal{O}] = \Delta$. To compute $[\mathcal{O}(x)]^\dagger$, we can map $\mathcal{O}$ to the cylinder and back, using (1.85) twice. The result is

$$[\mathcal{O}(x)]^\dagger = |x|^{-\Delta}[\mathcal{O}(t,\mathbf{n})]^\dagger = |x|^{-\Delta}\mathcal{O}(-t,\mathbf{n}) = |x|^{-2\Delta}\mathcal{O}(x')\,, \qquad x'^\mu = x^\mu/x^2. \tag{1.99}$$

The above formula has a simple interpretation: the time reflection $(t,\mathbf{n}) \mapsto (-t,\mathbf{n})$ maps the corresponding point $x = e^{t/R}\,\mathbf{n}$ in flat space to the inverted point $x' = e^{-t/R}\,\mathbf{n} = x/|x|^2$. Consequently, the adjoint state $\langle\mathcal{O}|$ is given by

$$\langle\mathcal{O}| = \lim_{x\to 0}|x|^{-2\Delta}\langle 0|\mathcal{O}(x') = \lim_{w\to\infty}|w|^{2\Delta}\langle 0|\mathcal{O}(w). \tag{1.100}$$

Similar formulas exists for adjoints of states with nonzero spin.

Without proof, we mention that the generators P_μ and K_μ are conjugate to one another [21]:

$$K_\mu^\dagger = P_\mu\,, \qquad P_\mu^\dagger = K_\mu\,. \tag{1.101}$$

This means that the adjoint to a descendant state

$$|\chi\rangle = P_{\mu_1}\cdots P_{\mu_j}|\mathcal{O}\rangle \tag{1.102}$$

is given by

$$\langle\chi| = \langle\mathcal{O}|K_{\mu_1}\cdots K_{\mu_j}\,. \tag{1.103}$$

Since any non-primary state is a descendant, the above rules completely define an inner product $\langle\Phi|\Psi\rangle$ in radial quantization. If all states have a positive norm with respect to this inner product, a theory is said to be *reflection positive*: this provides a natural generalization of unitarity on the Minkowski cylinder.

We will treat two examples to show how the above formalism can be used to compute actual matrix elements. First, we consider a set of scalar primaries $\{\mathcal{O}_i\}$ of identical scaling dimension Δ. If the two-point functions $\langle\mathcal{O}_i\mathcal{O}_j\rangle$ are given by

$$\langle\mathcal{O}_i(x)\mathcal{O}_j(y)\rangle = \frac{a_{ij}}{|x-y|^{2\Delta}} \tag{1.104}$$

then the matrix elements $\langle\mathcal{O}_i|\mathcal{O}_j\rangle$ are given by

$$\langle\mathcal{O}_i|\mathcal{O}_j\rangle = \lim_{\substack{x\to 0\\ y\to 0}}|x|^{-2\Delta}\langle[\mathcal{O}_i(x)]^\dagger\mathcal{O}_j(y)\rangle = \lim_{\substack{y\to 0\\ w\to\infty}}|w|^{2\Delta}\frac{a_{ij}}{|w-y|^{2\Delta}} = a_{ij}\,. \tag{1.105}$$

The matrix a_{ij} therefore must be positive definite in a unitary theory; this proves an assertion made in section 1.4.

As a second example, we consider a matrix element $\langle \mathcal{O}_i | \mathcal{O}_j(x) | \mathcal{O}_k \rangle$ involving three scalar primaries. Using the three-point function (1.50), the matrix element in question evaluates to

$$\langle \mathcal{O}_i | \mathcal{O}_j(x) | \mathcal{O}_k \rangle = \lim_{\substack{w \to \infty \\ y \to 0}} |w|^{2\Delta_i} \langle \mathcal{O}_i(w) \mathcal{O}_j(x) \mathcal{O}_k(y) \rangle = \frac{c_{ijk}}{|x|^{\Delta_j + \Delta_k - \Delta_i}}. \tag{1.106}$$

1.6.3 Unitarity constraints on CFTs

Above, we defined an inner product on the Hilbert space of a CFT. It turns out that there exists an easy criterion that determines whether this inner product is unitary. Roughly speaking, unitarity requires that all primary states $|\mathcal{O}_i\rangle$ and all descendant states $P_{\mu_1} \cdots P_{\mu_j} |\mathcal{O}_i\rangle$ have a positive norm. [10] These norms can be computed using the conformal algebra (1.15): therefore they depend on the scaling dimension Δ and the $SO(d)$ quantum numbers of the primary $\mathcal{O}_i$.

Through this argument, sufficient conditions for unitarity can be formulated as lower bounds on scaling dimensions of primary operators, depending on the $SO(d)$ representation of the primary in question. The precise bounds for scalar and spin-ℓ primaries are [60, 82]

$$\begin{aligned} \ell = 0: &\qquad \Delta \geqslant (d-2)/2 \quad \text{or} \quad \Delta = 0, \\ \ell > 0: &\qquad \Delta \geqslant \ell + d - 2. \end{aligned} \tag{1.107}$$

These bounds are all saturated in known theories: $\Delta = 0$ is the dimension of the unit operator, and $\Delta = (d-2)/2$ is the dimension of the free scalar field. Similarly, spin-ℓ conserved currents automatically have dimension $\Delta = \ell + d - 2$; such currents are easily constructed in free theories. The converse holds too: a spin-ℓ operator with a dimension saturating the unitary bound (1.107) is automatically conserved, and a scalar of dimension $\Delta = (d-2)/2$ has trivial correlation functions [83, 84].

Unitarity also puts constraints on three-point function coefficients. If $\mathcal{O}_i, \mathcal{O}_j, \mathcal{O}_k$ are three hermitian scalar primaries, then it follows from Eq. (1.106) that

$$c_{ijk} = \langle \mathcal{O}_i | \mathcal{O}_j(x) | \mathcal{O}_k \rangle = \overline{\langle \mathcal{O}_k | \mathcal{O}_j(x) | \mathcal{O}_i \rangle} = \overline{c_{kji}}\,, \tag{1.108}$$

provided that $|x| = 1$. Because c_{ijk} is symmetric in its indices, it follows that c_{ijk} is real. This result extends to scalar-scalar-spin ℓ correlation functions (see [14] for a careful proof).

10. We use the fact that in a unitary CFT, there exists an orthonormal basis of primary operators, obeying $\langle \mathcal{O}_i | \mathcal{O}_j \rangle = \delta_{ij}$. Consequently, descendants of different primaries do not overlap. If such a basis does not exist, there are necessarily null or negative-norm states present.

1.7 Operator product expansion

We now turn our attention to a useful property of CFTs, known as the *operator product expansion* (OPE). The OPE entails that the product of any two (primary) operators $\mathcal{O}_1(x_1)\mathcal{O}_2(x_2)$ admits a short-distance expansion in the limit $x_2 \to x_1$:

$$\mathcal{O}_1(x_1)\mathcal{O}_2(x_2) = \sum_{\mathcal{O}_k \text{ primary}} \mathcal{F}_{12k}(x_{12}, \partial_2)\, \mathcal{O}_k(x_2)\,, \tag{1.109}$$

where the sum runs over all primary operators $\mathcal{O}_k$ in the theory and $\mathcal{F}_{12k}$ is a (for now undetermined) differential operator. For simplicity, all $SO(d)$ indices are suppressed in this equation.

The above OPE (1.109) $\mathcal{O}_1 \times \mathcal{O}_2$ must be understood as a relation between correlation functions:

$$\langle X\mathcal{O}_1(x_1)\mathcal{O}_2(x_2)\rangle = \sum_{\mathcal{O}_k \text{ primary}} \mathcal{F}_{12k}(x_{12}, \partial_2)\, \langle X\mathcal{O}_k(x_2)\rangle \tag{1.110}$$

where $X = \mathcal{O}_{j_1}(y_1)\cdots\mathcal{O}_{j_n}(y_n)$ is a string of other operators. We will briefly argue *why* this relation is valid.[11] Let us suppose that the points x_1 and x_2 are 'close together', in the sense that there exists a sphere $\mathscr{S}$ separating the points $\{x_1, x_2\}$ from $\{y_1, \ldots, y_n\}$ in the correlation function (1.110). We can then apply radial quantization around the center w of $\mathscr{S}$, inserting a complete basis of states $\mathbb{1} = \sum_n |n\rangle\langle n|$ at the surface $\mathscr{S}$:

$$\langle 0|X\mathcal{O}_1(x_1)\mathcal{O}_2(x_2)|0\rangle = \sum_n \langle 0|X|n\rangle\langle n|\mathcal{O}_1(x_1)\mathcal{O}_2(x_2)|0\rangle. \tag{1.111}$$

By the state-operator correspondence, the states $|n\rangle$ correspond to operators $\mathcal{O}$ inserted at w; we can therefore write the above as

$$\sum_{\text{all operators } \mathcal{O}} f_{\mathcal{O}}(x_{12})\, \langle X\mathcal{O}(w)\rangle, \qquad f_{\mathcal{O}}(x_{12}) = \langle \mathcal{O}|\mathcal{O}_1(x_1)\mathcal{O}_2(x_2)|0\rangle. \tag{1.112}$$

To get this formula in the desired form (1.110), we separate the contributions from primaries and descendants in the above sum and resum the descendants. This way, we can rewrite the above formula as

$$\sum_{\mathcal{O}_k \text{ primary}} \widetilde{\mathcal{F}}_k(x_{12}, \partial_w)\, \langle X\mathcal{O}_k(w)\rangle. \tag{1.113}$$

As a final step, we need shift the exchanged operator $\mathcal{O}_k(w)$ to the point x_2. This is done by expanding $\mathcal{O}_k(w) = \mathcal{O}_k(x_2) + (w - x_2)^\mu \partial_\mu\, \mathcal{O}_k(x_2) + \ldots$, which changes the precise form of $\widetilde{\mathcal{F}}_k$. By a trivial rewriting, we obtain the desired result (1.110).

The above argument gives a sharp condition for the OPE to hold, namely the existence of a sphere that separates x_1, x_2 from all other operator insertions y_j. With some additional

11. A much more complete treatment is given in Ref. [21].

work, it may be shown that the OPE is *convergent*, even at finite $x_1 - x_2$; we refer to [85, 86, 21] for more details.

The differential operators $\mathcal{F}_{ijk}(x_{12}, \partial_2)$ appearing in (1.109) are fixed by conformal invariance, as we will discuss now. The crucial idea is that the OPE $\mathcal{O}_i \times \mathcal{O}_j \sim \mathcal{O}_k$ is in one-to-one correspondence with the three-point function $\langle \mathcal{O}_k(y)\mathcal{O}_i(x_1)\mathcal{O}_j(x_2)\rangle$ [61, 62]. For simplicity, let us assume that all three operators are scalars. We can always translate $x_2 \to 0$ and relabel $x_1 \to x$. Recall that the three-point function is restricted by conformal invariance to the form (1.50)

$$\mathcal{J}(x,y) \equiv \langle \mathcal{O}_k(y)\mathcal{O}_i(x)\mathcal{O}_j(0)\rangle = \frac{c_{ijk}}{|x|^{\Delta_{ijk}}|y|^{\Delta_{jki}}|x-y|^{\Delta_{ikj}}} \tag{1.114}$$

writing $\Delta_{abc} \equiv \Delta_a + \Delta_b - \Delta_c$ as before. In the domain $|x| < |y|$, the product $\mathcal{O}_i(x)\mathcal{O}_j(0)$ can be expanded using the OPE:

$$\begin{aligned}\mathcal{J}(x,y) &= \lim_{\epsilon\to 0} \sum_{\mathcal{O}_{k'} \text{ primary}} \mathcal{F}_{ijk'}(x,\partial_\epsilon)\,\langle \mathcal{O}_k(y)\mathcal{O}_{k'}(\epsilon)\rangle \\ &= \lim_{\epsilon\to 0} \mathcal{F}_{ijk}(x,\partial_\epsilon)\,\langle \mathcal{O}_k(y)\mathcal{O}_k(\epsilon)\rangle \\ &= \lim_{\epsilon\to 0} \mathcal{F}_{ijk}(x,\partial_\epsilon)\,\frac{1}{|y-\epsilon|^{2\Delta_k}}\,.\end{aligned} \tag{1.115}$$

To pass from the first to the second line, we assume that all primaries are orthogonal, so only the term with $k' = k$ contributes to the sum. In order to fix $\mathcal{F}_{ijk}$, we simply notice that the OPE (1.115) must reproduce the correlator (1.114). It is now easy to establish that $\mathcal{F}_{ijk}(x,\partial)$ has the following properties:

— $\mathcal{F}_{ijk}$ is proportional to c_{ijk};

— by rotation invariance, $\mathcal{F}_{ijk}(x,\partial)$ can only depend on $|x|$, $x\cdot\partial$ and ∂^2;

— under a dilatation $x \to \lambda x$, $\mathcal{F}_{ijk}$ scales as

$$\mathcal{F}_{ijk}(\lambda x, \lambda^{-1}\partial) = \lambda^{-\Delta_{ijk}}\mathcal{F}_{ijk}(x,\partial)\,. \tag{1.116}$$

We deduce that $\mathcal{F}_{ijk}$ is of the following form:

$$\mathcal{F}_{ijk}(x,\partial) = \frac{c_{ijk}}{|x|^{\Delta_{ijk}}} \sum_{m,n=0}^{\infty} \beta_{mn}(x\cdot\partial)^m (x^2\partial^2)^n\,. \tag{1.117}$$

The precise coefficients β_{mn} above are determined by matching (1.115) to a Taylor expansion of the correlator (1.114) around $x = 0$. Up to terms of order x^3, we have for example [12]

$$\begin{aligned}\mathcal{F}_{ijk}(x,\partial) = \frac{c_{ijk}}{|x|^{\Delta_{ijk}}}\Bigg[1 + \frac{\Delta_k+\Delta_{ij}}{2\Delta_k}x\cdot\partial + \frac{(\Delta_k+\Delta_{ij})(\Delta_k+\Delta_{ij}+2)}{8\Delta_k(\Delta_k+1)}(x\cdot\partial)^2 \\ - \frac{\Delta_k^2-\Delta_{ij}^2}{16\Delta_k(\Delta_k+1)(\Delta_k-\nu)}x^2\partial^2 + \mathrm{O}(|x|^3)\Bigg].\end{aligned} \tag{1.118}$$

12. For completeness, we remark that explicit expressions for the differential operators $\mathcal{F}$ are known in some cases [17–19, 15], but they are not required in the rest of this thesis.

It is straightforward to show that the coefficients β_{mn} depend on the 'external' dimensions Δ_i and Δ_j only through their difference $\Delta_{ij} = \Delta_i - \Delta_j$. Because the coefficient c_{ijk} controls the leading OPE behaviour as $x \to 0$, they are also known as *OPE coefficients*.

Having established the relation between the OPE and three-point functions, it is easy to see which primaries $\mathcal{O}_k$ contribute a particular OPE $\mathcal{O}_i \times \mathcal{O}_j$. In this thesis, we will only be interested in the case where $\mathcal{O}_i$ and $\mathcal{O}_j$ are both scalars. Recall from section 1.4 that only traceless symmetric tensor operators can have a nonvanishing three-point function with two scalars. Consequently, only TSTs (and not other $SO(d)$ representations) appear in a scalar-scalar OPE $\mathcal{O}_1 \times \mathcal{O}_2$. Moreover, if both scalars are identical ($\mathcal{O}_1 = \mathcal{O}_2$), then only tensor operators of even spin appear (cf. the argument at the end of section 1.4).

1.7.1 Conformal block decomposition

Let us now consider a correlation function of four identical scalars φ, which is of the form (cf. Sec. 1.4)

$$\langle \varphi(x_1)\varphi(x_2)\varphi(x_3)\varphi(x_4)\rangle = \frac{\mathcal{G}(u,v)}{|x_{12}|^{2\eta}|x_{34}|^{2\eta}}, \qquad \eta = [\varphi] \tag{1.119}$$

for some function $\mathcal{G}(u,v)$ that only depends on the cross-ratios u and v. It turns out that $\mathcal{G}(u,v)$ is completely determined by the OPE, and therefore the three-point functions of the theory. To prove this, we apply the OPE *twice* to the correlator (1.119), both to the operator product $\varphi(x_1)\varphi(x_2)$ and to $\varphi(x_3)\varphi(x_4)$. The question where these OPEs converge will be postponed until the next section. Schematically, this double OPE can be expressed as a double sum over all primary TST operators in the theory:

$$\langle \varphi(x_1)\varphi(x_2)\varphi(x_3)\varphi(x_4)\rangle = \sum_{\substack{\mathcal{O}_i,\mathcal{O}_j \\ \text{primary TST}}} \mathcal{F}_{\varphi\varphi i}(x_{12},\partial_2)\,\mathcal{F}_{\varphi\varphi j}(x_{34},\partial_4)\,\langle \mathcal{O}_i(x_2)\mathcal{O}_j(x_4)\rangle. \tag{1.120}$$

Working in a theory where the two-point functions are diagonal, Eq. (1.120) collapses to a single sum:

$$\langle \varphi(x_1)\varphi(x_2)\varphi(x_3)\varphi(x_4)\rangle = \sum_{\mathcal{O}\text{ prim. TST}} (c_{\varphi\varphi\mathcal{O}})^2\,\mathcal{W}_{\mathcal{O}}(x_1,x_2,x_3,x_4). \tag{1.121}$$

where we have extracted the OPE coefficients $c_{\varphi\varphi\mathcal{O}}$ from the differential operators $\mathcal{F}_{\phi\phi\mathcal{O}}$. The function $\mathcal{W}_{\mathcal{O}}$ resums the contribution of the primary $\mathcal{O}$ and its descendants to the correlator $\langle\varphi\varphi\varphi\varphi\rangle$. It may be shown [87] that $\mathcal{W}_{\mathcal{O}}$ has the same transformation properties under conformal transformations as the four-point function $\langle\varphi(x_1)\phi(x_2)\phi(x_3)\varphi(x_4)\rangle$, meaning that it can be written as

$$\mathcal{W}_{\mathcal{O}}(x_1,x_2,x_3,x_4) = \frac{1}{|x_{12}|^{2\eta}|x_{34}|^{2\eta}}\,G_{\mathcal{O}}(u,v) \tag{1.122}$$

for some function $G_{\mathcal{O}}(u,v)$ that only depends on u and v. Such a function is called a *conformal block* or a *conformal partial wave*, and it encodes the contribution of a primary $\mathcal{O}$

and its descendants to the function $\mathcal{G}(u,v)$ appearing in the correlator (1.119):

$$\mathcal{G}(u,v) = \sum_{\mathcal{O} \text{ prim. TST}} (c_{\varphi\varphi\mathcal{O}})^2 \, G_{\mathcal{O}}(u,v) \tag{1.123}$$

as follows from Eq. (1.122). This is the desired result: we have shown that the *a priori* arbitrary function $\mathcal{G}(u,v)$ is completely fixed by conformal invariance, and that it depends only on the OPE coefficients c_{ijk} of the theory.

The x-dependence of $\mathcal{G}(u,v)$ is completely encoded by the conformal blocks $G_{\mathcal{O}}(u,v)$ appearing in Eq. (1.123). Notice that these functions are *universal*, in the sense that depend on the dimension and spin of $\mathcal{O}$, but not on any details of the CFT under consideration.

For completeness, we note the conformal block decomposition (1.123) applies to all CFT four-point functions, not just those of identical scalars. In the case of four non-identical scalars, we have

$$\langle \phi_1(x_1)\phi_2(x_2)\phi_3(x_3)\phi_4(x_4)\rangle \sim \mathcal{G}_{1234}(u,v)\,, \quad \mathcal{G}_{1234}(u,v) = \sum_{\mathcal{O} \text{ prim. TST}} c_{12\mathcal{O}}c_{34\mathcal{O}} \, G_{\mathcal{O}}(u,v)\,. \tag{1.124}$$

The general case differs from the decomposition (1.123) in two ways: first, operators of any spin $\ell \geqslant 0$ are summed over here, whereas only even spins contribute to the correlator of identical scalars (cf. the discussion in section 1.7). Second, in the general case the conformal blocks $G_{\mathcal{O}}(u,v)$ depend not only on the dimension and spin of $\mathcal{O}$, but also on the external dimensions Δ_{12} and Δ_{34}. The same applies to four-point functions of non-scalar operators; the situation there is however significantly more complicated, see e.g. [87, 66, 88, 89].

Domain of convergence

We have yet to analyze the domain of convergence of the conformal block decomposition (1.122). In what follows, we use a particular sequence of conformal transformations to pass from a general configuration of the points $\{x_1, x_2, x_3, x_4\} \in \mathbb{R}^d$ to a specific configuration that depends on a single complex parameter, greatly simplifying the 'kinematics' of the problem.

First, the point x_4 can be moved to infinity using an SCT, and a subsequent translation puts x_1 at the origin. The points $\{x_1, x_2, x_3\}$ then span a plane that passes through the origin, which after a rotation can be made to align with the (12)-plane. We parametrize the latter by a complex coordinate $\zeta = x^1 + ix^2$. By a combined dilatation and rotation in the ζ-plane, x_3 can be moved to the point $\zeta = 1$, which leaves $x_2 \equiv z$ as the only free parameter. In this special configuration, the points x_i are thus given by

$$x_1 = 0, \quad x_2 = z, \quad x_3 = 1, \quad x_4 = \infty\,. \tag{1.125}$$

This configuration of points is shown in Fig. 1.2. In the kinematics of Eq. (1.125), the cross

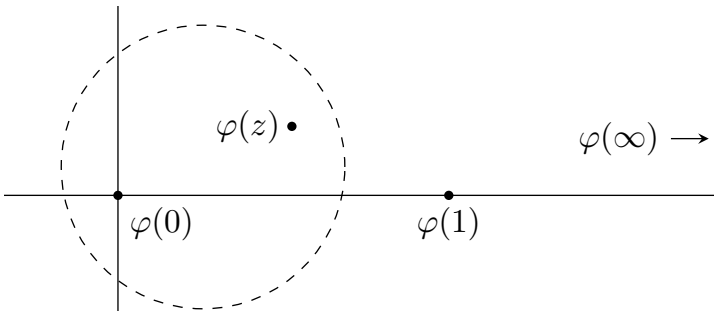

Figure 1.2: Configuration described from (1.125) in the (12) plane. Dashed: example of a circle separating $\{0, z\}$ from $\{1, \infty\}$.

ratios are given by

$$u = z\bar{z}, \quad v = (1-z)(1-\bar{z}), \qquad \bar{z} = z^*. \tag{1.126}$$

In two dimensions, the above kinematics are well-known; in $d > 2$ dimensions, the parametrization of the cross ratios was first used by Dolan and Osborn [15].

It is now straightforward to see when the conformal block decomposition is valid. For the OPE $\varphi(0) \times \varphi(z)$ to converge, the points $\{0, z\}$ must be separated from the points $\{1, \infty\}$ by a circle in the z-plane. Such a circle exists for all z outside of the half-line $[1, \infty)$. No additional condition comes from imposing convergence of the $\varphi(1) \times \varphi(\infty)$ OPE.

We therefore expect the conformal blocks $G_{\mathcal{O}}(z, \bar{z})$ to be smooth, real-valued functions everywhere on the domain $z \in \mathbb{C} \setminus [1, \infty)$. It is instructive to compare this prediction to closed-form expressions for conformal blocks in two [19, 90] and four [15, 16] dimensions. [13] These expressions make use of the hypergeometric function ${}_2F_1(a, b; c; z)$:

$${}_2F_1(a, b; c; z) = \sum_{n=0}^{\infty} \frac{(a)_n (b)_n}{(c)_n} \frac{z^n}{n!}\,. \tag{1.127}$$

The coefficients of ${}_2F_1(a, b; c; z)$ are written in terms of the Pochhammer symbol

$$(x)_n \equiv \frac{\Gamma(x+n)}{\Gamma(x)} = x(x+1)\cdots(x+n-1)\,, \qquad n \in \mathbb{N}\,. \tag{1.128}$$

The series (1.127) converges absolutely on the unit disk [14] but has a branch cut starting at $z = 1$. Away from the branch cut $[1, \infty)$ on the real axis, the hypergeometric function can be analytically continued (see e.g. sections 2.1.3 and 2.1.4 of Ref. [92]). Using the shorthand notation

$$k_\beta(z) = z^{\beta/2}\, {}_2F_1\big(\tfrac{1}{2}(\beta - \Delta_{12}), \tfrac{1}{2}(\beta + \Delta_{34}); \beta; z\big)\,, \tag{1.129}$$

the conformal block $G_{\Delta,\ell}$ for an operator of spin ℓ and dimension Δ is then

$$G_{\Delta,\ell}(z, \bar{z}) = k_{\Delta+\ell}(z) k_{\Delta-\ell}(\bar{z}) + (z \leftrightarrow \bar{z}) \tag{1.130a}$$

13. Many details and references concerning the two-dimensional case can be found in Ref. [91].

14. On the circle $|z| = 1$, the series (1.127) converges absolutely if $\Re(a + b - c) < 0$, it converges conditionally (away from $z = 1$) if $0 \leqslant \Re(a + b - c) < 1$, and it diverges on $|z| = 1$ otherwise [92].

in $d = 2$, and

$$G_{\Delta,\ell}(z,\bar{z}) = \frac{z\bar{z}}{z-\bar{z}}\left[k_{\Delta+\ell}(z)k_{\Delta-\ell-2}(\bar{z}) - (z \leftrightarrow \bar{z})\right] \tag{1.130b}$$

in $d = 4$. The analytic structure of the 2d and 4d conformal blocks is therefore the same as the analytic structure of the hypergeometrics, apart from $z = 0$ where they behave as $G_{\Delta,\ell} \sim (z\bar{z})^{\Delta/2}$.

1.7.2 Conformal bootstrap

We can use the conformal block decomposition from the previous section to revisit the relations (1.54) expressing the constraints coming from Bose symmetry (in this context also known as *crossing symmetry*) on the functions $\mathcal{G}_{1234}(u,v)$. Symmetry under the exchange $\phi_1(x_1) \leftrightarrow \phi_3(x_3)$ for example required that

$$v^{(\Delta_2+\Delta_3)/2}\,\mathcal{G}_{1234}(u,v) = u^{(\Delta_1+\Delta_2)/2}\,\mathcal{G}_{3214}(v,u). \tag{1.131}$$

To use a conformal block decomposition, we want to apply the OPE on both sides of this equation simultaneously. On the LHS, this requires that both OPEs (12) and (34) exist, while on the RHS we require the (23) and (14) OPEs. Suppose for now that these conditions are all satisfied for suitable values of u and v. In that case, Eq. (1.131) can be expanded as a sum over all primaries $\mathcal{O}$ in the theory:

$$\begin{aligned} v^{(\Delta_2+\Delta_3)/2} \sum_{\mathcal{O}=(\Delta,\ell)} c_{12\mathcal{O}}c_{34\mathcal{O}}\,G_{\Delta,\ell}(u,v;\Delta_{12},\Delta_{34}) \\ = u^{(\Delta_1+\Delta_2)/2} \sum_{\mathcal{O}=(\Delta,\ell)} c_{32\mathcal{O}}c_{14\mathcal{O}}\,G_{\Delta,\ell}(v,u;-\Delta_{23},\Delta_{14})\,, \end{aligned} \tag{1.132}$$

where we have made the dependence of the conformal blocks on the external dimensions Δ_i explicit. This equation involves both the *spectrum* of a CFT (the set of primary operators $\mathcal{O}_{\Delta,\ell}$) and its OPE coefficients c_{ijk}. As such, it will form a non-trivial consistency requirement on the CFT data $\{\mathcal{O}_{\Delta,\ell}, c_{ijk}\}$. Equations as (1.133) that follow from crossing symmetry are known as *bootstrap equations* [10–12].

Notice that for every four-point function $\langle\mathcal{O}_1\mathcal{O}_2\mathcal{O}_3\mathcal{O}_4\rangle$ in a given CFT, an equation of the form (1.133) may be written down. It seems very ambitious to attack this full system of equations at once. In what follows, we will therefore focus on a single correlator of four identical fields φ of dimension $[\phi] = \eta$, in which case crossing symmetry requires that

$$v^\eta \sum_{\mathcal{O}=(\Delta,\ell)} \lambda_{\mathcal{O}}\,G_{\Delta,\ell}(u,v) = u^\eta \sum_{\mathcal{O}=(\Delta,\ell)} \lambda_{\mathcal{O}}\,G_{\Delta,\ell}(v,u)\,, \qquad \lambda_{\mathcal{O}} = (c_{\varphi\varphi\mathcal{O}})^2\,. \tag{1.133}$$

We have yet to discuss the domain of validity of the crossing equation (1.133); as before, we wil do so using the z-coordinate. Recall from the previous section that the (12) $\to$ (34)

OPE converges away from the branch cut $[1,\infty)$. The exchange $x_1 \leftrightarrow x_3$ is equivalent to exchanging $z \to 1-z$; the two OPEs in the (23) $\to$ (14) channel therefore converge if z is outside of the interval $(-\infty, 0]$. In summary, the bootstrap equation (1.133) is well-defined for every z in the domain

$$\mathbb{C} \setminus (-\infty, 0] \cup [1, \infty)\,. \tag{1.134}$$

To solve the crossing symmetry equation (1.133), explicit expressions for the conformal blocks are needed. Recall from the previous section that conformal blocks in the (12) $\to$ (34) channel converge absolutely inside the unit disk $|z| < 1$. The conformal blocks in the (14) $\to$ (23) channel are obtained by replacing $z \to 1-z$, and thus converge absolutely on the disk $|z-1| < 1$. Without analytically continuing the conformal blocks, the crossing symmetry equation (1.133) is therefore valid inside the domain $\max\{|z|, |z-1|\} < 1$.

Notice now that the point $z = 1/2$ plays a special role with respect to crossing symmetry: it is the only point left invariant by the exchange $x_1 \leftrightarrow x_3$. Starting with Ref. [14], it has become customary to study the bootstrap equation (1.133) in a neighborhood of this point. To be precise, the authors of Ref. [14] Taylor expand the bootstrap equation around $z = \bar{z} = 1/2$, keeping only a finite number of derivatives in the real and imaginary directions. This derivative expansion has radius of convergence $1/2$, due to the singularities at $z = 0, 1$. We schematically draw the various domains of convergence in Fig. 1.3.

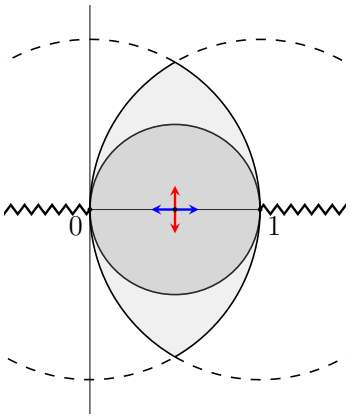

Figure 1.3: Light shaded area: domain of convergence of the conformal blocks in the z-plane. Dark shaded area: domain of convergence of the series expansion around $z = 1/2$. Zigzag lines: branch cuts of the conformal blocks. The arrows indicate how the Taylor expansion around $z = 1/2$ must be understood.

The Taylor expansion reduces the crossing symmetry equation to a system of N linear equations, where N is the total number of derivatives that is taken into account. After fixing a spectrum $\{\mathcal{O}_{\Delta,\ell}\}$, these equations involve the squared OPE coefficients $\lambda_{\mathcal{O}} = (c_{\varphi\varphi\mathcal{O}})^2$ as unknown parameters. Generically, such a system is easy to solve, as long as sufficiently many primary operators are added (such that the system is underdetermined). Unitary however

implies that $c_{\varphi\varphi\mathcal{O}}$ is real, meaning that $\lambda_{\mathcal{O}}$ is positive; this requirement makes the linear system much less trivial to solve. Using unitarity, it turns out that only certain spectra $\{\mathcal{O}_{\Delta,\ell}\}$ are consistent with crossing symmetry: if the $\varphi \times \varphi$ OPE is schematically given by

$$\varphi \times \varphi \sim \mathbb{1} + \varphi' + \left(\text{scalars of dimension} > [\varphi']\right) + \text{non-scalar primaries}\,, \tag{1.135}$$

then it can e.g. be shown that $[\varphi']$ is bounded from above [14].

In practice, different linear programming methods are used to either solve the crossing equation or to rule out a possible solution, depending on the spectrum $\{\mathcal{O}_{\Delta,\ell}\}$. It is outside the scope of this thesis to explain the methods used in any detail: we refer the reader to the papers [93–99, 7, 100–104, 9, 105–114] to understand the various numerical methods that are currently in use. [15]

All of these methods have in common that they require as input derivatives of conformal blocks $G_{\Delta,\ell}(z,\bar{z})$ for arbitrary values of Δ and ℓ, evaluated that the point $z = 1/2$:

$$(\partial/\partial z)^m\,(\partial/\partial\bar{z})^n\,G_{\Delta,\ell}(z,\bar{z})\Big|_{z=1/2}. \tag{1.136}$$

The method described above specializes to the point $z = 1/2$, although it may very well be possible that future applications of the bootstrap focus on different points z_0. For $d = 2$ and $d = 4$ dimensions, the closed-form expressions (1.130) may be used to compute these derivatives, but for odd (or even noninteger) d, no simple strategy is known to find the above derivatives. This problem will be dealt with in much detail in chapters 2 and 3.

1.8 Casimir differential equations

We conclude this introductory chapter by reviewing a method proposed by Dolan and Osborn in Ref. [16] to compute conformal blocks. [16] For concreteness, we focus on the correlator $\langle\varphi(x_1)\varphi(x_2)\varphi(x_3)\varphi(x_4)\rangle$ of four identical scalars, and we assume that the operators $\varphi(x_1)\cdots\varphi(x_4)$ are radially ordered. Eventually, we are interested in finding a differential equation that governs a conformal partial wave $G_{\mathcal{O}}(u,v)$ appearing in partial wave expansion of $\langle\varphi\varphi\varphi\varphi\rangle$.

Let us first focus on the function $W_{\mathcal{O}}(x_1,x_2,x_3,x_4)$, defined in Eq. (1.121). To single out the contribution of $W_{\mathcal{O}}$, we use the projection operator

$$\sum_{|n\rangle\in\mathcal{B}} |n\rangle\langle n| \tag{1.137}$$

15. See also Refs. [115, 116] for an approach to the bootstrap that is not manifestly based on unitarity.
16. For other discussions of this method, we refer to [14, 66, 49].

where $\mathcal{B}$ is an orthonormal basis of the span of $|\mathcal{O}\rangle$ and its descendants $P_\mu|\mathcal{O}\rangle$, $P^2|\mathcal{O}\rangle$, et cetera. We then have

$$W_{\mathcal{O}}(x_1,x_2,x_3,x_4) = \frac{1}{(c_{\varphi\varphi\mathcal{O}})^2}\sum_{|n\rangle\in\mathcal{B}}\langle 0|\varphi(x_1)\varphi(x_2)|n\rangle\langle n|\varphi(x_3)\varphi(x_4)|0\rangle \tag{1.138}$$

after dividing by the OPE coefficients $c_{\varphi\varphi\mathcal{O}}$ to get the correct normalization from Eq. (1.121). Next, we recall that the conformal generators L_{AB} act as first-order differential operators $\mathcal{L}_{AB}$ on the fields $\varphi(x_i)$:

$$[L_{AB},\varphi(x_i)] \equiv \mathcal{L}^{(i)}_{AB}\,\varphi(x_i) \tag{1.139}$$

The explicit form of the $\mathcal{L}_{AB}$ is derived in Eq. (1.35), but will not be needed for the rest of this argument. In particular, the linear combination $\mathcal{L}^{(1)}_{AB}+\mathcal{L}^{(2)}_{AB}$ 'passes through' the product $\varphi(x_1)\varphi(x_2)$ in the matrix element $\langle 0|\varphi(x_1)\varphi(x_2)|n\rangle$:

$$\begin{aligned}\left(\mathcal{L}^{(1)}_{AB}+\mathcal{L}^{(2)}_{AB}\right)\langle 0|\varphi(x_1)\varphi(x_2)|n\rangle &= \langle 0|[L_{AB},\varphi(x_1)\varphi(x_2)]|n\rangle \\ &= -\langle 0|\varphi(x_1)\varphi(x_2)L_{AB}|n\rangle.\end{aligned} \tag{1.140}$$

In passing from the first to the second line, we used that $\langle 0|L_{AB}=0$ by conformal invariance. The above trick holds for every term when acting on (1.138), hence

$$\left(\mathcal{L}^{(1)}_{AB}+\mathcal{L}^{(2)}_{AB}\right)W_{\mathcal{O}} = -\frac{1}{(c_{\varphi\varphi\mathcal{O}})^2}\sum_{|n\rangle\in\mathcal{B}}\langle 0|\varphi(x_1)\varphi(x_2)L_{AB}|n\rangle\langle n|\varphi(x_3)\varphi(x_4)|0\rangle. \tag{1.141}$$

Let us now define the second-order differential operator

$$\mathcal{E}_{12} = \frac{1}{2}\left(\mathcal{L}^{(1)}_{AB}+\mathcal{L}^{(2)}_{AB}\right)\left(\mathcal{L}^{(1),AB}+\mathcal{L}^{(2),AB}\right) \tag{1.142}$$

that acts on x_1 and x_2.[17] From the above reasoning, acting with $\mathcal{E}_{12}$ on the function $W_{\mathcal{O}}$ is equivalent to acting with the quadratic Casimir $\mathscr{C}_2$ on the intermediate states $|n\rangle$:

$$\mathcal{E}_{12}\,W_{\mathcal{O}}(x_1,x_2,x_3,x_4) = \frac{1}{(c_{\varphi\varphi\mathcal{O}})^2}\sum_{|n\rangle\in\mathcal{B}}\langle 0|\varphi(x_1)\varphi(x_2)\mathscr{C}_2|n\rangle\langle n|\varphi(x_3)\varphi(x_4)|0\rangle. \tag{1.143}$$

This sum can be computed term by term in n. Let us focus on the primary state $|\mathcal{O}\rangle$ first. If $\mathcal{O}$ has dimension Δ and spin ℓ, then $|\mathcal{O}\rangle$ is an eigenstate of the quadratic Casimir:

$$\mathscr{C}_2|\mathcal{O}\rangle = c^{(2)}_{\Delta,\ell}|\mathcal{O}\rangle\,, \qquad c^{(2)}_{\Delta,\ell} = \Delta(\Delta-d)+\ell(\ell+d-2)\,. \tag{1.144}$$

The eigenvalue $c^{(2)}_{\Delta,\ell}$ can be computed explicitly from Eq. (1.20), using the observation that $K_\mu|\mathcal{O}\rangle$ vanishes. The second term in $c^{(2)}_{\Delta,\ell}$ comes from the $SO(d)$ Casimir $\mathcal{C}_2$ that was computed in Eq. (1.41). Next, we remark that the Casimir $\mathscr{C}_2$ has the same eigenvalue acting on a descendant state $|n\rangle \neq |\mathcal{O}\rangle$: this follows from the fact that $\mathscr{C}_2$ commutes with P_μ. Consequently, the function $\mathcal{W}_{\mathcal{O}}(x_1,x_2,x_3,x_4)$ obeys a second-order partial differential equation [20, 87]:

$$\left[\mathcal{E}_{12}-c^{(2)}_{\Delta,\ell}\right]\mathcal{W}_{\mathcal{O}}(x_1,x_2,x_3,x_4) = 0\,. \tag{1.145}$$

17. The indices on $\mathcal{L}^{(i)}_{AB}$ are to be raised according to the Minkowski metric on $SO(d+1,1)$, cf. section (1.2).

Finally, we notice that the conformal block $G_{\Delta,\ell}(u,v)$ is by definition proportional to $\mathcal{W}_{\mathcal{O}}(x_1,x_2,x_3,x_4)$, cf. equation (1.122). The above differential equation therefore descends to one for $G_{\Delta,\ell}(u,v)$, schematically given by

$$\mathcal{D}_{u,v}\, G_{\Delta,\ell}(u,v) = c^{(2)}_{\Delta,\ell}\, G_{\Delta,\ell}(u,v)\,, \tag{1.146}$$

where $\mathcal{D}_{u,v}$ is a second-order differential operator in the coordinates u and v. An explicit formula for $\mathcal{D}_{u,v}$ is given in [16], Eq. (1.8). The equation (1.146) is called a *Casimir differential equation* for the conformal block $G_{\Delta,\ell}(u,v)$. In order to completely determine $G_{\Delta,\ell}(u,v)$, boundary conditions need to be specified, that essentially follow from the behaviour of the $\varphi(x_1)\times\varphi(x_2)\sim\mathcal{O}(x_2)$ OPE as $x_1\to x_2$ [15]. We will make these conditions precise in the next chapter.

Similarly, a fourth-order differential equation exists for $G_{\Delta,\ell}(u,v)$, obtained by acting with the quartic Casimir $\mathscr{C}_4$ (1.23):

$$\begin{aligned}\mathscr{C}_4|\mathcal{O}\rangle &= c^{(4)}_{\Delta,\ell}|\mathcal{O}\rangle\,,\\ c^{(4)}_{\Delta,\ell} &= \Delta^2(\Delta-d)^2+\tfrac{1}{2}d(d-1)\Delta(\Delta-d)\\ &\quad+\ell^2(\ell+d-2)^2+\tfrac{1}{2}(d-1)(d-4)\ell(\ell+d-2).\end{aligned} \tag{1.147}$$

Note that only terms on the first line of Eq. (1.23) contribute, because K_μ annihilates $|\mathcal{O}\rangle$. Furthermore, we have used both $SO(d)$ Casimirs (1.41). The resulting quartic Casimir differential equation is shown in Eq. (4.14) of Ref. [20].

Chapter 2

Conformal blocks in radial coordinates [1]

In chapter 1, we presented a first view at *conformal blocks*, functions of the cross-ratios u and v that encode the contribution of a primary operator to four-point functions in a conformal field theory. Because these conformal blocks play an important role in the conformal bootstrap program, the current chapter (as well as the next one) is devoted to computing them.

Little is known in general about conformal blocks. In fact, the closed-form results in $d = 2$ and $d = 4$ dimensions displayed in Eq. (1.130) are essentially the only exact expressions for spin-ℓ conformal blocks in d dimensions. [2] Early applications of the bootstrap, such as [14], were therefore limited to studying bootstrap equations in two and four dimensions. In general d, an approach to evaluating the conformal blocks and their derivatives was developed in 2012 in [7], and applied in a first bootstrap analysis of the 3d Ising model.

Nonetheless, conformal blocks remain rather mysterious special functions. The purpose of this chapter is to 'demystify' them via a concrete approach. We use an idea that is rarely used in $d > 2$ CFT but standard in the 2d CFT literature [12], namely that conformal blocks are sums of matrix elements in radial quantization; all conformal blocks together sum up to a four-point function. Recently [21], this point of view proved useful to study the convergence rate of the conformal block decomposition. Here, we develop it to its logical end.

We start in section 2.1 by showing how conformal blocks can be represented using radial quantization. The Dolan-Osborn variable z arises naturally, when placing one operator at the radial quantization origin and by mapping a second operator to infinity. The conformal blocks admit an expansion in terms of the radial coordinate $|z|$ and the angular variable

1. This chapter is a reworked version of [117], which was written in collaboration with S. Rychkov.
2. It is also possible to compute conformal blocks in $d = 6$ (or higher even d), see [16].

$\theta = \arg\, z$.

In section 2.2, we develop a different series expansion of conformal blocks in radial quantization, inserting the operators symmetrically around the origin. This geometry defines a new radial coordinate ρ, which has several advantages compared to the z-coordinate. In particular, the ρ-series expansion converges in the full domain of regularity of the conformal blocks; moreover, it has a faster converge rate.

The ρ-series has various potential applications to the conformal bootstrap program; we outline two in section 2.3. A summary of the results is given in section 2.4.

Appendix A contains a proof that coefficients appearing in the ρ-expansion are bounded.

2.1 Conformal blocks in the Dolan-Osborn coordinates

In this thesis, we will only be concerned with scalar four-point functions in the Euclidean domain, although a generalization to non-scalar four-point functions is possible. For simplicity, we discuss here the correlator of four identical scalars, which is fixed by conformal invariance

$$\langle \phi(x_1)\phi(x_2)\phi(x_3)\phi(x_4)\rangle = \frac{g(u,v)}{|x_{12}|^{2\Delta_\phi}|x_{34}|^{2\Delta_\phi}}\,, \tag{2.1}$$

where $g(u,v)$ is a function of the conformally invariant cross ratios u and v. The partial wave decomposition of this correlator takes the form:

$$g(u,v) = \sum_{\mathcal{O}} f_{\mathcal{O}}^2\, G_{\mathcal{O}}(u,v), \tag{2.2}$$

where the $G_{\mathcal{O}}(u,v)$ are the conformal blocks of the primary operators appearing in the $\phi\times\phi$ OPE and $f_{\mathcal{O}} \equiv f_{\phi\phi\mathcal{O}}$ are their OPE coefficients. We recall that in this conformal block decomposition, the only exchanged primaries are traceless symmetric tensors of even spin ℓ.[3] The function $g(u,v)$ computed from this expansion must satisfy the crossing symmetry equation

$$v^{\Delta_\phi} g(u,v) = u^{\Delta_\phi} g(v,u)\,, \tag{2.3}$$

which imposes constraints on the dimensions, spins, and OPE coefficients $f_{\mathcal{O}}$ of the exchanged operators. However, our main interest here is not in how to extract these constraints (this will be briefly discussed in section 2.3), but in the conformal blocks themselves.

Starting from the work of Dolan and Osborn [15, 16], it has become customary to express conformal blocks by changing coordinates from u, v to z and $\bar{z} \equiv z^*$:

$$u = z\bar{z}, \qquad v = (1-z)(1-\bar{z})\,. \tag{2.4}$$

3. In a four-point function of non-identical scalar operators, tensor operators of odd spin are exchanged as well.

The geometrical meaning of the new variables has been discussed in Sec. 1.7.1; we recall that it arises by assigning three points to $0, 1, \infty$ as in Fig. 2.1.

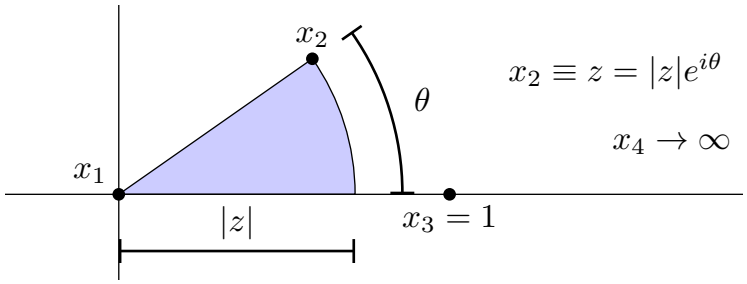

Figure 2.1: By conformal symmetry, three operators can be put at $x_1 = 0$, $x_3 = (1, 0, \ldots, 0)$, $x_4 \to \infty$, with the fourth point x_2 somewhere in the (12)-plane parametrized by the complex coordinate z.

The complex coordinate z is consistently used in $d = 2$ dimensional CFT, yet its utility for general d is not a priori obvious. Refs. [15, 16] discovered that conformal blocks in $d = 4$ and in all even dimensions take particularly simple expressions in these coordinates. We will not specify any particular dimension d for now. In fact, the conformal blocks depend analytically on d (when keeping all other data fixed), hence the crossing symmetry equation can be formally considered for all d, as was done e.g. in the context of the Wilson-Fisher theory [118]. [4]

To avoid possible misunderstanding, we should stress that although we parametrize the conformal blocks by a complex variable z, we never use complex analysis. In $d = 2$ dimensions, conformal blocks factorize as a holomorphic times antiholomorphic function [91], meaning that $G_{\mathcal{O}}(z, \bar{z}) = f(z)\widetilde{f}(\bar{z})$ for suitable functions $f, \widetilde{f}$. This property does not hold for general d; we will simply treat conformal blocks as real functions in the z-plane. In practice, we will parametrize the z-plane using the radial coordinates $|z|$ and $\theta = \arg z$.

2.1.1 Dolan-Osborn kinematics in radial quantization

To exhibit the general structure of conformal blocks in the $z, \bar{z}$ variables, we propose to use radial quantization, as introduced in section 1.6. Our goal is to express the conformal blocks $G_{\mathcal{O}}(z, \bar{z})$ in terms of matrix elements of operators on the cylinder $\mathbb{R} \times S^{d-1}$, parametrized by the coordinates $(t, \mathbf{n})$. For simplicity, we set the radius R of the cylinder to one.

The flat-space four-point function with points assigned as in Fig. 2.2 maps to the cylinder matrix element

$$\langle \phi | \phi(t_3, \mathbf{n}_3) \phi(t_2, \mathbf{n}_2) | \phi \rangle \,. \tag{2.5}$$

4. **Note added**: after the publication of this work, various other analyses of CFTs in fractional d have been undertaken [107, 110, 112].

The operators inserted at zero and infinity map to the radial quantization in- and out-states $|\phi\rangle$ and $\langle\phi|$. The other two insertions are at the cylinder times $t_2 = \log|z|$ and $t_3 = 0$. We

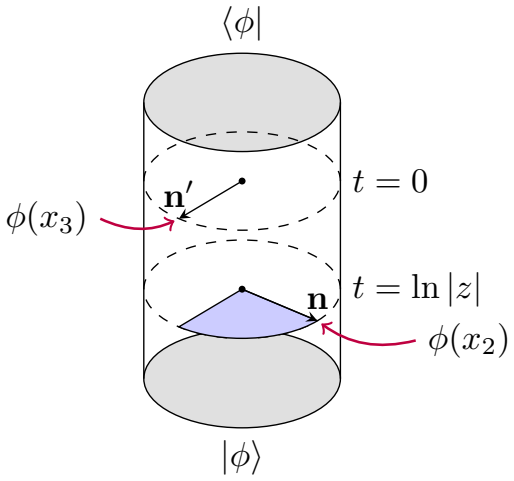

Figure 2.2: Using a Weyl transformation, the configuration in Fig. 2.1 is mapped onto a cylinder matrix element with operators inserted as shown.

keep both unit vectors $\mathbf{n}_2$ and $\mathbf{n}_3$ explicit for future use, but the only rotationally invariant parameter is their scalar product

$$\mathbf{n}_2 \cdot \mathbf{n}_3 = \cos\theta, \quad \theta = \arg z\,. \tag{2.6}$$

In order to find expressions for the conformal blocks, we first note that in the configuration with $x_1 = 0$ and $x_4 \to \infty$, the flat-space correlator can be expressed as

$$\langle\phi|\phi(x_3)\phi(x_2)|\phi\rangle = \lim_{\substack{x_1\to 0\\ w\to\infty}} |w|^{2\Delta_\phi}\langle\phi(x_1)\phi(x_2)\phi(x_3)\phi(w)\rangle = \frac{g(u,v)}{|x_2|^{2\Delta_\phi}}\,. \tag{2.7}$$

As a consequence, the function $g(u,v)$ may be rewritten as follows:

$$g(u,v) = |x_2|^{2\Delta_\phi}\langle\phi|\phi(x_3)\phi(x_2)|\phi\rangle \tag{2.8a}$$

$$= e^{t_2\Delta_\phi}\,\langle\phi|\phi(0,\mathbf{n}_3)\phi(t_2,\mathbf{n}_2)|\phi\rangle. \tag{2.8b}$$

In the second line, we have mapped the operators to the cylinder, using $t_3 = 0$ and $\phi(t_2,\mathbf{n}_2) = e^{t_2\Delta_\phi}\phi(x_2)$. The next step is to express (2.8b) by inserting a complete basis of energy eigenstates on S^{d-1}:

$$\langle\phi|\phi(0,\mathbf{n}_3)\phi(t_2,\mathbf{n}_2)|\phi\rangle = \sum_E e^{(E-\Delta_\phi)t_2}\langle\phi|\phi(0,\mathbf{n}_3)|E\rangle\langle E|\phi(0,\mathbf{n}_2)|\phi\rangle \tag{2.9}$$

where we use the Heisenberg picture on the cylinder, cf. Eq. (1.90):

$$\langle E|\phi(t_2,\mathbf{n}_2)|\phi\rangle = \langle E|e^{Ht_2}\phi(0,\mathbf{n}_2)e^{-Ht_2}|\phi\rangle = e^{t_2(E-\Delta_\phi)}\langle E|\phi(0,\mathbf{n}_2)|\phi\rangle. \tag{2.10}$$

Specializing to the Dolan-Osborn coordinates with $t_2 = \ln|z|$, we obtain

$$g(u,v) = \sum_E |z|^E \langle\phi|\phi(0,\mathbf{n}_3)|E\rangle \langle E|\phi(0,\mathbf{n}_2)|\phi\rangle, \tag{2.11}$$

after the cancellation of both factors of $e^{t_2\Delta_\phi} = |z|^{\Delta_\phi}$.

The exchanged states $|E\rangle$ on the sphere are in one-to-one correspondence with the local operators appearing in the OPE $\phi \times \phi$. For now we do not distinguish between primary and descendant states. Every state will come in a multiplet of $SO(d)$. In fact, only symmetric traceless tensor multiplets of spin $j \geqslant 0$ can couple for the considered correlator. [5] The right matrix element

$$\langle E_{\mu_1\cdots\mu_j}|\phi(0,\mathbf{n}_2)|\phi\rangle \tag{2.12}$$

must be a rank-j symmetric traceless tensor constructed out of the vector $\mathbf{n}_2$, which is fixed up to a constant:

$$\text{const.}\left(\mathbf{n}_2^{\mu_1}\mathbf{n}_2^{\mu_2}\ldots\mathbf{n}_2^{\mu_j} - \text{traces}\right). \tag{2.13}$$

Analogously, the left matrix element is fixed up to a constant, and so a general term in (2.11) will be proportional to [6]

$$(\mathbf{n}_2^{\mu_1}\mathbf{n}_2^{\mu_2}\ldots\mathbf{n}_2^{\mu_j} - \text{traces})(\mathbf{n}_3^{\mu_1}\mathbf{n}_3^{\mu_2}\ldots\mathbf{n}_3^{\mu_j} - \text{traces}) = \frac{2^j}{j!(\nu)_j}\text{Geg}_j^{(\nu)}(\mathbf{n}_2\cdot\mathbf{n}_3) \tag{2.14}$$

where $\text{Geg}_j^{(\nu)}(z)$ is a Gegenbauer polynomial. Gegenbauer polynomials are a particular class of spherical harmonics in $d = 2\nu + 2$ dimensions. In low dimensions, they reduce to familiar special functions:

$$d = 2: \qquad \lim_{\nu\to 0}\frac{j!}{(\nu)_j}\text{Geg}_j^{(\nu)}(\cos\theta) = 2\cos(j\theta), \quad (j > 0) \tag{2.15a}$$

$$d = 3: \qquad \text{Geg}_j^{(1/2)}(\cos\theta) = P_j(\cos\theta), \tag{2.15b}$$

$$d = 4: \qquad \text{Geg}_j^{(1)}(\cos\theta) = U_j(\cos\theta), \tag{2.15c}$$

where P_j is a Legendre polynomial and U_j is a Chebyshev polynomial of the second kind. We conclude that the function $g(u,v)$ appearing in the four point function (2.1) must have an expansion of the form:

$$g(u,v) = 1 + \sum p_{E,j}\,|z|^E \text{Geg}_j^{(\nu)}(\cos\theta), \qquad p_{E,j} \geqslant 0. \tag{2.16}$$

where the sum is over all local operators of dimension E and spin j appearing in the OPE $\phi \times \phi$. Although the coefficients $p_{E,j}$ are left undetermined by this argument, we do know that they must be non-negative. This is because for $\mathbf{n}_2 = \mathbf{n}_3$ the configuration in Fig. 2.2

5. One cannot construct an antisymmetric tensor out of a single vector $\mathbf{n}$, and so the corresponding matrix elements necessarily vanish.

6. This contraction formula follows from the theory of spherical harmonics and harmonic polynomials, see [37], Vol.2 Section 11.2, Lemma 1, and [119], Chapter 4.

becomes reflection-positive. The matrix elements in (2.11) are then complex conjugates of each other.

The appearance of Gegenbauer polynomials in this result is not surprising, as they already arise in the theory of angular momentum in quantum mechanics. When two spinless particles scatter through a spin-j resonance, it is well known that the amplitude is given by the Legendre polynomial of the scattering angle (see Fig. 2.3).

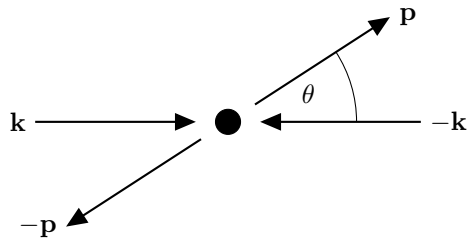

Figure 2.3: Elastic center-of-mass scattering of two scalar particles. When a spin-j resonance dominates the scattering process, the amplitude is proportional to $P_j(\cos\theta)$.

Consider now a particular primary operator $\mathcal{O}$ of dimension Δ and spin ℓ occurring in the $\phi \times \phi$ OPE. If we restrict the sum (2.16) to its conformal multiplet, it must represent the conformal block of $\mathcal{O}$. The conformal multiplet will have descendants of integer-spaced dimensions $\Delta + n$ with spins at level n taking values [7]

$$j = \ell + n, \ell + n - 2, \ldots, \max(\ell - n, \ell - n \bmod 2)\,. \tag{2.17}$$

Moreover, the coefficients $p_{E,j}$ within one conformal multiplet are not independent, since the matrix elements for the descendants will be all proportional to the basic OPE coefficient $f_{\mathcal{O}}$. We conclude that the conformal block must have the following expansion:

$$G_{\Delta,\ell}(u,v) = \sum_{n=0}^{\infty} |z|^{\Delta+n} \sum_j A_{n,j} \frac{\mathrm{Geg}_j^{(\nu)}(\cos\theta)}{\mathrm{Geg}_j^{(\nu)}(1)}\,, \qquad A_{n,j} \geqslant 0, \tag{2.18}$$

where the positive coefficients $A_{n,j}$ are some universal functions of Δ, ℓ, and d that are fixed by conformal symmetry. We normalize the total conformal block by the condition $A_{0,\ell} = 1$. [8] The Gegenbauer normalization factors

$$\mathrm{Geg}_j^{(\nu)}(1) = (2\nu)_j / j! \tag{2.19}$$

are included in (2.18) for later convenience and also to ensure a smooth $\nu \to 0$ limit for $d = 2$.

7. For short representations (e.g. those of conserved currents or a free scalar field) some of these spins will not be there.

8. This normalization relates to the one used by Dolan and Osborn in [15, 16] as $G^{\text{here}}_{\Delta,\ell} = (-2)^l (\nu)_\ell / (2\nu)_\ell G^{\text{there}}_{\Delta,\ell}$.

The formula (2.18) is the main result of this section. It should be noted that Ref. [16] already used an expansion of conformal blocks into Gegenbauer polynomials, because they turn out to form a convenient basis for solving the Casimir differential equation recursively (see the next section). Ref. [120], Eq. (78), observed that in any number of dimensions conformal blocks can be expanded in $\cos(j\,\theta)$ with positive coefficients. For $d = 2$ our result says the same, although for general d our conclusion is stronger. To obtain their result, one runs the above argument classifying states into multiplets with respect to the $SO(2)$ subgroup of $SO(d)$ acting in the (12)-plane. In particular, the Gegenbauer polynomials for any $\nu \geqslant 0$ have positive expansions in $\cos(j'\,\theta)$, $j' \leqslant j$.

The region of convergence of the expansion (2.18) will be limited to $|z| < 1$, which is the condition for the operators ϕ_2 and ϕ_3 in (2.5) to be time-ordered on the cylinder. However, the actual domain X of regularity (cf. the discussion in Sec. 1.7.1) of the conformal block as a function of z is larger; it is given by the complex plane minus the $[1, +\infty)$ cut along the real axis:

$$X = \mathbb{C} \setminus [1, +\infty)\,. \tag{2.20}$$

Everywhere in this region the blocks will be real-analytic, except at $z = 0$ because of the $|z|^{\Delta}$ factor . In section 2.2 below we will construct expansions convergent in the full region X, but first we would like to study the coefficients of the expansion (2.18).

2.1.2 Expansion coefficients from the Casimir equation

We would like to compute the coefficients $A_{n,j}$ in (2.18). In principle, this can be done following the radial quantization method to its logical end: imposing the constraints of conformal invariance in the OPE and evaluating the norms of the descendants. The example of scalar exchanged primaries and their first two descendant levels was considered in [21].

However, it is far more efficient to use the method based on Casimir differential equations, first proposed in [16] and reviewed in section 1.8. The idea is that the conformal block satisfies an eigenvalue equation of the form

$$\mathcal{D}_{u,v}\, G_{\Delta,\ell}(u,v) = c^{(2)}_{\Delta,\ell}\, G_{\Delta,\ell}(u,v), \qquad c^{(2)}_{\Delta,\ell} = \Delta(\Delta - d) + \ell(\ell + d - 2), \tag{2.21}$$

where $\mathcal{D}_{u,v}$ is a second-order partial differential operator. In the $z, \bar{z}$-coordinates, the operator $\mathcal{D}$ takes the form [16]

$$\tfrac{1}{2}\mathcal{D} = [z^2(1-z)\partial_z^2 - z^2\partial_z] + [\bar{z}^2(1-\bar{z})\partial_{\bar{z}}^2 - \bar{z}^2\partial_{\bar{z}}] + 2\nu\frac{z\bar{z}}{z-\bar{z}}\left[(1-z)\partial_z - (1-\bar{z})\partial_{\bar{z}}\right]. \tag{2.22}$$

For our purposes it will be convenient to express it in the coordinates

$$s = |z|, \quad \xi = \cos\theta = (z + \bar{z})/(2|z|)\,. \tag{2.23}$$

We find:

$$\begin{aligned}
\mathcal{D} &= \mathcal{D}_0 + \mathcal{D}_1, \\
\mathcal{D}_0 &= s^2\partial_s^2 + (2\nu+1)\left[\xi\,\partial_\xi - s\,\partial_s\right] - \left(1-\xi^2\right)\partial_\xi^2, \\
\mathcal{D}_1 &= s\left[-\xi s^2\partial_s^2 + 2\left(1-\xi^2\right)s\,\partial_s\partial_\xi - \xi s\,\partial_s - \left(2\nu+\xi^2\right)\partial_\xi + \xi\left(1-\xi^2\right)\partial_\xi^2\right].
\end{aligned} \tag{2.24}$$

The terms are grouped in such a way that $\mathcal{D}_0$ preserves homogeneity in s while $\mathcal{D}_1$ increases it by one unit.

We now apply this operator to (2.18), which we write as

$$G_{\Delta,\ell} = \sum_{n=0}^{\infty}\sum_j A_{n,j}\mathcal{P}_{\Delta+n,j}, \qquad \mathcal{P}_{E,j}(s,\xi) \equiv s^E \frac{j!}{(2\nu)_j}\mathrm{Geg}_j^{(\nu)}(\xi)\,. \tag{2.25}$$

Using the properties of Gegenbauer polynomials, it is easy to see that $\mathcal{P}_{E,j}$ are eigenfunctions of $\mathcal{D}_0$. The eigenvalue depends on the dimension and spin in the same way as the Casimir:

$$\mathcal{D}_0\,\mathcal{P}_{E,j} = c^{(2)}_{E,j}\,\mathcal{P}_{E,j}\,. \tag{2.26}$$

The $\mathcal{D}_1$ also acts simply in this basis:

$$\begin{aligned}
\mathcal{D}_1\,\mathcal{P}_{E,j} &= -\gamma^+_{E,j}\mathcal{P}_{E+1,j+1} - \gamma^-_{E,j}\mathcal{P}_{E+1,j-1}, \\
\gamma^+_{E,j} &= \frac{(E+j)^2(j+2\nu)}{2(j+\nu)}, \qquad \gamma^-_{E,j} = \frac{(E-j-2\nu)^2 j}{2(j+\nu)}.
\end{aligned} \tag{2.27}$$

Applying these formulas, equation (2.21) can be solved order by order in s. We find that the coefficients $A_{n,j}$ must satisfy the following recursion relation:

$$\left(c^{(2)}_{\Delta+n,j} - c^{(2)}_{\Delta,\ell}\right)A_{n,j} = \gamma^+_{\Delta+n-1,j-1}A_{n-1,j-1} + \gamma^-_{\Delta+n-1,j+1}A_{n-1,j+1}. \tag{2.28}$$

Starting from the initial conditions

$$A_{0,j} = \delta_{j\ell} \tag{2.29}$$

this recursion determines all coefficients $A_{n,j}$. One can check that

$$c^{(2)}_{\Delta+n,j} - c^{(2)}_{\Delta,\ell} > 0, \qquad \gamma^\pm_{E,j} \geqslant 0 \tag{2.30}$$

if Δ satisfies unitarity bounds and j is in the range (2.17). So the coefficients generated by the recursion are manifestly positive, in agreement with the previous section.

For illustration, here is what the solution at the first two levels looks like:

$$\begin{aligned}
A_{1,\ell+1}, A_{1,\ell-1} =& \frac{(\Delta+\ell)(\ell+2\nu)}{4(\ell+\nu)}, \frac{(\Delta-\ell-2\nu)\ell}{4(\ell+\nu)}\,, \\
A_{2,\ell+2}, A_{2,\ell}, A_{2,\ell-2} =& \frac{(\Delta+\ell)(\Delta+\ell+2)^2(\ell+2\nu)(\ell+2\nu+1)}{32(\Delta+\ell+1)(\ell+\nu)(\ell+\nu+1)}, \\
& \frac{(\Delta+\ell)(\Delta-\ell-2\nu)[(\Delta-\nu)\ell(\ell+2\nu)+(\Delta-2\nu)(\nu-1)]}{16(\Delta-\nu)(\ell+\nu+1)(\ell+\nu-1)}, \\
& \frac{(\Delta-\ell-2\nu)(\Delta-\ell-2\nu+2)^2\ell(\ell-1)}{32(\Delta-\ell-2\nu+1)(\ell+\nu)(\ell+\nu-1)}.
\end{aligned} \tag{2.31}$$

Notice that low spins do not require a separate treatment: only descendants with positive spin $j \geqslant 0$ may contribute to the conformal block, and indeed coefficients multiplying Gegenbauers with spin $j < 0$ (like $A_{1,\ell-1}$ for $\ell = 0$ and $A_{2,\ell-2}$ for $\ell = 0, 1$) vanish automatically. This follows from the fact that $\gamma^{-}_{E,0} = 0$ and so (2.27) makes sense also for $j = 0$.

The recursion (2.28) has been found previously by Dolan and Osborn [16], Eq. (3.12), who arrived at the ansatz (2.25) as the way to diagonalize the homogeneous part of $\mathcal{D}$. They were expanding in Jack polynomials symmetric functions in two variables $z, \bar{z}$, which are identical to our $\mathcal{P}_{E,j}$. They also give a closed-form solution of this recursion, Eq. (3.19), which is however rather complicated (it involves ${}_4F_3$). In practice, it may be faster to evaluate the coefficients directly from the recursion.

2.1.3 Decoupling of descendants for the leading twist [9]

One interesting special case where the recursion can be solved easily is for the 'leading twist' operators $\mathcal{O}$ of dimension

$$\Delta = \ell + d - 2, \qquad \ell = 0, 1, 2 \dots . \tag{2.32}$$

In this case we find that at each level, only the maximal allowed spin $j = \ell + n$ has a nonzero coefficient. At the first two levels, this can be seen happening in Eq. (2.31). For general n, this single nonzero coefficients takes the form: [10]

$$A_{n,\ell+n} = \frac{(\ell+\nu)_n (\ell+2\nu)_n}{n!(2\ell+2\nu)_n} . \tag{2.33}$$

The massive decoupling of descendants implied by this result can be understood as follows. The descendants at level n are obtained by acting with n derivatives

$$\partial_{\mu_1}\partial_{\mu_2}\dots\partial_{\mu_n}\mathcal{O} . \tag{2.34}$$

If a μ_i is contracted with an index of $\mathcal{O}$, such a state simply vanishes, because for $\ell \geqslant 1$ the dimension (2.32) is the minimal value allowed by the unitarity bound and corresponds to a conserved current. If some of the μ_i are contracted with each other, we get a state involving ∂^2 which has spin strictly less than $\ell + n$. We should show that such states decouple. Since they do not have zero norm, this can only happen via vanishing of the matrix elements in (2.11). Equivalently, this means that the following limit of the three point function should vanish:

$$\lim_{x_1\to\infty} |x_1|^{2\Delta_\phi} \langle \phi(x_1)\phi(x_2)\partial_y^2\mathcal{O}(y)\rangle = 0 . \tag{2.35}$$

9. This section is independent of the main line of reasoning and can be skipped on the first reading.
10. For $d = 3$, this result is agreement with the integral representation in [20], Eq. (6.20).

Since the three point function $\langle\phi\phi\mathcal{O}\rangle$ is known explicitly (see e.g. [15]), this is easy to check. Sending $x_1 \to \infty$, $x_2 \to 0$, the three point function becomes

$$\begin{aligned}\langle\phi|\phi(0)\mathcal{O}_{\mu_1\dots\mu_\ell}(y)\rangle &= \lambda_{\mathcal{O}}(y_{\mu_1}\cdots y_{\mu_\ell}/|y|^{d-2+2\ell} - \text{traces}) \\ &\propto \partial_{\mu_1}\cdots\partial_{\mu_\ell}\frac{1}{|y|^{d-2}}\,.\end{aligned} \tag{2.36}$$

That the second line takes care of the trace subtractions in the first line (up to a constant factor) is obvious: it gives a tensor which has the right scaling in y and is also automatically traceless (as well as conserved), due to the fact that the function $1/|y|^{d-2}$ is harmonic in d dimensions. For the same reason, this formula implies that ∂^2-descendants decouple.

We should stress that the decoupling of ∂^2-descendants at leading twist is peculiar to the kinematic configuration of Fig. 2.1. In particular, it will not happen when the points are inserted symmetrically with respect to the origin, as in the next section. This is because Eq. (2.35) is only true in the infinite x_1-limit.

2.2 Conformal blocks in the ρ coordinate

We now wish to analyze the four point function (2.1) in a different, more symmetric, configuration of operator insertions, shown in figure 2.4: specifically, we map the points x_i to

$$x_1 = -\rho, \quad x_2 = \rho, \quad x_3 = 1, \quad x_4 = -1, \qquad \rho \in \mathbb{C}\,. \tag{2.37}$$

The parameter ρ can be fixed by imposing that the above configuration is related to the z-configuration by a conformal transformation. It is easy to construct a Möbius transformation that maps the configuration of Fig. 2.1 to the ρ-kinematics, namely

$$\zeta \;\mapsto\; -\frac{(1+\rho)\zeta - 2\rho}{(1+\rho)\zeta - 2}\,, \tag{2.38}$$

which is completely fixed by imposing that $\infty \mapsto -1$, $1 \mapsto 1$ and $0 \mapsto -\rho$. If we furthermore require that $z \mapsto \rho$, we find the following relation between the z and ρ coordinates:

$$\rho = \frac{z}{(1+\sqrt{1-z})^2} \quad \Leftrightarrow \quad z = \frac{4\rho}{(1+\rho)^2}\,. \tag{2.39}$$

Alternatively, the above formula (2.39) can be found by requiring that the cross ratios u and v agree.

The ρ-coordinate was considered in [21], where it was used to give an optimal estimate for the convergence rate of the decomposition of a four point function as a sum of conformal blocks, Eq. (2.2). Here we will use ρ to analyze the blocks themselves. As discussed at the end of section 2.1, the blocks are expected to be regular in the region $z \in \mathbb{C} \setminus [1, +\infty)$. The

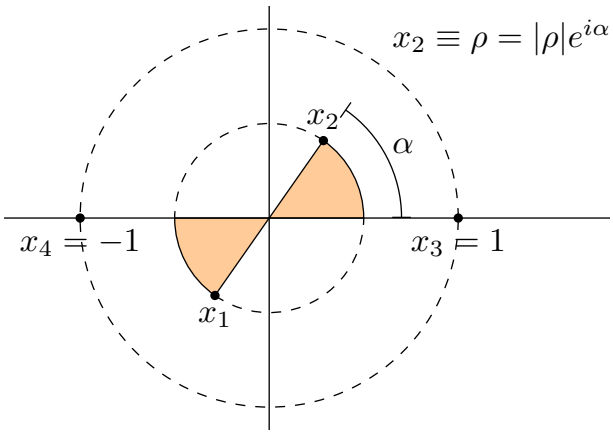

Figure 2.4: This more symmetric configuration of operation insertions can be obtained from the one in Fig. 2.1 by a global conformal transformation.

function $\rho(z)$ maps this region onto the unit disk (see Fig. 2.5).[11] This suggests that this coordinate should be particularly suitable to analyze the blocks. To begin with, conformal block representations as power series in ρ will converge for $|\rho| < 1$, which is the full region of interest. Other advantages will be discussed below.

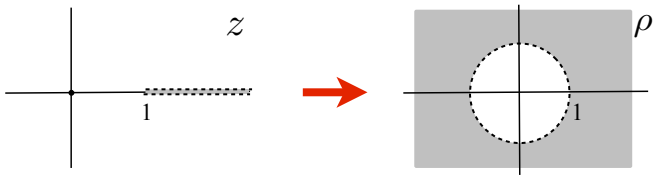

Figure 2.5: The ρ coordinate maps the regularity domain X onto the unit disk.

Fig. 2.6 shows what the configuration of Fig. 2.4 looks like after the Weyl transformation to the cylinder. This picture is similar to Fig. 2.2, however the final and initial states have a slightly different form:

$$\langle 0|\phi(0,-\mathbf{n}')\phi(0,\mathbf{n}') \quad \text{resp.} \quad \phi(t,\mathbf{n})\phi(t,-\mathbf{n})|0\rangle \quad \text{for } t = \ln|\rho|. \tag{2.40}$$

As before, the dependence on the energy of an exchanged state is given by a factor of $e^{tE} \to |\rho|^E$:

$$\langle E|\phi(t,\mathbf{n})\phi(t,-\mathbf{n})|0\rangle = |\rho|^E \langle E|\phi(0,\mathbf{n})\phi(0,-\mathbf{n})|0\rangle. \tag{2.41}$$

The argument of section 2.1 that spin-j states are encoded by Gegenbauer polynomials of $\mathbf{n}\cdot\mathbf{n}'$ also goes through unchanged, and again the configuration with $\mathbf{n}' = \mathbf{n}$ is reflection

11. The easiest way to see this is to note that the inverse function $z(\rho)$ maps any point $\rho = e^{i\alpha}$ on the unit circle $|\rho| = 1$ to

$$\rho = e^{i\alpha} \;\mapsto\; \frac{1}{\cos^2(\alpha/2)} \in [1,+\infty).$$

In particular, $\rho = -1$ corresponds to $z = \infty$.

positive.

We can therefore state the following analog of Eqs. (2.18),(2.25): conformal block of a dimension Δ, spin ℓ primary will have an expansion:

$$G_{\Delta,\ell} = \sum_{n=0}^{\infty} \sum_{j} B_{n,j} \mathcal{P}_{\Delta+n,j}(r,\eta), \qquad B_{n,j} \geqslant 0, \tag{2.42}$$

where

$$r \equiv |\rho|, \quad \eta = \cos \arg \rho \,. \tag{2.43}$$

The non-negative coefficients $B_{n,j}$ in this new expansion will of course be different from $A_{n,j}$. The spins j at level n will still be subject to the constraint (2.17). However, notice that only even spin states can be exchanged since the initial state $\phi(\rho)\phi(-\rho)|0\rangle$ is symmetric with respect to $\rho \to -\rho$.[12] We conclude that only even levels n will have nonzero $B_{n,j}$.[13] This is unlike in (2.25) where all levels have $A_{n,j} \neq 0$.

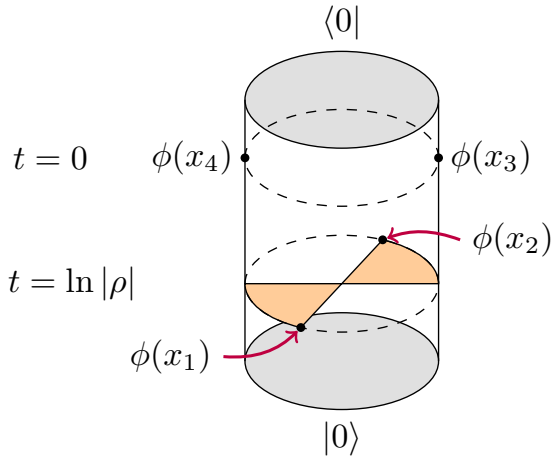

Figure 2.6: The analog of Fig. 2.2 for the new configuration.

We now turn to the problem of determining the coefficients $B_{n,j}$. The first method is to convert from the old expansion (2.25) whose coefficients $A_{n,j}$ we already know how to compute. From (2.39), the relevant variables are related by:

$$s = \frac{4r}{1+2r\eta+r^2}\,, \quad \xi = \frac{\eta(1+r^2)+2r}{1+2r\eta+r^2}\,. \tag{2.44}$$

Substituting into (2.25) and expanding the denominators, we will get a power series of the form

$$\sum_{n=0}^{\infty} r^{\Delta+n}\, Q_n(\eta), \tag{2.45}$$

12. In fact the exchange $1 \leftrightarrow 2$ corresponds to $z \to z/(z-1)$, which is equivalent to $\rho \to -\rho$.

13. In an analogous expansion for a four point function of non-identical primaries, states of all levels will be exchanged. However, if $\Delta_1 = \Delta_2$ and $\Delta_3 = \Delta_4$, then again only even levels will appear. This is even though the exchanged primary may have both even and odd spin in this case.

with $Q_n(\eta)$ certain polynomials in η. To extract $B_{n,j}$, we have to reexpand $Q_n(\eta)$ into the basis of Gegenbauers. This will give $B_{n,j}$ at level n as a linear combination of $A_{n',j'}$ for $n' \leqslant n$.

The second method is to set up an independent recursive procedure for $B_{n,j}$ based on the Casimir equation. The operator $\mathcal{D}$ in r, η coordinates takes the form:

$$\mathcal{D} = \mathcal{D}_0 + \widetilde{\mathcal{D}}, \tag{2.46}$$

where the homogeneity-preserving part $\mathcal{D}_0$ is the same as in (2.24) with $s \to r$, $\xi \to \eta$. The homogeneity-increasing part is given by

$$\widetilde{\mathcal{D}} = 4r^2 \left\{ \left[\frac{1-2\eta^2+r^2}{1+r^4-2r^2(2\eta^2-1)} - \frac{\nu}{1-r^2} \right] r\partial_r + \frac{2\eta(1-\eta^2)}{1+r^4-2r^2(2\eta^2-1)} \partial_\eta \right\}. \tag{2.47}$$

Its action in the $\mathcal{P}_{E,j}$ basis will look like

$$\widetilde{\mathcal{D}}\, \mathcal{P}_{E,j} = - \sum_{n=2,4,\ldots} \sum_{j'} \Gamma_{E,j}^{E+n,j'} \mathcal{P}_{E+n,j'} \,. \tag{2.48}$$

The series is over positive even n, since only such powers of r occur in the expansion of $\widetilde{\mathcal{D}}$.

The dependence of the Γ coefficients on j' is found with the help of the following identities involving the Gegenbauer polynomials (the radial dependence of $\mathcal{P}_{E,j}$ is not important here):

$$\begin{aligned} (2\eta^2-1)\mathcal{P}_{E,j} &= a_j^- \mathcal{P}_{E,j-2} + a_j^0 \mathcal{P}_{E,j} + a_j^+ \mathcal{P}_{E,j+2} \,, \\ 2\eta(1-\eta^2)\partial_\eta \mathcal{P}_{E,j} &= b_j^- \mathcal{P}_{E,j-2} + b_j^0 \mathcal{P}_{E,j} + b_j^+ \mathcal{P}_{E,j+2} \,, \end{aligned} \tag{2.49}$$

where

$$\begin{aligned} a_j^- &= \frac{j(j-1)}{2(j+\nu)(j+\nu-1)}, \quad a_j^0 = \frac{\nu(1-\nu)}{(j+\nu+1)(j+\nu-1)}, \quad a_j^+ = \frac{(j+2\nu+1)(j+2\nu)}{2(j+\nu+1)(j+\nu)} \,, \\ b_j^- &= \frac{j(j-1)(j+2\nu)}{2(j+\nu)(j+\nu-1)}, \quad b_j^0 = \frac{j(j+2\nu)\nu}{(j+\nu+1)(j+\nu-1)}, \quad b_j^+ = -\frac{(j+2\nu+1)(j+2\nu)j}{2(j+\nu+1)(j+\nu)}. \end{aligned} \tag{2.50}$$

For example, for $n = 2$ we get

$$\Gamma_{E,j}^{E+2,j-2} = 4(Ea_j^- - b_j^-), \quad \Gamma_{E,j}^{E+2,j} = 4\left[E(a_j^0+\nu) - b_j^0\right], \quad \Gamma_{E,j}^{E+2,j+2} = 4(Ea_j^+ - b_j^+). \tag{2.51}$$

The recursion relation for the $B_{n,j}$ takes the form:

$$\left(c_{\Delta+n,j}^{(2)} - c_{\Delta,\ell}^{(2)}\right) B_{n,j} = \sum_{n'=0,2,\ldots n-2} \sum_{j'} \Gamma_{\Delta+n',j'}^{\Delta+n,j} B_{n',j'} \,, \tag{2.52}$$

At level 0 we have the initial condition:

$$B_{0,j} = k\, \delta_{j\ell} \,. \tag{2.53}$$

We will set $k = 1$, keeping in mind that the normalization of section 2.1 would correspond to $k = 4^{\Delta}$.

To find the $B_{n,j}$ up to level N, one needs first to compute the coefficients $\Gamma^{E+n,j'}_{E,j}$ for $n \leqslant N$. For example, Eq. (2.51) is sufficient to find the solution for level 2:

$$B_{2,\ell-2} = \frac{\ell(\ell-1)(\Delta-\ell-2\nu)}{2(\ell+\nu-1)(\ell+\nu)(\Delta-\ell-2\nu+1)}, \qquad B_{2,\ell} = \nu\frac{\Delta\nu(\nu-1)+(\Delta-1)\ell(\ell+2\nu)}{(\Delta-\nu)(\ell+\nu+1)(\ell+\nu-1)},$$
$$B_{2,\ell+2} = \frac{(\Delta+\ell)(\ell+2\nu)(\ell+2\nu+1)}{2(\Delta+\ell+1)(\ell+\nu)(\ell+\nu+1)}. \tag{2.54}$$

2.2.1 Comparison between the z and ρ expansions

We have presented two ways to expand the conformal blocks: the "z-series" (2.25) and the "ρ-series" (2.42). We will now argue that the second expansion is more efficient, in the sense that it converges more rapidly and fewer terms need to be evaluated in order to get a good approximation. This happens because of the better choice of the expansion parameter and the better asymptotic behavior of the series coefficients.

Let us start with the expansion parameters. The interesting range for the ρ coordinate is the unit disk $|\rho| < 1$. The ρ-series will converge absolutely, everywhere in this disk. To prove this, we first restrict the expansion of the conformal block to the positive real axis:

$$G_{\Delta,\ell}(\rho > 0 \text{ real}) = \sum_{n=0}^{\infty} \rho^{\Delta+n}\,\beta_n, \qquad \beta_n = \sum_j B_{n,j} \geqslant 0. \tag{2.55}$$

Now fix $\rho_* \geqslant 0$. By positivity of the β_n, the sequence

$$g_N(\rho_*) = \sum_{n=0}^{N} \rho_*^{\Delta+n}\,\beta_n \tag{2.56}$$

grows monotically with N: therefore either it converges or it grows unboundedly (meaning that $\lim_N g_N(\rho_*) = \infty$). The latter cannot occur for $\rho_* < 1$, because it would mean a physical singularity in the conformal block. We conclude that the expansion (2.55) converges pointwise on $[0, 1)$.

As a corollary, it follows that $G_{\Delta,\ell}(\rho)$ increases on the interval $[0, 1)$. To see this, notice that for any two points ρ_1, ρ_2 satisfying $0 \leqslant \rho_1 \leqslant \rho_2 < 1$, we have

$$G_{\Delta,\ell}(\rho_1) = \sum_{n=0}^{\infty} \rho_2^{\Delta+n}\left[\beta_n(\rho_1/\rho_2)^{\Delta+n}\right] \leqslant G_{\Delta,\ell}(\rho_2). \tag{2.57}$$

We will now prove a stronger statement, namely that for any $\epsilon > 0$, convergence is *uniform* on $[0, 1-\epsilon]$.[14] Notice that in this interval, the invidual terms in the expansion (2.55) are bounded as follows:

$$|\rho^{\Delta+n}\,\beta_n| \leqslant \beta_n\,(1-\epsilon)^{\Delta+n} \equiv M_n. \tag{2.58}$$

14. The definition of uniform convergence and various theorems are discussed in Sec. 7.7 of [121].

By the Weierstrass M-test, it is sufficient to show that sum $\sum M_n$ is finite

$$\sum_{n=0}^{\infty} M_n = G_{\Delta,\ell}(\rho = 1-\epsilon) < \infty, \tag{2.59}$$

from which uniform converge follows.

Elsewhere on the disk $|\rho| < 1$ (i.e. away from the real axis), convergence will be only better. For general ρ, the conformal block can be expanded as

$$G_{\Delta,\ell}(\rho = re^{i\alpha}) = \sum_{n=0}^{\infty} r^{\Delta+n}\,\gamma_n(\alpha), \qquad \gamma_n(\alpha) = \sum_j B_{n,j}\frac{\mathrm{Geg}_j^{(\nu)}(\cos\alpha)}{\mathrm{Geg}_j^{(\nu)}(1)}. \tag{2.60}$$

On the interval $[-1,1]$, the Gegenbauer polynomials $\mathrm{Geg}_j^{(\nu)}(x)$ take their (absolute) maximum at $x = 1$. The coefficient $\gamma_n(\alpha)$ is therefore always smaller (in absolute sense) than β_n. Physically, this follows by the Cauchy inequality: $\gamma_n(\alpha)$ is the product of two matrix elements, which for real $\alpha = 0$ become Hermitian conjugates of one another [21]. In particular, if we only keep the first N terms in the conformal block expansion, the 'tail' (i.e. the error induced by this truncation) is smaller away from the real axis:

$$\left|\sum_{n=N+1}^{\infty} \gamma_n(\alpha)\, r^{\Delta+n}\right| \leqslant \sum_{n=N+1}^{\infty} \beta_n\, r^{\Delta+n}\,. \tag{2.61}$$

Since the RHS goes to zero uniformly as $N \to \infty$, the LHS must do so at an even faster rate.

The same argument can be used to show that the z-series will converge absolutely in the disk $|z| < 1$. As we discussed, this does not even cover the full regularity region of the conformal blocks. Moreover, from the second Eq. (2.39) we have

$$|z(\rho)/\rho| > 1 \qquad (|\rho| < 1)\,. \tag{2.62}$$

So even in the region where both series converge, the ρ-series will always have a strictly smaller expansion parameter.

An additional bonus appears when considering conformal blocks for equal external dimensions. As we have seen, in this case the ρ-series involves only even levels. So, the effective expansion parameter becomes ρ^2. In conformal bootstrap applications, one usually uses conformal blocks evaluated near $z = 1/2$, which would correspond to $\rho = 3 - 2\sqrt{2} \approx 0.17$ and $\rho^2 \approx 0.03$.

Let us now examine the expansion coefficients. We are interested in their asymptotic behavior when Δ or ℓ become large. In the large-Δ limit the coefficients $A_{n,j}$ at level n grow as

$$A_{n,j} \underset{\Delta\to\infty}{\sim} \mathrm{O}(\Delta^n)\,. \tag{2.63}$$

For $n = 1, 2$ this can be seen in Eqs. (2.31). The reason for this growth is that the operator $\mathcal{D}_1$ is second order in ∂_s, and consequently the coefficients $\gamma^{\pm}_{E,j}$ in (2.27) are $\mathrm{O}(E^2)$. On the

other hand the factor in the RHS of the recursion relation:

$$c^{(2)}_{\Delta+n,j} - c^{(2)}_{\Delta,\ell} = 2n\Delta + n(n-d) + j(j+d-2) - \ell(\ell+d-2) \tag{2.64}$$

increases only linearly in Δ. So, going up one level in n, the coefficients $A_{n,j}$ gain one power in Δ.

Turning to the second expansion, we encounter a crucial difference. Unlike $\mathcal{D}_1$, the operator $\widetilde{\mathcal{D}}$ in (2.46) is only first order in ∂_r. So the coefficients Γ entering the $B_{n,j}$ recursion grow only linearly in E, and this growth cancels when dividing by (2.64). Contrary to the previous case, going one level up in the recursion relation does not increase the leading power of Δ. We conclude that the coefficients $B_{n,j}$ remain bounded in the large-Δ limit. For $n = 2$ this is illustrated by Eqs. (2.54).

Keeping more careful track of the size of the relevant factors, one can show the following sharper statement (see appendix A). Each coefficient $B_{n,j}$ is uniformly bounded in the full range of Δ and ℓ allowed by the unitarity bounds, with the bound depending only on the level n and on d:

$$\max_{\Delta,\ell}\Big(\max_{j} B_{n,j}\Big) \leqslant b(n,d)\,. \tag{2.65}$$

The region close to the free scalar limit $\ell = 0$, $\Delta \to \nu$ is understood excluded when taking the maximum. As is well known, the scalar conformal block becomes singular in this limit. Physically this is due to the fact that the free scalar must be decoupled from everything else. In our representation, the singularity first shows up in the coefficient $B_{2,0} \sim (\Delta - \nu)^{-1}$, see Eq. (2.54), and then feeds into higher levels.

Consider now the growth of the conformal block for real $\rho \to 1$. It can be shown using the results of Ref. [7] [15] that in this limit the conformal block has a power-law like singularity of the form:

$$G_{\Delta,\ell}(\rho \text{ real}) \underset{\rho\to 1}{\sim} \frac{1}{(1-\rho)^{d-2}} \qquad \left(\log\frac{1}{1-\rho} \text{ for } d=2\right). \tag{2.66}$$

These asymptotics can be used to make a rigorous statement about the growth of the coefficients $\beta_n = \sum_j B_{n,j}$. We recall from Eq. (2.55) that the β_n appear in the expansion of $G_{\Delta,\ell}$ restricted to the real axis. Given the fact that the β_n are positive and that the conformal block expansion converges for all $\rho < 1$, the Hardy-Littlewood tauberian theorem [122, theorem 7.4] implies for $d > 2$ that

$$\sum_{n=0}^{N} \beta_n \underset{N\to\infty}{\sim} N^{d-2} \tag{2.67}$$

for any Δ and ℓ. Assuming that the sequence $\{\beta_n\}$ itself has a power-law like growth at large n, we must have

$$\beta_n \underset{n\to\infty}{\sim} n^{d-3}. \tag{2.68}$$

15. This follows for $\ell = 0$ from the explicit ${}_3F_2$ representation on the real line, Eq. (4.10) of [7], and remains valid for $\ell \geqslant 1$ by the recursions in Appendix A of [7].

It would be interesting to know how the ratio β_n/n^{d-3} behaves for small and intermediate n. The simplest possibility which accommodates both (2.65) and (2.68) is that $\beta_n \leqslant c(d)n^{d-3}$ for all n, Δ and ℓ. However, further study is needed to check this hypothesis.

The case $d = 2$, where the Hardy-Littlewood tauberian theorem does not apply, requires special attention. It is certainly *not* true that

$$\sum_{n=0}^{N} \beta_n \underset{N\to\infty}{\sim} \text{constant}, \tag{2.69}$$

because in that case Abel's theorem [121, theorem 8.2] implies that the limit $G_{\Delta,\ell}(\rho \to 1)$ is finite. In various special cases, we find that $\beta_n \sim (a \ln n + b)/n$ as $n \to \infty$, meaning that the partial sums $\sum_{n\leqslant N} \beta_n$ asymptote to $a\,(\ln N)^2/2 + b \ln N$ as $N \to \infty$. It may be interesting to check these asymptotics at a more rigorous level, starting either from explicit expressions for the 2d conformal blocks or using "logarithmic" tauberian theorems [123, 124].

To finish this section, we would like to demonstrate how the highlighted differences between the z- and ρ-series can be seen in the explicit expressions for the conformal blocks available for even d. These expressions [19, 15, 16, 20] are written in terms of the functions

$$k_a(z) = z^{a/2}{}_2F_1(a/2, a/2; a; z) \tag{2.70}$$

with $a = \Delta + \ell$ and $\Delta - \ell - 2\nu$. For large Δ, the z^n coefficient in the expansion of the ${}_2F_1$ grows as $a^n \sim \Delta^n$. This is the same growth as in (2.63). However, when the ρ variable is used, the function k_a can be transformed using a hypergeometric identity [38, Eq. 9.134.3]

$$k_a\left[\frac{4\rho}{(1+\rho)^2}\right] = (4\rho)^{a/2}{}_2F_1\left[\begin{matrix}1/2,\, a/2\\ (a+1)/2\end{matrix}; \rho^2\right]. \tag{2.71}$$

As advertised, this is a function of ρ^2 and the expansion coefficients

$$\frac{(1/2)_n (a/2)_n}{n!\,(a/2+1/2)_n} \underset{a\to\infty}{\sim} \frac{(1/2)_n}{n!} + \mathrm{O}(1/a) \tag{2.72}$$

do not grow with a.[16]

2.3 Outlook: potential applications to the conformal bootstrap

In the previous section, we introduced a new way to represent the conformal blocks, by expanding them in the polar coordinates associated with the complex variable ρ. Our interests in the blocks stems from the role they play in the conformal bootstrap program.

16. We warn the reader that analysis of the coefficients β_n à la Hardy-Littlewood is done at *fixed* Δ, and that the $\Delta \to \infty$ blocks from Eq. (2.72) do not satisfy the growth required by the Hardy-Littlewood theorem.

We believe that our new representation will turn out quite useful in this context. Here we will list several ideas, leaving their complete development for the future.

We recall that most existing applications of the bootstrap program in $d \geqslant 3$ dimensions follow a scheme first proposed in [14]. This scheme focuses on a single bootstrap equation, that is obtained by substituting the conformal block expansion (2.2) into the crossing symmetry constraint (2.3) and takes the form:

$$(v^{\Delta_\phi} - u^{\Delta_\phi}) + \sum_i f_i^2 \left[v^{\Delta_\phi} G_{\Delta_i,\ell_i}(u,v) - (u \leftrightarrow v)\right] = 0\,. \tag{2.73}$$

The sum is over all primary operators $\mathcal{O}_i$ appearing in the OPE $\phi \times \phi$, with Δ_i, ℓ_i, f_i their dimensions, spins, and OPE coefficients. The unit operator $\mathbb{1}$ contribution is separated explicitly: its conformal block is trivial

$$G_{\text{unit}}(u,v) = G_{\text{unit}}(v,u) = 1\,, \qquad (\Delta_{12} = \Delta_{34} = 0) \tag{2.74}$$

and its OPE coefficient equals one:

$$\phi(x)\phi(0) = \frac{1}{|x|^{2\Delta_\phi}}\mathbb{1} \;+\; \text{other operators.} \tag{2.75}$$

We would like to highlight two practical issues regarding this sum rule.

First, we remark that the bootstrap equation (2.73) looks rather complicated, and in practice it is usually replaced by a finite-dimensional constraint that is less constraining than the full bootstrap equation (2.73), but more tractable. As explained in section 1.7.2, it is customary to Taylor expand the bootstrap equation up to a large order around the point $z = 1/2$, corresponding to $u = v = 1/4$.

A second issue is that the conformal blocks appearing in (2.73) are complicated functions, even for $d = 4$ where explicit expressions in terms of hypergeometrics are known. Some simplifications occur for specific values of Δ, but this does not help, since the dimensions of $\mathcal{O}_i$ are unknown and should be allowed to vary freely between the unitarity bound and infinity. For generic Δ, conformal block derivatives at $z = 1/2$ must be evaluated numerically. [17] For this reason all the studies cited above used numerical analysis. Moreover, this evaluation is an expensive operation and often presents a computational bottleneck.

We will now describe new ways of approaching these issues, made possible by the ρ-series representation.

17. For even d, these derivatives can be written via the ${}_3F_2$ functions (see appendix B.1 of [95]). It is not known at present how to use these analytic expressions in practice, rather than as a starting point for the numerical evaluation.

2.3.1 Inexpensive derivative evaluation for all Δ and ℓ

Let us briefly review the existing ways of evaluating conformal blocks and their derivatives at the point $z = \bar{z} = 1/2$. For even d, one uses the explicit representations of Dolan and Osborn [15, 16]. For $d = 4$ they take the form:

$$G_{\Delta,\ell}(z,\bar{z}) = \frac{z\bar{z}}{z-\bar{z}}[k_{\Delta+\ell}(z)k_{\Delta-\ell-2}(\bar{z}) - (z \leftrightarrow \bar{z})]\,. \tag{2.76}$$

By this formula, partial derivatives of $G_{\Delta,\ell}(z,\bar{z})$ can be represented as quadratic forms in the derivatives of the function $k_a(z)$, defined in Eq. (2.70). One can now create an interpolated lookup table of $k_a(z)$'s derivatives at $z = 1/2$ for a range of a. This is a time-consuming operation, because the hypergeometric function in (2.70) is expensive to evaluate. However, one needs to do this only once. Once the table is created and stored, partial derivatives of (2.76) can be computed quickly for any Δ and ℓ. Such a strategy was used in [93, 94, 96–98], and a similar one in [95]. More recently, Ref. [99] found a way to dispense with the lookup table altogether, computing the derivatives of $k_a(z)$ at $z = 1/2$ via a very rapidly convergent infinite product representation.

Turning to general d, a method to evaluate conformal block derivatives was developed in Ref. [7], where it was used to study the 3d Ising model. This method combines a variety of ideas. One begins by evaluating partial derivatives along the $z = \bar{z}$ line, first for $\ell = 0$ and $\ell = 1$ using explicit ${}_3F_2$ expressions found by [7], then for higher ℓ using the recursion relations from [20] reducing those blocks to the lower-spin ones. Then, partial derivatives in the orthogonal direction are computed *à la* Cauchy-Kovalevskaya, using the fact that the conformal blocks satisfy a second-order partial differential equation.

The ρ-series gives a new way to evaluate conformal blocks and their derivatives, which works for general d and around any z. To achieve the necessary precision, one needs to evaluate the coefficients $B_{n,j}$ as a function of Δ and ℓ up to a sufficiently high order, using the recursion relation (2.52). It is important that the necessary number of terms will be independent of Δ and ℓ, because of the bound (2.65). For example, to be able to compute the conformal blocks with double precision (10^{-16}) one would need the coefficients up to level

$$n \approx 16/\log_{10}(1/\rho)\,, \tag{2.77}$$

which gives $n \approx 20$ for $z = 1/2$. This number is a bit of an underestimate, because it assumes that the sum of the coefficients at level n is uniformly bounded, while in fact it grows with n as in Eq. (2.68). Also more levels will be needed if one wants to evaluate derivatives.

It should also be rather easy to generalize the ρ-series method to the case of unequal external dimensions $\Delta_1 \neq \Delta_2$ and $\Delta_3 \neq \Delta_4$. The extra terms in the Casimir operator for unequal external dimensions are all first order in derivatives [16]. So, the operator $\widetilde{\mathcal{D}}$ will remain first order, and we can expect that the boundedness properties of the coefficients

$B_{n,j}$ will still hold. Such a generalization will be useful for the conformal bootstrap analysis of several scalar correlators simultaneously.

2.3.2 Truncated bootstrap equation with an error estimate

Rather than using a derivative expansion around $z = 1/2$, one could also try to do bootstrap imposing the bootstrap equation point by point at several $z = z_i$, rather than in the Taylor expansion around $z = 1/2$. We would like to discuss here the issues arising if one wants to implement this technique. Conformal block evaluation for any z can be done with the ρ-series. The next question is then how to distribute the sampling points. To get an idea, let us consider the rate of convergence of the conformal block decomposition (2.2). As shown in Ref. [21], the error induced by truncating (2.2) at some maximal dimension $\Delta = \Delta_*$ is exponentially small:

$$\left| \sum_{\mathcal{O}:\Delta(\mathcal{O})\geqslant\Delta_*} f_{\mathcal{O}}^2 \, G_{\mathcal{O}}(z,\bar{z}) \right| \lesssim \frac{\Delta_*^{4\Delta_\phi}}{\Gamma(4\Delta_\phi+1)} |\rho(z)|^{\Delta_*} . \tag{2.78}$$

To be precise, this estimate was shown to hold for $\Delta_* \gg \Delta_\phi/(1-|\rho(z)|)$. Most importantly, it holds in an arbitrary CFT with no extra assumptions about the $\phi \times \phi$ OPE. For example, it might seem that having too many operators at high Δ, or a single operator with a huge OPE coefficient, might invalidate this bound. However, the proof in [21] shows that such situations cannot occur in a consistent CFT.

The estimate (2.78) is relevant to our discussion, because in most practical approaches to the bootstrap one has to truncate the spectrum of considered operators from above (to make the problem finite). Now we know that the error induced by this operation is controlled by $|\rho(z)|$, while the error in the crossed channel will be controlled by $|\rho(1-z)|$. Therefore it seems natural to distribute the points z_i in a region of the form (see Fig. 2.7)

$$\lambda(z) = \max(|\rho(z)|, |\rho(1-z)|) \leqslant \lambda_c \, , \tag{2.79}$$

where λ_c should be chosen commensurately with the eventual dimension cutoff Δ_*.

One way to choose Δ_* is so that the error (2.78) is below the numerical precision one is working with (say double precision) everywhere within the region (2.79). Alternatively, one can choose Δ_* lower, so that the error is non-negligible. Then one has to include this error estimate directly into the bootstrap equation. Such a modified equation takes the form:

$$\begin{aligned} &\left| v^{\Delta_\phi} - u^{\Delta_\phi} + \sum_{\Delta(\mathcal{O})\leqslant\Delta_*} f_{\mathcal{O}}^2 \left[v^{\Delta_\phi} G_{\mathcal{O}}(u,v) - (u \leftrightarrow v) \right] \right| \leqslant E(z,\bar{z}) \, , \\ &E(z,\bar{z}) \simeq \frac{\Delta_*^{4\Delta_\phi}}{\Gamma(4\Delta_\phi+1)} \max\left(|1-z|^{2\Delta_\phi} |\rho(z)|^{\Delta_*}, |z|^{2\Delta_\phi} |\rho(1-z)|^{\Delta_*} \right) . \end{aligned} \tag{2.80}$$

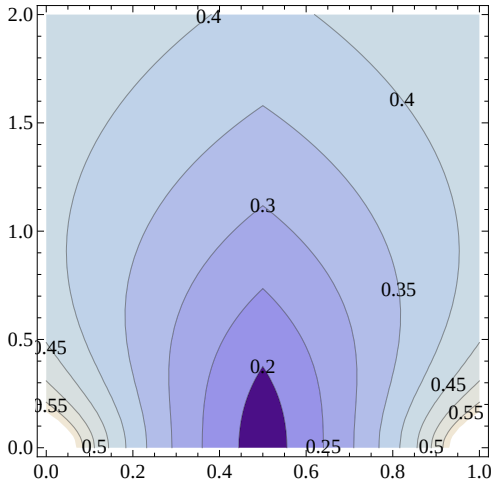

Figure 2.7: The contour plot of the function $\lambda(z)$ in the plane $(\mathrm{Re}\, z, \mathrm{Im}\, z)$. Only the region $\mathrm{Im}\, z \geqslant 0$ is shown, since the conformal blocks are symmetric in $z, \bar{z}$.

We think it would be interesting to try to carry out bootstrap analysis based on this 'truncated bootstrap equation' rather than the conventional technique of expanding around $z = 1/2$. There are many free parameters to choose: Δ_*, λ_c, the number of points z_i at which to impose (2.80); furthermore, the points can be different in many different ways over the region (2.79). Once all these parameters are fixed, the problem of deciding whether (2.80) has a solution with $f^2_{\mathcal{O}} \geqslant 0$ can be solved via the same linear programming algorithms that are used in other bootstrap computations.

It's worth pointing out an additional feature of Eq. (2.80), which makes it particularly useful when the conformal blocks are computed via the ρ-series, whose coefficients can be computed up to arbitrary order but whose closed form is unknown. Namely, it remains valid when the conformal blocks $G_{\mathcal{O}}(u, v)$ are replaced by the "truncated blocks"—the partial sums of the ρ-series up to the level $\Delta + n \geqslant \Delta_*$. This is because the error estimate (2.78) is in fact valid when the contributions of all states of dimension above Δ_* are included into the LHS (and not just the conformal multiplets of primaries above Δ_*). It is in this stronger form that the error estimate was proved in Ref. [21].

2.4 Summary

In this chapter we presented a new type of expansion for $d > 2$ conformal blocks, rooted in their physical meaning as sums of exchanged states in radial quantization. We explained how quantum mechanics fixes the structure of conformal block in radial coordinates: it is an integer-spaced power series in the r with angular dependence given by Gegenbauer polynomials. The coefficient of each term is positive as a consequence of unitarity. These

coefficients are easy to find using recursion relations that are derived from the quadratic Casimir equation.

We highlighted the existing freedom in the choice of the radial coordinates. It is the same freedom as when expanding the product of two operators $\phi(x_1)\phi(x_2)$ into a sum of operators inserted in some point x_0, which becomes the radial quantization origin. Each choice gives a different representation of the same conformal block, and it is not a priori clear which one is more convenient. In this paper we analyzed in detail two natural choices, the end point $x_0 = x_1$, and the middle point $x_0 = (x_1 + x_2)/2$.

The end point choice (section 2.1) corresponds to working with the complex variable z often used to represent conformal blocks, with explicit ${}_2F_1$ representations available in even dimensions d. For general d considered here, we expand conformal blocks in a power series in $|z|$ times Gegenbauers. The expansion coefficients $A_{n,j}$ satisfy a three-term recursion relation, also derived earlier from a different point of view by Dolan and Osborn [16]. An unpleasant feature of these expansions is that the coefficients at level n grow with the exchanged primary dimension as Δ^n. For large Δ many terms need to be evaluated to get a good approximation to the conformal block.

Choosing the middle point (section 2.2), one passes from z to the complex variable

$$\rho = \frac{z}{(1+\sqrt{1-z})^2}\,. \tag{2.81}$$

This variable was recently used in Ref. [21] to study convergence of the conformal block decomposition. As we showed here, this is also an ideal variable for constructing rapidly convergent expansions of the conformal blocks themselves. The expansion coefficients $B_{n,j}$ satisfy a recursion relation which is a bit more involved than for the $A_{n,j}$: the coefficients at level n are linear combinations of coefficients at all levels $n-2$, $n-4$, ... up to zero, while for $A_{n,j}$ only the level $n-1$ contributes. But this complication pays off: the resulting coefficients do not exhibit any growth with Δ or ℓ. This means that the coefficients computed and stored up to some large and fixed level N can be used to evaluate conformal blocks of arbitrary dimension and spin with uniform accuracy.

We believe that our ρ-series expansions will find future use in the bootstrap program. Two possibilities are described in section 2.3. In the following chapter, we will develop a way to compute conformal blocks inexpensively, using the ideas from section 2.3.1.

Chapter 3

Conformal blocks in the diagonal limit [1]

3.1 Introduction

In the previous chapter, we revisited the conformal block decomposition of scalar correlation functions $\langle\phi_1(x_1)\phi_2(x_2)\phi_3(x_3)\phi_4(x_4)\rangle$, where the fields ϕ_i are of scaling dimension Δ_i. Our main result was that any conformal block $G_{\mathcal{O}}(u,v)$ in such an expansion admits various series expansions of the form

$$G_{\mathcal{O}}(r,\theta) = \sum_{n,j} C_{n,j}\, r^{\Delta_{\mathcal{O}}+n}\, \mathrm{Geg}_j^{(\nu)}(\cos\theta)\,, \qquad [\nu = (d-2)/2]. \tag{3.1}$$

We singled out two particular representations, corresponding to a "z" and a "ρ" configuration of the four points x_1, x_2, x_3, x_4. The coefficients $C_{n,j}$ in the series expansion (3.1) depend on the chosen kinematics, the dimension Δ and spin ℓ of the exchanged operator $\mathcal{O}$, the spacetime dimension d and furthermore on $\Delta_{12} = \Delta_1 - \Delta_2$ and $\Delta_{34} = \Delta_3 - \Delta_4$ if the external scalar operators $\phi_1, \ldots, \phi_4$ are non-identical.

As we showed, both expansions (3.1) converge absolutely inside the unit disk $|r| < 1$, so they can be used to numerically compute the value of $G_{\mathcal{O}}(r,\theta)$ to arbitrary precision. This requires knowledge of the coefficients $C_{n,j}$ for arbitrary Δ and ℓ (and Δ_{12} and Δ_{34}, if applicable), at least up to a level $N \gg 1$. For the z-kinematics, these coefficients are known in closed form, or otherwise they can be easily computed by means of a two-term recursion relation. For the ρ-kinematics, the coefficients are *not* known in closed form, and furthermore the recursion relation used to compute them becomes increasingly involved as n increases.

1. This chapter is a reworked version of Ref. [125], which was written in collaboration with H. Osborn and S. Rychkov.

Moreover, most bootstrap applications do not require the actual value of conformal blocks at various points z_i or ρ_i inside the unit disk: rather, they take as input derivatives of $G_{\mathcal{O}}(z,\bar{z})$ at a given point z_0 on the 'diagonal' $z=\bar{z}$. It is the goal of this chapter to compute such derivatives efficiently, both in the z and ρ kinematics.

In the previous chapter, our focus was on the four-point function of identical scalars. We now consider a more general case, the correlator $\langle\phi_1\phi_2\phi_3\phi_4\rangle$ of four non-identical scalars. By conformal invariance, the latter must be of the form

$$\langle\phi_1(x_1)\phi_2(x_2)\phi_3(x_3)\phi_4(x_4)\rangle = \left(\frac{|x_{24}|}{|x_{14}|}\right)^{\Delta_{12}}\left(\frac{|x_{14}|}{|x_{13}|}\right)^{\Delta_{34}}\frac{g(u,v)}{|x_{12}|^{\Delta_1+\Delta_2}|x_{34}|^{\Delta_3+\Delta_4}}\,, \tag{3.2}$$

where $g(u,v)$ is a function of the conformally invariant cross-ratios u and v only. The four-point function (3.2) can be expanded into conformal partial waves corresponding to the primaries $\mathcal{O}$ appearing in the operator product expansions (OPEs) $\phi_1\times\phi_2$ and $\phi_3\times\phi_4$This gives the following series representation for the function $g(u,v)$:

$$g(u,v) = \sum_{\mathcal{O}} f_{12\mathcal{O}} f_{34\mathcal{O}}\, G_{\Delta,\ell}(u,v)\,, \tag{3.3}$$

Here the $G_{\Delta,\ell}(u,v)$ are the universal parts of the conformal partial waves; these are the conformal blocks mentioned above. They depend on the dimension Δ and spin ℓ of the exchanged primary $\mathcal{O}$, as well as on the external dimension differences Δ_{12} and Δ_{34}. The $f_{ij\mathcal{O}}$ are the OPE coefficients which depend on the CFT in question. In the case of non-identical scalars, the OPE coefficients $f_{12\mathcal{O}}$ and $f_{34\mathcal{O}}$ are in general different.

An equivalent representation of the conformal blocks is expressed in terms of the symmetric functions of variables $z,\bar{z}$ which are related to u,v via

$$u = z\bar{z}, \qquad v = (1-z)(1-\bar{z})\,. \tag{3.4}$$

To make contact with the literature [15, 16, 20], we will use a slightly different notation for the conformal block $G_{\Delta,\ell}(u,v)$ in this chapter, namely

$$G_{\Delta,\ell}(u,v) = F_{\lambda_1\lambda_2}(z,\bar{z})\,, \tag{3.5}$$

for

$$\Delta = \lambda_1+\lambda_2, \quad \ell = \lambda_1-\lambda_2 \in \{0,1,2,\ldots\}\,. \tag{3.6}$$

The normalization of conformal blocks is a matter of choice, for us [2]

$$F_{\lambda_1\lambda_2}(z,z) \sim z^{\Delta} \quad \text{as} \quad z\to 0\,. \tag{3.7}$$

The work in this chapter is mainly motivated by a numerical approach to computing conformal blocks that was developed by El-Showk et al. [7], where it was applied in the

2. Note that the limit $z\to 0$ is taken along the real axis. This is the same normalization as the one used in the previous chapter.

bootstrap analysis of the 3d Ising model. Rather than solving the Casimir differential equation directly, the method advocated there computes the conformal blocks first on the "diagonal" $z = \bar{z}$, which turns out to be significantly simpler than for general $z, \bar{z}$. Then, one computes derivatives in the direction normal to the diagonal, using recursion relations following from a second-order partial differential equation (PDE) that the blocks satisfy. While this method cannot compute the blocks at a finite distance from the diagonal,[3] it proved very efficient in computing them in the derivative expansion around $z = \bar{z} = 1/2$. The latter information is sufficient for applying the existing conformal bootstrap algorithms.

Motivated by [7], here we analyze in more detail the diagonal limit of conformal blocks. The central part of the chapter is section 3.2, where we systematically derive ordinary differential equations (ODEs) satisfied on the diagonal. While it is well known that conformal blocks as functions of $z, \bar{z}$ satisfy PDEs (which arise from eigenvalue equations for the Casimir operator), it is by no means evident that the diagonal limit satisfies an equation by itself. As we will see, this follows from an interplay between the well-known quadratic and the rarely-used quartic Casimir PDEs.

Next, in section 3.4 we propose to use the ODEs from section 3.2 as a basis for an efficient algorithm which can numerically compute conformal blocks and their derivatives around any point on the diagonal. This algorithm is a generalization and an improvement of the method used in [7] for the case of equal external scalar dimensions.

We summarize the main aspects of this chapter in section 3.5. Appendix B discusses how our ODEs can be used to generate power series expansions of the conformal blocks.

3.2 Differential equations on the diagonal

Mathematically, conformal blocks in d-dimensional CFTs can be extended to symmetric functions of two complex variables z and $\bar{z}$, analytic everywhere in $\mathbb{C}^2$ except for branch points at $z, \bar{z} = 0,1$ and ∞. This is merely a trick: when actually evaluating conformal blocks in Euclidean space, it is necessary to impose $\bar{z} = z^*$.

In this chapter we study conformal blocks on the "diagonal" $z = \bar{z}$. For the Euclidean section $z = x + iy$, $\bar{z} = x - iy$, for x, y real, the limit $y \to 0$ is in general singular when it approaches the branch cut $x \in [1, \infty)$[4]. Away from the cut, for arbitrary complex z, the

3. See [16] or the previous chapter for a proposal on how to do this, using power series expansions around $z, \bar{z} = 0$.

4. This is also apparent from the four-dimensional result (1.130) which can be expressed in the form $\frac{f(z)\,g(\bar{z}) - f(\bar{z})\,g(z)}{z - \bar{z}}$ where $f(z), g(z)$ have branch cuts along the real axis for $z > 1$. Hence for $x > 1$, $f(z), f(\bar{z})$ and $g(z), g(\bar{z})$ approach different limits as $y \to 0$ and the denominator is not cancelled.

limit $\bar{z} \to z$ is well-defined and conformal blocks on the diagonal will be denoted by

$$f_{\lambda_1\lambda_2}(z) = F_{\lambda_1\lambda_2}(z,z)\,. \tag{3.8}$$

For most conformal bootstrap applications we require real z and $0 < z < 1$, which includes the crossing symmetric point $z = \bar{z} = 1/2$. These functions allow a power series expansion of the form

$$f_{\lambda_1\lambda_2}(z) = z^{\Delta}\sum_{n=0}^{\infty} a_n z^n\,, \qquad a_0 = 1\,, \tag{3.9}$$

where $a_0 = 1$ follows from the normalization condition (3.7). Following an argument in the previous chapter, CFT properties imply that $z^{-\Delta} f_{\lambda_1\lambda_2}(z)$ is analytic in z with singularities at $z = 1, \infty$ and so this expansion is convergent for $|z| < 1$ (see also [21]).

As functions of z and $\bar{z}$, conformal blocks satisfy various PDEs, derived by acting on the four-point function with the Casimir operators of the conformal group and demanding that conformal partial waves be eigenfunctions. For general d, there are quadratic and quartic Casimir operators, as explained in section 1.8. The corresponding second- [16] and fourth-order [20] PDEs are

$$\Delta_2\, F_{\lambda_1\lambda_2} = c_2\, F_{\lambda_1\lambda_2}\,, \qquad \Delta_4\, F_{\lambda_1\lambda_2} = c_4\, F_{\lambda_1\lambda_2}\,, \tag{3.10}$$

where ($\nu = (d-2)/2$)

$$\begin{aligned} c_2 &= \lambda_1(\lambda_1 - 1) + \lambda_2(\lambda_2 - 1 - 2\nu) = \tfrac{1}{2}[\ell(\ell+2\nu) + \Delta(\Delta - 2 - 2\nu)]\,,\\ c_4 &= \ell(\ell+2\nu)(\Delta-1)(\Delta-1-2\nu)\,, \end{aligned} \tag{3.11}$$

and the differential operators can be written as

$$\Delta_2 = D_z + D_{\bar{z}} + 2\nu\frac{z\bar{z}}{z-\bar{z}}\Big[(1-z)\frac{\mathrm{d}}{\mathrm{d}z} - (1-\bar{z})\frac{\mathrm{d}}{\mathrm{d}\bar{z}}\Big]\,, \tag{3.12}$$

$$\Delta_4 = \left(\frac{z\bar{z}}{z-\bar{z}}\right)^{2\nu}(D_z - D_{\bar{z}})\left(\frac{z\bar{z}}{z-\bar{z}}\right)^{-2\nu}(D_z - D_{\bar{z}})\,, \tag{3.13}$$

in terms of the one-dimensional differential operator of the ${}_2F_1$ type:

$$D_z \equiv D_z(a,b) = (1-z)z^2\frac{\mathrm{d}^2}{\mathrm{d}z^2} - (a+b+1)\,z^2\frac{\mathrm{d}}{\mathrm{d}z} - ab\,z\,. \tag{3.14}$$

Here and below we denote $a = -\frac{1}{2}\Delta_{12}$ and $b = \frac{1}{2}\Delta_{34}$. The above operator D_z has the functions $k_\beta(z)$ from Eq. (1.129) as eigenfunctions:

$$D_z(a,b)\,k_\beta(z) = \tfrac{1}{4}\beta(\beta-2)\,k_\beta(z). \tag{3.15}$$

For $\ell = 0$ (when the exchanged operator $\mathcal{O}$ is a scalar) the quartic eigenvalue c_4 vanishes. In this case the quartic Casimir equation actually reduces to a second-order PDE [20]

$$\big(D_z - D_{\bar{z}}\big)F_{\lambda\,\lambda} = 0\,. \tag{3.16}$$

Crucially, the two PDEs (3.10, 3.16) can be combined to yield a single ODE that controls the 'diagonal' part of the conformal block. Conformal blocks are symmetric functions of $z, \bar{z}$ and near the diagonal (3.8) can be extended to a power series expansion of the form:

$$F_{\lambda_1\lambda_2}(z,\bar{z}) = f_{\lambda_1\lambda_2}(t) + \tfrac{1}{4}(z-\bar{z})^2 g_{\lambda_1\lambda_2}(t) + \mathrm{O}\big((z-\bar{z})^4\big), \quad t = \tfrac{1}{2}(z+\bar{z})\,. \tag{3.17}$$

Clearly the t-coordinate parametrizes the diagonal $z = \bar{z}$. Only even powers of $(z-\bar{z})$ can appear, because $F_{\lambda_1\lambda_2}(z,\bar{z})$ must be symmetric under $z \leftrightarrow \bar{z}$. Remark that the quadratic Casimir equation at $z = \bar{z}$ gives one relation between $f \equiv f_{\lambda_1\lambda_2}$ and $g \equiv g_{\lambda_1\lambda_2}$:

$$\left[\tfrac{1}{2}(1-z)z^2\frac{\mathrm{d}^2}{\mathrm{d}z^2} - (1+a+b+\nu)z^2\frac{\mathrm{d}}{\mathrm{d}z} - 2ab\,z - c_2\right] f(z) + (1+2\nu)(1-z)z^2 g(z) = 0\,. \tag{3.18}$$

A second relation follows from the quartic Casimir equation, which reduces to a third-order PDE on the diagonal, so that the $\mathrm{O}\big((z-\bar{z})^4\big)$ terms omitted in (3.17) do not contribute. This relation takes the schematic form

$$P_3(\mathrm{d}_z) f(z) + P_2(\mathrm{d}_z) g(z) = 0\,. \tag{3.19}$$

In addition, for $\ell = 0$, substituting (3.17) into (3.16) and looking at the $\mathrm{O}(z-\bar{z})$ terms gives an equation of the form

$$Q_2(\mathrm{d}_z) f(z) + Q_1(\mathrm{d}_z) g(z) = 0\,, \tag{3.20}$$

The P_i and Q_i in the last two equations are certain differential operators of degree i with polynomial coefficients, whose precise form is important for what follows but is of no particular interest to write them down explicitly.

With the help of (3.18), we can eliminate $g(z)$ from (3.19) and (3.20). This gives ODEs for $f(z)$ by itself, fourth-order for the general case, and third-order for $\ell = 0$:

$$D_z^{(4,3)} f_{\lambda_1\lambda_2}(z) = 0\,, \tag{3.21a}$$

$$D_z^{(3,2)} f_{\lambda\,\lambda}(z) = 0\,, \tag{3.21b}$$

where in general $D^{(n)}$ is a differential operators of the form

$$D_z^{(n)} = (z-1)^{n-1} z^n \frac{\mathrm{d}^n}{\mathrm{d}z^n} + \sum_{r=2}^{n-1} (z-1)^{r-1} p_r(z)\, z^r \frac{\mathrm{d}^r}{\mathrm{d}z^r} + \sum_{r=0,1} p_r(z)\, z^r \frac{\mathrm{d}^r}{\mathrm{d}z^r}\,, \tag{3.22}$$

denoting by $p_r(z)$ polynomials of degree

$$\deg p_r(z) = \begin{cases} n-r, & r > 2\,, \\ n-1, & r = 0, 1\,. \end{cases} \tag{3.23}$$

The differential operators are symmetric functions of a, b and so, with $P = 2ab$, $S = a + b$, the operator in (3.21a) is determined by

$$\begin{aligned}
p_3(z) &= (4S - 2\nu + 7)z + 4\nu - 2\,,\\
p_2(z) &= [2P + (S - \nu + 2)(5S - \nu + 5)]z^2 + 2\,[c_2 - P + (3S - \nu + 3)(2\nu - 1)]z\\
&\quad + 4\nu^2 - 2\nu - 2c_2\,,\\
p_1(z) &= [4P + (2S + 1)(S - \nu + 2)](S - \nu + 1)z^3\\
&\quad + [c_2(4S - 2\nu + 1) + 2(2S + 1)(S - \nu + 1)(2\nu - 1) + P(-4S + 10\nu - 5)]z^2\\
&\quad + [-6\nu P + P + 2(2S + 1)\nu(2\nu - 1) + c_2(-4S + 6\nu + 1)]z - 2c_2(2\nu + 1)\,,\\
p_0(z) &= 2P(S - \nu)(S - \nu + 1)z^3 + (S - \nu)[c_2(2S - 1) + P(6\nu - 1)]z^2\\
&\quad + [c_4 + 2(2\nu + 1)(c_2(S - 1) + P\nu)]z - c_4 + 2c_2(2\nu + 1)\,,
\end{aligned} \tag{3.24}$$

with c_2, c_4 as in (3.11). In (3.21b)

$$\begin{aligned}
p_2(z) &= (3S - \nu + 3)z + 2\nu\,,\\
p_1(z) &= [2P + (2S + 1)(S - \nu + 1)]z^2 + 2(c_2 - P + 2S\nu + \nu)z - 2c_2\,,\\
p_0(z) &= 2P(S - \nu)z^2 + [P(2\nu + 1) + c_2(2S - 1)]z + 2c_2\,,
\end{aligned} \tag{3.25}$$

where here $c_2 = 2\lambda(\lambda - 1 - \nu)$. With these expressions for the differential operators, the ODEs in (3.21) are the main result for this chapter. They allow for a direct analysis of the diagonal limit of conformal blocks.

In passing, let us briefly show that the differential operators $D_z^{(n)}$ above are consistent with the permutation $\phi_1(x_1) \leftrightarrow \phi_2(x_2)$, which changes $a \to -a$ but leaves b invariant. In the z-kinematics, the swap $x_1 \leftrightarrow x_2$ is equivalent to changing

$$z \;\mapsto\; z' = \frac{z}{z - 1}, \qquad \bar{z} \;\mapsto\; \bar{z}' = \frac{\bar{z}}{\bar{z} - 1} \tag{3.26}$$

as follows by imposing that the cross ratios u and v are invariant. Under this change of coordinate, the conformal blocks transform as [15, 16, 20]

$$F_{\lambda_1\lambda_2}(z', \bar{z}')\big|_{a\to -a} = (-1)^\ell\,(1 - z)^b(1 - \bar{z})^b\,F_{\lambda_1\lambda_2}(z, \bar{z})\,. \tag{3.27}$$

Specializing to the diagonal limit $\bar{z} \to z$, we have

$$f_{\lambda_1\lambda_2}(z')\big|_{a\to -a} = e^{\pm i\pi\Delta}\,(1 - z)^{2b}\,f_{\lambda_1\lambda_2}(z)\,. \tag{3.28}$$

The factor $e^{\pm i\pi\Delta}$ arises since $z \to z'$ maps $[0, 1) \;\to\; (-\infty, 0]$, with $\pm$ according which side of the branch cut on the negative axis $f_{\lambda_1\lambda_2}(z')$ is evaluated on. This leads to a consistency requirement on the operators D_z. On the one hand, the function $f(z')$ on the LHS is a

solution to $D_{z'} f(z') = 0$ in the z'-coordinate, but at the same time $f(z)$ on the RHS solves $D_z f(z) = 0$. By an explicit computation, it can indeed be shown that the $D_z^{(n)}$ satisfy

$$\begin{aligned}(1-z)^{2b-2} D_z^{(4)} (1-z)^{-2b} &= D_{z'}^{(4)}\big|_{a\to -a}\,,\\ (1-z)^{2b-1} D_z^{(3)} (1-z)^{-2b} &= D_{z'}^{(3)}\big|_{a\to -a}\,.\end{aligned} \tag{3.29}$$

A similar relation can be checked for the exchange $\phi_3(x_3) \leftrightarrow \phi_4(x_4)$, which changes $b \to -b$.

3.3 Frobenius' method

Differential operators of the form (3.22) have regular singular points at $0, \infty, 1$. (This is easiest seen after dividing by $(z-1)^{n-1}$, which brings these operators to their canonical form.) This implies that power series solutions of $D_z^{(n)} u(z) = 0$ with leading behaviour

$$u(z) \underset{z\to z_0}{\sim} (z - z_0)^\alpha\,, \qquad z_0 \in \{0, 1, \infty\} \tag{3.30}$$

can be constructed via Frobenius' method. [5] The characteristic exponents α are determined by indicial equations of n-th order (one for every singular point z_0 separately). We are eventually interested in expansions around $z_0 = 0$, but for completeness we will first classify all characteristic exponents α (also for $z_0 = 1, \infty$), since this is a relatively simple way to characterize the differential operators $D_z^{(n)}$. Finding and solving the indicial equations is straightforward; explicitly, we find that the different roots α are given in terms of Δ, ℓ, a, b, ν by

0	∞	1
Δ	$2a$	0
$2 + 2\nu - \Delta$	$2b$	$-2a - 2b$
$\ell + 1 + 2\nu$	$a + b - \nu$	$-a - b - \nu$
$1 - \ell$	$1 + a + b - \nu$	$1 - a - b - \nu$

(3.31a)

for $D^{(4)}$ (general ℓ), and

0	∞	1
Δ	$2a$	0
$2 + 2\nu - \Delta$	$2b$	$-2a - 2b$
1	$a + b - \nu$	$-a - b - \nu$

(3.31b)

for $D^{(3)}$ ($\ell = 0$ only). As a consistency check, we note that Δ is an exponent for both differential operators.

Let us now return to the case of physical interest, namely to find solutions of the form $f(z) = z^\Delta \sum a_n z^n$. Frobenius' method gives recursion relations by which all the coefficients

5. We refer the reader to [126, 127] for some background about ordinary differential equations.

a_n in (3.9) can be determined from $a_0 = 1$. These recursions, four-term for the general case and three-term for $\ell = 0$, are given in appendix B.

The reader may remark that for particular values of Δ, Frobenius' method breaks down: this can occur when Δ is smaller than one of the other exponents α by an integer. These special cases are treated separately in appendix B.

In section 3.4 we will explain how these and related recursions can be used to efficiently evaluate conformal blocks in the derivative expansion around any point on the diagonal (and in particular the point $z = \bar{z} = 1/2$ relevant for the conformal bootstrap applications).

3.4 Computing conformal blocks and their derivatives efficiently

In this section we will present an efficient algorithm to compute conformal blocks in the derivative expansion around any point $z = \bar{z} = t_0$ on the diagonal. Such expansions form the basic input for the numerical conformal bootstrap algorithms, where $t_0 = \frac{1}{2}$ is normally used. Our algorithm is an extension of the method first used in [7].

Let us now slightly formalize the problem. We start by generalizing the 'near-diagonal' expansion (3.17). If we denote by $h_{m,n}$ conformal blocks derivatives with respect to the coordinates t, s (related by simple rescalings to a, b in [7]), we can write

$$F_{\lambda_1\lambda_2}(z,\bar{z}) = \sum_{m,n\geqslant 0} \frac{1}{m!n!}\, h_{m,n}\, (t-t_0)^m s^n\,, \tag{3.32}$$

where

$$z = t + \sqrt{s}, \quad \bar{z} = t - \sqrt{s} \quad \Leftrightarrow \quad t = (z+\bar{z})/2, \quad s = (z-\bar{z})^2/4. \tag{3.33}$$

The diagonal corresponds to $s = 0$ and (3.17) corresponds to keeping just $n = 0, 1$. Conformal blocks being symmetric in $z \leftrightarrow \bar{z}$, ensures that the expansion is in integer powers of s.

The first observation is that the derivatives in the direction orthogonal to the diagonal (s-derivatives) can be recursively determined from the derivatives along the diagonal. This follows from a so-called Cauchy-Kovalevskaya argument that was used before in Ref. [7]: for completeness, we reproduce it here. The recursion between different derivatives follows from the quadratic Casimir equation in (3.10) and has the following schematic structure:

$$h_{m,n} = \sum_{m'\leqslant m-1} (\ldots) h_{m',n} + \sum_{m'\leqslant m+2} \left[(\ldots) h_{m',n-1} + (n-1)(\ldots) h_{m',n-2}\right]\,. \tag{3.34}$$

The above equation is obtained by inserting the Ansatz (3.32) into the quadric Casimir PDE. The precise coefficients for $a, b = 0$ and for $t_0 = \frac{1}{2}$ were given in [7]; extension to a, b nonzero

and general $0 < t_0 < 1$ is straightforward. By this recursion, moving one unit up in n we lose two units in m. So knowing the derivatives $h_{m,0}$ for $m = 0, \ldots, m_{\max}$ is sufficient to compute $h_{m,n}$ for all $m + 2n \leqslant m_{\max}$. In practical applications of numerical bootstrap, it is common to use the derivatives in such a triangular table with $m_{\max}$ up to O(20) or more.

Hence, we are reduced to computing the derivatives $h_m \equiv h_{m,0}$ along the diagonal. We next observe that h_m satisfy another set of recursion relations as a consequence of the ODEs (3.21). These recursions have the schematic form:

$$m(m-1)(m-2)(m-3)h_m = \sum_{m'=\min(0,m-7)}^{m-1} (\ldots)h_{m'} \quad (\ell = 1, 2, \ldots)\,, \tag{3.35}$$

$$m(m-1)(m-2)h_m = \sum_{m'=\min(0,m-5)}^{m-1} (\ldots)h_{m'} \quad (\ell = 0)\,. \tag{3.36}$$

The coefficients follow trivially from (3.21) so we do not give them here. Assuming that the first few h_m are known (namely for $m = 0, 1, 2, 3$ for general ℓ and $m = 0, 1, 2$ for $\ell = 0$), the rest can be found by these recursions.

Thus, it remains to find a method to compute the derivatives h_m at low m. This can be done as follows. Conformal blocks on the diagonal have an expansion (3.9) around $z = 0$. As we explained in section 3.2, the expansion coefficients a_n are fixed by the ODEs (3.21). The closed-form expressions for a_n are not available, but they can be found up to an arbitrary order via the recursion relations given in appendix B. Crucially, since $z = 0$ is a regular singular point, the single normalization condition $a_0 = 1$ is sufficient to determine all of a_n. This is unlike the recursions (3.35) for derivatives h_n around a regular point $0 < t_0 < 1$ where derivatives up to the equation order minus one have to be supplied as the initial condition.

A natural method to compute the h_m at low m is then just to evaluate a_n up to a sufficiently high order N, and to sum up the series (3.9) by differentiating term by term:

$$h_m = (\partial_z)^m f_{\lambda_1\lambda_2}(z)|_{z=t_0} \approx \sum_{n=0}^{N} a_n(\Delta+n)(\Delta+n-1)\ldots(\Delta+n-m)\, t_0^{\Delta+n-m}\,. \tag{3.37}$$

We propose to use this method but with a small modification, which greatly improves its numerical efficiency. Namely, we will evaluate the conformal blocks and their derivatives expanding not in z but in the variable ρ introduced in the previous chapter. We recall that it is related to z by

$$\rho = \frac{z}{(1+\sqrt{1-z})^2}, \qquad z = \frac{4\rho}{(1+\rho)^2}\,. \tag{3.38}$$

For ρ the points $0, 1, \infty$ are mapped to $0, 1, -1$ and $z \to z' = z/(z-1)$ corresponds to $\rho \to -\rho$. The corresponding expansion coefficients will be denoted b_n:

$$f_{\lambda_1\lambda_2}(\rho) = (4\rho)^\Delta \sum_{n=0}^{\infty} b_n \rho^n, \qquad b_0 = 1\,. \tag{3.39}$$

We also recall that the coefficients a_n grow as Δ^n for large Δ, while b_n remain bounded in this limit. So for large Δ more and more terms will have to be retained in the z-series, while the ρ-series will not suffer from this drawback.

The ODEs (3.21) in the variable ρ take the following form:

$$\mathcal{D}_4 f_{\lambda_1\lambda_2}(\rho) = 0, \qquad \mathcal{D}_3 f_{\lambda\,\lambda}(\rho) = 0, \tag{3.40}$$

where

$$\begin{aligned}
\mathcal{D}_4 = {}& (\rho-1)^3\rho^4(\rho+1)^4\frac{\mathrm{d}^4}{\mathrm{d}\rho^4} + 2(\rho-1)^2\rho^3(\rho+1)^3\big\{(2\nu+5)\rho^2+8S\rho+2\nu-1\big\}\frac{\mathrm{d}^3}{\mathrm{d}\rho^3}\\
&- 2(\rho-1)\rho^2(\rho+1)^2\Big\{[c_2-(\nu+4)(2\nu+3)]\rho^4+4[P-3S(2\nu+3)]\rho^3\\
&\qquad - 2\left[20S^2+2\nu^2+c_2+4P+3\nu-5\right]\rho^2+4[P+S(3-6\nu)]\rho-2\nu^2+c_2+\nu\Big\}\frac{\mathrm{d}^2}{\mathrm{d}\rho^2}\\
&- 2\rho(\rho+1)\Big\{(2\nu+3)[c_2-2(\nu+1)]\rho^6+[12\nu P+6P+8c_2S-8S(\nu+1)(2\nu+3)]\rho^5\\
&\qquad + \left[4\{-4(4\nu+3)S^2-2\nu^2+8P(S-\nu)+\nu+3\}-c_2(2\nu+5)\right]\rho^4\\
&\qquad - 4\left[P(16S-10\nu+5)+2S\left(8S^2+4\nu^2+2c_2-5\right)\right]\rho^3\\
&\qquad + \left[-2\nu c_2+c_2+16P(2S-2\nu+1)-2\left(16S^2+\nu-1\right)(2\nu-1)\right]\rho^2\\
&\qquad + \left[2P(6\nu-1)+8S\left(-2\nu^2+\nu+c_2\right)\right]\rho+c_2+2c_2\nu\Big\}\frac{\mathrm{d}}{\mathrm{d}\rho}\\
&+ (1-\rho)\big\{[c_2(4\nu+2)-c_4]\rho^6+2[-c_4+2c_2(2S+1)(2\nu+1)+4P\nu(2\nu+1)]\rho^5\\
&\quad + \left[c_4-16P(-6\nu S+S+2\nu^2-3\nu)+2c_2\left(16S^2+16S\nu+8S+6\nu-1\right)\right]\rho^4\\
&\quad + 4\left[c_4+2c_2(2S+1)(4S+2\nu-1)+4P\{8S^2+(6-4\nu)S+\nu(2\nu-3)\}\right]\rho^3\\
&\quad + \left[c_4-16P\{-6\nu S+S+\nu(2\nu-3)\}+2c_2\{16S^2+8(2\nu+1)S+6\nu-1\}\right]\rho^2\\
&\quad + 2[-c_4+2c_2(2S+1)(2\nu+1)+4P\nu(2\nu+1)]\rho-c_4+c_2(4\nu+2)\big\},
\end{aligned}$$

and

$$\begin{aligned}
\mathcal{D}_3 = {}& (\rho-1)^2\rho^3(\rho+1)^3\frac{\mathrm{d}^3}{\mathrm{d}\rho^3} + 2(\rho-1)\rho^2(\rho+1)^2\big\{(\nu+3)\rho^2+6S\rho+\nu\big\}\frac{\mathrm{d}^2}{\mathrm{d}\rho^2}\\
&- 2\rho(\rho+1)\big\{(c_2-2\nu-3)\rho^4+4(P-S(2\nu+3))\rho^3\\
&\qquad + \left[-2c_2-8P-2\left(8S^2+\nu\right)+1\right]\rho^2+4[P-2S\nu]\rho+c_2\big\}\frac{\mathrm{d}}{\mathrm{d}\rho}\\
&- 2(\rho-1)\big\{c_2\rho^4+2[2Sc_2+c_2+P+2P\nu]\rho^3\\
&\qquad + 2[4Sc_2+c_2+2P(4S-2\nu+1)]\rho^2+2[2Sc_2+c_2+P+2P\nu]\rho+c_2\big\}.
\end{aligned}$$

They imply recursion relations which determine all b_n starting from $b_0 = 1$. We do not present these recursions here, since they are totally analogous to those for the a_n given and analyzed in appendix B.

Our method for evaluating h_m for low m is thus as follows. First evaluate b_n up to a sufficiently high order N so that the series

$$(\partial_\rho)^m f_{\lambda_1\lambda_2}(\rho)|_{\rho=\rho_0} \approx \sum_{n=0}^{N} b_n(\Delta+n)(\Delta+n-1)\dots(\Delta+n-m)\rho_0^{\Delta+n-m}, \quad \rho_0 \equiv \rho(t_0), \tag{3.41}$$

give a good approximation to the RHS for all $0 \leqslant m \leqslant m_0$, where m_0 is the maximal needed derivative order. The accuracy of this approximation can be controlled via the asymptotics of the b_n coefficients, which can be understood from the recursion relations that they satisfy. For the reasons given above, the needed number of terms N in this series will be much smaller than in (3.35). Via the inverse change of variables $\rho \to z$, the derivatives in z can then be expressed as linear combinations of derivatives in ρ.

3.5 Summary

In this chapter, we focused on a concrete problem in the theory of conformal blocks: the computation of conformal blocks and their derivatives on the diagonal $z = \bar{z}$. The main result of this chapter was that the diagonal contribution $f_{\lambda_1\lambda_2}(z)$ obeys an ODE which is of fourth order for spin $\ell > 0$ and third order for $\ell = 0$. Such differential equations were known before only for spins $\ell = 0, 1$ and only for the case of equal external scalar dimensions $\Delta_1 = \Delta_2$, $\Delta_3 = \Delta_4$ [7]. The quartic Casimir played a key role in deriving these ODEs.

Furthermore, in section 3.4 we proposed an algorithm for an efficient numerical evaluation of conformal blocks and their derivatives around any point on the diagonal, generalizing the method first used in [7] for the case of equal external scalar dimensions. We expect that such an algorithm will prove immediately useful in conformal bootstrap applications.

One particular application of this algorithm involves the d-dimensional Ising model. Starting from [14] and until the publication of this work, all numerical conformal bootstrap studies have focused on correlators with equal external dimensions. The Ising model has both a 'spin' operator σ and an 'energy' operator ϵ as lowest-dimension operators. Using our algorithm, it seems feasible to perform a simultaneous analysis of several four-point functions, e.g. $\langle\sigma\sigma\sigma\sigma\rangle$, $\langle\sigma\sigma\epsilon\epsilon\rangle$, and $\langle\epsilon\epsilon\epsilon\epsilon\rangle$. Conformal blocks needed for the $\langle\sigma\sigma\epsilon\epsilon\rangle$ correlator could not be computed before, as they involve unequal external dimensions in two out of three OPE channels. [6]

This point also marks the end of the first part of this thesis, which focuses on conformal blocks: all following chapters solely focus on the Truncated Conformal Space Approach. Some closing remarks concerning conformal blocks are presented in the Discussion, section 8.

6. **Note added**: this analysis has been done (in $d = 3$) in 2014 by Kos, Poland and Simmons-Duffin [9, 128]. The results described in the previous chapter played an important role, as they paved the way to recursion relations used by these authors [103].

Chapter 4

TCSA for scalar fields $d > 2$ dimensions [1]

4.1 Introduction

In the introduction to this thesis, we have set the stage for the Truncated Conformal Space Approach (TCSA). In the rest of this thesis, we intend to use this method to study two different RG flows starting at the free, massless scalar CFT. Because these computations are somewhat involved, the current chapter is intended as a first introduction to the TCSA. It is organized as follows: we start in section 4.2 with a general discussion of the TCSA. Section 4.3 is devoted to the free massless scalar in d dimensions. We focus on the CFT description of the spectrum of theory, via radial quantization. We touch on various technical issues: the construction of the Hilbert space using a graph theory method, the computation of the Gram matrix and the fact the Hilbert space in question has various redundancies (null states) for integer d. As a byproduct of this discussion, we show in section 4.3.5 that the free massless scalar in a fractional number of dimensions is a non-unitary theory—its Hilbert space contains negative-norm states.

4.2 Truncated Conformal Space Approach: general setup

We would like to study an RG flow obtained by perturbing a d-dimensional CFT by a scalar operator $\mathcal{V}$ (assumed to be primary) that is *relevant*, e.g. that has scaling dimension $\Delta_{\mathcal{V}} < d$. [2] How can one find an appropriate scheme to deal with such RG flows? First, we

1. This and all subsequent chapters are based on Ref. [129], written in collaboration with S. Rychkov and B. C. van Rees.
2. The generalization to several perturbing operators is straightforward.

remark that a CFT by itself does not need to be regulated in the UV. In fact, many possible regulators (e.g. putting the theory on a lattice) will break the conformal group down to a smaller group, even before introducing the perturbation $\mathcal{V}$.

We do need to regulate the CFT in the infrared. Notice that we already know examples of IR regulators that preserve conformal invariance: using Weyl invariance, we can put the theory on any finite, conformally flat geometry. On such a background, conformal invariance is only broken when the perturbation $\mathcal{V}$ is turned on.

The cylinder $\mathbb{R} \times S^{d-1}$ is a particularly natural choice, because it manifestly preserves $SO(d)$ invariance. Furthermore, radial quantization endows the cylinder with a Hamiltonian, which maps to the CFT dilatation generator in flat space. The CFT local operators $\mathcal{O}_i$ of dimensions Δ_i map to states $|i\rangle$ on the cylinder. In the theories we will be considering here, there will be a unique ground state corresponding to the unit operator, with energy zero. [3]

The Hamiltonian of the perturbed theory on the cylinder is

$$H = H_{\text{CFT}} + V, \quad V = \lambda \int_\Sigma \mathcal{V}(t=0,\mathbf{n}) \tag{4.1}$$

where the coordinates $(t, \mathbf{n})$ parametrize the cylinder and the integral is taken over the timeslice $\Sigma \cong S^{d-1}$:

$$\int_\Sigma f(t,\mathbf{n}) \equiv \int_{S^{d-1}} f(t,\mathbf{n})\, R^{d-1} \mathrm{d}\mathbf{n}. \tag{4.2}$$

By dimensional analysis, the coupling λ has mass dimension $[\lambda] = d - \Delta_{\mathcal{V}}$. The key idea is to think about this Hamiltonian as an infinite matrix in the Hilbert space of unperturbed CFT states $|i\rangle$. The CFT Hamiltonian in this basis is simply related to the CFT operator dimensions: [4]

$$H_{\text{CFT}}|i\rangle = R^{-1}\Delta_i\, |i\rangle. \tag{4.3}$$

The matrix $\langle i|V|j\rangle$ decomposes as factor into a prefactor that depends on λ and R and a coefficient $f_{\mathcal{O}_i^\dagger \mathcal{V} \mathcal{O}_j}$

$$\langle i|V|j\rangle = R^{-1}(\lambda R^{d-\Delta_{\mathcal{V}}})\, f_{\mathcal{O}_i^\dagger \mathcal{V} \mathcal{O}_j} \tag{4.4}$$

that is determined by a flat-space CFT three-point function:

$$f_{\mathcal{O}_i^\dagger \mathcal{V} \mathcal{O}_j} \equiv R^{\Delta_{\mathcal{V}}} \int_{S^{d-1}} \langle i|\mathcal{V}(t=0,\mathbf{n})|j\rangle \, \mathrm{d}\mathbf{n} \tag{4.5a}$$

$$= \lim_{u\to 0} \int \delta(|x|-1)\, \langle [\mathcal{O}_i(u)]^\dagger \mathcal{V}(x) \mathcal{O}_j(0)\rangle \, \mathrm{d}^d x. \tag{4.5b}$$

In passing from Eq. (4.5a) to (4.5b) we have used that the scalar primary $\mathcal{V}$ transforms as

$$\mathcal{V}(t=0,\mathbf{n}) = R^{-\Delta_{\mathcal{V}}}\, \mathcal{V}(x=\mathbf{n}) \tag{4.6}$$

3. We will ignore the CFT Casimir energy density, nonzero in even dimensions. If needed, it's trivial to take it into account because it just shifts all eigenstates by const./R.

4. The actual matrix elements of the CFT Hamiltonian, given by $\langle i|H_{\text{CFT}}|j\rangle = R^{-1}\Delta_j \langle i|j\rangle$, are proportional to the Gram matrix $G_{ij} = \langle i|j\rangle$, see Sec. 4.3.3. In an orthonormal basis, both the Gram matrix and the matrix $\langle i|H_{\text{CFT}}|j\rangle$ are diagonal.

when mapped to flat space. In particular, it follows from Eq. (4.5b) that $f_{\mathcal{O}_i^\dagger \mathcal{V} \mathcal{O}_j}$ does not depend on R.

The dimensionless coupling $\lambda R^{d-\Delta_\mathcal{V}} =: \widetilde{\lambda}(R)$ from Eq. (4.4) determines whether the perturbation V is small. To be precise, the coupling λ defines an IR scale Λ_{IR} for the RG flow:

$$\Lambda_{\mathrm{IR}} \sim \lambda^{\frac{1}{d-\Delta_\mathcal{V}}} . \tag{4.7}$$

For $R \ll \Lambda_{\mathrm{IR}}^{-1}$ we are close to the UV regime: the coupling $\widetilde{\lambda}(R) \sim (R\,\Lambda_{\mathrm{IR}})^{d-\Delta_\mathcal{V}}$ is small, so V is a small correction to H_{CFT} and perturbation theory is reliable. To probe the IR physics, we must take instead

$$R \gg \Lambda_{\mathrm{IR}}^{-1} . \tag{4.8}$$

Here V cannot be treated as a small perturbation, and the right thing to do would be to diagonalize the whole Hamiltonian $H_{\mathrm{CFT}} + V$. But how can we do this given that this matrix is infinite?

The proposal by Yurov and Al. Zamolodchikov in Ref. [23] is to introduce a UV cutoff Λ_{UV} and to *truncate* the Hilbert space keeping only the states below this maximal energy:

$$E_i \leqslant \Lambda_{\mathrm{UV}} . \tag{4.9}$$

If the cutoff is chosen so that

$$\Lambda_{\mathrm{UV}} \gg \Lambda_{\mathrm{IR}} , \tag{4.10}$$

we can hope that the IR physics is not much affected. Let us furthermore assume that the UV CFT has a discrete spectrum, which will be true for most CFTs of interest. In this case, the truncated Hilbert space is finite-dimensional, H is a finite matrix and can be numerically diagonalized.

Many properties of a quantum field theory are encoded in its finite-volume spectrum, for example:

- the ground state dependence on R gives the vacuum energy density;
- the number of ground states encodes the symmetry breaking pattern (in the case of a global symmetry of the UV theory that is broken spontaneously in the IR);
- the excited states give the massive spectrum of the theory, including one-particle, many-particle, and bound states;
- for flows ending in conformal fixed points we can extract the spectrum of IR operator dimensions.

The truncation of the Hilbert space to states with energy $E \leqslant \Lambda_{\mathrm{UV}}$ necessarily induces truncation errors, which we expect to decrease when the cutoff Λ_{UV} is increased. However, increasing the cutoff also entails working with larger Hilbert spaces and requires more computational resources. The success of the TCSA therefore depends on whether we can get 'reasonable' results with numerically tractable Hilbert space sizes.

Both the original paper [23] and all the subsequent TCSA literature known to us consider $d = 2$. In two dimensions, it is very natural to put a QFT on $\mathbb{R} \times S^1$: this simply entails compactifying the spatial coordinate x as $x \sim x + 2\pi R$. The analog of this in $d > 2$ dimensions means compactifying on the torus T^{d-1}, which is not equivalent to the sphere S^{d-1}. In fact, there are many inequivalent ways to put a theory on a finite volume in $d > 2$: radial quantization requires however that we choose the cylinder $\mathbb{R} \times S^{d-1}$.

4.2.1 A case study for TCSA in d dimensions

In this thesis we will apply TCSA to study the Landau-Ginzburg theory, i.e. the free massless scalar theory perturbed by a linear combination of $:\phi^2:$ and $:\phi^4:$ operators. This is perhaps the simplest non-trivial d-dimensional RG flow. A priori, we are interested in $2 \leqslant d < 4$. However, in this first work we will have to stay away from the extremes of this range, since the TCSA analysis becomes complicated near these extremes.

The reason why d close to 2 is hard for TCSA is that the scalar dimension $\Delta_\phi = (d-2)/2$ approaches zero in this limit, and the free scalar spectrum becomes dense and eventually continuous in $d = 2$. [5] To have a sufficiently sparse spectrum, we will keep d not too close to 2.

On the other hand, the operator ϕ^4 becomes marginal in $d = 4$ dimensions. As we will see, TCSA works best for strongly relevant perturbing operators $\mathcal{V}$. The more relevant the operator is, the better-behaved perturbation problem is in the UV. The best situation is realized when

$$\Delta_{\mathcal{V}} < d/2\,, \tag{4.11}$$

which for the perturbations considered here means

$$d < 8/3 \quad (\mathcal{V} = :\phi^4:), \qquad d < 4 \quad (\mathcal{V} = :\phi^2:)\,. \tag{4.12}$$

When (4.11) is satisfied, the perturbation is simply UV-finite. At $\Delta_{\mathcal{V}} = d/2$ the vacuum energy becomes divergent, as can be seen at second order in perturbation theory. Other UV divergences appear if we further increase $\Delta_{\mathcal{V}}$, and these also affect the couplings of nontrivial local operators (including $\mathcal{V}$ itself). These short-distance divergences have to be handled in the usual QFT way – by adding counterterms. In this first work we would like to avoid dealing with UV divergences, so we will stay within the bounds (4.12). This does not mean however that we will altogether ignore cutoff dependence. Even in the range (4.12) when there are no UV divergences, the accuracy of the method for a finite cutoff will be influenced by power-suppressed corrections. This important issue will be discussed below.

5. The paper [130] discussing the two-dimensional Landau-Ginzburg theory using the TCSA (but in a different basis of operators) was submitted to the arXiv the same day as our work. **Note added**: an alternative analysis of the 2d Landau-Ginzburg flow, starting at the theory of a free massive boson, has been done in Ref. [131].

As the reader must have noticed, we are considering the case of fractional d on equal footing with the physically interesting integer d. We will see that the TCSA problem allows a natural continuation to general d.

4.3 Free scalar in d dimensions

In this section we will discuss the UV CFT at which our RG flows will be starting—the free massless scalar CFT in d dimensions, which has already been discussed in section 1.4.3. These results presented here lay the groundwork for the numerical investigations and for the renormalization, studied in the subsequent sections.

The local operators of the free boson theory are built by taking products of the fundamental field ϕ and of its derivatives, e.g.

$$:\partial^{n_1}\phi\cdots\partial^{n_k}\phi: \qquad (n_j \geqslant 0) \tag{4.13}$$

where some or all of the vector indices on the derivatives may be contracted. The operators are all inserted at the same point, and the normal-ordering sign means as usual that we do not consider Wick contractions within the operator when computing its correlation functions with other operators.

We can classify the operators according to their spin, i.e. their $SO(d)$ representation. When we put the theory on the cylinder, the spin of an operator becomes the spin of the state into which it maps under the state-operator correspondence. Eventually we will perturb the theory by adding to the Hamiltonian an integral of a scalar operator over the sphere, as in Eq. (4.1). Since this perturbation preserves rotation symmetry of the sphere, the Hamiltonian matrix will split into blocks corresponding to the states of the same spin.[6] Crucially, $SO(d)$ invariance is not broken by introducing a cutoff Λ_{UV}, because rotations do not mix states with different energy.

The scalar sector contains most of the states we are interested in: the ground state, one-particle states at rest, and two-particle states in the center-of-mass frame. In the large-R limit, many of the states of higher spin will correspond to spin-0 states slightly boosted along the sphere. In principle, there could also exist additional states with intrinsic spin, which could be thought of as bound states of fundamental scalars at strong coupling. This would be analogous to vector mesons in gauge theories with matter. In this thesis we however focus exclusively on the scalar sector.

The scalar boson (with arbitrary ϕ^2 and ϕ^4 couplings) has an additional parity symmetry P that commutes with the TCSA Hamiltonian. States are therefore classified not only by

6. In some 2d TCSA papers, such as Ref. [24], the term 'momentum' rather than 'spin' is used.

their spin quantum numbers, but also by their parity. As a simplifying technical assumption, we will restrict ourselves to states with $P = +1$.

4.3.1 Constructing the Hilbert space

We now turn our attention to the Hilbert space of the free boson. By the state-operator correspondence, introducing a UV cutoff Λ_{UV} is equivalent to only keeping states that correspond to operators with dimension

$$\Delta \leqslant \Delta_{\max} \equiv R\,\Lambda_{\mathrm{UV}}. \tag{4.14}$$

Constructing the scalar, parity-even sector of the truncated Hilbert space is a well-defined group theory problem, namely to find all parity-even scalars of scaling dimension $\Delta \leqslant \Delta_{\max}$ in the tensor product of the spin-j tensors

$$\partial_{\mu_1} \cdots \partial_{\mu_j} \phi. \tag{4.15}$$

It seems however more convenient to use a graph theory approach. Notice that a basis of scalar, parity-even operators is formed by operators of the form Eq. (4.13) having all indices contracted. Such an operator can be drawn as a graph, by mapping every ϕ to a separate vertex and by drawing an index contraction as an edge between two vertices. As an example, the graph corresponding to the operator $:\phi^2\,\phi_{,\mu}\,\phi_{,\mu\nu\rho}\,\phi_{,\nu\rho}:$ is displayed below:

Because of the equation of motion $\partial^2\phi = 0$, we can ignore operators containing contractions of derivatives acting on the same ϕ. As in the example above, two vertices may be connected by more than one edge. In graph theory, graphs obeying these conditions are called *multigraphs without loops*.[7] Depending on how derivatives are contracted, the graphs may have one or several connected components. Notice finally that isomorphic graphs correspond to identical operators, so they should not be counted separately.

Using this graph theory formalism, it is straightforward to find all scalar, parity-even operators $\{\mathcal{O}_i\}$ below a certain cut-off dimension $\Delta_{\max}$. Some details are given in appendix C. By the state-operator correspondence, the truncated Hilbert space $\mathcal{H}$ is spanned by the states $|\mathcal{O}_i\rangle = \mathcal{O}_i(0)|0\rangle$. For $d = 3$, the spin-0 states with lowest energy are for example

$$|0\rangle,\ |\phi\rangle,\ |\phi^2\rangle,\ \ldots\ ,|\phi^5\rangle,\ |(\partial_\mu\phi)^2\rangle,\ \ldots. \tag{4.16}$$

7. We can also replace n parallel edges by a single edge with n as a label. Then our graphs become simple edge-colored graphs.

Finally, we remark that the discussion above focussed on parity-even operators. Parity-odd operators involve a contraction with the Levi-Civita tensor $\epsilon_{\mu_1\cdots\mu_d}$. Notice that the $P=-1$ operators have quite high scaling dimensions, e.g. the lowest dimension one in $d=3$ is

$$\mathcal{O}_- = \epsilon^{\alpha\beta\gamma}\delta^{\mu_1\mu_2}\delta^{\nu_1\nu_2}\,\phi_{,\alpha}\,\phi_{,\beta\mu_1}\,\phi_{,\gamma\mu_2\nu_1}\,\phi_{,\nu_2} \tag{4.17}$$

which has dimension $[\mathcal{O}_-]=9$.

4.3.2 Primaries and descendants

CFT local operators can be divided into primaries and descendants (cf. section 1.3.2). The basis for the Hilbert space on the cylinder includes of course all states, those corresponding to primaries and to descendants. In 2d TCSA applications, it is customary to organize the Hilbert space into a set of primary states $|h_i,\bar{h}_i\rangle$ and descendant states, which are obtained by acting with the Virasoro generators $L_{-1},L_{-2},\ldots$ and $\bar{L}_{-1},\bar{L}_{-2},\ldots$. In that case, matrix elements involving descendants can be reduced using the Virasoro algebra to matrix elements $\langle h_1,\bar{h}_1|\mathcal{V}|h_2,\bar{h}_2\rangle$ that involve only primaries [12]. The latter are OPE coefficients of the UV CFT, assumed to be known. This way, all matrix elements $\langle i|V|j\rangle$ can be computed using some straightforward computer algebra [132]. In particular, this strategy works for strongly coupled CFTs, such as the Lee-Yang model [23] and the tricritical Ising model [24].

It seems natural to adapt this strategy to the conformal algebra in $d>2$ dimensions, where descendants are generated only by P_μ. However, the Hilbert space basis of graph theory states is not suited to this method, since a generic state $|\mathcal{O}_i\rangle\in\mathcal{H}$ is neither a primary nor a descendant, but a linear combination of both primary and descendant states. In principle, one could with some additional work classify all states in terms of primaries and descendants and imitate the 2d approach to compute all matrix elements. We will follow an alternative approach, which consists of working directly with the graph theory states $|\mathcal{O}_i\rangle$. This is possible because in our case the UV CFT is *free*, and all matrix elements $\langle\mathcal{O}_i|V|\mathcal{O}_j\rangle$ can be evaluated using Wick's theorem, bypassing the use of the conformal algebra.

Let us finally remark that the current mathematical understanding of the underlying algebraic structure for CFTs in fractional d appears to be rather incomplete. In practice, the computations in this thesis involve only scalar operators, which have all indices contracted; such computations can be done directly for fractional d by setting $\Delta_\phi=(d-2)/2$ and $\delta_\mu{}^\mu=d$. For computations involving non-scalar operators, a better understanding of $\mathfrak{so}(d)$ representation theory for fractional d may be necessary.

4.3.3 Gram matrix

Although the above construction provides a basis $|i\rangle = |\mathcal{O}_i\rangle$ for the truncated Hilbert space $\mathcal{H}$, this basis has no reason to be orthonormal or even orthogonal. Rather, we will have a nontrivial Gram matrix $G_{ij} \equiv \langle i|j\rangle$. This Gram matrix is an essential ingredient in the existing implementations of the TCSA in $d = 2$. In our case, the Gram matrix will not play a crucial role. In fact, as we will see below, the perturbed spectrum computation can be organized without using the Gram matrix at all. Nevertheless, the Gram matrix is a conceptually important object, so we would like to discuss in some detail its definition and evaluation.

As usual in radially quantized CFT, the map from a state $|\mathcal{O}_i\rangle$ to its conjugate $\langle\mathcal{O}_i|$ is defined with the help of the inversion transformation $\mathrm{I} \ : \ x_\mu \to x_\mu/x^2$ (see section 1.6.2). The Gram matrix is then defined as

$$G_{ij} = \lim_{x\to 0}\langle[\mathcal{O}_i(x)]^\dagger \mathcal{O}_j(x)\rangle\,, \tag{4.18}$$

where the conjugate operator $[\mathcal{O}_i(x)]^\dagger$ is inserted at the point $x' = \mathrm{I}(x)$. The rules for construction of the conjugate operators are as follows (ϕ is the fundamental scalar; $\mathcal{A}, \mathcal{B}$ any two fields in the theory):

1. $[\phi(x)]^\dagger = |x|^{-2\Delta_\phi}\,\phi\,(\mathrm{I}(x))$ (since ϕ is a primary),
2. $[\mathcal{A}(x)_{,\mu}]^\dagger = \frac{\partial}{\partial x^\mu}[\mathcal{A}(x)]^\dagger$ (since conjugation is antilinear),
3. $[:\mathcal{A}(x)\mathcal{B}(x):]^\dagger = \ :[\mathcal{A}(x)]^\dagger[\mathcal{B}(x)]^\dagger:$.[8]

Starting from Rule 1 and using Rule 2 repeatedly we can conjugate all derivatives of ϕ. Then by applying Rule 3 we can conjugate all normal-ordered products of derivatives, and in particular all scalar operators forming our basis.

Computation of the Gram matrix is thus reduced to evaluating two-point functions of operators made of several ϕ's acted upon by various derivatives. In principle, this is straightforward to do using Wick's theorem. The number of Wick contractions to perform can be dramatically reduced by using selection rules. To begin with, the only nonzero entries are those for which (a) $\mathcal{O}_i$ and $\mathcal{O}_j$ contain equal number of ϕ's , and (b) $\Delta_i = \Delta_j$. These two rules are subsumed by the following much more powerful rule. Let $N_\ell(\mathcal{O})$ be the number of times the ℓ^{th} derivative $\partial^\ell\phi$ occurs in the operator $\mathcal{O}$ (irrespectively of how its indices are contracted). Then the Gram matrix entry $\langle\mathcal{O}_i|\mathcal{O}_j\rangle$ can be nonzero only if

$$N_\ell(\mathcal{O}_i) = N_\ell(\mathcal{O}_j) \text{ for all } \ell = 0, 1, 2\ldots \tag{4.19}$$

8. To show this, start with $[\mathcal{A}(x)\mathcal{B}(y)]^\dagger = [\mathcal{A}(x)]^\dagger[\mathcal{B}(y)]^\dagger$, where the operators are inserted at the same radial quantization "time", so that no ordering issue arises. From here by induction in the number of fundamental fields we get $[:\mathcal{A}(x)\mathcal{B}(y):]^\dagger = \ :[\mathcal{A}(x)]^\dagger[\mathcal{B}(y)]^\dagger:$, and Rule 3 follows by taking the coincident point limit.

Physically, the selection rule (4.19) can be understood via canonical quantization, where N_j measures the occupation number of oscillators of spin ℓ – the selection rule is then a direct consequence of $SO(d)$ invariance. In practice, Eq. (4.19) implies that the Gram matrix is block diagonal, where the blocks correspond to sectors that have *all* occupation numbers $N_1, N_2, \ldots$ identical.

Putting it all together, the Gram matrix is thus evaluated as follows. First one computes the overlaps

$$\langle \partial^\ell_{\{\mu\}} \phi | \partial^\ell_{\{\nu\}} \phi \rangle \,, \tag{4.20}$$

by using the above prescription, or by using the conformal algebra, as explained e.g. in [21]. These are particular invariant tensors, symmetric and traceless in both groups of indices $\{\mu\}, \{\nu\}$. Overlaps between general scalar states are then computed by contracting the basic overlaps (4.20) between their constituents. Some additional details are given in appendix C.

Using this direct algorithm, we could compute the Gram matrix up to a rather high cutoff in operator dimension ($\Delta_{\max} = 23$ in $d = 4$). An alternative, indirect, method for computing the Gram matrix will be described in section 4.4.3. In any case, as we will see below, the spectrum computations can be organized avoiding the use of the Gram matrix.

4.3.4 Null states in integer d

Although the Gram matrix G_{ij} is non-trivial, it is natural to expect it to be positive-definite, in which case the states $|i\rangle$ can be made orthonormal by a suitable change of basis $|i\rangle \to U_i{}^j |j\rangle$. This turns out to be false: for integer $d \geqslant 3$, some states $|\chi\rangle$ in the Hilbert space are *null*, meaning that they have zero overlap with any other state $|\psi\rangle$ in the theory, i.e. $\langle \psi | \chi \rangle = 0$ for all states $\langle \psi |$. In particular, a null state has zero norm. The Gram matrix G_{ij} provides a simple way to characterize null states: a state $|\chi\rangle = \chi^i |i\rangle$ is null if and only if $G_{ij}\chi^j = 0$. Furthermore, the selection rule (4.19) implies that it is sufficient to check every block of the Gram matrix (with definite occupation numbers N_j) separately for the presence of null states.

Before we explain how to resolve this issue, we will discuss two simple examples of null states in $d = 3$. The simplest null state occurs in the sector with $N_2 = 4$ and $N_j = 0$ for all other j. This sector consists of two states:

$|1\rangle =$  , $\quad |2\rangle =$  , (4.21)

which have scaling dimension $\Delta = 4 + 2d \to 10$ in $d = 3$. Indeed, the Gram matrix in this sector

$$\begin{pmatrix} \langle 1|1\rangle & \langle 1|2\rangle \\ \langle 2|1\rangle & \langle 2|2\rangle \end{pmatrix} = \begin{pmatrix} 362880 & 181440 \\ 181440 & 90720 \end{pmatrix} \qquad (d = 3) \,, \tag{4.22}$$

has a null eigenvector $|\chi_1\rangle = |1\rangle - \frac{1}{2}|2\rangle$. To interpret this null state, we will rewrite the states $|1\rangle$ and $|2\rangle$ in terms of the field ϕ and its derivatives. Using the shorthand notation $\mathbf{M}_{\mu\nu} = \phi_{,\mu\nu}$, we have

$$|1\rangle = |\text{tr } \mathbf{M}^4\rangle, \quad |2\rangle = |(\text{tr } \mathbf{M}^2)^2\rangle. \tag{4.23}$$

The fact that $|\chi_1\rangle$ is null can now be proven from the properties of the matrix $\mathbf{M}$. In fact, the Cayley-Hamilton theorem asserts that $\mathbf{M}$ obeys a trace relation [9]

$$\mathbf{M}^3 - \tfrac{1}{2}(\text{tr } \mathbf{M}^2)\,\mathbf{M} - \tfrac{1}{3}(\text{tr } \mathbf{M}^3)\,\mathbb{1}_{3\times 3} = 0 \qquad (\text{tr } \mathbf{M} = 0, d = 3). \tag{4.24}$$

By multiplying the above relation with $\mathbf{M}$ and taking a trace, we immediately recover the fact that $|\chi_1\rangle$ is null.

Starting from the Cayley-Hamilton formula (4.24), it is easy to find many more null states. By for example multiplying it from both sides with the vector $\mathbf{V}_\mu = \phi_{,\mu}$, we find a second null state

$$|\chi_2\rangle = |\mathbf{V}\cdot\mathbf{M}^3\cdot\mathbf{V}\rangle - \tfrac{1}{2}|\mathbf{V}\cdot\mathbf{M}\cdot\mathbf{V}\,(\text{tr } \mathbf{M}^2)\rangle - \tfrac{1}{3}|\mathbf{V}\cdot\mathbf{V}\,(\text{tr } \mathbf{M}^3)\rangle \tag{4.25}$$

of dimension $\Delta = 3 + 5d/2 \to 21/2$ in $d = 3$. The same result can of course be obtained by calculating that $|\chi_2\rangle$ is a null eigenstate of the Gram matrix. Null states continue to appear at dimension $\Delta \geqslant 11$. [10]

Let us remark that the situation in integer $d \geqslant 4$ is completely analogous to the 3d case. At least one class of null states in integer d can be generated by the trace relation

$$\mathbf{M}^d - \tfrac{1}{2}(\text{tr } \mathbf{M}^2)\,\mathbf{M}^{d-2} - \tfrac{1}{3}(\text{tr } \mathbf{M}^3)\,\mathbf{M}^{d-3} + \ldots + c\,\mathbb{1}_{d\times d} = 0 \qquad (\text{tr } \mathbf{M} = 0). \tag{4.26}$$

The coefficient $c = (-1)^d \det \mathbf{M}$ in this equation can be written in terms of the traces $\text{tr } \mathbf{M}^2, \ldots, \text{tr } \mathbf{M}^d$. As in $d = 3$, we make no attempt to systematically describe all null states in integer $d > 3$.

The above discussion means that the Hilbert space $\mathcal{H}$ of graph theory states has various redundancies in integer d, originating from trace relations. These redundancies are an artefact of our description of the Hilbert space: the null states themselves are unphysical and do not contribute to correlation functions or matrix elements. As usual, the Hilbert space $\mathcal{H}'$ of physical states is obtained by modding out null states: $\mathcal{H}' = \mathcal{H}/\sim$, where

$$|\psi\rangle \sim |\psi\rangle + |\text{null}\rangle. \tag{4.27}$$

It is easy to see that the Gram matrix restricted to $\mathcal{H}'$ is positive-definite. In integer d, the original Hilbert space $\mathcal{H}$ should be thought of as an *extended* Hilbert space, which contains both physical and null states.

9. We remark that the matrix elements $\mathbf{M}_{\mu\nu}$ are operator-valued rather than c-numbers – in particular Eq. (4.24) should be understood as an operator equation in radial quantization.

10. We have not investigated whether all null states in $d = 3$ follow from the trace relation (4.24).

It may be interesting to compare the relative size of the Hilbert spaces $\mathcal{H}'$ and $\mathcal{H}$ for a given cutoff. In Fig. 4.1, we therefore display the number $N_0(\Delta)$ of physical states and the *total* number of states (both physical and null) at a given dimension Δ (restricted to the spin-0, $P = +1$ sector). The proportion of null states grows quickly: at $\Delta = 18$, which is the maximal cutoff we will be working with, about a quarter of all states are null.

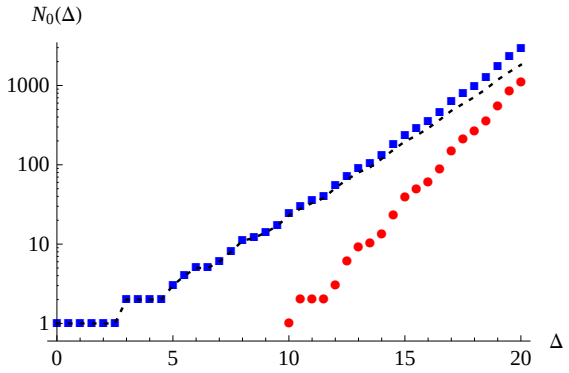

Figure 4.1: The number of scalar, parity-even states $d = 3$ (note the logarithmic scale). Blue squares: all states (physical + null). Red dots: null states. Black dotted curve: only physical states.

4.3.5 Non-unitarity at fractional d

The above discussion of null states raises an interesting question: what is the precise fate of the null states when one passes from integer d to a nearby fractional d? As we mentioned, these states are then no longer null, but are they positive- or negative-norm? We claim that some of these states acquire a negative norm.

To see a concrete example, let us take the operator $\mathcal{O} = \text{tr}\,\mathbf{M}^4 - \frac{1}{2}\,\text{tr}\,\mathbf{M}^2$ that corresponded to the first 3d null state $|\chi_1\rangle$ from section 4.3.4. By an explicit computation, its two point function for general d is given by

$$\langle \mathcal{O}(x)\mathcal{O}(0)\rangle = C(d-3)(d-2)^5(d-1)^2d^5(d+1)(d+2)(3d+8)|x|^{-2\Delta_\mathcal{O}}, \qquad C > 0\,. \quad (4.28)$$

Notice that the prefactor has zero at $d = 3$, which is of first order. For $2 < d < 3$ the two point function of $\mathcal{O}$ is negative, and so $\mathcal{O}$ must have an overlap with a negative-norm state. This example can be easily generalized to show that there are negative norm states for any fractional d.[11]

11. This argument is reminiscent of how Ref. [133] showed that analytic continuations of $O(n)$ models to fractional n contain negative-norm states.

Alternatively, we can compute the Gram matrix in the sector of $\mathcal{O}$ for general d:

$$8(d-2)^4(d-1)d^2(d+2)\begin{bmatrix} 4d^2\left(d^2+d+2\right) & 4d\left(2d^2+3d-6\right) \\ 4d\left(2d^2+3d-6\right) & d^4+5d^3-6d^2-36d+72 \end{bmatrix}. \tag{4.29}$$

Notice that this reduces to the matrix from Eq. (4.22) when for $d \to 3$. Substituting $d = 3-\epsilon$, one computes that one of the eigenvalues of the above matrix is $-31104\epsilon + \mathrm{O}(\epsilon^2)$, which is negative for sufficiently small $\epsilon > 0$.

The presence of negative-norm states means that the *free scalar theory in fractional d is not unitary*. To our knowledge, this observation has not been made before, although theories in fractional dimensions have been extensively studied, especially in relation to critical phenomena, where they form the basis of the epsilon expansion. As we will see below in section 7.3, the lack of unitarity will lead to the presence of complex energy eigenvalues, once the free theory is perturbed by the quartic coupling. However, the mass term alone leaves all energy levels real, as follows from a canonical quantization argument – see section 5.1.

It has to be said that the first negative norm state has a quite high dimension:

$$\Delta_{\text{neg}} = \begin{cases} 8+4\Delta_\phi & (2<d<3)\,, \\ 10+5\Delta_\phi & (3<d<4)\,. \end{cases} \tag{4.30}$$

This must be the reason why they have not been noticed until now. Since the density of states grows exponentially fast with dimension, a few negative norm states at high dimensions probably do not have a strong effect on the low-energy physics. In a recent conformal bootstrap study of the Wilson-Fisher fixed point in fractional dimensions [102] it was assumed that these theories were unitary, and very reasonable results were obtained. [12]

4.4 TCSA eigenvalue problem

4.4.1 Simple versus generalized eigenvalue problem

Before turning to the calculation of the matrix elements $\langle i|V|j\rangle$, it will be convenient to formally state the TCSA eigenvalue problem. Energy levels on the cylinder are solutions of the eigenvalue problem

$$H|\psi\rangle = E|\psi\rangle\,. \tag{4.31}$$

We will be looking for scalar eigenstates, expanding them in a basis of states $|j\rangle$:

$$|\psi\rangle = c^j|j\rangle \tag{4.32}$$

12. More evidence for the mildness of the unitarity violation is provided by recent calculation [134] of the free energy F of the free scalar and the Wilson-Fisher fixed point on S^d for non-integer d. It was found that F_d changes monotonically along the flow, just as for unitary theories in integer dimensions.

The states $|j\rangle$ will be in one-to one correspondence with the scalar local operators of the UV CFT (in this thesis, the free massless scalar theory). The Hamiltonian in this basis is represented by a matrix:

$$H|j\rangle = H^i{}_j|i\rangle\,. \tag{4.33}$$

In terms of this matrix, Eq. (4.31) becomes a simple eigenvalue problem

$$H^i{}_j\, c^j = E c^i\,. \tag{4.34}$$

Notice that the matrix $H^i{}_j$ is not hermitian. To transform the problem to a more familiar form, we consider the matrix elements

$$H_{ij} = \langle i|H|j\rangle\,. \tag{4.35}$$

We of course have

$$H_{ij} = G_{ik}H^k{}_j, \tag{4.36}$$

where $G_{ik} = \langle i|k\rangle$ is the Gram matrix discussed above. The matrix G_{ij} is hermitian, and H_{ij} is hermitian if the Hamiltonian is so as well, which is the case for the Landau-Ginzburg flows with real couplings considered here. Actually, for the operator bases considered in this work, these matrices will be real symmetric. We then have an equivalent symmetric generalized eigenvalue problem:

$$H_{ij}\, c^j = E\, G_{ij}\, c^j\,. \tag{4.37}$$

In most existing $d = 2$ TCSA implementations we are aware of, one starts by computing the matrices G_{ij} and H_{ij}, which naturally leads to the generalized eigenvalue problem (4.37). One then usually multiplies both sides by G^{-1} and transform to (4.34). [13] Here, we will choose an alternative path. Namely, we will directly compute the matrix $H^i{}_j$ and find eigenvalues from (4.34). The method for computing $H^i{}_j$ is described below in section 4.4.3.

4.4.2 Working in the presence of null states

As mentioned in section 4.3.4, the Hilbert space $\mathcal{H}$ of all graphs contains null states in integer d, arising from trace relations. When doing computations in a particular integer dimension $n \in \mathbb{N}$, it seems natural to work in a basis of physical states $\mathcal{H}'$ which is smaller than $\mathcal{H}$. However, when passing to fractional $d = n \pm \epsilon$, the trace relations cease to exist: consequently, all non-isomorphic graphs give rise to inequivalent states. In practice, this approach makes it difficult to compare results in integer and fractional dimensions: computing e.g. a spectrum in $d = 3$ dimensions requires working in a completely different basis than in $d = 3 \pm \epsilon$ dimensions. For simplicity, we therefore choose to work in the full

13. Strictly speaking, this is not necessary, since numerical methods for solving generalized eigenvalue problems are readily available.

Hilbert space $\mathcal{H}$ *both for integer and fractional* d. For integer d, this approach means that several unphysical states will appear in the spectrum. [14]

In presence of null states the discussion of section 4.4.1 needs to be reconsidered. In particular, the Hamiltonian matrix becomes ambiguous in integer d, since we can add an arbitrary null state to the RHS in (4.33):

$$H|i\rangle \to H|i\rangle + |\text{null}\rangle. \tag{4.38}$$

Also, the eigenvalue problem (4.31) has to be considered modulo addition of an arbitrary null state in the RHS. In practice, however, we do not have to deal with these subtleties. We will compute the Hamiltonian matrix as if there were no null states, [15] and solve the original eigenvalue problem (4.31). Our final spectrum for integer d will thus contain both physical and null state eigenvalues. It is easy to see that the physical state eigenvalues are the same as in the more rigorous treatment. [16] The null eigenvalues are unphysical: they need to be separated and thrown out. There are many ways to do this in practice: one can follow a null eigenvalue from the UV where its value is known; one can detect it by the presence of crossings with physical states (physical eigenvalues don't cross in RG flows which are not integrable); one can check the nullness of the corresponding eigenvector. For the low-lying spectrum this issue does not even arise, since the first null state has a relatively high scaling dimension.

4.4.3 Matrix elements via the OPE method

The CFT piece of the Hamiltonian matrix is diagonal:

$$(H_{\text{CFT}})^i{}_j = R^{-1}\Delta_j \delta^i{}_j \,. \tag{4.39}$$

The nontrivial part is to compute the matrix of the perturbation. We compute this by using the following *OPE method*. Namely, in radial quantization we are supposed to compute

$$\left(\int_{|x|=1} \mathcal{V}(x)\right) \mathcal{O}_j(0)\,, \tag{4.40}$$

where $\mathcal{V}$ is the perturbing operator (in our examples it will be $:\phi^2:$ or $:\phi^4:$), and $\mathcal{O}_j$ is the operator corresponding to the state $|j\rangle$. Notice that we have already mapped the operator

14. In future work focusing on integer d, it will probably make sense to eliminate the null states, in order to reduce the dimension of the Hilbert space and speed up the subsequent matrix diagonalization.

15. We keep d as a free parameter when computing matrix elements, and set d to the desired value before the diagonalization.

16. A key to this argument is that null states can only be mapped into null states by the Hamiltonian. In principle, the fact that we don't solve (4.33) modulo the appearance of a null state could lead to some physical eigenvectors disappearing, due to the Jordan block phenomenon. However, this is very non-generic and would be easily detectable as we are varying parameters such as couplings and the radius of the cylinder. We have never observed it happen.

$\mathcal{V}$ to flat space. Consider now the OPE

$$\mathcal{V}(x)\mathcal{O}_j(0) = \sum_k C_{k,\{\mu\}}(x)\mathcal{A}_k^{\{\mu\}}(0) \tag{4.41}$$

where $A_k(0)$ are local operators inserted at the origin, and $C_k(x)$ are c-number coefficient functions. Since we are in a free theory, this OPE can be worked out explicitly. Notice that while $\mathcal{V}$ and $\mathcal{O}_j$ will be scalars, many of the operators $\mathcal{A}_k$ will be tensors, and $\{\mu\}$ stands collectively for their indices, contracted with those of C_k. Now to evaluate (4.40) we just integrate the OPE term by term, which amounts to integrating the coefficients:

$$\sum_k \left(\int_{|x|=1} C_{k,\{\mu\}}(x) \right) \mathcal{A}_k^{\{\mu\}}(0)\,. \tag{4.42}$$

By rotation invariance, the integrals will produce invariant tensors, i.e. a number of Kronecker deltas connecting the indices in $\{\mu\}$. Contracting these with the indices of $\mathcal{A}_k^{\{\mu\}}$ will give scalar operators. Expressing the RHS of (4.42) in the original basis, we read off the matrix $V^i{}_j$. In the above discussion we were effectively setting R and g to unity. To restore the dependence in these parameters, we need to multiply the resulting matrix by $R^{-1}(gR^{d-\Delta_\mathcal{V}})$.

This, then, is how we compute the matrix entering the eigenvalue problem. Some additional implementation details are given in appendix C. Notice that this approach is more economical (involves fewer Wick contractions) than the direct computation of the three-point functions $\langle i|H|j\rangle$.

The matrices $V^i{}_j$ computed by the OPE method can be subjected to a check. We know that if we multiply them by the Gram matrix as in (4.36), the resulting matrix V_{ij} must be symmetric. As mentioned at the end of section 4.3.3, we can compute the Gram matrix directly up to a rather high cutoff. Up to this cutoff, we can then check the symmetry of V_{ij} for the ϕ^2 and ϕ^4 perturbations—this check works.

In some cases, the Gram matrix can be computed indirectly, by turning the above consistency check around. The logic is the following: given the matrices V^i_j for the ϕ^2 and ϕ^4 perturbations, we may classify all matrices Q_{ij} that are (a) symmetric, (b) subject to the selection rule (4.19) and (c) have the property that $Q_{ij}V^j_k$ is symmetric for both perturbation matrices. If the constraints (a)-(c) completely determine Q_{ij}, then Q_{ij} must coincide with the Gram matrix G_{ij}. It turns out that up to the highest cutoffs explored in this work, the solution to (a-c) is always unique, which means that we can always use this indirect method to compute G_{ij}.[17] It is by this method that we computed the Gram matrix used to count the negative norm states in figure 7.12.

17. We have noticed that this indirect method breaks down for even higher cutoffs in $d = 4$.

Chapter 5

The ϕ^2 flow in TCSA

In the previous chapter, we have set up the necessary formalism to do TCSA computations in the theory of the massless boson in d dimensions. We now turn our attention to a specific RG flow, namely the *massive* boson, which has the following TCSA description

$$H = H_{\text{CFT}} + V, \qquad V = \gamma \frac{m^2}{2} \int_\Sigma :\phi^2(t=0,\mathbf{n}):. \tag{5.1}$$

The coefficient γ is related to the normalization of ϕ: a unit-normalized two-point function $\langle\phi\phi\rangle$ requires that $\gamma = 1/(d-2)\mathrm{S}_d$ (see section 1.4.3).

Needless to say, this RG flow is considered for illustrative purposes only, as we expect to find the free massive scalar theory. In section 5.1, we use canonical quantization on the cylinder to compute both the Casimir and the energy spectrum along the RG flow. Section 5.2 is a short detour of the main line of thinking: it generalizes a known approach in 2d TCSA, namely to calculate such observables using conformal perturbation theory. We conclude in section 5.4 by showing the numerical results from TCSA.

5.1 Canonical quantization on the cylinder

Before doing any TCSA computations, we will compute the spectrum of the massive boson on the cylinder $\mathbb{R} \times S_R^{d-1}$ analytically, using canonical quantization. [1] Coupling the massive boson to curvature is completely analogous to the procedure for the massless boson, which was discussed in section 1.5). After adding a mass term $\frac{1}{2}m^2\phi^2$, we therefore have

$$S[\phi, g_{\mu\nu}] = \frac{1}{2}\int \mathrm{d}^d x \sqrt{|g|}\left[g^{\mu\nu}\partial_\mu\phi\partial_\nu\phi + (m^2 + \kappa\mathcal{R})\phi^2\right] \equiv \int \mathrm{d}^d x\sqrt{|g|}\mathcal{L}. \tag{5.2}$$

1. In this section, we work in Euclidean cylinder in order to be consistent with the conventions used in other chapters. The more familiar real-time approach of course leads to the same spectrum.

In TCSA, it is crucial that the UV theory (with $m^2 = 0$) is a CFT, which requires to set κ to the specific value κ_c from Eq. (1.79).[2] Specializing to the cylinder with radius R, the Ricci curvature is given by $\mathcal{R} = (d-1)(d-2)/R^2$.

Canonical quantization on S_R^{d-1} is similar to the familiar flat-space case. The only subtlety comes from the Laplacian, which has hyperspherical harmonics $f_{\ell,n}(\mathbf{n})$ as eigenfunctions [135, 119]:

$$-\Delta_{S_R^{d-1}} f_{\ell,n}(\mathbf{n}) = \frac{1}{R^2}\,\ell(\ell+d-2)\,f_{\ell,n}(\mathbf{n}), \qquad \ell \in \mathbb{N}_0. \tag{5.3}$$

The label ℓ indicates total angular momentum, whereas n is an additional quantum number that labels all different states in the spin-ℓ representation of $SO(d)$. The dimension of the spin-ℓ representation is given by

$$D(\ell) = \sigma_d(\ell) + \sigma_d(\ell-1)\,, \qquad \sigma_d(\ell) = \binom{\ell+d-2}{\ell}\,, \tag{5.4}$$

hence n runs over $n = 1, 2, \ldots, D(\ell)$. In low dimensions, these hyperspherical harmonics are familiar functions: for $d = 2$ they are simply $f_{\ell,\pm}(\mathbf{n}) \sim e^{\pm i\ell\varphi}$, and for $d = 3$ they are standard spherical harmonics, $f_{\ell,m}(\mathbf{n}) \sim Y_\ell^m(\theta,\varphi)$. A particular class of hyperspherical harmonics in any d is given by the Gegenbauer polynomials:

$$f_\ell(\mathbf{n}) \sim \mathrm{Geg}_\ell^{(\nu)}(\mathbf{n}\cdot\mathbf{n}'), \qquad \mathbf{n}' = \text{fixed}. \tag{5.5}$$

We will need some basic properties of the hyperspherical harmonics, all of which carry over from the $d = 3$ case. It will be convenient to introduce an L^2 inner product on S_R^{d-1}:

$$(\!(f,g)\!) \equiv \int_{S_R^{d-1}} f^*(\mathbf{n})\,g(\mathbf{n})\,R^{d-1}\mathrm{d}\mathbf{n}. \tag{5.6}$$

Clearly two harmonics $f_{\ell,n}$, $f_{\ell',n'}$ are orthogonal with respect to this inner product if $\ell \neq \ell'$. Consequently, we can always work in a completely orthonormal basis:

$$(\!(f_{\ell,n}, f_{\ell',n'})\!) = \delta_{\ell\ell'}\delta_{nn'}\,. \tag{5.7}$$

Furthermore, the hyperspherical harmonics are a complete basis of functions [136], in the sense that any function $\psi : S_R^{d-1} \to \mathbb{C}$ can be expanded as

$$\psi(\mathbf{n}) = \sum_{\ell=0}^{\infty}\sum_{n=1}^{D(\ell)} \psi_{\ell n}\, f_{\ell,n}(\mathbf{n})\,, \qquad \psi_{\ell n} = (\!(f_{\ell,n},\psi)\!). \tag{5.8}$$

This implies a completeness relation

$$\sum_{\ell=0}^{\infty}\sum_{n=1}^{D(\ell)} f_{\ell,n}(\mathbf{n}) f^*_{\ell,n}(\mathbf{n}') = \frac{1}{R^{d-1}}\delta(\mathbf{n}-\mathbf{n}') \tag{5.9}$$

2. This illustrates the fact that putting a QFT on curved space is ambiguous: here we use Weyl invariance of the UV theory to resolve this ambiguity. Any other choice of κ would give rise to a different spectrum on S_R^{d-1}, although in the limit $R \to \infty$ the κ-dependence drops out.

where the delta function $\delta(\mathbf{n})$ is defined as

$$\int_{S^{d-1}} \delta(\mathbf{n}-\mathbf{n}')\psi(\mathbf{n}')\,\mathrm{d}\mathbf{n} = \psi(\mathbf{n}). \tag{5.10}$$

After this rather technical discussion, the actual canonical quantization of the scalar field is straightforward. The field ϕ has a mode expansion

$$\phi(t,\mathbf{n}) = \sum_{\ell=0}^{\infty}\sum_{n=1}^{D(\ell)} \frac{1}{\sqrt{2\omega_\ell}}\left[a_{\ell n}\, e^{-\omega_\ell t}\, f_{\ell,n}(\mathbf{n}) + a^*_{\ell n}\, e^{\omega_\ell t}\, f^*_{\ell,n}(\mathbf{n})\right], \tag{5.11}$$

where the equation of motion fixes ω_ℓ to be

$$\omega_\ell = \sqrt{m^2 + (\ell+\nu)^2/R^2}\,. \tag{5.12}$$

As usual, we promote the modes $a_{\ell n}, a^*_{\ell n}$ to ladder operators $a_{\ell n}, a^\dagger_{\ell n}$ that satisfy the commutation rules

$$[a_{\ell n}, a^\dagger_{\ell' n'}] = \delta_{\ell\ell'}\delta_{nn'}\,, \qquad [a_{\ell n}, a_{\ell' n'}] = [a^\dagger_{\ell n}, a^\dagger_{\ell' n'}] = 0\,. \tag{5.13}$$

It may readily be checked that the field $\phi(t,\mathbf{n})$ and its conjugate $\pi(t,\mathbf{n}) = \delta S/\delta\dot\phi(t,\mathbf{n})$ satisfy canonical equal-time commutation relations

$$[\phi(t,\mathbf{n}),\phi(t,\mathbf{n}')] = [\pi(t,\mathbf{n}),\pi(t,\mathbf{n}')] = 0\,, \qquad [\phi(t,\mathbf{n}),\pi(t,\mathbf{n}')] = \delta(\mathbf{n}-\mathbf{n}')\,. \tag{5.14}$$

and that the Hamiltonian is given by

$$H = \sum_{\ell=0}^{\infty}\sum_{n=1}^{D(\ell)} \omega_\ell \left[a^\dagger_{\ell n} a_{\ell n} + \tfrac{1}{2}\right]. \tag{5.15}$$

As usual, the Fock space of the oscillators $a^\dagger_{\ell n}$ forms the Hilbert space of the theory.

5.1.1 Casimir energy

A first observable that we want to compute is the ground state energy $E_0(m^2)$ as a function of m^2. For the canonically quantized massive scalar, it is given by the zero point energy of all oscillators

$$E_{0,\mathrm{can}} = \frac{1}{2}\sum_{\ell=0}^{\infty} D(\ell)\,\omega_\ell\,, \tag{5.16}$$

with $D(\ell)$ given by Eq. (5.4). The canonical ground state energy (5.16) however does not match with the TCSA ground state energy. To see this, we will compute the latter to first order in conformal perturbation theory. This is the usual Rayleigh-Schrödinger perturbation theory applied to the Hamiltonian (5.1). At leading order in the perturbation [3] V, this gives

$$E_{0,\mathrm{TCSA}} = \langle 0|H_{\mathrm{CFT}}|0\rangle + \gamma\frac{m^2}{2}\langle 0|V|0\rangle + \mathrm{O}(m^4). \tag{5.17}$$

3. Strictly speaking, the small parameter in this expansion is the dimensionless coupling $\mu \equiv mR$. Although this is not manifest from Eq. (5.1), this can be shown by extracting the R-dependence from the matrix elements of V.

Since the conformal vacuum $|0\rangle$ has zero energy, the first term vanishes. Similarly, the second term is an integral over the one-point function $\langle\phi^2\rangle$, which vanishes by conformal invariance. We therefore expect that

$$E_{0,\mathrm{TCSA}} \sim \frac{1}{R}(mR)^4 \qquad \text{as} \quad m^2 \to 0 \tag{5.18}$$

up to a prefactor that we will compute later.

Now consider the Casimir energy as computed according to Eq. (5.16). Its dependence on m^2 comes completely from ω_ℓ, which can be expanded around $m^2 = 0$ as follows:

$$\omega_\ell = \frac{1}{R}\left[\ell + \nu + \frac{\mu^2}{2(\ell+\nu)} - \frac{\mu^4}{8(\ell+\nu)^3} + \mathrm{O}\big(\mu^6\big)\right], \quad \mu \equiv mR. \tag{5.19}$$

This has the wrong m^2-dependence: in order to match with the TCSA Casimir energy (5.18), the first two terms (that are constant resp. quadratic in m) must be subtracted from ω_ℓ. These subtractions can be justified by adding local counterterms to the bare action. [4]

After taking these subtractions into account, we will pass to the computation of the Casimir energy. For simplicity, we can rewrite the prefactor $D(\ell)$ from Eq. (5.4) as

$$D(\ell) = \frac{\ell+\nu}{\nu}\frac{(2\nu)_\ell}{\ell!} = \frac{2}{\Gamma(2\nu+1)}\frac{(\ell+\nu)\Gamma(\ell+2\nu)}{\Gamma(\ell+1)}. \tag{5.20}$$

Then after some algebra, we obtain

$$E_0 = \frac{1}{2}\sum_{\ell=0}^{\infty} D(\ell)\Big[\omega_\ell - \omega_\ell|_{m^2=0} - m^2\frac{\partial\omega_\ell}{\partial m^2}\Big|_{m^2=0}\Big] \tag{5.21}$$

$$= -\frac{\mu^2}{2\Gamma(2\nu+1)R}\sum_{\ell=0}^{\infty} H(\ell+\nu), \tag{5.22}$$

where

$$H(z) = \frac{\Gamma(z+\nu)}{\Gamma(z+1-\nu)}\frac{\sqrt{z^2+\mu^2}-z}{\sqrt{z^2+\mu^2}+z}. \tag{5.23}$$

Because of subtractions, the general term in the series behaves at large ℓ as $\ell^{2\nu-3} = \ell^{d-5}$. Consequently, the ground state energy is finite for $d < 4$.

For general R, we can compute E_0 by numerically summing the series (5.22). In the large volume limit $\mu \gg 1$, the sum will be dominated by large-ℓ terms and can be approximated by an integral. The leading behavior in this limit scales as the volume of the sphere, with a constant density set by the mass:

$$E_0 \approx -\frac{1}{R}C_d\,(mR)^d \qquad (R \gg m^{-1}), \tag{5.24}$$

4. The subtractions in (5.22) remove the divergences that originate from the normal ordering of the operators in the bare CFT Lagrangian and the bare ϕ^2 operator, respectively. These divergences are intrinsic to the CFT and not associated with the RG flow.

for

$$C_d = \frac{1}{2\Gamma(2\nu+1)} \int_0^\infty x^{2\nu-1} \frac{\sqrt{1+x^2}-x}{\sqrt{1+x^2}+x} \mathrm{d}x$$
$$= \frac{\Gamma(1-\nu)\Gamma\left(\nu+1/2\right)}{4\sqrt{\pi}\nu(\nu+1)\Gamma(2\nu+1)} \qquad (2<d<4)\,. \tag{5.25}$$

One can show that the first correction in this formula arises at order $1/R^2$. The presence of these terms that power-like in R is due to the curvature of the general d-dimensional sphere. Here we are observing such corrections in a free theory, and we expect them to be present in an interacting situation as well. This can be contrasted with what happens when a QFT is put on $\mathbb{R}\times T^{d-1}$ (which for $d=2$ is of course the same as $\mathbb{R}\times S^{d-1}$). In this case it has been observed long ago [137] that masses in an interacting theory are affected by terms which are exponentially small in the size of the torus.

5.1.2 Massive states on the cylinder

Apart from the Casimir energy, we are also interested in comparing the exact spectrum of the massive theory of the cylinder to the TCSA eigenvalues. This is a very simple exercise, since we have already canonically quantized the massive theory in section 5.1. All energy levels can be expressed in terms of ω_ℓ, which has the following small- and large-R asymptotics:

$$\omega_\ell \underset{R\to 0}{\sim} \frac{\ell+\nu}{R}\left[1+\mathrm{O}(\mu^2)\right], \qquad \omega_\ell \underset{R\to\infty}{\sim} m\left[1+\mathrm{O}(1/\mu^2)\right]. \tag{5.26}$$

Close to the UV, in the limit $R\to 0$, the energy of a spin-ℓ state becomes $(\nu+\ell)/R$, which is precisely the energy of the spin-ℓ tensor operator $\phi_{,\mu_1\cdots\mu_\ell}$ in the UV CFT. On the other hand, in the infinite volume-limit $R\to\infty$, the energy ω_ℓ converges to m, as it should. Notice the presence of power-like corrections $\sim R^{-2}$ to the massive spectrum as $R\to\infty$, as we already discovered for the Casimir energy.

Since we restrict our TCSA computation to the scalar, parity-even sector, we need to select only scalar, parity-even states in the massive theory. Out of all the one-particle states $a^\dagger_{\ell n}|0\rangle$, we can for example only match with the $\ell=0, n=1$ state, which has no momentum on the sphere; its energy is

$$E_1 = \sqrt{m^2+\nu^2/R^2} \qquad \text{(1 particle at rest)}. \tag{5.27}$$

Similarly, the state $(a^\dagger_{\ell=0,n=1})^j|0\rangle$ is a j-particle state at rest with energy jE_1.

More generally, scalar states can arise in a tensor product $a^\dagger_{\ell_1 n_1}\cdots a^\dagger_{\ell_j n_j}|0\rangle$ — this is a j-particle state, where the different particles are boosted along the sphere. Finding the scalars in such a tensor product is a problem that we already encountered in section 4.3.1, in the context of the construction of the Hilbert space. The problem therefore trivializes, and it is easy to see the scalar states of the massive theory are in one-to-one correspondence with the

scalar states in the UV CFT.[5] In particular, a CFT state $|\partial^{n_1}\phi\cdots\partial^{n_N}\phi\rangle$ corresponds to a massive state with energy

$$E=\sum_{i=1}^{N}\omega_{n_i}=\frac{1}{R}\sum_{i=1}^{N}\sqrt{\mu^2+(n_i+\nu)^2} \tag{5.28}$$

on the cylinder.

5.2 Intermezzo: computing observables using conformal perturbation theory

The massive boson has the attractive feature that it can be solved analytically along the RG flow, for any value of R. For non-integrable RG flows, it is not possible to compare TCSA results with exact spectra at finite R; at small R, Rayleigh-Schrödinger perturbation theory can however be used to compute the spectrum. In the context of perturbed CFTs, this method is also known as *conformal perturbation theory*, and it is a familiar technique in two-dimensional RG flows (see e.g. [25]). In this section, we extend some 2d results to d dimensions.

5.2.1 Casimir energy

Let us first consider the Casimir energy for a general TCSA Hamiltonian

$$H=H_{\text{CFT}}+g\int_{\Sigma}\mathcal{V}(t=0,\mathbf{n})\,. \tag{5.29}$$

We will later specialize to the massive boson and compare with the results found using canonical quantization. Suppose for simplicity that all states are orthogonal, and let $|0\rangle$ be the CFT ground state. According to perturbation theory, we then have

$$E_0=-g^2\sum_{i\neq 0}\frac{1}{E_i\langle i|i\rangle}\left|\langle i|\int_{\Sigma}\mathcal{V}(0,\mathbf{n})|0\rangle\right|^2+\mathrm{O}(g^3). \tag{5.30}$$

The $\mathrm{O}(g)$ term vanishes, because it is proportional to the CFT one-point function $\langle\mathcal{V}\rangle$. To compute the matrix element itself, we pass to flat space and expand around $x=0$:

$$\begin{aligned}\int\mathcal{V}(0,\mathbf{n})\,R^{d-1}\mathrm{d}\mathbf{n}\,|0\rangle&=R^{d-1-\Delta_{\mathcal{V}}}\int_{|x|=1}\mathcal{V}(x=\mathbf{n})|0\rangle\\&=R^{d-1-\Delta_{\mathcal{V}}}\int_{|x|=1}\left[\mathcal{V}(0)+\ldots+\frac{1}{(2n)!}(x\cdot\partial)^{2n}\mathcal{V}(0)+\ldots\right]|0\rangle.\end{aligned} \tag{5.31}$$

5. In integer d, the massive states are in correspondence with the *physical* states of the CFT – the null states should be discarded.

Notice that only even derivatives contribute, since the integral is even under $x \to -x$. After substituting $\partial_\mu \to iP_\mu$, the n-th term in this expansion is given by

$$\int_{|x|=1} \frac{(-1)^n}{(2n)!}(x\cdot P)^{2n}|\mathcal{V}\rangle = (-1)^n \frac{\mathrm{S}_d}{4^n n!(d/2)_n}|\mathcal{V}_n\rangle, \qquad |\mathcal{V}_n\rangle = (P^2)^n|\mathcal{V}\rangle. \tag{5.32}$$

The x-integral is done using

$$\int_{|x|=1} \mathrm{d}^{d-1}x\, x_{\mu_1}\cdots x_{\mu_{2n}} = \frac{\mathrm{S}_d}{2^n(d/2)_n}\left[\delta_{\mu_1\mu_2}\cdots\delta_{\mu_{2n-1}\mu_{2n}} + \text{permutations}\right], \tag{5.33}$$

and we note that on the right-hand side $(2n-1)!!$ different pairings of the indices $\{\mu_1,\ldots,\mu_{2n}\}$ appear. The state $|\mathcal{V}_n\rangle$ has energy $(\Delta_\mathcal{V}+2n)/R$ and is orthogonal to any other state; its norm is given by [6]

$$\langle\mathcal{V}_n|\mathcal{V}_n\rangle = 16^n n!(\Delta_\mathcal{V})_n(\Delta_\mathcal{V}-\nu)_n(d/2)_n\langle\mathcal{V}|\mathcal{V}\rangle. \tag{5.34}$$

Inserting this into Eq. (5.30), we find that the second-order correction to the Casimir energy is given by

$$E_0 = -\frac{1}{R}\widetilde{g}^2\mathrm{S}_d^2\langle\mathcal{V}|\mathcal{V}\rangle\sum_{n=0}^{\infty}\frac{(\Delta_\mathcal{V})_n(\Delta_\mathcal{V}-\nu)_n}{(\Delta_\mathcal{V}+2n)n!(d/2)_n} + \mathrm{O}(\widetilde{g}^3), \qquad \widetilde{g}\equiv gR^{d-\Delta_\mathcal{V}}. \tag{5.35}$$

The summand grows like $n^{2\Delta_\mathcal{V}-1-d}$ at large n, so it converges when $\Delta_\mathcal{V} < d/2$ and diverges when $\Delta_\mathcal{V} \geqslant d/2$: this is the advertised UV divergence from section 4.2.1. The computation of this sum is straightforward and gives

$$E_0 = -\frac{1}{R}\widetilde{g}^2\mathrm{S}_d^2\langle\mathcal{V}|\mathcal{V}\rangle\,\mathcal{K}_d(\Delta_\mathcal{V}) + \mathrm{O}(\widetilde{g}^3), \qquad (\Delta_\mathcal{V} < d/2) \tag{5.36}$$
$$\mathcal{K}_d(x) = \frac{\Gamma(d/2-x)\Gamma(d/2)}{4\Gamma(x)}\left[\frac{\Gamma(x/2)}{\Gamma[(d-x)/2]}\right]^2.$$

In the 2d case, we have $\mathcal{K}_2(x) = \frac{1}{4}\gamma(1-x)[\gamma(x/2)]^2$ for $\gamma(z)=\Gamma(z)/\Gamma(1-z)$, in accordance with known results [138, 25].

Notice that the case of multiple perturbations is straightforward. As long as the different operators $\mathcal{V}_a$ satisfy $\mathcal{V}_a(x)\mathcal{V}_b(0) \sim \delta_{ab}\mathbb{1}$, the Casimir energy at order $O(g^2)$ is the sum of contributions of the form (5.36). At order $O(g^3)$, this no longer holds.

For the massive boson (with $\mathcal{V} = {:}\phi^2{:}$), we have $\Delta_\mathcal{V} = d-2$, $\langle\mathcal{V}|\mathcal{V}\rangle = 2$, and $\widetilde{g} = \mu^2/[2(d-2)\mathrm{S}_d]$. Substituting this into (5.36), we obtain

$$E_0 = -\frac{1}{R}\frac{\mu^4}{2(d-2)^2}\mathcal{K}_d(d-2) + \mathrm{O}(\mu^6), \qquad (d<4) \tag{5.37}$$

which can be shown to agree with canonical quantization.

6. This follows by noticing that $\langle\mathcal{V}_n| = \langle\mathcal{V}|(K^2)^n$ and by recycling the computation of the matrix element $\langle\mathcal{V}|(K\cdot x)^n(P\cdot y)^n|\mathcal{V}\rangle$ done in section 3.3 of [21].

In practice, conformal perturbation theory predictions like the above can be used to check TCSA computations close to the UV: in the regime where $\widetilde{g} \ll 1$, the TCSA Casimir energy must agree with the perturbation theory result (5.35). Even better, keeping only states of dimension $\Delta \leqslant \Delta_{\max}$ means that the sum should be truncated at $n_{\max} = (\Delta_{\max} - \Delta_{\mathcal{V}})/2$: this way, the TCSA can be checked for different values of the cutoff.

5.2.2 Excited states

Similarly, the energy E_n of an excited state $|n\rangle$ can be computed using conformal perturbation theory. At first order, we have

$$E_n(g) = E_{n,\mathrm{CFT}} + \frac{\widetilde{g}}{\langle n|n\rangle}\langle n| \int_{|x|=1} \mathcal{V}(x)|n\rangle + \mathrm{O}(\widetilde{g}^2). \tag{5.38}$$

In particular, if $\mathcal{O}$ is a primary and $|n\rangle \equiv |\mathcal{O}\rangle$, the matrix element $\langle n| \int \mathcal{V}|n\rangle$ is proportional to the three-point function $\langle \mathcal{O}\mathcal{O}\mathcal{V}\rangle$.

Let us specialize to the massive theory and focus on the state $|n\rangle = |\phi^n\rangle$, which has norm $\langle \phi^n|\phi^n\rangle = n!$. The matrix element $\langle \phi^n|{:}\phi^2{:}|\phi^n\rangle$ can be computed using the OPE:

$${:}\phi^2(x){:}{:}\phi^n(0){:} \sim \frac{2n}{|x|^{d-2}}{:}\phi^n(0){:} + \dots, \tag{5.39}$$

hence

$$\langle \phi^n|{:}\phi^2(x){:}|\phi^n\rangle = \frac{2nn!}{|x|^{d-2}}. \tag{5.40}$$

Substituting this into Eq. (5.38), we obtain

$$E_n(m^2) = R^{-1}\left[n\nu + \frac{n\mu^2}{2\nu} + \mathrm{O}(\mu^4)\right]. \tag{5.41}$$

which agrees with canonical quantization.

5.3 TCSA setup

In section 5.1, we explained how to compute the Casimir energy and spectrum of the ϕ^2 flow. At this point, we will turn our attention to TCSA calculations in this theory. First, we need to choose in which dimension d the numerical computations are done. As already mentioned in section 4.2.1, the case $d \to 2$ is expected to be difficult, as the CFT spectrum is becoming dense in the limit. For $d > 4$ the vacuum energy will be divergent. Here we will show results for the physical value $d = 3$. We have also performed checks for other nearby values of d and they work equally well.

As mentioned in the previous chapter, we work with a fixed cutoff $\Delta \leqslant \Delta_{\max}$. As we vary R, this means that the effective UV cutoff varies too:

$$\Lambda_{\mathrm{UV}} = \Delta_{\max}/R \tag{5.42}$$

The TCSA can be expected to reproduce the IR spectrum roughly below this cutoff. As we increase R, the sliding cutoff decreases and eventually becomes comparable with m. At this point TCSA results can no longer be trusted. [7]

Furthermore, we recall from Sec. 4.4.2 that we will be working in an extended Hilbert space which for integer d is somewhat larger than the physical Hilbert space, since it includes some null states.

The success of any TCSA calculation will depend on whether reasonable results can be obtained with a manageable $\Delta_{\max}$. The computational bottleneck in TCSA computations is the diagonalization of the Hamiltonian matrix, which scales polynomially with the size of the Hilbert space. As a rule of thumb, we find that such an eigenvalue problem is feasible in `Mathematica` on a laptop or desktop computer if the Hilbert space contains at most $O(10^3 - 10^4)$ states. This should be compared with the actual number of states at low Δ, printed in Fig. 4.1. We consider cutoffs up to $\Delta_{\max} = 18$, which corresponds to 4573 scalar P-even states. [8]

5.4 Numerical results

We will now show our numerical TCSA results and compare them with theoretical expectations. The TCSA computation starts by constructing the truncated Hilbert space. We then construct the Hamiltonian matrix $H^i{}_j$. The CFT part is given by the diagonal matrix (4.39). The perturbing part is computed using the OPE method from section 4.4.3, for the operator $\mathcal{V} = :\phi^2:$. We then diagonalize the Hamiltonian matrix to find the spectrum of the perturbed theory.

Since the perturbation preserves the $\mathbb{Z}_2$ symmetry which maps $\phi \to -\phi$, the Hamiltonian matrix does not mix $\mathbb{Z}_2$-even and $\mathbb{Z}_2$-odd states. The two sectors have roughly equal number of states, and it makes sense to do the computation separately in each of them, reducing the size of the matrices to be diagonalized by factor ~ 2. The ground state belongs to the $\mathbb{Z}_2$-even sector.

7. The range of validity of TCSA will be somewhat extended due to the fact that the induced ground state energy is negative.

8. We note that the *total* number of states (of any spin, both primaries and descendants) in a d-dimensional CFT grows with Δ exponentially [139]

$$N(\Delta) \sim \exp\left[\lambda \Delta^{(d-1)/d}\right], \tag{5.43}$$

where λ is a theory-dependent constant – see [21] for a review. For the UV CFT in question (the free massless scalar), we have $\lambda = d[\zeta(d)]^{1/d}/(d-1)^{1+1/d}$, as has been computed in Ref. [139]. It can be argued that the number of states in every spin-ℓ subsector of the Hilbert space grows exponentially with the same exponent, although with a smaller prefactor.

5.4.1 Casimir energy

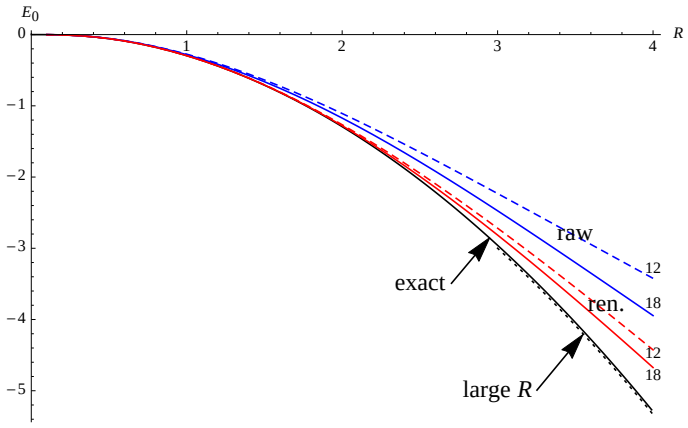

Figure 5.1: The ground state energy of the ϕ^2 flow in $d = 3$ as a function of R (we set $m = 1$). Solid black curve: theory prediction (5.22). Dotted black: theory limit at large R, Eq. (5.24). Blue curves marked 'raw': raw TCSA results, i.e. before applying any correction. Red curves marked 'ren.': renormalized TCSA results, see section 6.3.1. Dashed and solid TCSA curves correspond to cutoff $\Delta_{\text{max}} = 12(18)$.

In figure 5.1, we plotted E_0 as a function of R. In this and other plots in this section, we set $m = 1$, which means that we measure R in units of m^{-1} and energies in units of m. The black solid curve shows the theoretical prediction for $E_0(R)$ obtained by summing the series in Eq. (5.22). The TCSA results are displayed in blue (with the label 'raw'): results obtained at cutoff $\Delta_{\text{max}} = 12$ (18) are shown as a dashed (solid) line. We see that the agreement is good up to $R \sim 1$, while for larger R there are noticeable deviations.

It is clear that the results of TCSA computations depend on the chosen cutoff Δ_{max}. The more states are taken into account (or equivalently, the higher the cutoff), the better we expect the TCSA computations to agree with the exact Casimir energy. Indeed, the $\Delta_{\text{max}} = 18$ results are in better agreement with the exact result than the $\Delta_{\text{max}} = 12$ curve. In the next chapter, we will discuss this cutoff dependence in more detail. Furthermore, we will *renormalize* the TCSA Hamiltonian H, which entails adding counterterms to H in order to reduce the cutoff dependence. We have chosen to already display these 'renormalized' TCSA predictions in Fig. 5.1, plotted in red. The agreement with the exact results is greatly improved; it now extends up to $R \sim 2.5$. Notice that the corrected results also exhibit a smaller dependence on the cutoff.

5.4.2 Massive excitations

We now turn to the excitations above the vacuum. In figure 5.2 we plot the energies of these excitations, subtracting the vacuum energy. We have two plots, one for the $\mathbb{Z}_2$-even

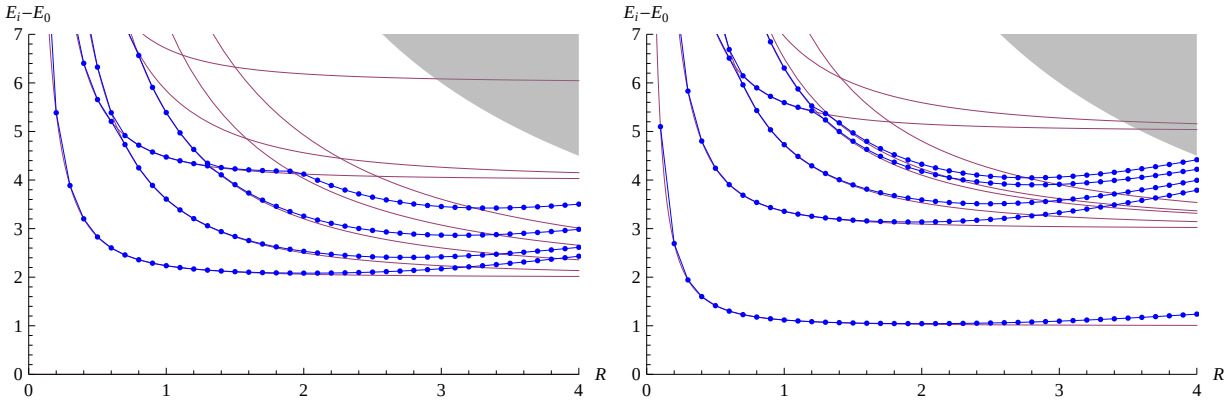

Figure 5.2: A few lowest massive excitations from the raw TCSA spectra at $\Delta_{\max} = 18$ (blue dots connected with a line to guide the eye) vs exact spectrum (magenta lines). Left(right): $\mathbb{Z}_2$-even (odd) sector. The gray region indicates the sliding UV cutoff (5.42).

and one for the $\mathbb{Z}_2$-odd sectors. To keep the plots from cluttering, we show the lowest five eigenvalues in each sector. Notice that in both cases we subtract the same quantity E_0, which is the lowest energy in the $\mathbb{Z}_2$-even sector. Blue dots are computed using TCSA for $\Delta_{\max} = 18$, while lines joining them are added to guide the eye.

In the same plot thin magenta lines show the exact free massive scalar spectrum, as discussed in section 5.1.2. In the $\mathbb{Z}_2$-even sector the lowest state corresponds to two particles at rest, while the states above it correspond to two particles with some angular momentum on the sphere combined in a state of total spin zero. Then there comes the state with four particles at rest etc. In the $\mathbb{Z}_2$-odd sector we recognize one particle at rest, three particles at rest, then three-particle states in relative motion, etc.

5.4.3 Discussion

In this chapter, we have produced some first numerical TCSA results and compared them to exact predictions. At this stage, it may be interesting to discuss the quality of the the TCSA results from section 5.4. We found that TCSA was reliable in the domain $R \lesssim 2.5$: is this a promising result?

To answer this, we first remark that this domain extends significantly beyond the radius of convergence $R_{\rm PT}$ of perturbation theory, which is $R_{\rm PT} = \frac{1}{2}(d-2) \to \frac{1}{2}$ in $d = 3$.[9] Second, we argue that $R \sim 2.5$ corresponds to a relatively large volume in physical units. The wavefunction of a massive particle has a characteristic length scale $\xi \sim 1/m$, whereas the circumference of the sphere is $L = 2\pi R$. The radius $R \sim 2.5$ therefore corresponds to a

9. As determined by the leading singularity in the exact expressions for the vacuum energy density and the massive spectrum (cf. Eq. (5.27), located at $m^2R^2 = -\nu^2$.

'box size' $L/\xi \sim 15$ which is significantly larger than 1. Third, we remark that the finite-volume effects are reasonably small at $R \sim 2.5$: the leading finite-size corrections to both the Casimir energy and the massive spectrum are of order $R^{-2} \sim 15\%$ there. This indicates that it should be possible to systematically estimate these finite-size effects from the TCSA data in order to obtain reliable $R \to \infty$ extrapolations. We have not taken this approach in the case of the massive scalar, but it may prove useful for non-integrable theories.

Finally, we point to the fact that the plots in 5.4 did not contain error bars: we only checked whether the TCSA results were reliable by computing the spectrum for two different values of the cutoff. In the next chapter, we will develop a more systematic method to deal with these truncation errors; in particular, in section 6.3.2 we recompute the massive spectrum using renormalized TCSA.

Chapter 6

Cutoff dependence and renormalization

In this chapter we will be concerned with the presence of the cutoff $\Delta_{\text{max}} \sim \Lambda_{\text{UV}} R$ in TCSA. We have already seen that computed spectra depend on Δ_{max}, but eventually we want to obtain predictions that are cutoff-independent. Fortunately, there exists a method to systematically reduce the cutoff-dependence: in this chapter, we develop the necessary formalism to do so. First, let us slightly formalize the problem. In the TCSA, as we advocated so far, we use a Hamiltonian with 'bare' couplings g_a:

$$H = H_{\text{CFT}} + g^a \int_\Sigma \mathcal{V}_a(t=0,\mathbf{n})\,, \tag{6.1}$$

where summation over a is understood. The dependence of the spectrum on the cutoff comes only from the size of the Hilbert space: the higher Δ_{max} is chosen, the more states are taken into account.

This begs the question of what happens in the limit $\Lambda_{\text{UV}} \to \infty$. We have already seen that this limit is not always well-defined: if $[\mathcal{V}_a] > d/2$ for one of the perturbing operators $\mathcal{V}_a$ the ground state energy diverges, cf. section 5.2.1. Such divergences have been observed in the 2d TCSA, for example in the RG flow induced by the so-called subleading energy operator ε' in the tricritical Ising model [24].

In this thesis, we avoid all UV divergences by restricting d to $d < 4$ for the ϕ^2 flow and $d < 8/3$ for the ϕ^4 flow. The 'continuum limit' $\Lambda_{\text{UV}} \to \infty$ is therefore finite. Still, the TCSA energy levels $E_n = E_n(\Lambda)$ depend on the cutoff. We will argue in this chapter that the cutoff dependence is power-law like: [1]

$$E_n(\Lambda) \;\sim\; \lim_{\Lambda\to\infty} E_n(\Lambda) \;+\; \frac{c_1}{\Lambda^{\alpha_1}} \;+\; \frac{c_2}{\Lambda^{\alpha_2}} \;+\; \ldots \qquad (0 < \alpha_1 < \alpha_2 < \ldots) \tag{6.2}$$

1. In special cases, a logarithmic cutoff dependence $\ln\Lambda$ or $\Lambda^n \ln\Lambda$ is also possible. This is however non-generic in interacting theories.

with the powers α_i depending on the RG flow under consideration and the state $|n\rangle$.[2] If $\alpha_1 \gg 1$ is large, the truncation effects in (6.2) decrease quickly with $\Delta_{\max}$, and using a moderate cutoff it will be possible to obtain a good approximation to the physical value $E_n(\Lambda \to \infty)$. If however $\alpha_1 = O(1)$, reducing the truncation error is numerically expensive.

As usual in quantum field theory, we may hope to improve this situation by adding Λ-dependent counterterms. This means adding to the bare Hamiltonian H an improvement term ΔH in such a way that the leading cutoff dependence is cancelled. Such ideas are not new: in lattice-regulated QFTs, a similar method [140] known as *Symanzik improvement* is well-studied. In the TCSA, improved Hamiltonians were first introduced in the context of boundary RG flows in two dimensions [35, 141, 142]; later, these ideas were applied to 2d bulk RG flows by Giokas and Watts [143].

This chapter is organized as follows. In Sec. 6.1, we study ϕ^4 theory in flat space as a toy model to make the above ideas about truncation errors and improvement quantitative. In section 6.2, we will formalize the problem in TCSA, and in section 6.2.2 we show how to compute leading counterterms to leading order. In section 6.3.1, we explain how this method applies to the ϕ^2 flow and recompute the massive spectrum from the previous chapter.

6.1 Warm-up: improving ϕ^4 theory in flat space

Before we start with a rather technical discussion about cutoff effects in TCSA, we want to illustrate the main points in a simpler setting. Let us consider the ϕ^4 theory in flat (Euclidean) space in $2 \leqslant d < 4$ dimensions, with Lagrangian

$$\mathscr{L} = \frac{1}{2}(\partial\phi)^2 + \frac{1}{2}m^2{:}\phi^2{:} + \frac{1}{4!}g{:}\phi^4{:}. \tag{6.3}$$

The ϕ^4 coupling g has mass dimension $[g] = 4-d$, and we take $m^2 > 0$. Perturbation theory is valid provided that

$$\frac{g}{m^{4-d}} \ll 1. \tag{6.4}$$

For convenience, we can set $g \equiv \lambda m^{4-d}$, such that λ is dimensionless; the above condition then translates to $\lambda \ll 1$. We can imitate the TCSA regulator by truncating all loop integrals at a fixed momentum scale $|k| = \Lambda$.[3] For Λ to be a UV cutoff, we require that $\Lambda \gg m$.

How do physical observables depend on this cutoff? As an example, we consider the four-point vertex function $\Gamma^{(4)}(p_1, p_2, p_3, p_4)$ at zero incoming momentum ($p_i = 0$). At one

2. If $\alpha_i < 0$, this indicates a UV divergence.

3. This is straightforward to implement at one-loop order, but requires some extra care to define at higher orders in perturbation theory.

loop, only the diagram displayed in fig. (6.1) contributes:

$$\Gamma^{(4)}(p_i = 0) = \lambda m^{4-d} - \frac{3}{2}\lambda^2 m^{2(4-d)} \int_{|k|<\Lambda} \frac{\mathrm{d}^d k}{(2\pi)^d} \frac{1}{(k^2+m^2)^2} \tag{6.5a}$$

$$= \lambda m^{4-d} - b\,\lambda^2 m^{2(4-d)} \int_0^\Lambda \frac{\kappa^{d-1}}{(\kappa^2+m^2)^2} \mathrm{d}\kappa, \qquad b \equiv \frac{3\,\mathrm{S}_d}{2(2\pi)^d}. \tag{6.5b}$$

Since the integrand grows as κ^{d-5} for large κ, the integral is UV-finite in the continuum limit $\Lambda \to \infty$ if $d < 4$.

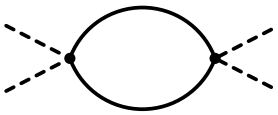

Figure 6.1: The only diagram contributing to $\Gamma^{(4)}$ at one-loop order.

Let us now make precise how $\Gamma^{(4)}$ depends on the cutoff. The Λ-dependence can be extracted by rewriting the loop integral in Eq. (6.5b):

$$m^{4-d} \int_0^\Lambda \frac{\kappa^{d-1}}{(\kappa^2+m^2)^2} \mathrm{d}\kappa = -\frac{\pi(d-2)}{4\sin(d\pi/2)} - \int_{\Lambda/m}^\infty \frac{x^{d-1}}{(x^2+1)^2} \mathrm{d}x\,. \tag{6.6}$$

The first term is physical, and encodes what remains after the cutoff Λ is sent to infinity. The second term encodes the truncation error; it may be systematically expanded as a series in m^2/Λ^2 as follows:

$$\int_{\Lambda/m}^\infty \frac{x^{d-1}}{(x^2+1)^2} \mathrm{d}x = \frac{1}{4-d}\left(\frac{m}{\Lambda}\right)^{4-d} - \frac{2}{6-d}\left(\frac{m}{\Lambda}\right)^{6-d} + \mathrm{O}(1/\Lambda^{8-d})\,. \tag{6.7}$$

In particular, we see that the leading truncation error in $\Gamma^{(4)}$ scales as $1/\Lambda^{4-d}$.

Usually in QFT, we have in mind that we are working in the continuum limit $\Lambda \to \infty$, in which (finite) cutoff effects like those of Eq. (6.7) vanish. For now, we consider Λ to be fixed, yet we will try to reduce the cutoff dependence by adding a counterterm to the action (6.3):

$$\mathscr{L} \;\to\; \mathscr{L} + \frac{1}{4!}\delta_\lambda(\Lambda) m^{4-d} {:}\phi^4{:}. \tag{6.8}$$

With the counterterm present, the vertex function is given by

$$\Gamma^{(4)}(p_i = 0) = [\Lambda - \text{indep.}] + \delta_\lambda(\Lambda) m^{4-d} + \frac{b\lambda^2 m^{4-d}}{4-d}\left(\frac{m}{\Lambda}\right)^{4-d} + \mathrm{O}(1/\Lambda^{6-d}). \tag{6.9}$$

By a judicious choice of the counterterm,

$$\delta_\lambda(\Lambda) = -\frac{b\lambda^2}{4-d}\left(\frac{m}{\Lambda}\right)^{4-d} \tag{6.10}$$

the leading dependence of vertex function $\Gamma^{(4)}$ on Λ can indeed be cancelled. In principle, we can also cancel subleading effects from Eq. (6.7) by adding suitable terms to $\delta_\lambda(\Lambda)$.

A more refined point of view is given by the renormalization group. Suppose that we cancel the cutoff dependence for some very large cutoff Λ_1. Next, we lower the cutoff by an infinitesimal amount $\delta\Lambda \ll \Lambda_1$, such that the new cutoff is given by $\Lambda_2 = \Lambda - \delta\Lambda$. Obviously, we should compensate for this change in cutoff by adjusting the counterterm δ_λ. After we have adjusted the counterterm, we can iterate the above procedure and flow to a much lower cutoff $\Lambda_n \ll \Lambda_1$.

The above logic can be used to obtain a differential equation that controls the counterterms. In order to simplify the next computation, we join the bare coupling λ and the counterterm δ_λ into the 'renormalized' coupling $\lambda_{\text{ren}}(\Lambda) = \lambda + \delta_\lambda(\Lambda)$. Notice first that the vertex function $\Gamma^{(4)}$ must be cutoff-independent, since it is a physical observable. From Eq. (6.5b), it follows that $\lambda_{\text{ren}}(\Lambda)$ must be adjusted as follows under a change in Λ:

$$\Lambda \frac{\partial}{\partial \Lambda} \lambda_{\text{ren}}(\Lambda) = b\, \lambda_{\text{ren}}(\Lambda)^2 m^{4-d} \frac{\Lambda^d}{(\Lambda^2 + m^2)^2}. \tag{6.11}$$

This RG equation is exact at one-loop order. The value of $\lambda_{\text{ren}}(\Lambda)$ is determined by integrating this ODE (either analytically or numerically) starting from an initial scale Λ_1. For the counterterm in question, we can extrapolate to $\Lambda_1 \to \infty$ and choose $\lambda_{\text{ren}}(\Lambda = \infty) = \lambda$ as an initial condition; when any of the observables is UV divergent, a different renormalization condition at some finite scale must be chosen.

If we drop the m^2 term in the denominator of (6.11), we can solve the above RG equation in closed form:

$$\begin{aligned} \lambda_{\text{ren}}(\Lambda) &= \lambda \left[1 + \frac{b\lambda}{4-d} (\mu/\Lambda)^{4-d} \right]^{-1} \\ &= \lambda - \lambda^2 \frac{b}{4-d} \left(\frac{m}{\Lambda} \right)^{4-d} + \lambda^3 \frac{b^2}{(4-d)^2} \left(\frac{m}{\Lambda} \right)^{8-2d} + \mathrm{O}(\lambda^4). \end{aligned} \tag{6.12}$$

By integrating the one-loop RG equation (6.11), we have not only obtained the leading counterterm (6.10), but infinitely many extra terms that correspond to higher-loop diagrams. We stress that only *some* higher-loop diagrams are taken into account: to obtain the full counterterm at order λ^{n+1}, an n-loop analysis is required.

We can now go on to compute $\Gamma^{(4)}$ at two and higher-loop order and find the appropriate counterterms. Notice however that in a superrenormalizable theory these higher-loop counterterms are cutoff-suppressed. This follows from power counting: the observable under consideration has mass dimension $[\Gamma^{(4)}] = 4 - d$, hence by dimensional analysis the n-loop contribution scales as

$$\Gamma^{(4)} \supset \frac{\text{cst.}}{\Lambda^{n(4-d)}} (\lambda m^{4-d})^{n+1} + \mathrm{O}(1/\Lambda^{n(4-d)+2}) \tag{6.13}$$

omitting terms that are suppressed by factors of m^2/Λ^2. If the cutoff is large compared to m, such terms are tiny at large enough n, *regardless of the value of* λ.

This last point is important in the context of TCSA. There, we are generally not in the perturbative regime, since the dimensionless couplings $g^a R^{d-\Delta_a}$ in the Hamiltonian may be of order one. Yet the above power counting argument explains that we can still use (conformal) perturbation theory at finite order to make the truncation error arbitrarily small. To be very concrete, let us return to the above example, setting the cutoff to $\Lambda/m = 10$ and choosing $d = 3$. If we want to make the truncation error in $\Gamma^{(4)}$ to be at most $O(10^{-n})$, then it is sufficient to compute counterterms at n-th order in perturbation theory, even if $\lambda \sim 1$.

We have so far focused on the ϕ^4 coupling, but the regulator Λ generates many more operators. The most obvious one is the mass renormalization $\delta m^2(\Lambda) :\phi^2:$ and the cosmological constant renormalization $\delta E_0(\Lambda)$. Usually, we do not keep track of the latter, since it is unobservable in flat space. In TCSA, the ground state energy is observable, cf. section 5.4. These counterterms (computed using the vertex function $\Gamma^{(2)}$ and the partition function Z) are generated by the diagrams in Fig. 6.2. By power counting, they scale with Λ as follows:

$$\delta m^2(\Lambda) \sim (\lambda m^{4-d})^2 \, (1/\Lambda)^{6-2d}\,, \tag{6.14a}$$

$$\delta E_0(\Lambda) \sim (\lambda m^{4-d})^2 \, (1/\Lambda)^{8-3d}\,. \tag{6.14b}$$

We remark that $\delta m^2(\Lambda)$ diverges logarithmically in $d = 3$ and that the cosmological constant diverges starting from $d = 8/3$, in agreement with conformal perturbation theory.

Figure 6.2: Left: the two-loop diagram contributing to $\Gamma^{(2)}$. Right: three-loop diagram contributing to the cosmological constant.

Many other operators are generated, most of which are irrelevant (in the RG sense) and strongly suppressed in $1/\Lambda$. It may for example be shown that $:\phi^6:$ and $:\phi^8:$ are generated with coefficients $1/\Lambda^{6-d}$ (resp. $1/\Lambda^{8-d}$).

It turns out that most of the lessons learned in this simple example generalize to the TCSA. This is unsurprising, because truncation effects only reflect the short-distance behaviour of the theory under consideration: the fact that TCSA puts the theory on the sphere S_R^{d-1} does not play a role. [4] We also remark that even in flat space, it is not necessary to compute counterterms using Feynman diagrams: we could just as well have computed the counterterms δ_λ, δm^2 and δE_0 using position space techniques [144]. In summary, we have seen that:

4. In particular, the counterterms computed in this method can be compared to those computed directly for the Landau-Ginzburg theory in TCSA, cf. appendix D.2.1.

— Truncation effects in a hard cutoff scheme are power-law like suppressed; in special cases (like the mass renormalization in $d = 3$), there can be logarithms;
— These cutoff effects can be systematically cancelled by demanding that well-chosen observables are cutoff-independent;
— In superrenormalizable theories (such as those used in the TCSA), it is sufficient to compute counterterms up to a finite order in perturbation theory;
— Computing counterterms computed by integrating RG equations partially resums higher orders in perturbation theory.

6.2 Cutoff dependence in TCSA

6.2.1 General remarks

Let us now turn to the actual problem at hand, namely the analysis of truncation effects that originate from the TCSA regulator. In TCSA, it seems easiest to discuss the cutoff dependence directly in terms of the Hamiltonian spectrum. We work in the Hilbert space of the unperturbed CFT on the cylinder, which is divided into the low (l) and high (h) energy parts:

$$\mathcal{H} = \mathcal{H}_l \oplus \mathcal{H}_h \,, \tag{6.15}$$

where $\mathcal{H}_l$ includes all states of energy up to $\Lambda_{\rm UV}$. The full Hamiltonian is a block matrix:

$$H = \begin{pmatrix} H_{ll} & H_{hl} \\ H_{lh} & H_{hh} \end{pmatrix} . \tag{6.16}$$

where H_{ab} maps $\mathcal{H}_b$ into $\mathcal{H}_a$. The TCSA truncated Hamiltonian is the upper left corner: $H_{ll} = H_{\rm TCSA}$. The full eigenvalue problem is

$$H.c = Ec, \quad c = (c_l, c_h)^t \,, \tag{6.17}$$

or, in components,

$$H_{ll}.c_l + H_{lh}.c_h = Ec_l \,, \qquad H_{hl}.c_l + H_{hh}.c_h = Ec_h \,. \tag{6.18}$$

Let us now eliminate c_h by using the second equation. We get:

$$\left(H_{ll} - H_{lh}.(H_{hh} - E)^{-1}.H_{hl}\right).c_l = Ec_l \,, \tag{6.19}$$

This exact equation should be compared to the truncated equation used in TCSA:

$$H_{ll}.\bar{c}_l = \bar{E}\bar{c}_l \qquad (\text{TCSA}) \,. \tag{6.20}$$

Here, we write $\bar{E}, \bar{c}$ rather than E, c to indicate that these are solutions to the *truncated* equation rather than Eq. (6.17).

We conclude that the TCSA will converge if the matrix correction in (6.19) can be neglected in the limit $\Lambda_{\rm UV} \to \infty$. Naively, this seems likely since it is suppressed by $H_{hh} - E$, and we are assuming that E belongs to the low-energy spectrum, while the eigenvalues of H_{hh} will be presumably large. However, the precise statement will depend also on the size of the matrix elements mixing $\mathcal{H}_h$ into $\mathcal{H}_l$. This mixing being due to the perturbation, we can expect that the importance of corrections will depend on $\Delta_{\mathcal{V}}$.

Let us view the problem from a practical angle. Suppose we know an eigenvalue $\bar{E}$ and the corresponding eigenvector $\bar{c}$ of the truncated problem (6.20). How can we correct $\bar{E}$ to get closer to the solution of the exact eigenvalue equation? Let us write the full Hamiltonian as

$$H = H_0 + H_1, \quad H_0 = \begin{pmatrix} H_{\rm TCSA} & 0 \\ 0 & H_{{\rm CFT},h} \end{pmatrix}, \quad H_1 = \begin{pmatrix} 0 & V_{lh} \\ V_{hl} & V_{hh} \end{pmatrix}. \tag{6.21}$$

We took into account that the off-diagonal elements H_{hl} and H_{lh} are associated only with the perturbation V. The eigenvalues of H_0 are known—these are the TCSA eigenvalues and the unperturbed eigenvalues of the diagonal $H_{{\rm CFT},h}$. We will now view H_1 as a perturbation and compute corrections to the TCSA eigenvalues. By the usual Rayleigh-Schrödinger perturbation theory we get:

$$E = \bar{E} + \langle \bar{c} | \Delta H | \bar{c} \rangle \,, \tag{6.22}$$

$$\Delta H = -V_{lh}.(H_{\rm CFT} - \bar{E})^{-1}.V_{hl} + \dots \tag{6.23}$$

Further corrections terms are simple to write down. For example, the next one is given by

$$V_{lh}.(H_{\rm CFT} - \bar{E})^{-1}.V_{hh}.(H_{\rm CFT} - \bar{E})^{-1}.V_{hl} \,. \tag{6.24}$$

We will only use the term shown in (6.23) in this paper, but in the future increasing the accuracy of the renormalization procedure will likely require mastering (6.24) and perhaps even further terms.

Our job is not yet finished, since evaluating the correction term (6.23) requires an infinite summation over the states in $\mathcal{H}_h$. It would be desirable to find a simplified approximate form for this correction:

$$\Delta H \approx \sum_c V_c \,, \tag{6.25}$$

where V_c act simply on $\mathcal{H}_l$. For example, V_c might be of the same form as V itself, i.e. an integral of a local operator $\mathcal{V}_c$ over the sphere. If this is the case, then adding ΔH to the TCSA Hamiltonian can be thought of as renormalizing the couplings, analogously to the discussion in the previous section.

A difference between the situation here and in section 6.1 is that the 'improvement term' ΔH is constructed *after* diagonalizing the bare Hamiltonian. In particular, it depends on the energy $\bar{E}$ of the state under consideration. At this stage, it is not obvious whether the same

improvement can be obtained by adding an improvement term $\Delta H'$ to the bare Hamiltonian H *before* diagonalizing. We will come back to this issue later.

6.2.2 Computation of ΔH via two-point functions

The above discussion has been completely abstract and applies to *any* perturbation V. We now specialize to a general TCSA perturbation

$$V = \sum_a g^a \int_\Sigma \mathcal{V}_a(t=0,\mathbf{n}) \tag{6.26}$$

where $\mathcal{V}_a$ is a primary scalar of dimension Δ_a. In the rest of this chapter, we will not write the sum over a explicitly.

To find the correction terms, we examine the matrix element of ΔH (6.23) between two states $i,j \in \mathcal{H}_l$:

$$(\Delta H)^i{}_j = -\sum_{E_n>\Lambda_{\rm UV}} \frac{(M_n)^i{}_j}{E_n-\bar{E}}\,, \qquad (M_n)^i{}_j \equiv \sum_{k:\Delta_k=\Delta_n} V^i{}_k V^k{}_j\,, \tag{6.27}$$

where $E_n = \Delta_n/R$ stands for the unperturbed CFT energy. We will estimate the large energy asymptotics of M_n. The key idea is to consider the correlation function:

$$\begin{aligned} C(t) &= \langle i|V(t/2)V(-t/2)|j\rangle \\ &= g^a g^b \langle i| \int_{S^{d-1}_R} d\mathbf{n}\, \mathcal{V}_a\left(t/2,\mathbf{n}\right) \int_{S^{d-1}_R} d\mathbf{n}' \mathcal{V}_b\left(-t/2,\mathbf{n}'\right)|j\rangle\,. \end{aligned} \tag{6.28}$$

We assume that $t>0$, in order for the above correlator to be time-ordered. The operators $V(t)$ and $\mathcal{V}_a(t,\mathbf{n})$ at time $t\neq 0$ are time-translated by the unperturbed Hamiltonian $H_{\rm CFT}$:

$$V(t) = e^{H_{\rm CFT}t}\, V(t=0)\, e^{-H_{\rm CFT}t}, \qquad \mathcal{V}_a(t,\mathbf{n}) = e^{H_{\rm CFT}t}\, \mathcal{V}_a(t=0,\mathbf{n})\, e^{-H_{\rm CFT}t}. \tag{6.29}$$

Inserting the resolution of unity $\mathbb{1} = \sum_k |k\rangle\langle k|$, this correlation function can be represented through the same M_n as

$$C(t) = \sum_n (M_n)_{ij} e^{-[\Delta_n - (\Delta_i+\Delta_j)/2]t}\,. \tag{6.30}$$

The large energy behavior of M_n can then be extracted from the part of $C(t)$ which is non-analytic as $t\to 0$, since the low energy states give rise to an analytic contribution.

A moment's thought shows that nonanalyticity for $t\to 0$ can appear only from the region where the nonintegrated correlator has a singularity, i.e. from $\mathbf{n}$ close to $\mathbf{n}'$. In this region we can use the OPE

$$\mathcal{V}_a(x)\mathcal{V}_b(y) \approx \sum_c f_{ab}{}^c \frac{\mathcal{V}_c(\frac{1}{2}(x+y))}{|x-y|^h}, \qquad h = h_{abc} = \Delta_a+\Delta_b-\Delta_c\,. \tag{6.31}$$

To the accuracy needed below, it will be sufficient to use only the shown leading term in the OPE. Moreover, we will be considering only scalars in the RHS of the OPE. With a Poincaré-invariant cutoff, non-scalar operators are not induced in the renormalization group flow. However, the TCSA regulator is more subtle. We break the Poincaré group to $SO(d)$ times dilatations. Furthermore, since we are working in a Hamiltonian formalism, we may find integrals of tensorial operators induced by the RG flow. As an example, the appearance of the stress tensor $T_{\mu\nu}$ on the RHS gives (after integrating over the sphere) a contribution of the form

$$\int_{S^{d-1}} n^\mu n^\nu T_{\mu\nu} \propto H_{\mathrm{CFT}} \tag{6.32}$$

so it leads to a renormalization of the coefficient of H_{CFT} in the TCSA Hamiltonian.[5] However, since the stress tensor and other operators with spin have high dimension, their effects will be suppressed compared to the effects of the scalars by a higher power of Λ_{UV}.

Each term in the OPE will give rise to a term in the $t \to 0$ asymptotics of the correlator. The prefactor will be given by the matrix element of $\mathcal{V}_c$ integrated over the sphere, while the dependence on t will come from the integral of the OPE kernel. Up to $O(t^2)$ accuracy we have (see Appendix D.1):

$$C(t) \supset B(h)\Gamma(h-d+1)t^{d-h-1}[1+O(t^2)] \times g^a g^b f_{ab}{}^c \langle i| \int_{S^{d-1}} \mathcal{V}_c(x)|j\rangle \,,$$
$$B(h) = \frac{2^{d-h}\pi^{d/2}}{\Gamma(h/2)\Gamma(h/2-\nu)} \,. \tag{6.33}$$

This non-analytic behavior can be reproduced provided that the large-dimension distribution of the coefficients M_n contains a component with a power law:

$$[M(\Delta)]_{ij} \supset \frac{B(h)}{[\Delta - \frac{1}{2}(\Delta_i+\Delta_j)]^{d-h}} g^a g^b f_{ab}{}^c \langle i| \int_{S^{d-1}} \mathcal{V}_c(x)|j\rangle \,. \tag{6.34}$$

It should be kept in mind that M_n is a discrete sequence, and so the given continuous distribution is supposed to approximate it only on average. Below we will discuss the accuracy of this approximation in more detail. Also, for the renormalization of the ϕ^2 flow we will work out the asymptotics of the sequence M_n via an alternative method.

For the moment, to get an expression for ΔH, we introduce the shown asymptotics into (6.27) and perform the sum approximating it by an integral. Gathering all the prefactors, reinstating the dependence on the coupling constant and on R, we obtain the following formula for the correction term:

$$\Delta H \approx -g^a g^b K_{ab}{}^c(\Lambda) \int_{S_R^{d-1}} \mathcal{V}_c(x) \tag{6.35}$$

$$K_{ab}{}^c(\Lambda) = f_{ab}{}^c \, B(h) \int_\Lambda^\infty \frac{1}{[t - \frac{1}{2}(\Delta_i+\Delta_j)/R]^{d-h}(t-\bar{E})} \mathrm{d}t, \quad h = h_{abc} \,. \tag{6.36}$$

5. This term is the analogue of wave function renormalization in ordinary perturbation theory.

For very large Λ we are allowed to drop the corrections due to $\bar{E}$ and $\Delta_i + \Delta_j$ in the denominator, which yields

$$K_{ab}{}^{c}(\Lambda) \simeq f_{ab}{}^{c}\,\frac{B(h)}{d-h}\frac{1}{\Lambda^{d-h}}, \qquad (\Lambda \gg \bar{E}, (\Delta_i+\Delta_j)/R). \tag{6.37}$$

As in section 6.1, we can in principle expand the integral from Eq. (6.36) as a series in $1/\Lambda$ to obtain subleading corrections.

6.2.3 RG improvement

In the above discussion we were assuming that ΔH is very small, and correcting eigenvalues by the leading-order perturbation formula (6.22) is adequate. For this, Λ_{UV} has to be taken sufficiently large so that the renormalizations of all the couplings implied by (6.36) are small compared to their values in the bare TCSA Hamiltonian. This condition is rather restrictive and in fact in our main example below—the Landau-Ginzburg flow—we will not be able to satisfy it, as the mass renormalization due to the quartic coupling will sometimes be comparable to the bare mass.

Concretely, using the form of ΔH given in (6.36) and assuming that the corrections due to $\Delta_i + \Delta_j$ and $\bar{E}$ can be ignored, this procedure results in RG equations of the form:

$$\Lambda\frac{\partial}{\partial\Lambda}g^{c}(\Lambda) = f_{ab}{}^{c}\,g^{a}(\Lambda)g^{b}(\Lambda)\,B(h)\frac{1}{\Lambda^{d-h}} \qquad (\Lambda \gg \bar{E}, (\Delta_i+\Delta_j)/R)\,. \tag{6.38}$$

In this way we obtain a flow in the space of Hamiltonians, which we can integrate all the way down to the desired cutoff Λ_{UV}. It may be expected that, under certain circumstances, the final 'resummed' Hamiltonian obtained by such a procedure will have a larger range of applicability (i.e. work for smaller Λ_{UV}) than the first-order correction formula. This will be the case if the subleading on the right-hand side of (6.23), such as (6.24), are less important than the terms we are proposing to resum.

As already mentioned, in the examples considered below we will want to keep track of the corrections due to $(\Delta_i + \Delta_j)/R$ and $\bar{E}$ in (6.36). These corrections are state-dependent, and taking them into account completely would require a separate RG flow for every value of these parameters—a complication that we wish to avoid. Instead, we would like to find a practical way to represent them by operators. The easiest way to do so is to expand in powers of the inverse cutoff and keep only the first-order terms. In that case we can replace Δ/R by H_{CFT} and $\bar{E}$ by H. For example, in the case where $\mathcal{V}_c = \mathbb{1}$, the first of these two subleading corrections can be thought of as 'wave function' renormalization of the coefficient of H_{CFT} in the TCSA Hamitonian, [6] while the second correction becomes a uniform overall rescaling of all couplings. Both of these can be taken into account easily by a slight modification

6. This shows once again that corrections due to integrals of non-scalar operators, T_{tt} in this case, can be induced by the flow with the TCSA cutoff. In the previous subsection, we pointed out that the correction due

of (6.38). The situation is more complicated if $\mathcal{V}_c \neq \mathbb{1}$. In this case, the expansion generates terms of the form [7]

$$H_{\rm CFT}.V_c + V_c.H_{\rm CFT}, \qquad H.V_c + V_c.H, \qquad V_c \equiv \int_{S_R^{d-1}} \mathcal{V}_c\,. \tag{6.39}$$

Not only are these terms not present in the original Hamiltonian, they are also of a qualitatively different type—they are not given as an integral of a local operator over the sphere. In other words, these terms are nonlocal. While this may seem confusing, a moment's thought shows that this was to be expected. The reason is that the TCSA regulator—throwing out all states above a certain energy—is not a fully local UV regulator. [8] So we have to learn to live with nonlocal correction terms. Fortunately, from the practical point of view the terms (6.39) pose no problem. First of all, they are easily computable, since they are given by products of matrices which we anyway have to compute in the earlier stages of the TCSA procedure. Secondly, although in principle the non-local terms would appear also on the right-hand side of the RG flow equations, which would substantially complicate the flow, in practice we found that they remain rather small compared to the local terms. This happens because their running is suppressed by one extra power of the cutoff. Therefore, in this work we will ignore backreaction of the non-local terms on the other running couplings.

Although the above procedure correctly takes into account the leading $\bar{E}/\Lambda$ dependence, we realized that expanding in $\bar{E}/\Lambda$ is actually not a reasonable thing to do at large R. The point is that the ground state energy E_0 grows at large R like R^{d-1}, and even for moderately large R becomes non-negligible compared to $\Lambda_{\rm UV}$. Whether this is a problem depends on the sign of E_0. If E_0 were to become large and positive, there would be no magic way out—the correction procedure would break down as soon as $E_0 \sim \Lambda_{\rm UV}$, as seen e.g. by the blow up of the integral in (6.36). Fortunately, the ground state energy density at large R is usually negative. [9] In this case, although E_0 becomes large in absolute value, nothing bad occurs with the correction in (6.36); it even decreases with respect to the $E_0 = 0$ case. However,

to the direct appearance of $T_{\mu\nu}$ in the OPE would be suppressed, since the corresponding coefficient h is quite large. However, here we are discovering another way for the appearance of this correction—as a subleading term accompanying the unit operator in the OPE.

7. Notice that these corrections, as written, preserve the hermiticity of the Hamiltonian.

8. The TCSA regulator reproduces exact correlators as long as the insertion points are separated in the *time* direction by $\gg {\Lambda_{\rm UV}}^{-1}$. In particular, correlation functions on a constant time slice are not faithfully reproduced no matter how far the points are separated in the space direction. By a fully local UV regulator we mean a regulator which reproduces exact correlation functions as long as points are separated in *some* direction, time or space, by $\gg {\Lambda_{\rm UV}}^{-1}$. E.g. the point splitting procedure, used in conformal perturbation theory, is a fully local regulator.

9. The second-order correction to the ground state energy is negative. Assuming that higher-order corrections don't change the situation, we may expect negative energy density at large R. Studying many examples of RG flows known in $d = 2$, this seems to be invariably true. The only exceptions happen when the dimension of the perturbing operator exceeds $d/2$. In this case the renormalized ground state energy density may be positive, although the non-renormalized, divergent energy density is still negative. In both concrete examples of $d > 2$ flows studied in this work, the ground state energy density is negative at large R.

were one to expand in $\bar{E}/\Lambda$, one would unnecessarily introduce large corrections even in this benign case.

We will therefore adopt the following prescription. We will replace the estimate $\bar{E}$ in (6.36) by $E_r+(\bar{E}-E_r)$ where E_r is a convenient reference energy that we estimate to be close to the expected value of $\bar{E}$. For example, we may choose E_r to be around the ground state energy as obtained by extrapolation from lower values of the radius, or around the energy of the first excited state. In fact, the end results for the spectrum should not depend much on the chosen value of E_r, which provides a consistency check for the method. We then expand not in $\bar{E}/\Lambda$ but instead in the difference $(\bar{E}-E_r)/\Lambda$, which is not expected to become large in the large volume limit. The RG evolution is then performed keeping track of the exact dependence on E_r (no expansion) through the simple substitution $\Lambda^{d-h+1} \to \Lambda^{d-h}(\Lambda - E_r)$ in the denominator of (6.38). Since we will expand in $(\bar{E}-E_r)/\Lambda$, the leading correction in (6.39) should be modified by replacing $H \to (H - E_r)$. In appendix D.2.1, we will see a concrete example of how this works, when discussing the Landau-Ginzburg flow.

6.2.4 Other treatments of renormalization

Cutoff dependence and renormalization have been discussed in the context of the $d = 2$ TCSA studies, most importantly in [143] (following [35, 142]). In particular, Section 3 of [143] discusses in detail how the cutoff dependence can be analyzed using the OPE, and gives renormalization group equations similar to our (6.38) for the couplings of the local operators. At leading order, then, their results are basically equivalent to ours. [10]

Ref. [143] also initiated a discussion of subleading terms. For example, the first of the two subleading terms in (6.39) may be discerned in their equations, for the special case where $\mathcal{V}_c$ is the identity operator. However, significant differences do exist between us and them at how these subleading effects are implemented.

According to the prescription in Section 4.2 of [143], on top of leading RG improvement, each IR state should get a subleading correction factor computed from the conformal perturbation theory applied to a UV state from which the IR state in question originates. This prescription, as well as a more recent detailed discussion in Section 3 of [145], are designed to fix up, order by order in the coupling, the discrepancies between TCSA and conformal perturbation theory. On the other hand, our discussion uses from the very beginning the fact that the true expansion parameter is the inverse cutoff rather than the couplings, which become large in the IR.

Let's illustrate the differences by looking at the correction in Eq. (6.22). Our derivation

10. A factor $\frac{1}{2}$ seems to be missing in their Eq. (3.7). Even having corrected this misprint, we did not manage to reproduce their figure 1(c).

demonstrates clearly that one should compute ΔH with the *nonperturbative* energy $\bar{E}$ and take the matrix element between the *nonperturbative* states $\bar{c}$. A similar correction in Eq. (3.11) of [145] uses the UV energy and the UV state in place of $\bar{E}$ and $\bar{c}$. At small R the two methods would give very similar results, but at large R the difference will be significant. Indeed, the IR states at large R will have a complicated composition, in which the original UV state carries little weight (see e.g. figure 6.5). Also the energy in the IR will get a very large correction, implying a large change in the denominator in (6.23). As a result the whole correction may be modified at $O(1)$. Out of curiosity, we compared our method to that of [145] for the ϕ^2 flow discussed in the next section. We found that at large R our method is more effective in reducing the discrepancy from the exact results.

It should be noted that [145], using their renormalization prescription, achieved an excellent agreement of TCSA data with the results obtained by exact integrability methods applicable for the model they studied. This success is puzzling to us, since as we explained we believe that their prescription is problematic at large R. This question deserves further analysis.

Finally, we would like to compare our renormalization prescription to the more recent one proposed in Ref. [131] for ϕ^4 theory in two dimensions, considered as a deformation of the *massive* free boson. There are many similarities between the approach taken there and in this thesis, but the precise methods used are quite different: the authors of Ref. [131] quantize the massive theory canonically on S^1 and use the resulting Fock space as a Hilbert space, keeping only states with a total energy $\leqslant E_{\max}$. As far as the renormalization procedures are concerned, both works take the exact equation (6.19) as a starting point. The precise meaning of the matrices H_{ll}, H_{hh}, etc. in both works is of course different, but we will not insist on these details.

After this point, the two renormalization procedures differ. In this work, ΔH is foremost a correction to the energy $\bar{E}$ of a state $|\bar{c}\rangle$, computed to first order in Rayleigh-Schrödinger perturbation theory. The actual renormalization procedure consists of two steps: first, we expand ΔH into a basis of local operators, see Eq. (6.36). In the second step, we compute their appropriate couplings by integrating RG equations. The physical motivation of this procedure is rooted in the renormalization group, cf. the discussion in section 6.1. The renormalization prescription in Ref. [131] is more streamlined: ΔH is considered as an operator (rather than a first-order correction to the spectrum) and computed directly in terms of the bare couplings appearing in the Hamiltonian. Only at the very end, ΔH is expanded in terms of local operators. Both prescriptions agree at leading order, but appear to differ at the level of subleading terms. This alternative method from Ref. [131] appears somewhat simpler to work with, and it may be interesting to revisit the TCSA renormalization using this new point of view.

6.3 Renormalization for the ϕ^2 flow

6.3.1 Renormalization details

The general method of renormalization was presented in section 6.2. Here we will describe particular issues which arise when the procedure is applied to the ϕ^2 flow. The leading contributions to the correction term ΔH are expected to come from the low-dimension operators in the $\phi^2 \times \phi^2$ OPE:

$$:\phi^2(x):\times:\phi^2(0):=\frac{2\mathrm{N}_d^2}{|x|^{2(d-2)}}\mathbb{1}+\frac{2\mathrm{N}_d}{|x|^{d-2}}:\phi^2:+:\phi^4:+\dots\,, \tag{6.40}$$

Here N_d is the normalization factor in the two point function of the canonically normalized massless scalar:

$$\langle\phi(x)\phi(0)\rangle=\mathrm{N}_d/|x|^{d-2},\quad \mathrm{N}_d=1/[(d-2)\mathrm{S}_d]\,. \tag{6.41}$$

Now, curiously, although the operators ϕ^2 and ϕ^4 appear in the OPE (6.40), their contributions to the renormalization corrections vanish. Indeed, the coefficient $B(h)$ given by (6.33) is zero for the corresponding h's. The reasons this happens are not difficult to understand; they are ultimately related to the fact that the UV CFT we are perturbing is free. Starting with ϕ^4, notice that since the dimensions factorize, $\Delta(\phi^4)=2\Delta(\phi^2)$, and the OPE kernel is just a constant. Clearly, the $t\to 0$ limit discussed in section 6.2.2 is perfectly analytic in this case, and so $B(h)$ must vanish. For ϕ^2, although the OPE kernel is singular, it is a harmonic function of $x-y$. By the mean value property, the integral of a harmonic function over a sphere is equal to its value at the center of the sphere. This implies that also in this case the $t\to 0$ limit is analytic, and $B(h)=0$.[11]

Thus the only leading non-vanishing correction is for $\mathcal{V}_c=\mathbb{1}$.[12] We will have to include this correction taking into account the subleading dependence on $\Delta_i+\Delta_j$ and $\bar{E}$. Indeed, were we to drop these subleading parts, we would get a constant counterterm which would shift all eigenvalues in the same way. This would have a chance to improve the agreement for the ground state energy, but would have no effect on the spectrum of massive excitations. However, the raw TCSA massive spectra in figure 5.2 do show noticeable deviations, which we would also like to improve.

In fact, we will be able to do even better. Not only will we include the above-mentioned subleading effects, but we will also take into account the discreteness of the sequence M_n.

11. This argument shows that, more generally, corrections will vanish for the ϕ^{n+m} and ϕ^{n+m-2} operators in the $\phi^n\times\phi^m$ OPE. This observation will be useful for the general Landau-Ginzburg flow in section D.2.1.

12. This also implies that the RG improvement discussed in section 6.2.3 is not of much use for this particular example: the mass parameter never appears on the right-hand side of the renormalization group equations (6.38), so their solution is straightforward and essentially given by (6.36), i.e. the unimproved equation.

Recall that the general formula (6.34) gives this sequence only on average. However, it turns out that for the ϕ^2 flow the tail of the M_n sequence can be worked out explicitly, independently of the argument in section 6.2.2. As we show in appendix D.2, M_n at $\Delta_n \gg \Delta_j$ is nonzero only if $\Delta_n - \Delta_j - \Delta(\phi^2) = 2p$ is an even integer, in which case it's given by

$$(M_n)^i{}_j = \frac{2(2\nu)_p(\nu)_p}{p!(\nu+1)_p}(\mathrm{N}_d\mathrm{S}_d)^2\delta^i{}_j \overset{d=3}{\to} \frac{2}{2p+1}(\mathrm{N}_d\mathrm{S}_d)^2\delta^i{}_j\,. \tag{6.42}$$

It's not difficult to see that on average this sequence does agree with the continuous distribution (6.34), which also provides a check for the general argument.

We next evaluate ΔH via Eq. (6.27). When doing the sum, we use the expression (6.42) for all terms. This is not quite true, since (6.42) was derived under the assumption $\Delta_n \gg \Delta_j$, which does not hold for the external states i, j just below and n just above the cutoff. However, the induced error cannot be large, since the states i, j close to the cutoff will anyway contribute little to the renormalization, having small weight in the eigenvector $\bar{c}$; see figure 6.5 below. We will therefore tolerate this little imprecision. The infinite sum over p becomes a ${}_4F_3$ hypergeometric sum, and specializing to $d = 3$ we obtain the digamma function $\psi(z)$. Reinstating the coupling and radius dependence, we get:

$$(\Delta H)^i{}_j \approx -(\tfrac{1}{2}m^2)^2\frac{R^3}{(d-2)^2}\frac{\psi((K_j+\Delta_j-R\bar{E})/2)-\psi(K_j/2)}{\Delta_j - R\bar{E}}\delta^i{}_j\,, \tag{6.43}$$

where K_j is defined as the smallest odd integer such that $\Delta_j + K_j > \Delta_{\max}$.

The leading term in ΔH for large $\Delta_{\max}$ is a state-independent correction $\propto \Delta_{\max}^{-1}$. As mentioned above, keeping only this correction would not be adequate. Instead, we will use the full expression (6.43) to compute corrected ('renormalized') eigenvalues E_{ren} from the raw TCSA eigenvalues $\bar{E}$ via the formula (6.22):

$$E_{\text{ren}} = \bar{E} + \bar{c}_i(\Delta H)^i{}_j\bar{c}^j\,. \tag{6.44}$$

It is these 'renormalized' results which were used to produce figures 5.1,6.3. Here $\bar{c}$ is the eigenvector corresponding to the raw TCSA eigenvalue $\bar{E}$. In this approach, each energy level is corrected separately.

Note that to apply formula (6.44) we need to compute both *right* eigenvector $\bar{c}^j$, as in (4.34), and the *left* eigenvector $\bar{c}_i$:

$$H^i{}_j\bar{c}^j = \bar{E}\bar{c}_j\,, \quad \bar{c}_iH^i{}_j = \bar{E}\bar{c}_i\,. \tag{6.45}$$

The eigenvectors are assumed normalized via $\bar{c}_i\bar{c}^i = 1$. Of course these two eigenvectors are related, up to normalization, via the Gram matrix:

$$\bar{c}_i \propto G_{ij}\bar{c}^j\,. \tag{6.46}$$

As mentioned in section 4.3.3, computing the full Gram matrix may be expensive, although we did find an indirect way to do it, described in section 4.4.3. If one has access to the

Gram matrix, one can use it to compute the left eigenvectors via (6.46). Without the Gram matrix, one simply finds $\bar{c}_i$ from the second eigenvalue problem in (6.45). [13]

6.3.2 Numerical results

In section 5.4, specifically Fig. 5.2, we displayed the 'raw' spectra for the massive boson, computed using the bare TCSA Hamiltonian at cutoff $\Delta_{\max} = 12$ (18). In figure 6.3 we show the same but for the spectra computed using renormalized TCSA. We see from these plots that renormalization extends the range of R where TCSA is in agreement with the exact results from $R \lesssim 2$ to $R \lesssim 3$.

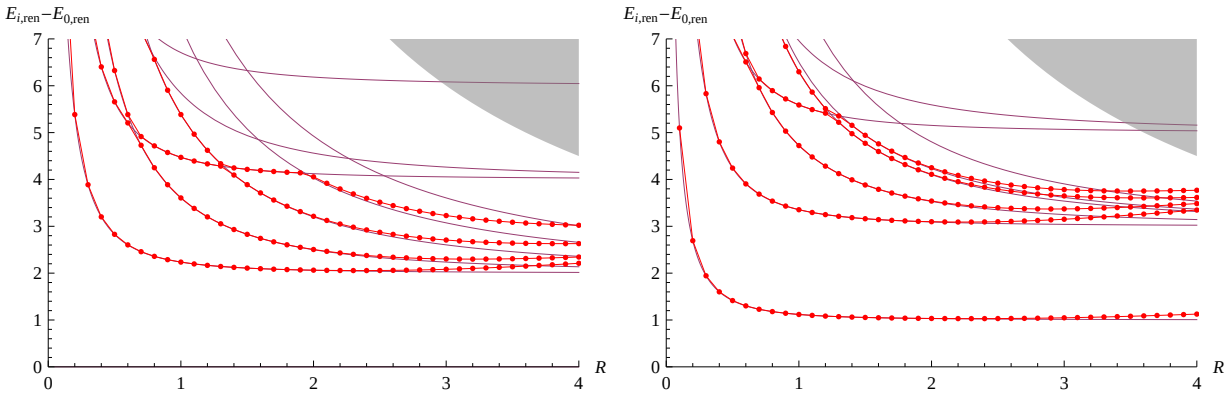

Figure 6.3: Same as figure 5.2, but for the renormalized TCSA spectra.

Figures 5.1 and 6.3 do demonstrate that our renormalization procedure works—upon applying the renormalization corrections, the discrepancy from the exact results is reduced compared to the raw TCSA data. Figure 6.4 demonstrates the same as a function of the UV cutoff: we show how the TCSA ground state energy and the massive spectrum converge to their exact values with the gradual increase of $\Delta_{\max}$. We do this plot for one value $R = 2$, but the picture is qualitatively the same for all R. This figure shows that not only the accuracy is greatly improved after the renormalization, but the convergence rate is also improved. This is because the error terms remaining after the leading renormalization subtractions are suppressed by higher powers of $1/\Lambda_{\text{UV}}$.

One last aspect we would like to discuss here is an assumption implicit in the entire procedure of renormalization, namely that the contribution of high energy states to low

13. It should be noted that the nonsymmetric eigenvalue problems are somewhat more difficult to solve numerically than the symmetric ones, and more prone to numerical instabilities. In our work we overcome the instabilities by applying the transformation $H \to (H-\sigma)^{-1}$ to the matrix H before diagonalization. This transformation focuses on the eigenvalues nearest to σ. We also checked some of our results by working at a higher number of digits. In future work, it would be interesting to keep looking for other, more numerically efficient diagonalization procedures.

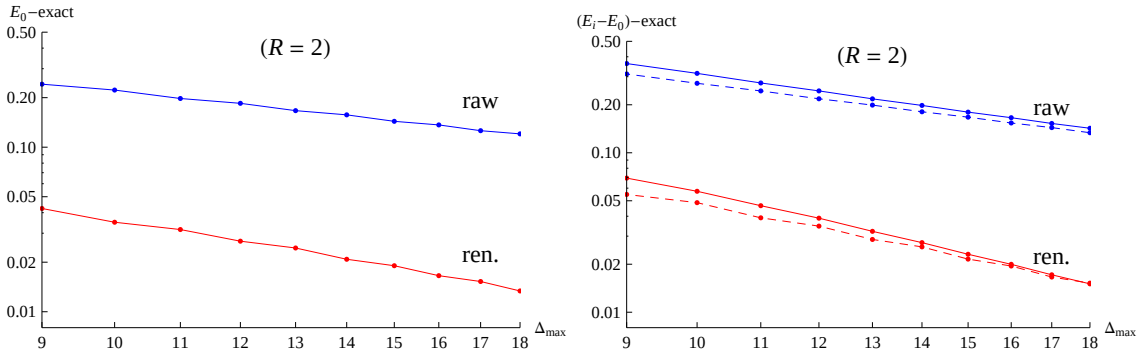

Figure 6.4: Convergence rate before and after renormalization. Left: ground state energy. Right: lightest states in the massive spectrum, $\mathbb{Z}_2$-even (solid) and $\mathbb{Z}_2$-odd (dashed).

energy observables is suppressed. It is possible to make this assumption more quantitative by studying the distribution of eigenstate components in energy, defined as:

$$w(\Delta) = \sum_{i:\Delta_i=\Delta} \bar{c}_i \, \bar{c}^i \,. \tag{6.47}$$

In figure 6.5, we plot this distribution for the lowest $\mathbb{Z}_2$-even massive excitation (the one which is interpreted as a state of two particles at rest) and for several values of R. As expected, for small R the distribution is strongly peaked at $\Delta = \Delta(\phi^2) = 1$. As R is increased, the distribution becomes wider and wider, but its high-energy tail does remain suppressed. The same qualitative behavior is true for the other states. One can wonder what it would mean if for very large R the distribution becomes flat or even peaked at high Δ. Does this ever happen for CFTs perturbed by a relevant operator? Presumably the method would completely break down for such R, but for the values of R explored in this work this does not happen.

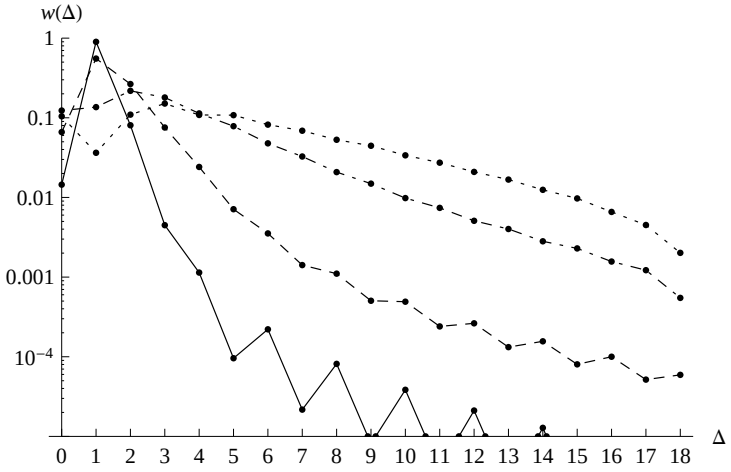

Figure 6.5: The distribution of eigenstate components in energy, Eq. (6.47), plotted for the lowest $\mathbb{Z}_2$-even massive excitation, for $R = 0.5$ (solid), 1 (dashed), 2 (dot-dashed), 3 (dotted).

Chapter 7

The Landau-Ginzburg flow

In the free massive flow considered in the previous chapter, we could compare TCSA results with their exact theoretical values for all observables. Although the massive flow forms a good pedagogical example of the TCSA in action, we would like to use the TCSA to study strong-coupling phenomena that do not occur in free theories. In this chapter, we will therefore apply the TCSA to a more interesting model, namely the ϕ^4 theory, described in flat space by the Euclidean action

$$S[\phi] = \int \mathrm{d}^d x \left(\tfrac{1}{2}(\partial\phi)^2 + V[\phi] \right), \qquad V[\phi] = \tfrac{1}{2} m^2 {:}\phi^2{:} + \lambda {:}\phi^4{:}. \tag{7.1}$$

In d dimensions, the quartic coupling λ has dimension $[\lambda] = 4 - d$, meaning that it is relevant when $d < 4$. In order for the potential to be bounded from below, we require that λ be positive.

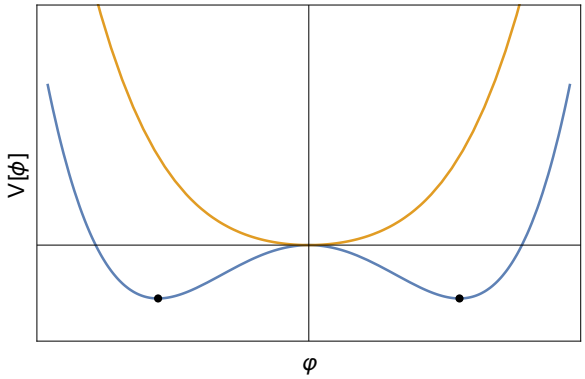

Figure 7.1: Orange (resp. blue) plot: ϕ^4 potential with $m^2 > 0$ (resp. $m^2 < 0$). Black dots: minima of $V[\phi]$ for $m^2 < 0$.

It is well-known that the action (7.1) displays spontaneous symmetry breaking at low energies. Qualitatively, this can be understood using a tree-level analysis of the action (7.1). When $m^2 > 0$, there is a unique vacuum with order parameter $\langle\phi\rangle = 0$, and the $\mathbb{Z}_2$ symmetry

$\phi \to -\phi$ is preserved. If on the other hand $m^2 < 0$, there are two vacua with

$$\langle \phi \rangle = \pm \sqrt{-\frac{m^2}{4\lambda}} \neq 0 \tag{7.2}$$

and the theory is in a broken phase, cf. figure 7.1. We do not expect the actual boundary between these phases be at $m^2 = 0$, because the ϕ^4 coupling additively renormalizes the bare mass. It is not even obvious whether the critical value of m^2 will be positive or negative. In our TCSA exploration of this theory, we will simply scan over a range of values of the bare mass m^2 to find its critical value.

Indeed, the action (7.1) is a phenomenological model for the $\mathbb{Z}_2$ phase transition that occurs in many systems, including ferromagnets and binary liquids [146]. A comprehensive explanation of the Landau theory of phase transitions is outside the scope of this thesis; we refer the reader to any of the textbooks [29, 31, 30] for more details. In the light of this analogy with the theory of phase transitions, the action (7.1) will also be referred to as *Landau-Ginzburg theory*.

It is the goal of this chapter to reproduce the above phase diagram using the TCSA. In section 7.1, we will explain in more detail how we expect to find symmetry breaking; the numerical results are presented and discussed in section 7.2. All TCSA computations in this chapter will be done in non-integer d, for which the Hilbert space is not positive-definite. The consequences of these unitarity violations are discussed in 7.3. In appendix D.2.1, we detail the renormalization procedure used.

7.1 Theoretical expectations

Let us now discuss more precisely the theoretical expectations for the TCSA Hamiltonian

$$H = H_{\text{CFT}} \; + \; \int_\Sigma \left[\frac{1}{2} m^2 {:}\phi^2{:} \; + \; \lambda \, {:}\phi^4{:} \right], \tag{7.3}$$

where H_{CFT} is the CFT Hamiltonian of the free massless boson. We will be agnostic about the sign of m^2 for now. The low-energy physics of this theory can only depend on the dimensionless ratio

$$t \equiv m^2 / \lambda^{2/(4-d)}. \tag{7.4}$$

The case of small quartic coupling corresponds to $|t| \gg 1$. In this regime the theory in the IR describes weakly interacting massive particles, and predictions can be obtained from perturbation theory. This is regardless of the sign of m^2. For positive (and still large) t, the perturbative vacuum is at $\phi = 0$, and the $\mathbb{Z}_2$ symmetry $\phi \to -\phi$ is preserved. On the other hand, for negative t, perturbation theory is developed around one of two degenerate vacua of the double-well potential displayed in Fig. 7.1, where the $\mathbb{Z}_2$ symmetry is spontaneously broken.

Any non-trivial physics must happen for $t = O(1)$, when the IR theory is strongly coupled, and perturbation theory is not useful. One generally expects that the $\mathbb{Z}_2$ broken and preserving phases extend into the strongly coupled region, where they are separated by a second-order phase transition at a critical value $t = t_c$, see figure 7.2. At $t = t_c$ the theory is expected to flow in the IR to a CFT, belonging to the Wilson-Fisher family of fixed points in the Ising model universality class.

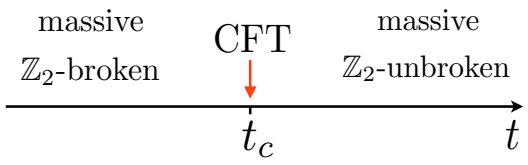

Figure 7.2: The commonly accepted phase diagram for the Landau-Ginzburg flow. Our calculations will indicate that $t_c > 0$ in $d = 2.5$ dimensions.

In this paper we will only study the $m^2 > 0$ (i.e. $t > 0$) part of the phase diagram. Instead of varying t as in figure 7.2, we will find it convenient to work in the units $m = 1$, and vary λ. Using TCSA, we will compute how the finite volume spectrum of the theory depends on λ. As we will see, for small λ the spectrum will be consistent with preserved $\mathbb{Z}_2$ symmetry, while for $\lambda > \lambda_c$ our calculations will indicate spontaneous $\mathbb{Z}_2$ symmetry breaking. Thus we will obtain qualitative confirmation of the phase diagram in figure 7.2, and quantitative information about the massive spectrum in the strongly coupled region. We will determine the critical value λ_c with some precision. For $\lambda = \lambda_c$ we will observe the mass gap going to zero, indicating that the IR theory is conformal. We will be able to get a rough estimate of the leading critical exponents at the phase transition point and compare them with the known values in the Ising universality class.

Notice that since our calculations indicate a positive value of $t_c = 1/\lambda_c^{(4-d)/2}$, the whole region $t < 0$ is expected to be in the $\mathbb{Z}_2$-broken phase. However, we have not explored this region numerically.

7.2 Numerical results

We will now perform TCSA analysis of the Landau-Ginzburg flow. We already remarked that the ϕ^4 perturbation induces UV divergences for $d \geqslant 8/3 \sim 2.67$. In order to avoid these UV divergences, we are forced to work in non-integer d. We choose the value $d = 2.5$, in order to stay far from the $d \to 2$ limit, where the spectrum of the free scalar CFT becomes dense. We will work with a cutoff of $\Delta_{\text{max}} = 17$, which corresponds to 5494 (4907) $\mathbb{Z}_2$-even (odd) states in $d = 2.5$.

As already mentioned above, we will set $m^2 = 1$. The spectrum will depend on λ and the TCSA radius R. We will explore the region $R \lesssim 3$ and $\lambda \lesssim 1.15$ (see figure 7.3). Raw TCSA without renormalization corrections would give converged predictions only in the lower left corner of this region, corresponding to weak coupling and small physical volume. To extend the range of applicability of the method, we will apply a renormalization procedure as described in section 6.2, with the theory specific details described in section D.2.1 below. To reduce the number of plots, we will only show results with all renormalization corrections taken into account.

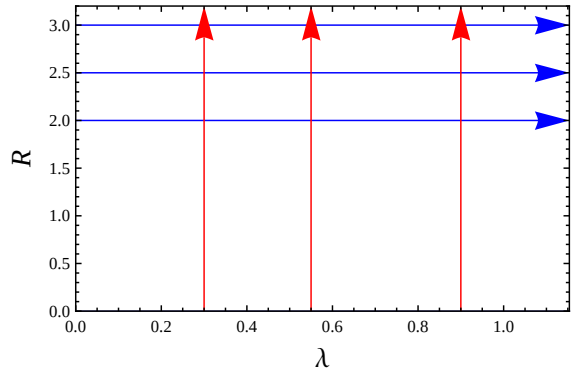

Figure 7.3: The range of R and λ explored in our study. Subsequent figures will show the spectrum dependence along the vertical and horizontal sections of this region, shown by the arrows.

Spectrum for a fixed R and varying λ

To visualize the spectrum dependence, we will plot it along a number of vertical and horizontal sections in the two-dimensional range in figure 7.3. Let us start with plots at a fixed R and varying λ. In figure 7.4 we show the results for $R = 2.5$. The ground state energy E_0 is defined as the lowest energy in the $\mathbb{Z}_2$ even sector. The excitation spectra are given by $E_i - E_0$, in the $\mathbb{Z}_2$-odd and the $\mathbb{Z}_2$-even sectors, respectively.

We see that as λ is increased, the excitation energies first decrease, and then, for $\lambda > \lambda_c \approx 0.5$ - 0.6, start increasing again. An interesting feature of the spectrum at $\lambda > \lambda_c$ is an approximate double degeneracy of states in the $\mathbb{Z}_2$-even and odd sectors, well visible for the vacuum and the first couple of excited levels. This behavior is the telltale sign that the theory for $\lambda > \lambda_c$ is in the phase of spontaneously broken $\mathbb{Z}_2$ symmetry. We then expect that the theory at $\lambda = \lambda_c$ is conformal. This expectation will be further tested below.

It may be somewhat counterintuitive that the $\mathbb{Z}_2$ symmetry breaks for a *positive* value of m^2 (remember that we fixed $m = 1$). In fact, there is no paradox. The m^2 is a UV parameter defining the initial direction of the flow, while the breaking is an IR phenomenon. As we flow

from UV to IR, m^2 is renormalized and the effective squared mass may become negative. [1] In other words, we may imagine that a double-well potential is generated by quantum effects. In this case there will be two degenerate vacua, and all excitations above the vacua should be degenerate as well. The degeneracy would be exact in infinite volume. In finite volume we expect some mixing due to the potential barrier tunneling, [2] so that the exact eigenstates are $\mathbb{Z}_2$-even or $\mathbb{Z}_2$-odd and split by a small amount (exponentially small for large volume). The mixing and the splitting are expected to become more important for higher energy states, for which the tunneling is not suppressed. All these intuitive expectations are confirmed by figure 7.4.

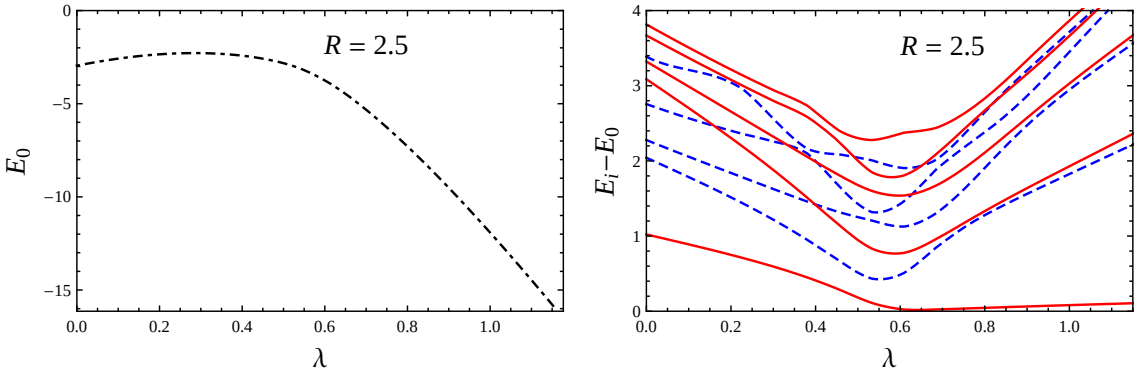

Figure 7.4: The ground state energy (left panel) and the spectrum of low-lying massive excitations (right panel) as a function of λ for $R = 2.5$. We plot 4 lowest $\mathbb{Z}_2$-even (dashed blue) and 5 lowest $\mathbb{Z}_2$-odd (solid red) states.

Another interesting feature of the spectra in figure 7.4 is the absence of level crossing: eigenstates belonging to the same $\mathbb{Z}_2$ sector don't cross. There are several values of λ when a pair of same $\mathbb{Z}_2$-parity eigenstates come close to each other, but then repel. This should be contrasted with the free massive flow spectra, which do show level crossings, reproduced by TCSA calculations. The difference stems from the fact that the ϕ^2 flow is integrable, while the Landau-Ginzburg flow is not. This way of distinguishing integrable and non-integrable flows has long been noticed in the $d = 2$ TCSA literature (see e.g. [24, 148]), and here we are observing it in $d > 2$.

Mass gap as a function of λ and determination of λ_c

We will now further test the expectation that the theory at $\lambda = \lambda_c$ is conformal. In figure 7.5 we plot the low-lying spectrum of excitations (just the first three states) for λ varying from 0 to 1.15 and for three values of $R = 2, 2.5, 3$. We see that the excitation energies

1. See section D.2.1 for the RG equations for the Landau-Ginzburg flow.
2. Such tunneling effects were for example studied in TCSA in Ref. [147].

are decreasing with R for λ near λ_c. This is especially noticeable for the second and third excited level. Away from λ_c the spectrum is relatively stable with R.[3]

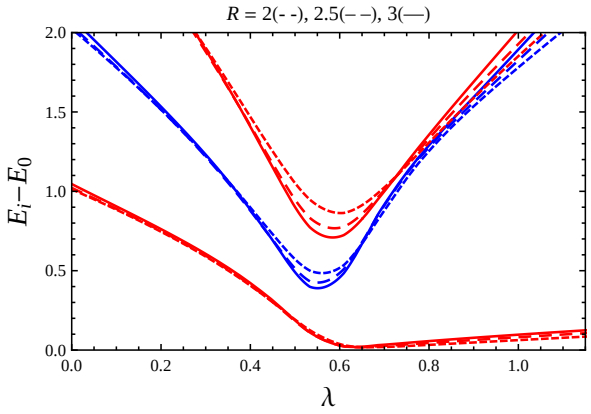

Figure 7.5: The spectrum of three lowest excitations as a function of λ for three values of R: 2 (short dashed), 2.5 (longer dashed), 3 (solid).

The decrease of the spectrum with R at $\lambda = \lambda_c$ is what one should expect if the critical theory is conformal. Indeed, for a flow ending in a conformal fixed point the excitation energies should behave at large R as $\Delta_i^{\rm IR}/R$ where $\Delta_i^{\rm IR}$ are the IR CFT operator dimensions. We will test this expectation in the next section.

Let us now determine the critical value of the coupling λ_c with some precision. According to the standard renormalization theory, the mass gap for λ near λ_c should depend on λ as

$$M_{\rm gap} \approx C|\lambda - \lambda_c|^\nu \,, \tag{7.5}$$

where ν is a critical exponent,[4] which in the case at hand is related to the dimension of ϵ—the first $\mathbb{Z}_2$-even scalar operator at the Wilson-Fisher fixed point:

$$\nu = 1/(d - \Delta_\epsilon) \,. \tag{7.6}$$

In our case the mass gap is $E_1 - E_0$ for $\lambda < \lambda_c$ and $E_2 - E_0$ for $\lambda > \lambda_c$. We will fit $E_1 - E_0$ in the region $\lambda < \lambda_c$ to determine λ_c and ν. We exclude the region $\lambda > 0.5$ from the fit since it is clearly affected by finite R effects which smear out the expected power-law behavior. We also exclude the region $\lambda < 0.3$ since Eq. (7.5) is expected to be valid only in the $\lambda \to \lambda_c$ limit. We thus perform the fit in an interval $[\lambda_1, \lambda_2]$, and to estimate the systematic uncertainty we vary λ_1 between 0.3 and 0.4 and λ_2 between 0.45 and 0.5. This gives the following rough estimates for the critical coupling and the exponent ν (see figure 7.6):

$$\lambda_c = 0.535 \text{ - } 0.555 \,, \quad \nu = 0.65 \text{ - } 0.8 \,, \tag{7.7}$$

with a positive correlation between λ_c and ν.

3. Or even slightly increasing. We observed that this slight increase of the spectrum with R is reduced when raising the cutoff, so it must be attributed to truncation effects.

4. This critical exponent ν should not be confused with the shorthand notation $\nu \equiv (d-2)/2$ used before.

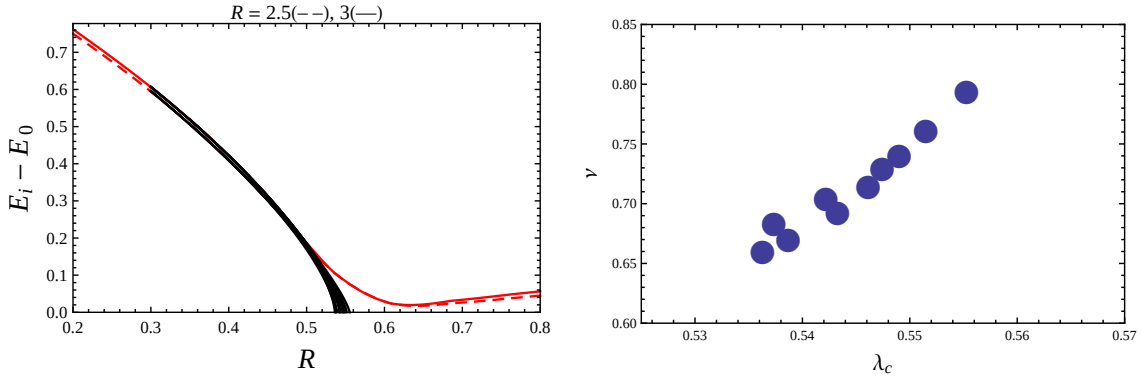

Figure 7.6: Left panel: We fit the $R = 2.5$ and $R = 3$ mass gap in the region $[\lambda_1, \lambda_2]$, for several λ_1 and λ_2 values chosen within the ranges $0.3 \ldots 0.4$ and $0.45 \ldots 0.5$, respectively. Right panel: a scatter plot for the λ_c and ν parameters resulting from these fits.

We will now compare our determination of ν with the results by other approaches. The dimension Δ_ϵ for $d = 2.5$ dimensions can be extracted from the Borel-resummed epsilon-expansion series [149]. It can also be determined from the conformal bootstrap under the assumption that the Wilson-Fisher fixed point lives at a kink in the region of the $(\Delta_\sigma, \Delta_\epsilon)$ plane [102]. The latter analysis was done under the assumption that the Wilson-Fisher fixed point in fractional dimensions is unitary, which as we now know is not necessarily true. However, as noticed in section 4.3.5, a small fraction of high-dimension negative-norm states should not have strong influence on the conformal bootstrap predictions. This probably explains why [102] found no disagreement with the results of [149]. Both analyses predict:

$$\Delta_\epsilon \approx 1.175 \qquad (d = 2.5)\,, \tag{7.8}$$

which gives a value $\nu \approx 0.755$, close to the upper end of the confidence interval for ν determined by our fitting procedure above. Assuming this precise value of ν and repeating the fits leads to a somewhat more accurate determination of the critical coupling:

$$\lambda_c \approx 0.55 \text{ - } 0.56\,. \tag{7.9}$$

Spectrum for a fixed λ and varying R

We next present how the spectrum depends on R for a fixed value of λ (figure 7.7). We pick three representative values of the quartic: $\lambda = 0.3$ for the $\mathbb{Z}_2$-preserving phase, $\lambda = 0.55$ near the presumed critical point, and $\lambda = 0.9$ in the $\mathbb{Z}_2$-breaking phase. We will now comment upon what we see in those plots, first for the ground state energy, and then for the massive spectra.

Ground state energy

The ground state energy is expected to grow for large R as a constant times R^{d-1}, corre-

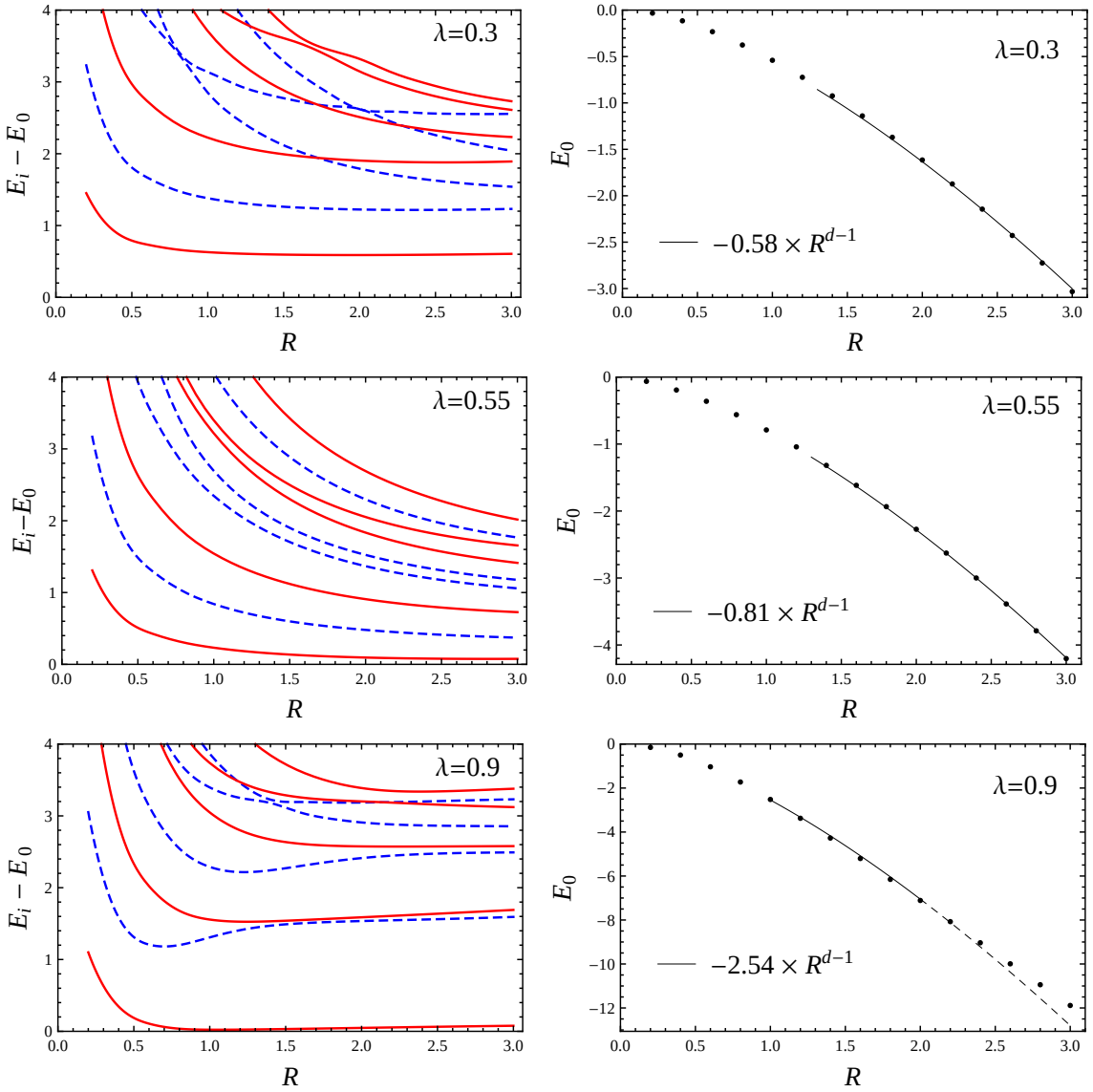

Figure 7.7: Left panels: The spectrum of excitations as a function of R for three values of the coupling: $\lambda = 0.3, 0.55, 0.9$. Solid red (dashed blue): $\mathbb{Z}_2$-odd (-even) states. Right panels: The ground state energy for the same couplings. Dots: numerical data. Black curves: fits of the data by $const.R^{d-1}$ in the range $R = 1.4$ - 3 ($R = 1$ - 2 for $\lambda = 0.9$).

sponding to a finite energy density (cosmological constant) induced by the RG flow. This behavior is clearly visible in the data for $\lambda = 0.3, 0.55$, while for $\lambda = 0.9$ the fit is not so good and there are significant deviations for $R \gtrsim 2$. These deviations decrease with $\Delta_{\max}$ and are thus due to truncation effects. Jumping a bit ahead, notice that there are no comparably flagrant deviations in the massive excitation spectrum for $\lambda = 0.9$ and large R. This is because the largest truncation effects are expected in the coefficient of the unit operator, which has the smallest possible dimension (0), and the unit operator affects the ground state energy but not the spectrum.

Excitations for $\lambda = 0.3$

Since the energies are observed to tend to finite nonzero limits for $R \to \infty$, we conclude that the IR theory is massive. The lightest $\mathbb{Z}_2$-odd state E_1 is a scalar particle of mass

$$M = \lim_{R\to\infty} (E_1 - E_0) \sim 0.6\,, \tag{7.10}$$

The next two excitations, belonging to the $\mathbb{Z}_2$-even sector, are readily interpreted as two-particle states. The former, of mass $\approx 2M$, must have both particles at rest, while in the latter the particles must be in relative motion with respect to each other, with total angular momentum zero. Higher up, we observe a state of three particles at rest, of mass $\approx 3M$, and orbital excitations thereof.

The appearance of this hierarchy of states, quantized in units of the lowest excitation, is a nontrivial consistency test on the results. It is also a prediction for the absence of bound states. *At weak coupling*, the two-particle interaction is repulsive in the $\mathbb{Z}_2$-symmetric phase of the ϕ^4 theory, so we wouldn't expect bound states. Our results show that this conclusion remains valid at strong(er) coupling. Notice that the physical mass M is significantly less than the bare mass m, so that the theory we are examining is presumably moderately to strongly coupled.

It is interesting to study the rate with which the excitation energies approach their infinite volume limits. Focussing first on the lowest excitation, the leading correction is expected to arise from coupling to curvature and scale as $1/R^2$:

$$E_1 - E_0 = M + \Delta M_{\rm curv} + \ldots\,, \quad \Delta M_{\rm curv} = \frac{A(d-2)^2}{8MR^2}\,, \tag{7.11}$$

where A is a (theory-dependent) constant. Indeed, when the theory is put in a weakly curved background, it should be possible to describe corrections to the lightest state energy by an effective Lagrangian of the same form as the free massive scalar Lagrangian (5.2) with $m \to M$ and an effective κ which will, in general, be different from κ_c in the UV. Then we get (7.11) with $A = \kappa/\kappa_c$.[5]

5. Notice that for $d = 2$ the curvature vanishes, and the modification of the mass spectrum is entirely due to boundary conditions. The leading correction in this case is exponentially small [137]: $E_1 - E_0 = M + O(e^{-\sqrt{3}/2ML})$, $L = 2\pi R$.

In figure 7.8 we test Eq. (7.11) for the lowest excitation of the $\lambda = 0.3$ spectrum. We see that it describes the large R approach reasonably well up to $R \sim 1.5$, where the truncation effects apparently kick in and make the error to increase rather than decrease with R. Fitting the correction in the range $R = 0.4$ - 1.5 we determine $M \approx 0.57$, $A \approx 1.05$.

One could wonder why A is so close to one in the case at hand. As already mentioned, we don't expect that A should be universal. We will encounter $A < 0$ below in the $\mathbb{Z}_2$-broken phase. Moreover, the coupling to curvature will be suppressed if the state in question is a pseudo-Goldstone boson, as may happen for more complicated flows with a continuous global symmetry. So, for the pion in QCD we expect $A \sim (m_\pi/\Lambda_{\rm QCD})^2 \ll 1$.

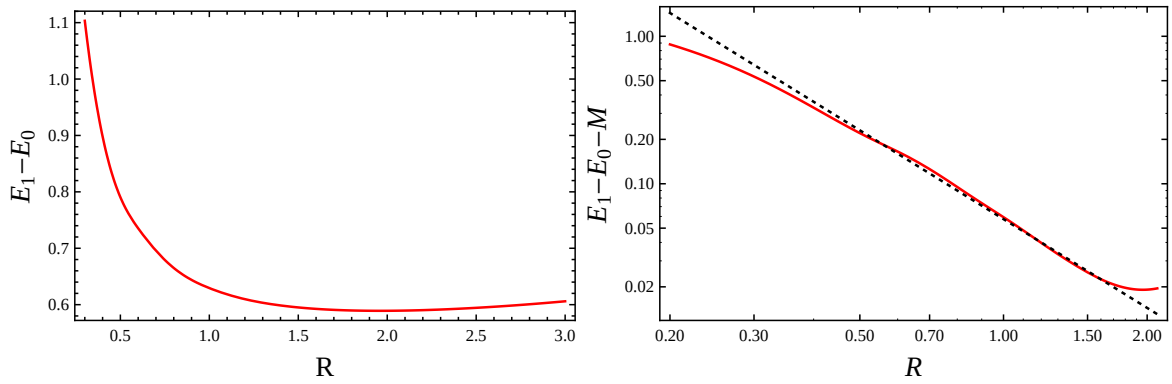

Figure 7.8: Left panel: the lowest $\mathbb{Z}_2$-odd excitation of the $\lambda = 0.3$ spectrum. We see that the excitation energy decreases for $R \lesssim 2$ and then starts somewhat increasing, likely due to truncation effects. In the right panel we test Eq. (7.11) in the range $R \lesssim 2$. Red curve: $E_1 - E_0 - M$ (log-log scale). Dotted line: $\Delta M_{\rm curv}$. The parameters $M = 0.57$, $A = 1.05$ have been determined by performing a fit in the range $R = 0.4$ - 1.5. The agreement is good.

We next discuss the rate of approach for the two-particle states, starting with the two-particle state at rest. The energy of this state can be approximated as

$$E_2 - E_0 = 2(M + \Delta M_{\rm curv}) + \Delta M_{\rm scat}\,, \tag{7.12}$$

where the last correction is due to the interaction (scattering) between two particles put into a finite volume. Since the interaction is short-range, we expect the leading correction of this type to scale as the inverse volume of the box [150]. In figure 7.9 we plot $E_2 - E_0 - 2M$ for the $\lambda = 0.3$ spectrum. We see that the difference is not well described by the finite-volume correction $2\,\Delta M_{\rm curv}$ alone. A much better agreement can be obtained including a correction with the scaling $\propto 1/R^{d-1}$, as would be expected from a scattering correction. Notice that the sign of the so determined scattering correction is positive, corresponding to a repulsion between the constituent particles. Indeed, as we already mentioned above, at weak coupling in the unbroken phase, $\lambda\phi^4$ interaction is repulsive; here we see the same effect persisting at strong coupling. In principle, it should be possible to relate the size of the scattering

correction to the scattering length, as was done for a flat torus by Lüscher [150]. In would be interesting to work out the corresponding theory for the sphere.

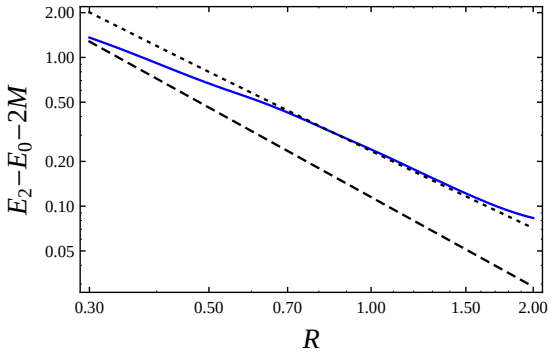

Figure 7.9: Blue curve: $E_2 - E_0 - 2M$ for the 'two-particles at rest' state in the $\lambda = 0.3$ spectrum (log-log scale). Dashed black line: $2 \times \Delta M_{\rm curv}$. We use the best fit value $M = 0.57$, $A = 1.05$. Dotted black: $2 \times \Delta M_{\rm curv}$ plus $\Delta M_{\rm scat} = 0.12/R^{d-1}$.

Finally, in figure 7.10 we plot the difference $E_i - E_0 - 2M$ for the lowest two orbital excitations in the two-particle sector, which should consist of two particles moving in the $\ell = 1$ and $\ell = 2$ angular momentum modes, combined to have the total angular momentum zero. Thus their finite volume mass correction should have an extra orbital term (see Eq. (5.12))

$$2 \times \Delta M_l, \quad \Delta M_l = \ell(\ell + d - 2)/(2MR^2)\,. \tag{7.13}$$

As is clear from figure 7.10, $E_i - E_0 - 2M$ decrease way too slowly with R to be described in the asymptotic region by just the sum of the curvature and orbital corrections. It must be that the difference is due to the scattering correction, although it looks hard to make a quantitative conclusion using the data in the $R < 3$ region.

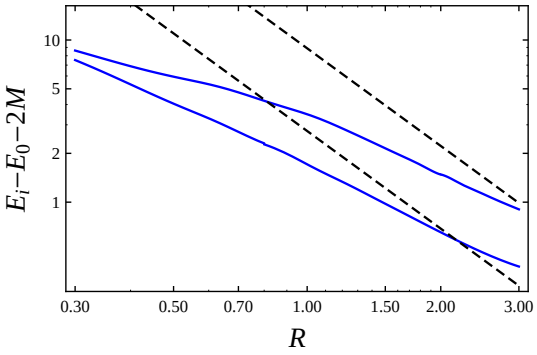

Figure 7.10: Blue curves: $E_i - E_0 - 2M$ for the lowest two orbital excitations in the two-particle sector of the $\lambda = 0.3$ spectrum corresponding (log-log scale). We excised by hand a state which asymptotes to $4M$ and thus looks like a four-particle state at rest. Dashed black lines: $2(\Delta M_{\rm curv} + \Delta M_l)$ for $l = 1, 2$.

Excitations for $\lambda = 0.55$

A very different behavior presents itself in the spectrum dependence on R for $\lambda = 0.55$, which is close to the critical coupling. Instead of energies tending to finite limits, we see them all gradually decrease with R.

As already mentioned in section 7.2, at $\lambda = \lambda_c$ we expect the excitation energies to scale at large R as Δ_i^{IR}/R, where Δ_i^{IR} are the IR CFT operator dimensions. To test this expectation, we plot in figure 7.11 the excitation energies times R. We vary λ in the range $0.53 \ldots 0.56$, roughly the range determined in section 7.2 to contain the critical coupling. Apart from the state ϵ in the $\mathbb{Z}_2$-even sector, of dimension ≈ 1.175 (see Eq. (7.8)), we expect

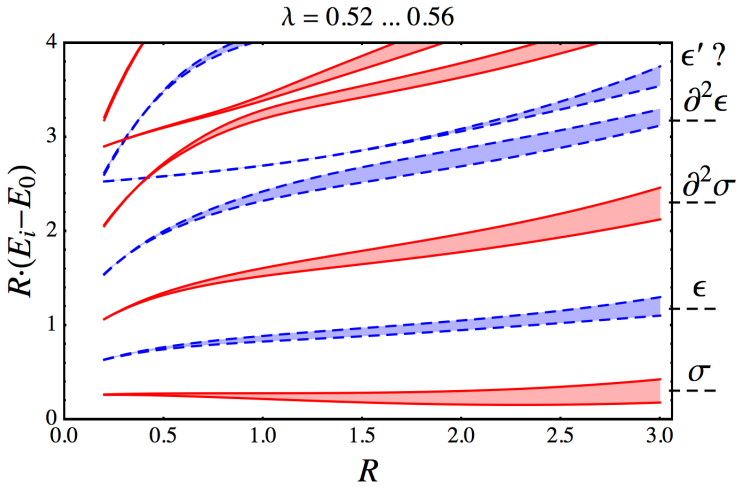

Figure 7.11: $\mathbb{Z}_2$-odd (red solid) and $\mathbb{Z}_2$-even (blue dashed) excitation energies multiplied by R, as a function of R. The shaded regions show the variation when λ varies in the range $0.53 \ldots 0.56$ (when the coupling is increased all the excitation energies go down). On the right border of the plot we indicate the expected dimensions of the lowest-lying states of the Wilson-Fisher fixed point in $d = 2.5$ dimensions (see the text). The curves must tend to the indicated finite limits. They do reach these limits for $R \approx 3$, but would overshoot them (except for σ) for larger R.

to see a $\mathbb{Z}_2$-odd operator σ of dimension ≈ 0.305 (as extracted again from [149, 102]). We also expect to see the states corresponding to operators $\partial^2\epsilon$ and $\partial^2\sigma$, of dimension two units higher. Finally, we may hope to see the next primary $\mathbb{Z}_2$-even operator ϵ', whose dimension for $d = 2.5$ is not precisely known but may be expected to lie between 3.5 and 4. [6]

Interestingly, for $R \approx 3$ we can observe all of the above mentioned states in the spectrum in figure 7.11, at the dimensions where they are supposed to be and with the right $\mathbb{Z}_2$ quantum number. The agreement of theory and our numerical results remains imperfect in that the curves don't really approach finite limits very well. Perhaps one could claim that for the lowest two states σ and ϵ, whose variation with R is not huge. However, the higher

6. It's 4 in $d = 2$ and in $d = 4 - \epsilon$, and ≈ 3.83 in $d = 3$ [151–153, 8].

states definitely exhibit growth with R and would overshoot the theoretical prediction for their dimension, were we to extend this plot to higher values of R. We hope that this issue will get resolved in the future by improving the accuracy of the method (see section D.2.1).

We would like to mention here that while TCSA should in principle be able to reproduce long-distance physics both in the gapped (massive) and the gapless (CFT) phases, it may not be the best approach from the point of view of numerical accuracy if one is interested *only* in the IR CFT. The conformal bootstrap is likely to give higher-precision results (see e.g. [7, 8, 103, 9, 114] for ongoing work concerning the Ising and $O(N)$ models in $d = 3$).

We would also like to mention in this respect the recent work [154] describing a Monte Carlo simulation of the critical point of the 3d Ising model not in the traditional $\mathbb{R}^3$ geometry, but in the $S^2 \times \mathbb{R}$ geometry, identical to the one used in this work. In principle, this method could be used to simulate the full flow, not just the critical point, but one has to be careful about the approach to the continuum limit, making sure that the quartic coupling becomes small at the cutoff scale. Another issue faced by the lattice simulations on $S^2 \times \mathbb{R}$ is that it is hard to lattice-discretize the theory on the two-sphere, because of its curvature. That is the reason why [154] uses a discretized icosahedron rather than the sphere. Preparatory work to find a true spherical discretization is ongoing [155, 156], and we are looking forward to realistic simulations.

Excitations for $\lambda = 0.9$

Finally, we consider the spectrum for $\lambda = 0.9$.[7] The first eye-catching feature of the spectrum is the approximate degeneracy of $\mathbb{Z}_2$-even and odd states in the region of large R. This degeneracy is clearly visible for the first excitation, which becomes degenerate with the vacuum, and for two more pairs of states. The interpretation of this phenomenon was already discussed in section 7.2—it means that the $\mathbb{Z}_2$-symmetry is spontaneously broken. There will be two vacua $|0\rangle_L$ (resp. $|0\rangle_R$), corresponding to the vacuum with $\langle\phi\rangle < 0$ (resp. $\langle\phi\rangle > 0$). By hermiticity, the matrix elements of the Hamiltonian between these states are of the form

$$H_{LL} = H_{RR} = E_0, \quad H_{LR} = H_{RL} = \delta_0\,. \tag{7.14}$$

The off-diagonal matrix element δ_0 depends on the tunneling rate between both wells, and therefore it decreases exponentially with the volume of space (see e.g. chapter 19 of [157]):

$$\delta_0 \sim \exp\left(-C\mathscr{V}\right), \qquad \mathscr{V} = \mathrm{Vol}(S^{d-1}_R) = \mathrm{S}_d\, R^{d-1}. \tag{7.15}$$

The coefficient $C > 0$ can in principle be computed, at least in a semi-classical approximation, but its precise value is not important for this argument. The eigenstates of the Hamiltonian

7. It's interesting to compare the discussion below with section VI of the contemporaneous work [130] devoted to Landau-Ginzburg flows in $d = 2$.

are then

$$|0,\pm\rangle = \frac{1}{\sqrt{2}}\left(|0\rangle_L \pm |0\rangle_R\right) , \tag{7.16}$$

and their energies are $E_{0,\pm} = E_0 \pm \delta_0$. Notice that the states $|0,\pm\rangle$ are even (odd) under $\phi \to -\phi$; as usual in quantum mechanics, we expect that the $\mathbb{Z}_2$-even combination will have a smaller energy than the $\mathbb{Z}_2$-odd one. From Eq. (7.15), we conclude that the splitting between both vacua decreases in the infinite-volume limit as $\exp(-\text{const.}\, R^{d-1})$.

A similar argument can be used to argue that the excited states $|i\rangle_L$ (resp. $|i\rangle_R$) above each well form $\mathbb{Z}_2$ even and odd energy eigenstates

$$|i,\pm\rangle = \frac{1}{\sqrt{2}}(|i\rangle_L \pm |i\rangle_R) , \tag{7.17}$$

with energies $E_{i,\pm} = E_i \pm \delta_i$. For these excited states, we confirm that the $\mathbb{Z}_2$ even state has lower energy than its odd counterpart: this can be seen in figure 7.7—in each of the three approximately degenerate pairs, the $\mathbb{Z}_2$-even state is the lower one.

The above tunneling argument seems to predict that the even/odd state pairs should be split roughly symmetrically with respect to the infinite volume limiting value. In fact, since the excitation energies are defined as $E_i - E_0$ and E_0 belongs to the $\mathbb{Z}_2$-even sector, we expect the $\mathbb{Z}_2$-even excitations to shift down by $(\delta_i - \delta_0)$, while the $\mathbb{Z}_2$-odd ones to move up by $(\delta_i + \delta_0)$. Since the tunneling probability strongly depends on the energy, we expect $\delta_0 \ll \delta_i$, and the shifts should be roughly symmetric. However, that's not what we see in the $\lambda = 0.9$ plots in figure 7.7—it rather looks that the negative shift of the $\mathbb{Z}_2$-even excitations is much larger than the positive shift of the $\mathbb{Z}_2$-odd ones. For the first pair of massive excitations, it even looks like both the $\mathbb{Z}_2$-odd and the $\mathbb{Z}_2$-even state have a negative shift.

The most natural explanation of this phenomenon is that we are forgetting the modification of the mass spectrum via coupling to curvature, see Eq. (7.11). This effect goes as $1/R^2$ and for low-lying states should be larger than the splitting, which is exponentially small in the volume of sphere. The fact that both states in the first $\mathbb{Z}_2$-odd/even pair have a negative shift can then be explained by taking A negative in Eq. (7.11).

In fact, it is not totally unexpected that A should be negative for the lowest massive excitation at $\lambda = 0.9$. The same occurs for the Landau-Ginzburg flow in the *weakly coupled* part of the $\mathbb{Z}_2$-broken phase, i.e. for negative m^2 and a small quartic coupling. We did not study this part of the phase diagram numerically, but it's easy to understand what happens analytically. The full mass parameter of the UV theory, including the coupling to curvature, is $m^2 + \kappa_c \mathcal{R}$. Since $m^2 < 0$, we have to reexpand the Lagrangian around the true vacuum, and when we do this, the mass parameter picks up the usual -2 factor. We thus conclude that $\kappa = -2\kappa_c$, giving $A = -2$ at weak coupling in the $\mathbb{Z}_2$ broken phase.

This finishes the discussion of splittings at finite R. Next, we would like to say a few words about the overall structure of the massive spectrum at large R. We identify the two

near-degenerate pairs of even/odd states with two massive excitations, of mass

$$M_1 \approx 1.6\,, \qquad M_2 \approx 2.5\,. \tag{7.18}$$

A very interesting feature of this spectrum is that $M_2 < 2M_1$. This is unlike the spectrum at $\lambda = 0.3$, which was neatly quantized in the units of the lightest excitation. In the situation at hand, the state of mass M_2 should probably be interpreted as a bound state of two M_1 particles.

The appearance of such bound states was found long ago, and their masses measured, in the lattice simulations of the broken phase of the Ising model and of the ϕ^4 theory in $d = 3$ dimensions [158]. In the weakly coupled regime, the existence of these states follows from the fact that the $\lambda\phi^4$ interaction becomes attractive in the broken phase, the cubic exchange diagrams overwhelming the repulsive effect of the contact term interaction [159]. Their binding energy, exponentially small at weak coupling, is known in the leading and first subleading exponential approximation [159, 160]. Apparently, here we are observing the same effect in $d = 2.5$ dimensions and at strong coupling.

7.3 Non-unitarity and complex energy levels

As we observed in section 4.3.5, the free massless scalar theory in fractional d is not unitary: its Hilbert space contains negative norm states. In $d = 2.5$ the lowest negative-norm state occurs for $\Delta = 9$. In figure 7.12 we show the total number of scalar states and the number of negative norm states as a function of Δ.

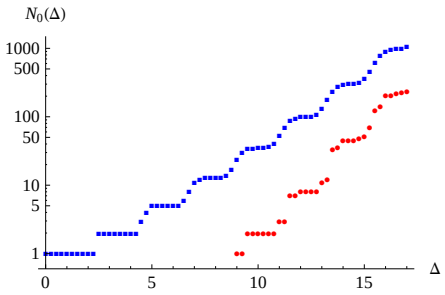

Figure 7.12: The number of scalar P-even states in the Hilbert space of free massless scalar theory in $d = 2.5$ on the cylinder. Blue squares: all states. Red dots: negative-norm states.

What are the consequences of having these negative-norm states? One expected consequence is that once we perturb the theory, complex eigenvalues will appear. The purely massive perturbation $\frac{1}{2}m^2\phi^2$ is an exception, since in this case the spectrum should agree with the canonical quantization spectrum, which is fully real-valued, cf. section 5.1.

What if we turn on $\lambda\phi^4$? As we saw in the previous sections, numerics indicate that the

low-energy spectrum is still real. This may not be so surprising, since the negative norm states all have high energies. To see complex eigenvalues, we may expect to have to go to high energies. We will now present several computations which show that complex eigenvalues do occur.

Let us first of all examine the case of very small R. In this limit we can treat m and λ as perturbations, with dimensional couplings m^2R^2 and $\lambda R^{d-4\nu}$. The second coupling decreases less slowly as $R \to 0$, and will dominate at very small R. The effects of the perturbation is to split the degenerate energy levels of the CFT Hamiltonian. The splittings are proportional to the eigenvalues of the perturbation diagonalized within each degenerate subspace. In high-energy subspaces, which contain negative-norm states, some of the eigenvalues may and do turn out to be complex. We find that this happens for the first time at $\Delta = 11.5$, which is an 88-dimensional subspace with 7 negative-norm states. We find that the matrix of the ϕ^4 perturbation within this subspace has one pair of complex conjugate eigenvalues $\approx 1.85 \pm 0.04i$. This implies that for very small R the energy levels will be complex.

The above argument is confirmed numerically in figure 7.13, where we show the spectrum around $\Delta = 11.5$ for $m^2 = 1$, $\lambda = 0.55$, and $0 < R < 0.15$. We see precisely one pair of complex conjugate eigenvalues emerging out of the $\Delta = 11.5$ group for small R. For larger R, the spectrum shows intricate structure. We see many avoided level crossings in the real part of the spectrum. We also see a second pair of complex conjugate eigenvalues appearing at $R \approx 0.04$ and then disappearing at $R \approx 0.07$. Zooming in on this line of complex eigenvalues, one notices that it joins collision points for pairs of real eigenvalues.

This last observation may seem to create a minor paradox. Didn't we say that the Landau-Ginzburg flow is not integrable, and that in non-integrable flows energy levels do not cross? The resolution is that this last statement requires a qualification in presence of negative norm states. If two energy levels which head for a collision are both positive-norm (or both negative-norm), they will generically repel. However, in a subspace with non-sign-definite Gram matrix, no-level-crossing rule does not apply. To see this, consider a toy-model 2×2 symmetric generalized eigenvalue problem

$$H.c = E\, G.c\,, \qquad H = \begin{pmatrix} h_{11} & h_{12} \\ h_{12} & h_{22} \end{pmatrix}, \quad G = \begin{pmatrix} 1 & 0 \\ 0 & \sigma \end{pmatrix}, \tag{7.19}$$

where $\sigma = \pm 1$ depending on whether we are dealing with a subspace of positive or non-sign-definite norm. We are assuming that the Hamiltonian matrix is symmetric and real. The distance between the two eigenvalues is controlled by the discriminant:

$$D = (h_{11} - \sigma h_{22})^2 + \sigma h_{12}^2\,. \tag{7.20}$$

For $\sigma = 1$ the discriminant is a sum of two squares, and level crossing cannot generically happen. On the other hand, for $\sigma = -1$ the discriminant is not positive definite, and can

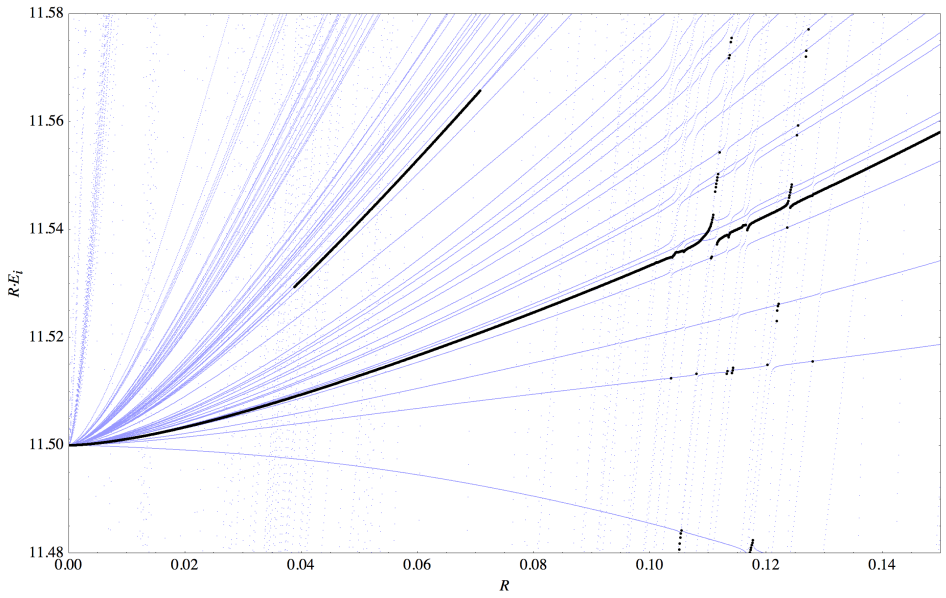

Figure 7.13: The spectrum around $\Delta = 11.5$ for $m^2 = 1$, $\lambda = 0.55$, and $0 < R < 0.15$ with a step of 10^{-4}. We are plotting energy levels multiplied by R. Light blue: real eigenvalues. Black: real part of eigenvalues with nonzero imaginary part. These are raw TCSA data with $\Delta_{\text{max}} = 12$.

readily change sign if the off-diagonal matrix element increases beyond a critical value. When this happens, we go from having two real eigenvalues to a complex conjugate pair.

As another illustration, in figure 7.14 we show the spectrum with $R\,E_i \in [8, 11]$ for the same couplings as above but in a wider range $0 < R < 2$. We clearly see several points where real eigenvalues collide and form a complex conjugate pair, which sometimes reemerges as a pair of real eigenvalues for a slightly larger value of R. The most prominent such collision happens at $R \approx 0.7$.

To resolve the multitude of eigenvalue curves in figures 7.13, 7.14, we had to compute the spectrum with a very small R step. For reasons of speed and numerical stability, we have performed these bulky computations with a relatively small Δ_{max}. Since the complex eigenvalues observed in these plots lie relatively close to the cutoff, their energies are likely to shift considerably when the cutoff is increased. However, we don't expect the complex eigenvalues to disappear. In fact, we performed checks for a few selected values of R, computing the spectrum with a higher cutoff and, for higher numerical stability, with a higher number of digits rather than at machine precision. The complex eigenvalues were always present.

Notice that the eigenstates corresponding to the complex eigenvalues necessarily have zero norm (computed with respect to the Gram matrix). In a *unitary* theory a state of zero norm has zero overlap with any other state. Such a state is unphysical; it can be kept in the

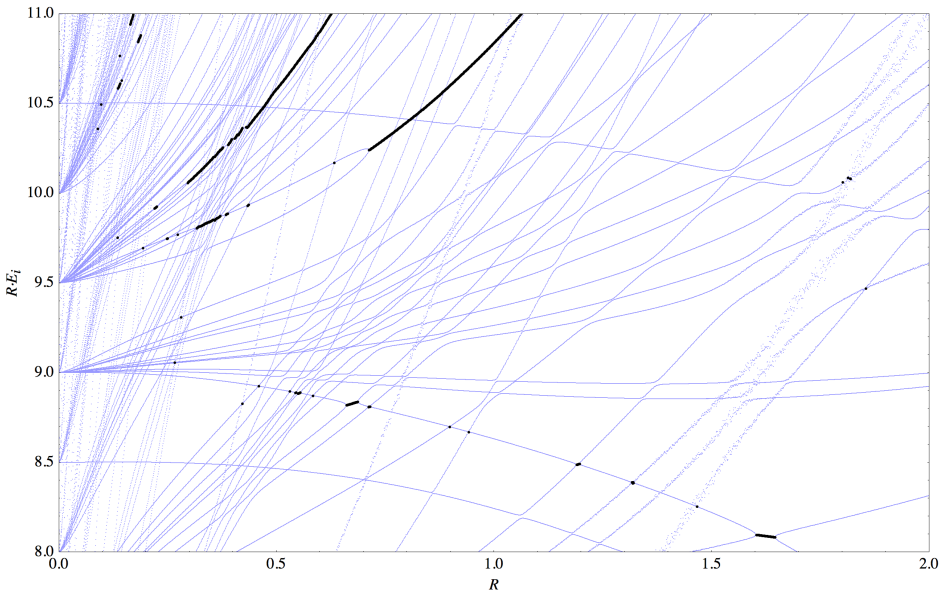

Figure 7.14: The spectrum at $R\,E_i \in [8, 11]$ for $m^2 = 1$, $\lambda = 0.55$, and $0 < R < 2$ with a step of 10^{-3}. We are plotting energy levels multiplied by R. Light blue: real eigenvalues. Black: real part of eigenvalues with nonzero imaginary part. These are raw TCSA data with $\Delta_{\max} = 11$. The jittering spread noticeable in some of the eigenvalue curves at $R \gtrsim 1.5$ is due to numerical instabilities in the `Mathematica` diagonalization routine.

Hilbert state or thrown out without physical consequence. This was the situation with the scalar theory in $d = 3$ in section 5, whose extended Hilbert state included some null states, but only as a matter of convenience. In a non-unitary theory, as the one we are discussing now, states of zero norm do not in general have zero overlap with other states. They cannot be removed from the theory without modifying it.

To summarize, the Landau-Ginzburg theory in $d = 2.5$ dimensions is a non-unitary interacting quantum field theory. Its spectrum on a sphere of finite radius contains negative-norm states with real energies, as well as zero-norm (but physical) states with complex energies. The negative-norm and zero-norm states belong to the high-energy part of the spectrum, and so their effect on the low-energy physics may not be huge, but the mere presence of these states is a proof that the theory is not unitary. We expect complex eigenvalues to be present also in the limit $R \to \infty$. In particular, the critical point of the theory should have operators with complex scaling dimensions. The same should be true for theories in any fractional d.

Chapter 8

Discussion and outlook

This thesis focused on two distinct, but related concepts. The first chapters were devoted to conformal blocks, special functions that encode the contribution of a single conformal family to a CFT four-point function. Pragmatically, conformal blocks can be thought of as solutions to a second-order PDE, the Casimir differential equation. In special cases, this PDE can be solved analytically, but in odd d (or even non-integer d), new ideas are needed to systematically compute conformal blocks.

In chapter 2, we computed conformal blocks in radial quantization. Although this does not lead to closed-form expressions, radial quantization shows that conformal blocks admit a series expansion in polar coordinates. Unitarity and conformal invariance were used to prove various properties of such expansions: they imply that the expansion coefficients are positive, that the expansion converges uniformly and that the conformal block is analytic inside the unit disk. For practical applications, we advocated the use of a ρ-coordinatethat covers the full range of regularity of the conformal blocks and has a rapidly convergent series expansion.

The subsequent chapter 3 focused on a practical problem, namely the computation of conformal blocks on the diagonal $z = \bar{z}$. This diagonal plays an important role in the conformal bootstrap program: in most applications, conformal blocks are expanded around the point $z = \bar{z} = 1/2$. The key result from this chapter was that two Casimir differential equations (the quadratic and quartic one) can be combined to produce a single fourth-order ODE on the diagonal (third-order for scalars). Frobenius' method gives a practical way to solve the ODE in question. Combined with a Cauchy-Kovalevskaya argument, we explained how Frobenius method' gives an efficient way for computing derivatives around any point t_0 on the diagonal.

Since the above work was published, it has found applications in the conformal bootstrap. These applications use a rational approximation of conformal blocks in the ρ-coordinate, first

proposed by Kos, Poland and Simmons-Duffin [103]. Notably, these rational approximations to conformal blocks were applied in computations of critical exponents of the 3d Ising model, by analyzing a single correlator [8] and multiple correlators simultaneously [9]. More rececently, two publicly available algorithms (SDPB and JuliBootS) for bootstrap computations have made use of the ρ-coordinate [128, 161].

We would like to mention at least one possible generalization that pertains to conformal blocks contributing to a non-scalar four-point function $\langle \mathcal{O}_1 \mathcal{O}_2 \mathcal{O}_3 \mathcal{O}_4 \rangle$ [87, 66]. [1] In that case, we must consider all operators $\mathcal{O}$ that appear in both the $\mathcal{O}_1 \times \mathcal{O}_2$ and $\mathcal{O}_3 \times \mathcal{O}_4$ OPEs. Depending on the $\mathcal{O}_i$, not only spin-j traceless symmetric tensor operators may contribute, but also tensors of mixed symmetry or even fermionic operators. The conformal blocks $G_{\mathcal{O}}$ can still be computed in radial quantization, for example in the ρ kinematics; the matrix elements there will be of the form

$$\langle 0|\mathcal{O}_1(0,-\mathbf{n})\mathcal{O}_2(0,\mathbf{n})|E,\lambda\rangle \quad \text{and} \quad \langle E',\lambda'|\mathcal{O}_3(0,\mathbf{n}')\mathcal{O}_4(0,-\mathbf{n}')|0\rangle,$$

where λ, λ' label $SO(d)$ representations. By contracting such matrix elements, we can find the corresponding 'building blocks' for the ρ series expansion, that will however no longer be Gegenbauer polynomials in $\mathbf{n} \cdot \mathbf{n}'$. We expect that the expansion coefficients can still be found by means of the Casimir differential equation. It would be interesting to carry out this computation in detail.

More speculatively, we note that the conformal blocks restricted to the diagonal are particularly simple: they are functions of a single variable and are solutions to an ODE, rather than a PDE. Whenever $\Delta_1 = \Delta_2$, the ODE in question can even be solved analytically, yielding a sum over ${}_3F_2$ hypergeometric functions. [2] We believe that it may be interesting to consider the crossing symmetry equation restricted to the diagonal. In particular, if it is possible to express the cross-channel blocks $f_{\lambda_1\lambda_2}(1-z)$ in terms of the normal blocks $f_{\lambda_1'\lambda_2'}(z)$, this would open the door to better understanding crossing symmetry analytically. In various special cases (e.g. in the large-N limit), such analytic results have already been obtained [162, 120, 163–165].

In the second part of this thesis, we presented a generalization of the Truncated Conformal Space Approach to $d > 2$ dimensions. We studied two flows starting at the free massless boson. In chapter 5, we computed the spectrum of the massive boson in $d = 3$ on the cylinder analytically, and compared these predictions to numerical TCSA results, finding that the data were reliable well beyond perturbation theory. Second, we considered the Landau-Ginzburg theory in $d = 2.5$: there, we found that $\mathbb{Z}_2$ symmetry of the theory was broken at strong coupling, and we obtained critical exponents that were roughly in agreement (within error bars) with their exact values. In order to obtain these results, we used a renormalization

1. This problem is already fully understood in two-dimensional CFT [91].
2. These closed-form solutions are presented in the published version of chapter 3, i.e. Ref. [125].

group method to reduce the cutoff dependence that is inherent to the TCSA.

These initial results open the door to several new problems. Various RG flows are closely related to the Landau-Ginzburg flow: we point to the $O(N)$ theory and the tricritical Ising model (generated by a ϕ^6 interaction). At a first glance, it does not appear very complicated to adapt our methods to study these theories using the TCSA.

Likewise, we only considered the ϕ^4 theory in $d = 2.5$, where it is UV-finite. For physical reasons, it would be interesting to consider the $d = 3$ case: this however entails dealing with a logarithmic divergence for the ϕ^2 operator. To get high-accuracy results for the IR spectrum and for critical exponents, it may be necessary to first obtain a better understanding of cutoff effects. In any case, we believe that the renormalization procedure proposed in this work can be significantly improved, e.g. by developing a systematic way to deal with subleading truncation effects.

A technical, but conceptually important matter was non-unitarity of the free boson in fractional d. We showed that the free, massless theory was non-unitary for any non-integer d and using numerical TCSA methods, we established that the Landau-Ginzburg Hamiltonian had complex energy eigenvalues on the cylinder. It should be possible to obtain a better insight into these unitarity violations by studying the Wilson-Fisher theory in $d = 4 - \epsilon$ dimensions [166], which is perturbative. For future bootstrap applications in fractional d, it may also be interesting to have rigorous (or at least asymptotic) bounds on unitarity violations in terms of OPE coefficients and scaling dimensions.

Next, one may consider RG flows starting at free CFTs with a richer field content. Starting from a CFT with both fermions and scalars, one may consider the Yukawa, Gross-Neveu or Gross-Neveu-Yukawa interactions [167]. Even more interesting are gauge theories (either Abelian or non-Abelian), although it is not quite obvious how to implement gauge invariance in the TCSA framework. This is an important problem for the future.

A different research direction involves computing new observables, different from the spectrum of the Hamiltonian. Various 2d TCSA studies have already computed form factors and one-point functions [168, 169]. In $d > 2$ dimensions, it would be interesting to have access to correlation functions to probe RG flows (or Wilson loops, in the case of gauge theories).

We would like to conclude on a more general note. The TCSA is a natural scheme to investigate RG flows that start at strongly coupled CFTs for which the CFT data are known (as is the case for the Virasoro minimal models). Let us make two different remarks with regard to this point. First, we are not aware of any non-SUSY strongly coupled CFT in $d > 2$ that is 'solved', in the sense that its low-energy spectrum (up to $\Delta_{\text{max}} \sim 20$) and OPE coefficients can be computed to high precision. Can conformal bootstrap techniques be

refined in order to provide these data as input to the TCSA? Second, many interesting RG flows in $d > 2$ (like 4d Yang-Mills theory) emanate from free theories in the UV. For such theories, alternative Hamiltonian truncation methods may also be promising: we have in mind light-cone methods (see e.g. [170–174]) and truncation methods that use a Fock space basis (see e.g. [175, 176, 131]). Surprisingly, few of these methods have been explored in $d \geqslant 3$ dimensions. Nevertheless, we are optimistic that such truncation methods will prove to be useful in the near future as a quantitative approach to understanding strongly coupled QFTs.

Acknowledgements

Appendix A

Boundedness of the ρ-series coefficients

In this appendix we show that the coefficients $B_{n,j}$ on each level n are uniformly bounded for all Δ and ℓ, as stated in Eq. (2.65). We have already shown in the main text that $B_{n,j}$ remain bounded as $\Delta \to \infty$ for each fixed ℓ. So here it suffices to consider the case of ℓ large with respect to n, say $\ell \geqslant n$.

We will proceed by induction, and assume that the inequality has already been shown for all levels $n' < n$. Using Eq. (2.52), the bound at level n will follow if we show that

$$\Gamma^{\Delta+n,j}_{\Delta+n',j'}/(c^{(2)}_{\Delta+n,j} - c^{(2)}_{\Delta,\ell}) \tag{A.1}$$

is bounded by a constant which depends only on n and ν.

Our first observation is that the Γ's satisfy the bound

$$\left|\Gamma^{\Delta+n,j}_{\Delta+n',j'}\right| \leqslant \text{const}\,\Delta + \text{const} \tag{A.2}$$

with constants which depends only on n and ν. To show this, notice that large contributions to Γ's appear from only two sources. First, through the action of $r\partial_r$, which gives a factor of $(\Delta + n')$. Second, through the action of $2\eta(1-\eta^2)\partial_\eta$, which gives factors $b_{j'} = \mathrm{O}(j')$. On the other hand, all the factors produced via the expansion of denominators in (2.47) will depend only on n and ν. Notice in particular that $a_j = \mathrm{O}(1)$.

Passing to the Casimir difference in (A.1), we write it as

$$c^{(2)}_{\Delta+n,j} - c^{(2)}_{\Delta,\ell} = k^2 + 2k(\ell - n + \nu) + 2n(\tau + n - 1)\,, \tag{A.3}$$

where $j = \ell - n + k$, $k = 0, 2, \ldots, 2n$, and $\tau = \Delta - \ell - 2\nu \geqslant 0$ by the unitarity bounds. Since we are assuming $\ell \geqslant n$, this is a manifestly monotonically increasing function of k and n.

Consider first the case $k \geqslant 2$. In this case we have a lower bound:

$$c^{(2)}_{\Delta+n,j} - c^{(2)}_{\Delta,\ell} \geqslant [(\text{A.3}) \text{ for } k = n = 2] = 4(\Delta - \nu) \qquad (k \geqslant 2)\,. \tag{A.4}$$

Combining this with (A.2), we see that (A.1) is indeed bounded independently of Δ and ℓ, except in the region near the free scalar unitarity bound $\Delta = \nu$, excluded from consideration as discussed in the main text.

It remains to consider the case $k = 0$, when the Casimir difference

$$c^{(2)}_{\Delta+n,\ell-n} - c^{(2)}_{\Delta,\ell} = 2n(\tau + n - 1) \tag{A.5}$$

can remain small even though both Δ and ℓ become large. However, precisely in this case the bound (A.2) can also be improved. The relevant recursion relation coefficients are

$$\Gamma^{\Delta+n,\ell-n}_{\Delta+n',j'=\ell-n'}\,. \tag{A.6}$$

The coefficients with $j' \neq \ell - n'$ will be zero, because lowering the spin via Eqs. (2.49) is accompanied by raising the dimension by at least the same amount. We will now show that all coefficients of the form (A.6) are bounded by $\text{cst}\,\tau + \text{cst}$. Together with (A.5), this will prove the boundedness of $B_{n,\ell-n}$ and will complete the proof.

For the case $n - n' = 2$, this stronger bound can already be suspected in the expression (2.51) for $\Gamma^{E+2,j-2}_{E,j}$, which contains two near-canceling terms. In detail, this coefficient can be expressed as

$$\Gamma^{\Delta+n'+2,\ell-n'-2}_{\Delta+n',\ell-n'} = 4(\tau + 2n')a^-_{\ell-n'}, \tag{A.7}$$

and satisfies the claimed bound, since $a^-_j \leqslant 1/2$ for all j.

For the general case, we notice that the action of $\widetilde{\mathcal{D}}$ on $\mathcal{P}_{\Delta+n',\ell-n'}$ can be written as follows:

$$\widetilde{\mathcal{D}}\,\mathcal{P}_{\Delta+n',\ell-n'} = -\frac{4(\tau + 2n')a^-_{\ell-n'}}{1 - 2r^2(2\eta^2 - 1)}\mathcal{P}_{\Delta+n'+2,\ell-n'-2} + \ldots \tag{A.8}$$

Here we computed explicitly the action of $(1 - 2\eta^2)r\partial_r$ and $2\eta(1 - \eta^2)\partial_\eta$. We omitted many terms $(\ldots)$ which cannot contribute to the relevant Γ coefficients, because they raise the dimension without lowering the spin by the same amount. The Γ coefficients (A.6) with $n - n' = 4, 6, \ldots$ are obtained by expanding the denominator in (A.8). They are given by

$$\Gamma^{\Delta+n,\ell-n}_{\Delta+n',\ell-n'} = 2(\tau + 2n') \prod_{j=\ell-n',\ell-n'-2,\ldots,\ell-n+2} (2a^-_j)\,, \tag{A.9}$$

and clearly satisfy the claimed bound.

The reader will have noticed that the coefficients $B_{n,\ell-n}$, which required a separate analysis in the above proof, satisfy a recursion relation among themselves. This is because

the relevant Γ's in (A.6) vanish for $j' \neq \ell - n'$. Due to this fact, these coefficients can in fact be computed explicitly:

$$B_{2m,\ell-2m} = \frac{(1/2)_m}{m!} \frac{(\ell+1-2m)_{2m}}{(\ell+\nu+1-2m)_{2m}} \frac{(\tau/2)_m}{(\tau/2+1/2)_m} \,. \tag{A.10}$$

Their boundedness is also obvious from this formula.

Appendix B

Recursion relations for a_η

Via Frobenius' method, the ODEs (3.21) imply recursion relations for the coefficients a_n in (3.9), four-term for general ℓ:

$$n(\Delta+\ell+n-1)(\Delta-\ell+n-2\nu-1)(2\Delta+n-2\nu-2)a_n=\sum_{i=1}^{3}\gamma_{i,n}\,a_{n-i}, \tag{B.1}$$

where

$$\begin{aligned}
\gamma_{1,n} &= 3n^4+\big(4S+12\Delta-10\nu-19\big)\,n^3\\
&\quad+\big[8\nu^2-2(6S+15\Delta-22)\nu-4c_2+2P+3(2\Delta-3)(2S+3\Delta-5)\big]n^2\\
&\quad+\big[12\Delta^3+12S\Delta^2-57\Delta^2-36S\Delta+90\Delta+4(2S+4\Delta-5)\nu^2+26S\\
&\qquad+P(4\Delta-6\nu-5)-2(3\Delta-4)(4S+5\Delta-8)\nu+c_2(-4S-8\Delta+6\nu+13)-47\big]n\\
&\quad+\big[\Delta(3\Delta-4\nu-10)+S(4\Delta-4\nu-6)+6\nu+9\big](\Delta-1)(\Delta-2\nu-2)\\
&\quad+c_4+P(\Delta-2\nu-1)(2\Delta-2\nu-3)\\
&\quad+c_2\big[-10\nu+S(-4\Delta+4\nu+6)+\Delta(-4\Delta+6\nu+13)-11\big],\\
\gamma_{2,n} &= (\Delta+n+S-\nu-2)\big\{-3n^3+\big[-5S-9\Delta+5(\nu+4)\big]n^2\\
&\quad+\big[2c_2-4P-3(7\nu+15)+S(-10\Delta+8\nu+21)+\Delta(10\nu+40-9\Delta)\big]n\\
&\quad+c_2(2S+2\Delta-5)+P(-4\Delta+6\nu+7)\\
&\qquad-(\Delta-2)\big[S(5\Delta-8\nu-11)+\Delta(3\Delta-5\nu-14)+11\nu+17\big]\big\},\\
\gamma_{3,n} &= (\Delta+2a+n-3)(\Delta+2b+n-3)(\Delta+n+S-\nu-3)(\Delta+n+S-\nu-2),
\end{aligned}$$

and three-term for $\ell=0$:

$$n(\Delta+n-1)(2\Delta+n-2\nu-2)\,a_n=\sum_{i=1}^{2}\xi_{i,n}\,a_{n-i}\,, \tag{B.2}$$

for

$$\begin{aligned}\xi_{1,n} &= 2n^3 + 3\big(S + 2\Delta - \nu - 3\big)\, n^2 \\ &\quad + \big[2P + S(6\Delta - 4\nu - 9) + 7\nu + \Delta(5\Delta - 4\nu - 16) + 13\big] n \\ &\quad + \tfrac{1}{2}\big[2P + (\Delta - 2)(2S + \Delta - 2)\big](2\Delta - 2\nu - 3)\,, \\ \xi_{2,n} &= -(\Delta + 2a + n - 2)(\Delta + 2b + n - 2)(\Delta + S + n - \nu - 2)\,.\end{aligned}$$

Apart from a few cases listed below, these recursion relations determine a_n for $n \geqslant 1$ starting from $a_0 = 1$ and imposing $a_n = 0$ for $n < 0$. The exceptions occur when the factor multiplying a_n in the LHS vanishes for some $n = n_0 \geqslant 1$. These are the cases when Δ is smaller by the positive integer, n_0, than the largest characteristic exponent at $z = 0$ in (3.31). Frobenius' method requires a special treatment in such situations. As we will see below, in our case potential ambiguities can be resolved using as an extra physical input the fact that conformal blocks should be continuous functions of Δ.

There are actually only three exceptional cases consistent with the unitarity bounds and assuming $d \geqslant 2$. We consider them one by one.

1. $\ell > 0, \Delta = \ell + 2\nu, n_0 = 1$ in (B.1)

This corresponds to a spin $\ell > 0$ primary higher spin conserved current saturating the unitarity bound. Conformal block of such a primary are defined only for $a = b = 0$, since three-point functions with scalars of unequal dimension vanish by imposing conservation. Thus we should not worry that eq. (B.1) predicts $a_1 \to \infty$ for a or b nonzero and $\Delta \to \ell + 2\nu$. However, for $a = b = 0$ conformal blocks should be continuous in this limit.

Indeed, for $n = 1$ and $a = b = 0$, $\gamma_{1,1}$ factorizes:

$$\gamma_{1,1} = \tfrac{1}{2}(\Delta - \ell - 2\nu)(2\Delta - 2\nu - 1)\Delta(\Delta + \ell)\,. \tag{B.3}$$

The offending factor $(\Delta - \ell - 2\nu)$ now appears on both sides of the recursion relation defining a_1. Cancelling this factor gives an equation for a_1 which is continuous in the full range including the unitarity bound. Once a_1 is computed according to this prescription, the rest of the coefficients follow from the recursion relation unambiguously.

We note in passing that the diagonal limit of spin ℓ blocks saturating the unitarity bound is known in closed form for arbitrary d, see section 2.1.3 and Eq. (2.33) in particular.

2. $\ell = 0, \Delta = \nu + \frac{1}{2}, n_0 = 1$ in (B.2)

Again, these conformal blocks can and should be defined by continuity. Namely, one can check that for $n = 1$ and any a and b the RHS of (B.2) factorizes, so that the problematic factor $(2\Delta - 2\nu - 1)$ can be cancelled from both sides of the recursion relation. Once a_1 is defined this way, the rest of the coefficients follow from the recursion.

3. $\ell = 0, \Delta = \nu, n_0 = 2$ in (B.2)

This case corresponds to a scalar field at the unitarity bound, so it is not particularly interesting. This conformal block can occur only in the free scalar theory, and only if the external field dimensions differ by the free scalar dimension ε. We have in mind the OPE $:\phi\mathcal{O}:\times\mathcal{O}\supset\phi$. One can check that in this case, i.e. for $a, b = \pm\varepsilon/2$, the free scalar block can be defined by continuity exactly as above. Namely the RHS of (B.2) for $n = 2$ can be factored (plugging in a_1 computed in the previous recursion step) and the offending factor cancelled. For all the other choices of a, b the scalar block diverges when $\Delta \to \nu$.

Appendix C

TCSA computations in practice

In this appendix, we present some methods and algorithms that were used in finding a basis for the Hilbert space, constructing the OPE matrices $V_i{}^j$ for both the ϕ^2 and the ϕ^4 interaction, and for computing the Gram matrix directly.

C.1 Constructing the Hilbert space

First, we focus on constructing the Hilbert space $\mathcal{H}$ for the free scalar CFT, containing all scalar and parity-even states with energy $\leqslant \Delta_{\text{max}}$. All necessary ideas are explained in section 4.3.1. We recall that states in $\mathcal{H}$ are in one-to-one correspondence with composite operators $:\partial^{k_1}\phi\cdots\partial^{k_n}\phi:$ that have all derivatives contracted. These operators can in turn be represented as graphs, each ϕ being denoted as a vertex and an index contraction corresponding to an edge that joins two vertices. Note that a graph Γ with V vertices and E edges maps to an operator with scaling dimension

$$\Delta_\Gamma = \tfrac{1}{2}(d-2)\,V + 2E, \tag{C.1}$$

hence imposing $\Delta_\Gamma \leqslant \Delta_{\text{max}}$ restricts the values V and E can take. We also recall that isomorphic graphs represent the same local operator, hence only one graph per isomorphism class must be added to the Hilbert space (otherwise, one introduces additional null states).

In the graph theory language, the set of necessary graphs can then be constructed using the following algorithm:

1. Build a list of all connected *simple* graphs (having at most one edge joining any two vertices), subject to the constraint (C.1). Test this list for isomorphisms, and keep only one graph per isomorphism class.
2. Given any connected simple graph Γ, build all multigraphs of the same topology satisfying (C.1) by adding edges in all possible ways. Keep only one graph for every

isomorphism class. This yields a list of all connected multigraphs.

3. Join these connected multigraphs in all possible ways, with the total number of vertices V and edges E satisfying (C.1).

The resulting set of all disconnected multigraphs then forms a basis for the truncated Hilbert space $\mathcal{H}$. We stress that this procedure does not take null states in integer d into account, see section 4.3.4.

Both in principle and in practice, all above graph manipulations can be done in `Mathematica`. We remark however that `Mathematica` has limited support for multigraphs, and in particular the function `IsomorphicGraphQ` that tests whether two graphs are isomorphic does not support them. The specialized graph theory package `NetworkX` [1] for Python is a useful alternative.

C.2 OPE matrices

Next, we turn to the computation of the OPE matrices. Let us denote these OPE matrices as $\left(C_{[N]}\right)_i^{\ j}$ for $N = 2, 4$:

$$\frac{1}{\mathrm{S}_d}\int_{|x|=1} \mathrm{d}^{d-1}x\, :\phi^N(x):|\mathcal{O}_i\rangle \equiv \left(C_{[N]}\right)_i^{\ j}|\mathcal{O}_j\rangle \ + \text{ states with } \Delta \geqslant \Delta_{\max}\,. \tag{C.2}$$

An approach for calculating the OPE matrices was sketched in section (4.4.3). In summary, the OPE matrices $C_{[N]}$ are computed state-by-state: for any i, we pick the state $|\mathcal{O}_i\rangle$ and compute the left-hand side of Eq. (C.2); after expanding it in the basis $\{|\mathcal{O}_j\rangle\}$, the coefficients $(C_{[N]})_i^{\ j}$ can be read off. This procedure is well-defined in fractional d, but ambiguous for integer d due to the presence of null states; for integer d, we therefore define the OPE coefficients by analytic continuation in d.

These OPEs can be computed in the following way:

1. Use Wick's theorem to expand the state $:\phi^N(x):|\mathcal{O}_i\rangle = :\phi^N(x)::\mathcal{O}_i(0):|0\rangle$.
2. Expand any factors of $\phi(x)$ around $x = 0$.
3. Integrate the result over the sphere S^{d-1} using the spherical integral (5.33).

Let us illustrate the above algorithm using a concrete example: we take $N = 2$ and compute the OPE of $\int \phi^2(x)$ with the in-state $|\mathcal{O}_i\rangle = |(\partial_\mu\phi)^2\rangle$.

1. For our example, this gives

$$\begin{aligned}:\phi^2(x):|(\partial_\mu\phi)^2\rangle = 2\langle\phi(x)\partial_\mu\phi(0)\rangle^2|0\rangle \\ + 4\,\langle\phi(x)\partial_\mu\phi(0)\rangle\,|\phi(x)(\partial^\mu\phi)\rangle + |\phi(x)^2(\partial_\mu\phi)^2\rangle\,.\end{aligned} \tag{C.3}$$

1. This can be found at the website http://networkx.github.io.

The factors $\langle\phi(x)\partial^k\phi(0)\rangle$ are easily worked out using

$$\langle\phi(x)\partial_{\mu_1}\cdots\partial_{\mu_\ell}\phi(0)\rangle = 2^\ell(\nu)_\ell\frac{x_{\mu_1}\cdots x_{\mu_\ell}-\text{traces}}{|x|^{d-2+2\ell}}\,. \tag{C.4}$$

Applying this to the OPE (C.3), we obtain

$$:\phi^2(x):|(\partial_\mu\phi)^2\rangle = \frac{2(d-2)^2}{|x|^{2d-2}}|0\rangle + \frac{4(d-2)x^\mu}{|x|^d}|\phi(x)\,\partial_\mu\phi\rangle + |\phi(x)^2\,(\partial_\mu\phi)^2\rangle. \tag{C.5}$$

2. Let us work this out explicitly for the second term in Eq. (C.5):

$$x^\mu|\phi(x)\,\partial_\mu\phi\rangle = x^\mu|\phi\,\partial_\mu\phi\rangle + x^\mu x^{\lambda_1}|\partial_{\lambda_1}\phi\,\partial_\mu\phi\rangle + \frac{1}{2!}x^\mu x^{\lambda_1}x^{\lambda_2}|\phi_{,\lambda_1\lambda_2}\,\phi_{,\mu}\rangle + \dots. \tag{C.6}$$

Note that adding a derivative of ϕ increases the dimension of a state by one unit. As a consequence, these Taylor expansions must be truncated after a finite number of terms.

3. For the first term in (C.5), this integration is trivial. For the second term, we obtain

$$\frac{1}{\mathrm{S}_d}\int_{|x|=1}\mathrm{d}^{d-1}x\,\frac{x^\mu}{|x|^d}|\phi(x)\,\partial_\mu\phi\rangle = (1/d)\delta^{\mu\alpha}|\partial_\alpha\phi\partial_\mu\phi\rangle = (1/d)|(\partial_\mu\phi)^2\rangle \tag{C.7}$$

because all higher-order terms vanish after integration. Performing the integral over the third term of (C.3) as well, we find that

$$\begin{aligned}\frac{1}{\mathrm{S}_d}\int_{|x|=1}\mathrm{d}^{d-1}x{:}\phi^2(x){:}|(\partial_\mu\phi)^2\rangle = 2(d-2)^2|0\rangle + \frac{4(d-2)}{d}|(\partial_\mu\phi)^2\rangle + |\phi^2(\partial_\mu\phi)^2\rangle \\ + \frac{1}{d}|(\partial_{\lambda_1}\phi)^2(\partial_\mu\phi)^2\rangle + \frac{1}{2d(d+2)}|(\phi_{,\lambda_1\lambda_2})^2(\phi_{,\mu})^2\rangle + \dots\end{aligned} \tag{C.8}$$

Here, we have only written down the first terms that come from expanding the state $|\phi(x)^2(\partial_\mu\phi)^2\rangle$ in (C.5) around $x=0$.

.

C.2.1 Index-free formalism

The algorithm presented in Sec. (C.2) can produce large expressions: derivatives of the two-point function Eq. (C.4) contain many different trace terms and the spherical integration (5.33) results in a sum of many different tensor structures. To avoid both of these issues, we can use an index-free formalism for traceless symmetric tensors [177, 178]. [2] The rationale behind this formalism is that any TST $T_{\mu_1\cdots\mu_\ell}$ can be encoded using an auxiliary vector u^μ that satisfies $u^2=0$. After contracting with such a vector, the result is a polynomial in u:

$$T(u) \equiv T_{\mu_1\cdots\mu_\ell}\,u^{\mu_1}\cdots u^{\mu_\ell}. \tag{C.9}$$

2. See [65, 87] for a pedagogical treatment.

Using the differential operator

$$\mathcal{D}_\mu[u] \equiv \left(\nu + u^\alpha \frac{\partial}{\partial u^\alpha}\right) \frac{\partial}{\partial u^\mu} - \frac{1}{2} u_\mu \frac{\partial^2}{\partial u^\alpha \partial u_\alpha}, \qquad \nu \equiv (d-2)/2 \tag{C.10}$$

the original tensor, with open indices, can be recovered:

$$T_{\mu_1 \cdots \mu_\ell} = \frac{1}{\ell!(\nu)_\ell} \mathcal{D}_{\mu_1 \cdots \mu_\ell}[u]\, T(u)\,. \tag{C.11}$$

Here we have used the shorthand notation

$$\mathcal{D}_{\mu_1 \cdots \mu_\ell}[u] \equiv \mathcal{D}_{\mu_1}[u] \cdots \mathcal{D}_{\mu_\ell}[u]\,. \tag{C.12}$$

Let us apply this to the computation of OPE matrices.

Encoding states as differential operators

As a first application of the index-free formalism, we show that it is possible to encode any state $|\mathcal{O}_i\rangle$ as a differential operator acting on a polynomial. For concreteness, let us consider the state $|\mathcal{A}\rangle = |\phi^2\,(\phi_{,\mu_1 \cdots \mu_8})^2\rangle$. Using two auxiliary vectors v_1, v_2, both satisfying $v_i^2 = 0$, $|A\rangle$ can be rewritten as

$$|\mathcal{A}\rangle = \mathscr{D}_{\mathcal{A}}[v]\, |\phi^2\,(v_1 \cdot \partial)^8 \phi\,(v_2 \cdot \partial)^8 \phi\rangle\,, \tag{C.13}$$

where

$$\mathscr{D}_{\mathcal{A}}[v] = \frac{1}{[8!(\nu)_8]^2} \mathcal{D}_{\mu_1 \cdots \mu_8}[v_1] \mathcal{D}_{\mu_1 \cdots \mu_8}[v_2] \tag{C.14}$$

is a differential operator that acts on the auxiliary vectors v_i^μ. This formula follows directly from Eq. (C.11).

Next, notice that the differential operator $\mathscr{D}_{\mathcal{A}}[v]$ commutes with the OPE, in the sense that

$$:\!\phi^N(x)\!:|\mathcal{A}\rangle = \mathscr{D}_{\mathcal{A}}[v] \left[:\!\phi^N(x)\!:\mathcal{A}(0;v)\right] |0\rangle\,, \tag{C.15}$$

where

$$\mathcal{A}(x;v) = \ :\!\phi^2(x)\,(v_1 \cdot \partial_x)^8 \phi(x)\,(v_2 \cdot \partial_x)^8 \phi(x)\!:. \tag{C.16}$$

The advantage of this approach is that OPE manipulations no longer involve sums of many different tensor structures that come from derivatives of two-point functions, such as in. Eq. (C.4). In fact, after contracting with an auxiliary vector v_i^μ, any such derivative $\langle \phi(x)(v_i \cdot \partial)^\ell \phi(0)\rangle$ consists of a single term:

$$\langle \phi(x)(v \cdot \partial)^\ell \phi(0)\rangle = 2^\ell (\nu)_\ell \frac{(x \cdot v)^\ell}{|x|^{d-2+2\ell}}\,, \qquad (v^2 = 0)\,. \tag{C.17}$$

As a next step, the operator $\mathscr{D}_{\mathcal{A}}[v]$ is used to contract as many indices as possible. As an example, we isolate a single term from the $\phi^4 \times \mathcal{A}$ OPE:

$$:\!\phi^4(x)\!:|\mathcal{A}\rangle \ \supset \ \left[\mathscr{D}_{\mathcal{A}}[v]\, \langle \phi(x)\,(v_1 \cdot \partial)^8 \phi(0)\rangle \langle \phi(x)\,(v_2 \cdot \partial)^8 \phi(0)\rangle\right] |\phi^2(x)\rangle. \tag{C.18}$$

Acting with $\mathscr{D}_{\mathcal{A}}[v]$ on the two-point functions, we obtain

$$:\phi^4(x):|\mathcal{A}\rangle \;\supset\; \frac{2^8(\nu)_8(2\nu)_8}{|x|^{2d-4+2\ell}}|\phi^2(x)\rangle. \tag{C.19}$$

Notice in particular that the auxiliary vectors v_i^μ are no longer present.

Spherical integrals

After manipulating the OPE, what remains to be done is a number of spherical integrals. The index-free formalism can be used to simplify their computation drastically. In order to explain this improvement, we consider a typical integral that arises when calculating OPE coefficients:

$$\frac{1}{\mathrm{S}_d}\int_{|x|=1}\mathrm{d}^{d-1}x\, x^{\mu_1}\cdots x^{\mu_8}x^{\nu_1}x^{\nu_2}x^{\rho_1}\cdots x^{\rho_6}|\phi_{,\mu_1\cdots\mu_8}\,\phi_{,\nu_1\nu_2}\,\phi_{,\rho_1\cdots\rho_6}\rangle. \tag{C.20}$$

As explained below Eq. (5.33), performing this integral yields a sum of $15!! \sim 2\cdot 10^6$ tensors, all of which need to be contracted with the state $|\phi_{,\mu_1\cdots\mu_8}\,\phi_{,\nu_1\nu_2}\,\phi_{,\rho_1\cdots\rho_6}\rangle =: |\Psi\rangle$. Notice however that the state $|\Psi\rangle$ is traceless in all indices μ_i, ν_i and ρ_i; this means that a large fraction of these tensor contractions will vanish. In fact, the integral (C.20) must be proportional to $|\Psi\rangle$ itself, since there are no other ways to contract the indices.

Fortunately, the index-free formalism allows for a major simplication. The key point is the following: because the state $|\Psi\rangle$ is traceless in three groups of indices, we may subtract various traces from the integrand

$$\begin{aligned} &x^{\mu_1}\cdots x^{\mu_8}x^{\nu_1}x^{\nu_2}x^{\rho_1}\cdots x^{\rho_6} \\ &\qquad\to\quad (x^{\mu_1}\cdots x^{\mu_8}-\text{traces})\,(x^{\nu_1}x^{\nu_2}-\text{trace})\,(x^{\rho_1}\cdots x^{\rho_6}-\text{traces}) \end{aligned} \tag{C.21}$$

without changing the result. This new integrand is a product of three TSTs, that we can encode using the auxiliary vectors u_1, u_2, u_3, all of which satisfy $u_i^2 = 0$:

$$x^{\mu_1}\cdots x^{\mu_8}x^{\nu_1}x^{\nu_2}x^{\rho_1}\cdots x^{\rho_6} \;\to\; (x\cdot u_1)^8\,(x\cdot u_2)^2\,(x\cdot u_3)^6\,. \tag{C.22}$$

The resulting integral can be calculated by taking derivatives of a generating function:

$$\frac{1}{\mathrm{S}_d}\int_{|x|=1}\mathrm{d}^{d-1}x\,(x\cdot u_1)^8\,(x\cdot u_2)^2\,(x\cdot u_3)^6 = (\partial_{\tau_1})^8(\partial_{\tau_2})^2(\partial_{\tau_3})^6\,\mathrm{GF}_3(u;\tau)\Big|_{\tau_i=0}, \tag{C.23}$$

$$\mathrm{GF}_n(u;\tau)\equiv\frac{1}{\mathrm{S}_d}\int_{|x|=1}\mathrm{d}^{d-1}x\,\exp\left(\sum_{i=1}^n\tau_i\,x\cdot u_i\right). \tag{C.24}$$

The generating function in question may be calculated explicitly:

$$\mathrm{GF}_n(u;\tau) = {}_0F_1\left[\frac{d}{2};\frac{1}{2}\sum_{i<j}\tau_i\tau_j\,u_i\cdot u_j\right], \qquad (u_i^2=0) \tag{C.25}$$

where ${}_0F_1[a;x]$ is a confluent hypergeometric function:

$$ {}_0F_1[a;x] = \sum_{n=0}^{\infty} \frac{x^n}{(a)_n n!}\,. \tag{C.26} $$

The proof of (C.25) is as follows: for any vector w^μ, we can use Eq. (5.33) to obtain

$$ \frac{1}{\mathrm{S}_d} \int_{|x|=1} \mathrm{d}^{d-1}x\, e^{w\cdot x} = \sum_{n=0}^{\infty} \frac{(w^2)^n}{(2n)!} \frac{(2n-1)!!}{2^n (d/2)_n} = {}_0F_1\left[\frac{d}{2}; \frac{w^2}{4}\right]. \tag{C.27} $$

To obtain the second equality, we use that $(2n-1)!! = 2^n (1/2)_n$ and $(2n)! = 4^n n! (1/2)_n$. Setting

$$ w^\mu = \sum_{i=1}^{n} \tau_i\, u_i^\mu\,, \tag{C.28} $$

leads immediately to the desired result.

Using formula (C.25), we obtain

$$ \frac{1}{\mathrm{S}_d} \int_{|x|=1} \mathrm{d}^{d-1}x\, (x\cdot u_1)^8\, (x\cdot u_2)^2\, (x\cdot u_3)^6 = \frac{40320}{d(d+2)\cdots(d+14)}\, (u_1\cdot u_2)^2 (u_1\cdot u_3)^6. \tag{C.29} $$

Strictly speaking, we should open now up all indices again using the differential operators (C.10). However, this step is superfluous: all different tensor structures that appear and their multiplicities can be directly read off from (C.29). For the case under consideration, we find that the integral (C.20) evaluates to

$$ \frac{40320}{d(d+2)\cdots(d+14)}\, |\phi_{,\nu_1\nu_2\rho_1\cdots\rho_6}\, \phi_{,\nu_1\nu_2}\, \phi_{,\rho_1\cdots\rho_6}\rangle. \tag{C.30} $$

This method can be straightforwardly extended to any tensor integral; in general, several different terms appear after integrating.

C.3 Gram matrix

In section 4.3.3, we explained all rules needed to computate the Gram matrix $G_{ij} = \langle \mathcal{O}_i | \mathcal{O}_j \rangle$. In this section, we will explain how to exploit the index-free formalism to improve the method presented there. Let us first fix the notation. We will calculate some matrix element $\langle \mathcal{A}|\mathcal{B}\rangle$, writing $\mathcal{A}$ as $\mathcal{A} = :\varphi_1 \cdots \varphi_n:$. Here, φ_i is a shorthand notation: it represents the field ϕ, acted on by k_i derivatives. Similarly, $\mathcal{B}$ is written as $\mathcal{B} = :\widetilde{\varphi}_1 \cdots \widetilde{\varphi}_n:$, where $\widetilde{\varphi_j}$ is equal to ϕ but with k'_j derivatives acting on it. By assumption, both states are scalars, hence all derivatives will be contracted.

Notice that we can always order the fields in $\mathcal{A}$ and $\mathcal{B}$ in order of increasing spin, such that $k_1 \leqslant k_2 \leqslant \ldots \leqslant k_m$, and similarly $k'_1 \leqslant \ldots \leqslant k'_n$. To $\mathcal{A}$ (resp. $\mathcal{B}$) we can then associate the partition

$$\mathcal{P}_\mathcal{A} = (k_1, k_2, \ldots, k_n), \qquad \mathcal{P}_\mathcal{B} = (k'_1, k'_2, \ldots, k'_n). \tag{C.31}$$

In section 4.3.3, we established that the matrix element $\langle \mathcal{A}|\mathcal{B}\rangle$ vanishes unless $\mathcal{P}_\mathcal{A} = \mathcal{P}_\mathcal{B}$. We also proved that

$$[\mathcal{A}(x)]^\dagger = :[\varphi_1(x)]^\dagger \cdots [\varphi_n(x)]^\dagger: . \tag{C.32}$$

Then Wick's theorem implies that

$$\langle \mathcal{A}|\mathcal{B}\rangle = \lim_{x,y\to 0} \sum_{\sigma\in S_n} \langle [\varphi_1(x)]^\dagger \widetilde{\varphi}_{\sigma(1)}(y)\rangle \cdots \langle [\varphi_n(x)]^\dagger \widetilde{\varphi}_{\sigma(n)}(y)\rangle. \tag{C.33}$$

The sum runs over all $n!$ permutations that form the symmetric group S_n. All factors $\langle [\varphi_i(x)]^\dagger \widetilde{\varphi}_{\sigma(i)}(y)\rangle$ can be calculated by taking derivatives of the two-point function

$$\langle [\phi(x)]^\dagger \phi(y)\rangle = \frac{1}{(1 - 2x\cdot y + x^2y^2)^{(d-2)/2}} \tag{C.34}$$

and using the fact that derivatives commute with taking the adjoint:

$$[\partial_{\mu_1} \cdots \partial_{\mu_\ell} \phi(x)]^\dagger = \frac{\partial}{\partial x^{\mu_1}} \cdots \frac{\partial}{\partial x^{\mu_\ell}} [\phi(x)]^\dagger. \tag{C.35}$$

Alternatively, the calculation can be done using the conformal algebra (1.15); this follows by writing

$$|\phi_{,\nu_1\cdots\nu_\ell}\rangle \equiv \lim_{y\to 0} \frac{\partial}{\partial y^{\nu_1}} \cdots \frac{\partial}{\partial y^{\nu_\ell}} \phi(y)|0\rangle = i^\ell P_{\nu_1} \cdots P_{\nu_\ell} |\phi\rangle, \tag{C.36a}$$

$$\langle \phi_{,\mu_1\cdots\mu_\ell}| \equiv \lim_{x\to 0} \frac{\partial}{\partial x^{\mu_1}} \cdots \frac{\partial}{\partial x^{\mu_\ell}} \langle 0|[\phi(x)]^\dagger = (-i)^\ell \langle \phi| K_{\mu_1} \cdots K_{\mu_\ell}. \tag{C.36b}$$

The order of the different P_μ's (resp. K_μ's) is unimportant, as $[P_\mu, P_\nu] = [K_\mu, K_\nu] = 0$. All matrix elements can then be worked out using the conformal algebra (1.15) and

$$M_{\mu\nu}|\phi\rangle = K_\mu|\phi\rangle = 0\,, \qquad D|\phi\rangle = -i\nu|\phi\rangle\,, \tag{C.37}$$

since ϕ is a scalar primary of dimension $[\phi] = \nu = \frac{1}{2}(d-2)$.

As a simple example, consider the operator $\mathcal{A} = :(\partial_\mu\phi)^2:$ and let's compute the norm $\langle \mathcal{A}|\mathcal{A}\rangle$ according to the above methods. According to (C.33), we must calculate

$$\langle \mathcal{A}|\mathcal{A}\rangle = 2\left[\lim_{x,y\to 0} \frac{\partial}{\partial x^\mu}\frac{\partial}{\partial y^\nu} \langle [\phi(x)]^\dagger \phi(y)\rangle\right]^2 \tag{C.38}$$

since both permutations in S_2 act identically. Working out the derivatives as follows

$$\lim_{x,y\to 0} \frac{\partial}{\partial x^\mu}\frac{\partial}{\partial y^\nu} \langle [\phi(x)]^\dagger \phi(y)\rangle = (d-2)\delta_{\mu\nu}\,, \tag{C.39}$$

we obtain the result $\langle\mathcal{A}|\mathcal{A}\rangle = 2d(d-2)^2$. Alternatively, using the conformal algebra, we would have

$$\langle\mathcal{A}|\mathcal{A}\rangle = 2\langle\partial_\mu\phi|\partial_\nu\phi\rangle^2 = 2\langle\phi|K_\mu P_\nu|\phi\rangle^2 = 2(2\delta_{\mu\nu}\langle\phi|iD|\phi\rangle)^2\,. \tag{C.40}$$

which gives the same result.

Index-free approach

A more efficient way to calculate matrix elements again the index-free approach from section C.2.1. Following section (C.2.1), we can decompose any matrix elements $\langle\mathcal{A}|\mathcal{B}\rangle$ as

$$\langle\mathcal{A}|\mathcal{B}\rangle = \mathscr{D}_\mathcal{A}[u]\mathscr{D}_\mathcal{B}[v]\; p(u,v) \tag{C.41}$$

where $\mathscr{D}_\mathcal{A}[u]$ (resp. $\mathscr{D}_\mathcal{B}[v]$) is a differential operator that acts on auxiliary vectors u_i^μ (resp. v_j^μ), and $p(u,v)$ is the polynomial

$$p(u,v) \equiv \langle(u_1\cdot\partial)^{k_1}\phi\cdots(u_n\cdot\partial)^{k_n}\phi|(v_1\cdot\partial)^{k'_1}\phi\cdots(v_n\cdot\partial)^{k'_n}\phi\rangle \tag{C.42a}$$

$$= \sum_{\sigma\in S_n}\langle(u_1\cdot\partial)^{k_1}\phi|(v_{\sigma(1)}\cdot\partial)^{k'_{\sigma(1)}}\phi\rangle\cdots\langle(u_n\cdot\partial)^{k_n}\phi|(v_{\sigma(n)}\cdot\partial)^{k'_{\sigma(n)}}\phi\rangle. \tag{C.42b}$$

Notice that $p(u,v)$ only depends on the partitions $\mathcal{P}_\mathcal{A} = \mathcal{P}_\mathcal{B}$ of both states, and not on the way the indices in both states are contracted. Any matrix element $\langle(u_i\cdot\partial)^k\phi|(v_j\cdot\partial)^{k'}\phi\rangle$ consists of a single term:

$$\langle(u_i\cdot\partial)^k\phi|(v_j\cdot\partial)^{k'}\phi\rangle = \delta_{kk'}\,2^k k!(\nu)_k(u_i\cdot v_j)^k\,,\qquad (u_i^2 = v_j^2 = 0)\,. \tag{C.43}$$

The delta function $\delta_{kk'}$ enforces the selection rule (4.19). Practically speaking, this means that $p(u,v)$ factorizes into a product of polynomials that encode spin-ℓ states.

As an example, consider the operator $\mathcal{A} = :\phi_{,\mu}\,\phi_{,\nu}\,\phi_{,\mu\nu}:$. Let us try to compute its norm $\langle\mathcal{A}|\mathcal{A}\rangle$ using the index-free formalism. The differential operators $\mathscr{D}_\mathcal{A}[u]$, $\mathscr{D}_\mathcal{A}[v]$ for this state are given by

$$\mathscr{D}_\mathcal{A}[u] = \frac{1}{[1!(\nu)_1]^2 2!(\nu)_2}\mathcal{D}_{\lambda_1}[u_1]\mathcal{D}_{\lambda_2}[u_2]\mathcal{D}_{\lambda_1\lambda_2}[u_3],$$
$$\mathscr{D}_\mathcal{A}[v] = \frac{1}{[1!(\nu)_1]^2 2!(\nu)_2}\mathcal{D}_{\mu_1}[v_1]\mathcal{D}_{\mu_2}[v_2]\mathcal{D}_{\mu_1\mu_2}[v_3].$$

According to Eq. (C.42a), the polynomial $p(u,v)$ is given by

$$p(u,v) = \langle u_1\cdot\partial\phi\; u_2\cdot\partial\phi\;(u_3\cdot\partial)^2\phi \mid v_1\cdot\partial\phi\; v_2\cdot\partial\phi\;(v_3\cdot\partial)^2\phi\rangle$$
$$= 2d(d-2)^3(u_1\cdot v_1\,u_2\cdot v_2 + u_1\cdot v_2\,u_2\cdot v_1)(u_3\cdot v_3)^2.$$

Applying the differential operators $\mathscr{D}_{\mathcal{A}}[u]$ and $\mathscr{D}_{\mathcal{A}}[v]$ to $p(u,v)$, we find that

$$\langle \mathcal{A}|\mathcal{A}\rangle = 2(d-2)^3(d-1)d(d+2)\,.$$

Appendix D

Renormalization in TCSA: computations

D.1 Asymptotics of $C(t)$

In this appendix we will give some details concerning the derivation of Eq. (6.33). We start from the definition of $C(t)$ in Eq. (6.28). We do the Weyl transformation which maps the correlation function on the cylinder into one in flat space. In flat space the operation insertions look like:

$$w \int_{S_r^{d-1}} dx\, \mathcal{V}_a(x) \int_{S_{1/r}^{d-1}} dy\, \mathcal{V}_b(y)\,, \qquad r = e^{t/2}\,, \tag{D.1}$$

where

$$w = r^{\Delta_a}(1/r)^{\Delta_b} = 1 + (\Delta_a - \Delta_b)t/2 + O(t^2)\,. \tag{D.2}$$

is the product of factors picked up by the operators under the Weyl transformation. To the shown order in t, which is the one we need, the effect of w will average to zero when summed over $a \leftrightarrow b$. We next use the flat space OPE:

$$\mathcal{V}_a(x)\mathcal{V}_b(y) \to |x-y|^{-h}[V_c(x) - \tfrac{1}{2}(x-y)^\mu \partial_\mu \mathcal{V}_c(x) + \ldots]\,. \tag{D.3}$$

Instead of inserting the RHS operator at the middle-point as in (6.31), we put it at one of the endpoints, since this facilitates the subsequent integration. However, the needed accuracy then requires the inclusion of the shown first subleading term.

We now have to do the integral over y running over the sphere of radius $1/r = e^{-t/2}$. By rotation invariance we can take $x = (\vec{0}, r)$. The nonanalytic behavior of the integral as $t \to 0$ will come from the region of the y sphere closest to x, i.e. its northern cap, which we parameterize as

$$y = (\vec{\rho}, \sqrt{e^{-t} - \rho^2})\,, \quad |x-y|^2 \approx \rho^2(1+t) + t^2\,, \tag{D.4}$$

where we kept the approximation needed to get $C(t)$ to $O(t^2)$. We are led to evaluate the integral

$$\int_0^\infty d\rho \frac{\mathrm{S}_{d-1}\rho^{d-2}}{[\rho^2(1+t)+t^2]^{h/2}}[V_c(x)-(t/2)\partial_z V_c(x)]\,. \tag{D.5}$$

Rescaling $\rho \to \rho/\sqrt{1+t}$ and doing the integral over ρ we obtain

$$(1+t)^{-(d-1)/2}t^{d-1-h}\mathrm{S}_{d-1}\frac{\Gamma((d-1)/2)\Gamma((h-d+1)/2)}{2\Gamma(h/2)}[V_c(x)-(t/2)\partial_z V_c(x)]\,. \tag{D.6}$$

Next we replace $V_c(x)-(t/2)\partial_z V_c(x) \approx V_c(\bar{x})$, $\bar{x} = e^{-t/2}x$. The factor $(1+t)^{-(d-1)/2}$ is absorbed when we transform the remaining integral in $x \in S_r^{d-1}$ into an integral in $\bar{x}$ over the unit sphere. The remaining coefficient in (D.6) equals $B(h)\Gamma(h-d+1)$ in (6.33).

D.2 M_n sequence for $\phi^2 \times \phi^2$

The purpose of this appendix is to derive Eq. (6.42), which gives the exact asymptotics for the M_n sequence in the case of the ϕ^2 perturbation. We thus consider the matrix $V^i{}_j$ defined as

$$\int_{|x|=1} :\phi^2(x):|\mathcal{O}_j\rangle \equiv V^i{}_j|\mathcal{O}_i\rangle. \tag{D.7}$$

We will describe two methods to get the answer. The first one is direct: we will study the matrix elements $V^k{}_j$ and $V^i{}_k$ and identify the states of energy $\Delta_k \gg \Delta_i, \Delta_j$ which contribute to the sum defining M_n. To compute $V^k{}_j$, we consider the OPE $\phi^2(x)\times\mathcal{O}_j(0)$. By Wick's theorem, we can write:

$$\begin{aligned} :\phi^2(x):\mathcal{O}_j(0) \;=\; & :\phi^2(x)\mathcal{O}_j(0): \\ & + \sum \langle\phi(x)\partial_{(\alpha)}\phi(0)\rangle :\phi(x)\hat{\mathcal{O}}_j(0): \\ & + \sum \langle\phi(x)\partial_{(\alpha)}\phi(0)\rangle\langle\phi(x)\partial_{(\beta)}\phi(0)\rangle\hat{\hat{\mathcal{O}}}_j(0)\,. \end{aligned} \tag{D.8}$$

Here in the second and third line we put terms where one or two ϕ's out of $\phi^2(x)$ are contracted with the ϕ's making up $\mathcal{O}_j$, which can possibly carry several derivatives denoted collectively as (α), (β). The operators $\hat{\mathcal{O}}_j$ and $\hat{\hat{\mathcal{O}}}_j$ are $\mathcal{O}_j$ minus the contracted parts.

The operators in the third line have all dimension $< \Delta_j$, so they are not relevant for the asymptotics. The operators coming from the second line will appear by expanding $\phi(x)$ under the normal ordering sign into the Taylor series and picking up terms which will not vanish upon integration over the unit sphere, with $\langle\phi(x)\partial_{(\alpha)}\phi(0)\rangle$ as a weight. A moment's thought shows that the only surviving operators will be $:\partial_{(\alpha)}\phi(x)\hat{\mathcal{O}}_j(0):$, i.e. where $\phi(x)$ is expanded at order α. These operators have dimension Δ_j and are also irrelevant for the asymptotics.

Thus, all the operators with asymptotically large dimensions come from the first line. Expanding around $x = 0$ and integrating, we get:

$$\int_{|x|=1} :\phi^2(x)\mathcal{O}_j(0):|0\rangle = \sum_{p=0}^{\infty} \frac{\mathrm{S}_d}{p!\, 4^p (d/2)_p} |\Box^p(\phi^2)\mathcal{O}_j\rangle \,. \tag{D.9}$$

Here $\Box \equiv \partial^2$, and we used the integral (5.33).

We conclude that the large dimension states appearing in the OPE are the states $|\Box^p(\phi^2)\mathcal{O}_j\rangle$, whose dimension is $\Delta_j + \Delta(\phi^2) + 2p$. To complete the calculation, we need to compute $V^i{}_k$ for k being one of these states and $\mathcal{O}_i$ an operator of low scaling dimension. We have

$$\begin{aligned}\int_{|x|=1} :\phi^2(x)::\Box^p(\phi^2)\mathcal{O}_j(0): \;=\; & \int_{|x|=1} 2^{p+1}\langle\phi(x)\partial_{\mu_1}\cdots\partial_{\mu_p}\phi(0)\rangle^2 :\mathcal{O}_j(0): \\ & + \text{operators of high dimension.}\end{aligned} \tag{D.10}$$

This equation expresses the fact that the only way to lower the dimension drastically is to contract both ϕ's out of ϕ^2 with ϕ's under the $\Box^p$ sign. The first line evaluates to

$$\mathrm{S}_d \mathrm{N}_d^2\, 2^{2p+1}(2\nu)_p(\nu)_p|\mathcal{O}_j\rangle \,. \tag{D.11}$$

Multiplying the factors in (D.9) and (D.11), we obtain exactly Eq. (6.42).

D.2.1 Renormalization details for the ϕ^4 flow

The renormalization in the Landau-Ginzburg flow is determined through the leading OPEs of the deforming operators in (7.3), given by

$$\begin{aligned}\phi^2(x)\times\phi^2(0) &= \frac{2\,\mathrm{N}_d^2}{|x|^{h_{220}}}\mathbb{1} + \dots\,, \\ \phi^4(x)\times\phi^4(0) &= \frac{24\,\mathrm{N}_d^4}{|x|^{h_{440}}}\mathbb{1} + \frac{96\,\mathrm{N}_d^3}{|x|^{h_{442}}}\phi^2 + \frac{72\,\mathrm{N}_d^2}{|x|^{h_{444}}}\phi^4 + \dots\,, \\ \phi^2(x)\times\phi^4(0) &= \frac{12\,\mathrm{N}_d^2}{|x|^{h_{422}}}\phi^2 + \dots\,,\end{aligned} \tag{D.12}$$

where $h_{ijk} = \Delta(\phi^i) + \Delta(\phi^j) - \Delta(\phi^k) = (i + j - k)\nu$. We have $\nu = 1/4$ in $d = 2.5$.

In the RHS of (D.12) we omitted the operators whose associated function $B(h)$ vanishes because of the remark in footnote 11. All the retained operators have nonzero $B(h)$ and will be relevant for the renormalization. The effect of ϕ^2 and ϕ^4 in the RHS will be to make the couplings λ and m^2 non-trivial functions of the cutoff. We are in a position to use the RG-improved formalism of section 6.2.3.

A crucial ingredient in the renormalization is the relation between the above OPEs and the asymptotics of the matrix $(M_n)^i{}_j$ in (6.27). For the ϕ^2 flow we were able to determine the asymptotics of this matrix exactly including the discrete structure, see equation (6.42).

In the future, such exact asymptotics may be also worked out with the ϕ^4 coupling switched on, see the end of Appendix D.2 for a discussion, although the task looks more challenging. In this work, we will use the continuum approximation (6.34). We checked the accuracy of this approximation for many choices of external states i, j against the exact expression for M_n within the range $\Delta_n \leqslant \Delta_{\text{max}}$ where we know V and can compute M_n numerically. These checks convinced us that the approximation is adequate.

One such check is shown in figure D.1, where we plot both the exact and the approximate behavior of $(M_n)^i{}_j$ for $\mathcal{V} = :\phi^4:$ and for $\mathcal{O}_i = \mathcal{O}_j = :\phi^2:$. The blue dots represent the individual values (notice that M_n is nonzero only for half-integer Δ_n). The red dashed line shows moving average of these values within the interval $[\Delta - 1, \Delta + 1]$. The solid black line is our approximation as given in (6.34), including the contributions of all three leading operators in the $\phi^4 \times \phi^4$ OPE shown in (D.12). We see that the agreement between the moving average and the approximation becomes very good at $\Delta \sim 17$, which is also the cutoff we used in this study. The agreement for other choices of $\mathcal{O}_i$ and $\mathcal{O}_j$ is similarly good.

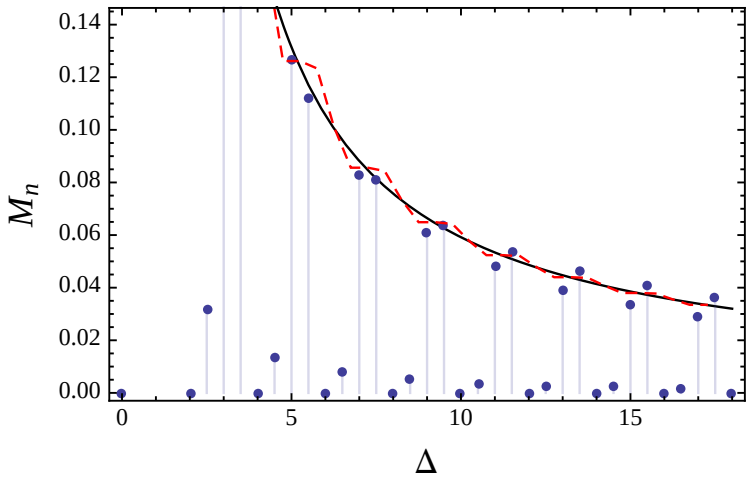

Figure D.1: The behavior of $(M_n)^i{}_j$ for the ϕ^4 deformation and one particular choice of i, j (see text). Exact values are given in blue (isolated dots), a moving average in red (dashed line), and our continuum approximation in black (smooth curve).

From the OPEs (D.12) we can directly generate the RG equations discussed in section 6.2.3 for the couplings of the local operators. They are given by:

$$\begin{aligned}
\frac{\delta g_0(\Lambda)}{\delta\Lambda} &= \frac{\tilde{f}_{220}\, g_2^2(\Lambda)}{\Lambda^{d-h_{220}}(\Lambda - E_r)} + \frac{\tilde{f}_{440}\, g_4^2(\Lambda)}{\Lambda^{d-h_{440}}(\Lambda - E_r)}\,, \\
\frac{\delta g_2(\Lambda)}{\delta\Lambda} &= \frac{\tilde{f}_{442}\, g_4^2(\Lambda)}{\Lambda^{d-h_{442}}(\Lambda - E_r)} + \frac{2\tilde{f}_{422}\, g_4(\Lambda) g_2(\Lambda)}{\Lambda^{d-h_{422}}(\Lambda - E_r)}\,, \\
\frac{\delta g_4(\Lambda)}{\delta\Lambda} &= \frac{\tilde{f}_{444}\, g_4^2(\Lambda)}{\Lambda^{d-h_{444}}(\Lambda - E_r)}\,,
\end{aligned} \tag{D.13}$$

where we denoted by g_0, g_2 and g_4 the coupling associated to $\mathbb{1}$, $:\phi^2:$, and $:\phi^4:$. We also

introduced

$$\tilde{f}_{abc} = f_{abc} B(h_{abc}) \tag{D.14}$$

with the OPE coefficients f_{abc} given in (D.12) and $B(h)$ was defined in (6.33). The renormalized couplings are then found by integrating these equations numerically from $\Lambda = \infty$ to the desired value of the cutoff $\Lambda = \Lambda_{\rm UV} = \Delta_{\rm max}/R$. We impose boundary conditions at infinity such that $g_0 = 0$ and g_2 and g_4 are given by their bare UV values:

$$g_4(\infty) = \lambda\,, \qquad g_2(\infty) = \tfrac{1}{2} m^2\,. \tag{D.15}$$

As we explained in section 6.2.3, the above RG equations depend on a reference energy E_r. In our study we found it convenient to choose E_r to be around the energy of the first excited state in the $\mathbb{Z}_2$ even sector. An estimate for this energy was obtained by extrapolating the earlier obtained results for lower values of the radius or the coupling, or by performing a quick computation with a smaller $\Delta_{\rm max}$.

We also discussed in section 6.2.3 the subleading dependence on $(\Delta_i + \Delta_j)/R$ and on $\bar{E} - E_r$. This dependence is taken into account by adding to the correction Hamiltonian the additional non-local terms given in (6.39). Their coefficients, which we denote as $g_i^{(H_{\rm CFT})}$ and $g_i^{(H)}$, are determined by solving separate RG flow equations. For example, for $i = 0$ we have

$$\begin{aligned} \frac{\delta g_0^{(H_{\rm CFT})}(\Lambda)}{\delta\Lambda} &= \frac{(d-h_{220})\tilde{f}_{220}\, g_2^2(\Lambda)}{\Lambda^{d-h_{220}+1}(\Lambda - E_r)} + \frac{(d-h_{440})\tilde{f}_{440}\, g_4^2(\Lambda)}{\Lambda^{d-h_{440}+1}(\Lambda - E_r)}\,, \\ \frac{\delta g_0^{(H)}(\Lambda)}{\delta\Lambda} &= \frac{\tilde{f}_{220}\, g_2^2(\Lambda)}{\Lambda^{d-h_{220}}(\Lambda - E_r)^2} + \frac{\tilde{f}_{440}\, g_4^2(\Lambda)}{\Lambda^{d-h_{440}}(\Lambda - E_r)^2}\,. \end{aligned} \tag{D.16}$$

The equations for other i are determined by modifying the corresponding equation in (D.13) in a similar manner. We integrate these equations with boundary conditions zero at infinity. Notice that we ignore the backreaction of these terms in the sense that they do not appear on the right-hand sides of the flow equations. [1]

In figure D.2 we present an example of the flow of several couplings. We see that g_2 receives substantial corrections, demonstrating the need for the RG improvement. On the other hand, we see that the relative change in g_4 is small, and that $g_0^{(H_{\rm CFT})}$ remains small compared to 1 (coefficient of $H_{\rm CFT}$ in the bare Hamiltonian) throughout the flow.

With the correction terms described up to now, the results we obtained already looked reasonable. We were however able to take into account one further correction, which turned

1. For $g_0^{(H_{\rm CFT})}$ and $g_0^{(H)}$, which multiply local terms in the Hamiltonian, it would be possible to incorporate such a backreaction rather easily. At every step of RG one should factor out the modified coefficient of $H_{\rm CFT}$, which leads to an overall rescaling of the remaining couplings. The product of all rescalings Z should be stored separately to undo the rescaling at the end of the computation. This procedure resembles wavefunction renormalization in perturbative RG. We implemented it, but found the numerical effect of this improvement to be very small.

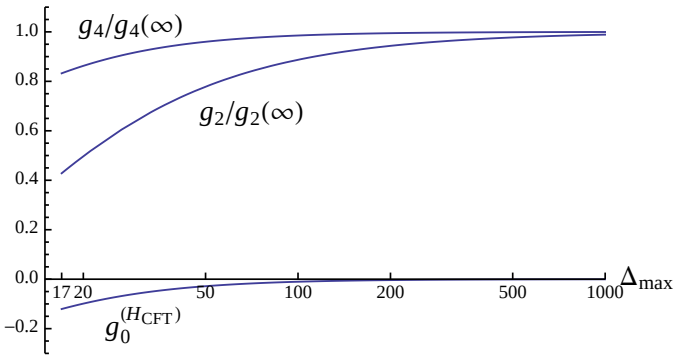

Figure D.2: The relative change in a few of the running couplings as a function of the cutoff. In this example we set $R = 3$, and $\lambda = 0.7$ and $m^2 = 1$ in the UV. We used $\bar{E}_r = -6$.

out to give a noticeable improvement mainly for small values of λ. Namely, we constructed a new nonlocal counterterm which completely takes into account the dependence on $(\Delta_i + \Delta_j)/R$ and $(\bar{E} - E_r)$, beyond expanding to first order as above. The coefficient of this correction is computed by running the RG flow again (once more ignoring the backreaction of this nonlocal term) but *separately* for each value of $\kappa = \frac{1}{2}(\Delta_i+\Delta_j)/R$ and $\bar{E}$. In equations, this means that we update this extra nonlocal correction in each RG step as follows,

$$\frac{\delta\Delta H^{\rm nl}(\kappa,\bar{E})_{ij}}{\delta\Lambda} = \sum_{a,b,c} g_a(\Lambda)g_b(\Lambda)\tilde{f}_{abc}\left(\int_{S^{d-1}}\mathcal{V}_c\right)_{ij}$$
$$\times\left\{\frac{1}{[\Lambda-\kappa]^{d-h_{abc}}(\Lambda-\bar{E})} - \frac{1}{\Lambda^{d-h_{abc}}(\Lambda-E_r)} - \frac{\bar{E}-E_r}{\Lambda^{d-h_{abc}}(\Lambda-E_r)^2} - \frac{(d-h_{abc})\kappa}{\Lambda^{d-h_{abc}+1}(\Lambda-E_r)}\right\}.$$

Inside curly brackets, we subtract the zeroth- and first-order terms in κ and $\bar{E} - E_r$, since these terms were already taken into account above.

Let us summarize. We integrate all the above RG equations from $\Lambda = \infty$ to $\Lambda = \Lambda_{\rm UV}$ and obtain the correction terms. We divide them into four groups:

— $\Delta H_{\rm loc}$ which reflects the change in all local couplings;

— ΔH_1 and ΔH_2 which include the nonlocal terms proportional to $H_{\rm CFT}.V_c + V_c.H_{\rm CFT}$ and $(H - E_r).V_c + V_c.(H - E_r)$, respectively;

— $\Delta H^{\rm nl}$.

It is now time for numerical diagonalization. We add $\Delta H_{\rm loc}$ and ΔH_1 directly to the bare TCSA Hamiltonian, and diagonalize. Let's call the resulting eigenvalues and eigenvectors E_n and c_n. In principle, we would also have liked to add ΔH_2 before the diagonalization. Unfortunately, we found that doing this destabilizes the numerics. This instability must have its origin in the fact that the factor $(H - E_r)$ is not small for states of high energy, and even for states of low energy it's not manifestly small, being a difference of two separately large quantities. We therefore chose to add the effect of ΔH_2 only after the numerical diagonalization. We found it necessary, and sufficient, to do this to the second order in

ΔH_2. The correction is computed by the usual Hamiltonian perturbation formula:

$$\Delta E_n = c_n.\Delta H_2.c_n + \sum_{m\neq n} \frac{(c_n.\Delta H_2.c_m)(c_m.\Delta H_2.c_n)}{E_n - E_m} \,. \tag{D.17}$$

The sum over m in the second-order term is rapidly convergent, and it's enough to sum over the first few eigenstates. Notice that one has to appropriately insert the right and left eigenvectors. This is not reflected in the notation but explained in detail in section 6.3.1.

Finally, we compute one last correction due to $\Delta H^{\rm nl}$, which turns out to be very small, so doing it to first order is sufficient:

$$(\Delta E_n)^{\rm nl} = c_n.\Delta H^{\rm nl}(E_n).c_n = (c_n)_i(\Delta H^{\rm nl}(E_n))^i{}_j(c_n)^j \,. \tag{D.18}$$

When evaluating this correction, we are supposed to set $\bar{E}$ in the definition of $\Delta H^{\rm nl}$ to the energy of the state we are correcting. Also recall that $\Delta H^{\rm nl}$ depends on $\kappa = \frac{1}{2}(\Delta_i + \Delta_j)/R$, and this dependence comes into play when evaluating the scalar product.

This completes the description of the renormalization procedure used to produce the plots in section 7.2. As the above discussion shows, an efficient implementation of the leading-order truncation effects given in (6.38) is subject to various subtleties, mostly due to the non-negligible presence of $(\Delta_i + \Delta_j)/R$ and $\bar{E}$ in the correction terms. In this exploratory paper we have not aimed to present a complete analysis of these effects. Instead, we discussed various recipes for dealing with them at a practical level. The details we provided should be sufficient to reproduce our results. In the future it would certainly be interesting to perform a more systematic study of all the subtleties.

Bibliography

[1] A. Zamolodchikov, "Irreversibility of the Flux of the Renormalization Group in a 2D Field Theory," *JETP Lett.* **43** (1986) 730–732.

[2] J. Polchinski, "Scale and Conformal Invariance in Quantum Field Theory," *Nucl.Phys.* **B303** (1988) 226.

[3] M. A. Luty, J. Polchinski, and R. Rattazzi, "The a-theorem and the Asymptotics of 4D Quantum Field Theory," *JHEP* **1301** (2013) 152, arXiv:1204.5221 [hep-th].

[4] A. Dymarsky, Z. Komargodski, A. Schwimmer, and S. Theisen, "On Scale and Conformal Invariance in Four Dimensions," arXiv:1309.2921 [hep-th].

[5] Y. Nakayama, "Scale invariance vs conformal invariance," *Phys.Rept.* **569** (2015) 1–93, arXiv:1302.0884 [hep-th].

[6] J. L. Cardy, "Conformal Invariance," in *Phase Transitions and Critical Phenomena*, C. Domb and J. L. Lebowitz, eds., vol. 11. Academic Press, 1987.

[7] S. El-Showk, M. F. Paulos, D. Poland, S. Rychkov, D. Simmons-Duffin, and A. Vichi, "Solving the 3D Ising Model with the Conformal Bootstrap," *Phys.Rev.* **D86** (2012) 025022, arXiv:1203.6064 [hep-th].

[8] S. El-Showk, M. F. Paulos, D. Poland, S. Rychkov, D. Simmons-Duffin, and A. Vichi, "Solving the 3d Ising Model with the Conformal Bootstrap II. c-Minimization and Precise Critical Exponents," *J.Stat.Phys.* **157** (2014) 869, arXiv:1403.4545 [hep-th].

[9] F. Kos, D. Poland, and D. Simmons-Duffin, "Bootstrapping Mixed Correlators in the 3D Ising Model," *JHEP* **1411** (2014) 109, arXiv:1406.4858 [hep-th].

[10] S. Ferrara, A. Grillo, and R. Gatto, "Tensor representations of conformal algebra and conformally covariant operator product expansion," *Annals Phys.* **76** (1973) 161–188.

[11] A. Polyakov, "Nonhamiltonian approach to conformal quantum field theory," *Zh.Eksp.Teor.Fiz.* **66** (1974) 23–42.

[12] A. Belavin, A. M. Polyakov, and A. Zamolodchikov, "Infinite Conformal Symmetry in Two-Dimensional Quantum Field Theory," *Nucl.Phys.* **B241** (1984) 333–380.

[13] D. Friedan, Z.-a. Qiu, and S. H. Shenker, "Conformal Invariance, Unitarity and Two-Dimensional Critical Exponents," *Phys.Rev.Lett.* **52** (1984) 1575–1578.

[14] R. Rattazzi, V. S. Rychkov, E. Tonni, and A. Vichi, "Bounding scalar operator dimensions in 4D CFT," *JHEP* **0812** (2008) 031, arXiv:0807.0004 [hep-th].

[15] F. Dolan and H. Osborn, "Conformal four point functions and the operator product expansion," *Nucl.Phys.* **B599** (2001) 459–496, arXiv:hep-th/0011040 [hep-th].

[16] F. Dolan and H. Osborn, "Conformal partial waves and the operator product expansion," *Nucl.Phys.* **B678** (2004) 491–507, arXiv:hep-th/0309180 [hep-th].

[17] S. Ferrara, A. Grillo, G. Parisi, and R. Gatto, "Covariant expansion of the conformal four-point function," *Nucl.Phys.* **B49** (1972) 77–98.

[18] S. Ferrara, A. Grillo, R. Gatto, and G. Parisi, "Analyticity properties and asymptotic expansions of conformal covariant green's functions," *Nuovo Cim.* **A19** (1974) 667–695.

[19] S. Ferrara, R. Gatto, and A. Grillo, "Properties of Partial Wave Amplitudes in Conformal Invariant Field Theories," *Nuovo Cim.* **A26** (1975) 226.

[20] F. Dolan and H. Osborn, "Conformal Partial Waves: Further Mathematical Results," arXiv:1108.6194 [hep-th].

[21] D. Pappadopulo, S. Rychkov, J. Espin, and R. Rattazzi, "OPE Convergence in Conformal Field Theory," *Phys.Rev.* **D86** (2012) 105043, arXiv:1208.6449 [hep-th].

[22] K. G. Wilson, "Confinement of Quarks," *Phys.Rev.* **D10** (1974) 2445–2459.

[23] V. Yurov and Al. B. Zamolodchikov, "Truncated Conformal Space Approach to Scaling Lee-Yang Model," *Int.J.Mod.Phys.* **A5** (1990) 3221–3246.

[24] M. Lassig, G. Mussardo, and J. L. Cardy, "The scaling region of the tricritical Ising model in two dimensions," *Nucl.Phys.* **B348** (1991) 591–618.

[25] T. R. Klassen and E. Melzer, "Spectral flow between conformal field theories in (1+1) dimensions," *Nucl.Phys.* **B370** (1992) 511–550.

[26] G. Feverati, F. Ravanini, and G. Takacs, "Truncated conformal space at $c = 1$, nonlinear integral equation and quantization rules for multi-soliton states," *Phys.Lett.* **B430** (1998) 264–273, arXiv:hep-th/9803104 [hep-th].

[27] C. Itzykson and J. Drouffe, *Statistical Field Theory. Vols 1 & 2.* Cambridge University Press, 1989.

[28] G. Mussardo, *Statistical Field Theory: An Introduction To Exactly Solved Models in Statistical Physics.* Oxford University Press, 2009.

[29] É. Brézin, *Introduction to Statistical Field Theory.* Cambridge University Press, 2010.

[30] G. Parisi, *Statistical Field Theory.* Addison-Wesley, 1988.

[31] J. L. Cardy, *Scaling and Renormalization in Statistical Physics.* Cambridge University Press, 1996.

[32] J. Binney, N. Dowrick, A. Fisher, and M. Newman, *The Theory of Critical Phenomena: An Introduction to the Renormalization Group.* Oxford University Press, 1992.

[33] J. Zinn-Justin, *Phase Transitions and Renormalization Group.* Oxford University Press, 2007.

[34] J. Zinn-Justin, *Transitions de phase et groupe de renormalisation.* EDP Sciences, 2005.

[35] G. Feverati, K. Graham, P. A. Pearce, G. Z. Toth, and G. Watts, "A Renormalisation group for TCSA," *J. Stat. Mech.* (2008) P03011, arXiv:hep-th/0612203 [hep-th].

[36] M. Abramowitz and I. A. Stegun, *Handbook of Mathematical Functions with Formulas, Graphs, and Mathematical Tables*. Applied Mathematics Series. National Bureau of Standards, 1964.

[37] H. Bateman, *Higher Transcendental Functions*, vol. I–III. McGraw-Hill, New York, 1953.

[38] I. Gradshteyn and I. Ryzhik, *Table of Integrals, Series, and Products*. Academic Press, 7th ed., 2007.

[39] P. Di Francesco, P. Mathieu, and D. Sénéchal, *Conformal Field Theory*. Springer, 1997.

[40] S. Ferrara, R. Gatto, and A. Grillo, "Conformal Algebra in Space-Time and Operator Product Expansion," *Springer Tracts Mod.Phys.* **67** (1973) 1–64.

[41] R. Blumenhagen and E. Plauschinn, *Introduction to Conformal Field Theory: With Applications to String Theory*, vol. 779 of *Lect. Notes Phys.* Springer, 2009.

[42] M. Schottenloher, *A Mathematical Introduction to Conformal Field Theory*. No. 759 in Lect. Notes Phys. Springer, 2008.

[43] P. Deligne, ed., *Quantum Fields and Strings: A Course for Mathematicians. Vol. 2*. American Mathematical Society, 1999.

[44] M. A. Shifman, *ITEP Lectures on Particle Physics and Field Theory. Vol. 2*. World Scientific, 1999.

[45] E. Kiritsis, *String Theory in a Nutshell*. Princeton University Press, 2007.

[46] J. Polchinski, *String Theory. Vols. 1 & 2*. Cambridge Univ. Press, 1998.

[47] A. M. Polyakov, *Gauge Fields and Strings*. Harwood Academic Publishers, 1987.

[48] K. Becker, M. Becker, and J. Schwarz, *String Theory and M-Theory: A Modern Introduction*. Cambridge University Press, 2007.

[49] A. Vichi, *A New Method to Explore Conformal Field Theories in Any Dimension*. PhD thesis, EPFL, 2011.

[50] P. H. Ginsparg, "Applied Conformal Field Theory," in *Les Houches lecture notes*. 1988. arXiv:hep-th/9108028 [hep-th].

[51] J. L. Cardy, "Conformal Invariance and Statistical Mechanics," in *Les Houches lecture notes*. 1988.

[52] J. Cardy, "Conformal Field Theory and Statistical Mechanics," in *Les Houches lecture notes*. 2008. arXiv:0807.3472 [cond-mat.stat-mech].

[53] S. Rychkov, "EPFL Lectures on Conformal Field Theory in $D \geqslant 3$ Dimensions," December 2012. http://sites.google.com/site/slavarychkov/.

[54] A. Schellekens, "Introduction to Conformal Field Theory," *Fortsch.Phys.* **44** (1996) 605–705.

[55] J. Kaplan, "Lectures on AdS/CFT from the Bottom Up," 2013. http://www.pha.jhu.edu/~jaredk.

[56] P. Cvitanović, *Group Theory: Birdtracks, Lie's and Exceptional Groups*. Princeton Univ. Press, 2008.

[57] S. Lagu and H. Laue, "The conformal group, its casimir operators, and a four-position operator," *Nuovo Cim.* **A20** (1974) 217–231.

[58] G. Mack and A. Salam, "Finite component field representations of the conformal group," *Annals Phys.* **53** (1969) 174–202.

[59] Lüscher, M. and Mack, G., "Global Conformal Invariance in Quantum Field Theory," *Commun.Math.Phys.* **41** (1975) 203–234.

[60] G. Mack, "All Unitary Ray Representations of the Conformal Group SU(2,2) with Positive Energy," *Commun.Math.Phys.* **55** (1977) 1.

[61] H. Osborn and A. Petkou, "Implications of conformal invariance in field theories for general dimensions," *Annals Phys.* **231** (1994) 311–362, arXiv:hep-th/9307010 [hep-th].

[62] J. Erdmenger and H. Osborn, "Conserved currents and the energy momentum tensor in conformally invariant theories for general dimensions," *Nucl.Phys.* **B483** (1997) 431–474, arXiv:hep-th/9605009 [hep-th].

[63] S. Weinberg, "Six-dimensional Methods for Four-dimensional Conformal Field Theories," *Phys.Rev.* **D82** (2010) 045031, arXiv:1006.3480 [hep-th].

[64] A. M. Polyakov, "Conformal symmetry of critical fluctuations," *JETP Lett.* **12** (1970) 381–383.

[65] M. S. Costa, J. Penedones, D. Poland, and S. Rychkov, "Spinning Conformal Correlators," *JHEP* **1111** (2011) 071, arXiv:1107.3554 [hep-th].

[66] D. Simmons-Duffin, "Projectors, Shadows, and Conformal Blocks," *JHEP* **1404** (2014) 146, arXiv:1204.3894 [hep-th].

[67] E. Elkhidir, D. Karateev, and M. Serone, "General Three-Point Functions in 4D CFT," *JHEP* **1501** (2015) 133, arXiv:1412.1796 [hep-th].

[68] M. S. Costa and T. Hansen, "Conformal correlators of mixed-symmetry tensors," *JHEP* **1502** (2015) 151, arXiv:1411.7351 [hep-th].

[69] J. Zinn-Justin, *Quantum Field Theory and Critical Phenomena.* Oxford Univ. Press, 2002.

[70] J. Callan, Curtis G., S. R. Coleman, and R. Jackiw, "A New improved energy - momentum tensor," *Annals Phys.* **59** (1970) 42–73.

[71] N. Birrell and P. Davies, *Quantum Fields in Curved Space.* Cambridge Univ. Press, 1982.

[72] J. L. Cardy and I. Peschel, "Finite Size Dependence of the Free Energy in Two-dimensional Critical Systems," *Nucl.Phys.* **B300** (1988) 377.

[73] A. Cappelli and A. Coste, "On the Stress Tensor of Conformal Field Theories in Higher Dimensions," *Nucl.Phys.* **B314** (1989) 707.

[74] C. P. Herzog and K.-W. Huang, "Stress Tensors from Trace Anomalies in Conformal Field Theories," *Phys.Rev.* **D87** (2013) 081901, arXiv:1301.5002 [hep-th].

[75] I. R. Klebanov, S. S. Pufu, and B. R. Safdi, "F-Theorem without Supersymmetry," *JHEP* **1110** (2011) 038, arXiv:1105.4598 [hep-th].

[76] J. L. Cardy, "Is There a c-Theorem in Four Dimensions?," *Phys.Lett.* **B215** (1988) 749–752.

[77] E. Gerchkovitz, J. Gomis, and Z. Komargodski, "Sphere Partition Functions and the Zamolodchikov Metric," *JHEP* **1411** (2014) 001, arXiv:1405.7271 [hep-th].

[78] B. Assel, D. Cassani, L. Di Pietro, Z. Komargodski, J. Lorenzen, and D. Martelli, "The Casimir Energy in Curved Space and its Supersymmetric Counterpart," arXiv:1503.05537 [hep-th].

[79] S. Fubini, A. J. Hanson, and R. Jackiw, "New approach to field theory," *Phys.Rev.* **D7** (1973) 1732–1760.

[80] J. Cardy, "Universal amplitudes in finite-size scaling: generalisation to arbitrary dimensionality," *J.Phys.* **A18** no. 13, (1985) L757–L760.

[81] J. L. Cardy, "Anisotropic Corrections to Correlation Functions in Finite Size Systems," *Nucl.Phys.* **B290** (1987) 355–362.

[82] S. Minwalla, "Restrictions imposed by superconformal invariance on quantum field theories," *Adv.Theor.Math.Phys.* **2** (1998) 781–846, arXiv:hep-th/9712074 [hep-th].

[83] S. Ferrara, A. Grillo, G. Parisi, and R. Gatto, "Canonical scaling and conformal invariance," *Phys.Lett.* **B38** (1972) 333–334.

[84] S. Weinberg, "Minimal fields of canonical dimensionality are free," *Phys.Rev.* **D86** (2012) 105015, arXiv:1210.3864 [hep-th].

[85] Lüscher, M., "Operator Product Expansions on the Vacuum in Conformal Quantum Field Theory in Two Space-Time Dimensions," *Commun.Math.Phys.* **50** (1976) 23.

[86] G. Mack, "Convergence of Operator Product Expansions on the Vacuum in Conformal Invariant Quantum Field Theory," *Commun.Math.Phys.* **53** (1977) 155.

[87] M. S. Costa, J. Penedones, D. Poland, and S. Rychkov, "Spinning Conformal Blocks," *JHEP* **1111** (2011) 154, arXiv:1109.6321 [hep-th].

[88] A. Dymarsky, "On the four-point function of the stress-energy tensors in a CFT," arXiv:1311.4546 [hep-th].

[89] F. G. Rejón-Barrera, "Bootstrapping CFT$_d$'s," Master's thesis, Universiteit van Amsterdam, 2014. http://dare.uva.nl/en/scriptie/501088.

[90] A. Zamolodchikov, "Conformal Symmetry in Two Dimensions: An Explicit Recurrence Formula for the Conformal Partial Wave Amplitude," *Commun.Math.Phys.* **96** (1984) 419–422.

[91] H. Osborn, "Conformal Blocks for Arbitrary Spins in Two Dimensions," *Phys.Lett.* **B718** (2012) 169–172, arXiv:1205.1941 [hep-th].

[92] H. Bateman and A. Erdélyi, *Higher transcendental functions, Vol. 1.* McGraw-Hill, 1955.

[93] V. S. Rychkov and A. Vichi, "Universal Constraints on Conformal Operator Dimensions," *Phys.Rev.* **D80** (2009) 045006, arXiv:0905.2211 [hep-th].

[94] F. Caracciolo and V. S. Rychkov, "Rigorous Limits on the Interaction Strength in Quantum Field Theory," *Phys.Rev.* **D81** (2010) 085037, arXiv:0912.2726 [hep-th].

[95] D. Poland and D. Simmons-Duffin, "Bounds on 4D Conformal and Superconformal Field Theories," *JHEP* **1105** (2011) 017, arXiv:1009.2087 [hep-th].

[96] R. Rattazzi, S. Rychkov, and A. Vichi, "Central Charge Bounds in 4D Conformal Field Theory," *Phys.Rev.* **D83** (2011) 046011, arXiv:1009.2725 [hep-th].

[97] R. Rattazzi, S. Rychkov, and A. Vichi, "Bounds in 4D Conformal Field Theories with Global Symmetry," *J.Phys.* **A44** (2011) 035402, arXiv:1009.5985 [hep-th].

[98] A. Vichi, "Improved bounds for CFT's with global symmetries," *JHEP* **1201** (2012) 162, arXiv:1106.4037 [hep-th].

[99] D. Poland, D. Simmons-Duffin, and A. Vichi, "Carving Out the Space of 4D CFTs," *JHEP* **1205** (2012) 110, arXiv:1109.5176 [hep-th].

[100] S. El-Showk and M. F. Paulos, "Bootstrapping Conformal Field Theories with the Extremal Functional Method," *Phys.Rev.Lett.* **111** no. 24, (2013) 241601, arXiv:1211.2810 [hep-th].

[101] C. Beem, L. Rastelli, and B. C. van Rees, "The $\mathcal{N} = 4$ Superconformal Bootstrap," *Phys.Rev.Lett.* **111** (2013) 071601, arXiv:1304.1803 [hep-th].

[102] S. El-Showk, M. Paulos, D. Poland, S. Rychkov, D. Simmons-Duffin, and A. Vichi, "Conformal Field Theories in Fractional Dimensions," *Phys. Rev. Lett.* **112** (2014) 141601, arXiv:1309.5089 [hep-th].

[103] F. Kos, D. Poland, and D. Simmons-Duffin, "Bootstrapping the $O(N)$ vector models," *JHEP* **1406** (2014) 091, arXiv:1307.6856 [hep-th].

[104] L. F. Alday and A. Bissi, "The superconformal bootstrap for structure constants," *JHEP* **1409** (2014) 144, arXiv:1310.3757 [hep-th].

[105] C. Beem, M. Lemos, P. Liendo, L. Rastelli, and B. C. van Rees, "The $\mathcal{N} = 2$ superconformal bootstrap," arXiv:1412.7541 [hep-th].

[106] L. F. Alday and A. Bissi, "Generalized bootstrap equations for $\mathcal{N} = 4$ SCFT," *JHEP* **1502** (2015) 101, arXiv:1404.5864 [hep-th].

[107] J. Golden and M. F. Paulos, "No unitary bootstrap for the fractal Ising model," *JHEP* **1503** (2015) 167, arXiv:1411.7932 [hep-th].

[108] S. M. Chester, J. Lee, S. S. Pufu, and R. Yacoby, "The $\mathcal{N} = 8$ superconformal bootstrap in three dimensions," *JHEP* **1409** (2014) 143, arXiv:1406.4814 [hep-th].

[109] S. M. Chester, J. Lee, S. S. Pufu, and R. Yacoby, "Exact Correlators of BPS Operators from the 3d Superconformal Bootstrap," *JHEP* **1503** (2015) 130, arXiv:1412.0334 [hep-th].

[110] S. M. Chester, S. S. Pufu, and R. Yacoby, "Bootstrapping $O(N)$ Vector Models in $4 < d < 6$," *Phys.Rev.* **D91** no. 8, (2015) 086014, arXiv:1412.7746 [hep-th].

[111] F. Caracciolo, A. C. Echeverri, B. von Harling, and M. Serone, "Bounds on OPE Coefficients in 4D Conformal Field Theories," *JHEP* **1410** (2014) 20, arXiv:1406.7845 [hep-th].

[112] N. Bobev, S. El-Showk, D. Mazac, and M. F. Paulos, "Bootstrapping SCFTs with Four Supercharges," arXiv:1503.02081 [hep-th].

[113] N. Bobev, S. El-Showk, D. Mazac, and M. F. Paulos, "Bootstrapping the Three-Dimensional Supersymmetric Ising Model," arXiv:1502.04124 [hep-th].

[114] F. Kos, D. Poland, D. Simmons-Duffin, and A. Vichi, "Bootstrapping the $O(N)$ Archipelago," arXiv:1504.07997 [hep-th].

[115] F. Gliozzi, "More constraining conformal bootstrap," *Phys.Rev.Lett.* **111** (2013) 161602, arXiv:1307.3111.

[116] F. Gliozzi and A. Rago, "Critical exponents of the 3d Ising and related models from Conformal Bootstrap," *JHEP* **1410** (2014) 042, arXiv:1403.6003 [hep-th].

[117] M. Hogervorst and S. Rychkov, "Radial Coordinates for Conformal Blocks," *Phys.Rev.* **D87** (2013) 106004, arXiv:1303.1111 [hep-th].

[118] S. Rychkov, "Conformal Bootstrap in Three Dimensions?," arXiv:1111.2115 [hep-th].

[119] E. Stein and G. Weiss, *Introduction to Fourier Analysis on Euclidean Spaces*. Mathematical Series. Princeton Univ. Press, 1971.

[120] A. L. Fitzpatrick, J. Kaplan, D. Poland, and D. Simmons-Duffin, "The Analytic Bootstrap and AdS Superhorizon Locality," *JHEP* **1312** (2013) 004, arXiv:1212.3616 [hep-th].

[121] W. Rudin, *Principles of mathematical analysis*, vol. 3. McGraw-Hill New York, 1964.

[122] J. Korevaar, *Tauberian Theory: A Century of Developments*, vol. 329 of *Grundlehren der mathematischen Wissenschaften*. Springer, 2004.

[123] K. Ishiguro, "Tauberian theorems concerning the summability methods of logarithmic type," *Proceedings of the Japan Academy* **39** no. 3, (1963) 156–159.

[124] K. Ishiguro, "A converse theorem on the summability methods," *Proceedings of the Japan Academy* **39** no. 1, (1963) 38–41.

[125] M. Hogervorst, H. Osborn, and S. Rychkov, "Diagonal Limit for Conformal Blocks in d Dimensions," *JHEP* **1308** (2013) 014, arXiv:1305.1321.

[126] G. Teschl, *Ordinary Differential Equations and Dynamical Systems*, vol. 140 of *Graduate Studies in Mathematics*. American Mathematical Society, 2012.

[127] E. Hille, *Ordinary Differential Equations in the Complex Domain*. Wiley, 1997.

[128] D. Simmons-Duffin, "A Semidefinite Program Solver for the Conformal Bootstrap," arXiv:1502.02033 [hep-th].

[129] M. Hogervorst, S. Rychkov, and B. C. van Rees, "Truncated conformal space approach in d dimensions: A cheap alternative to lattice field theory?," *Phys.Rev.* **D91** (2015) 025005, arXiv:1409.1581 [hep-th].

[130] A. Coser, M. Beria, G. P. Brandino, R. M. Konik, and G. Mussardo, "Truncated Conformal Space Approach for 2D Landau-Ginzburg Theories," *J.Stat.Mech.* **1412** no. 12, (2014) P12010, arXiv:1409.1494 [hep-th].

[131] S. Rychkov and L. G. Vitale, "Hamiltonian truncation study of the ϕ^4 theory in two dimensions," *Phys.Rev.* **D91** no. 8, (2015) 085011, arXiv:1412.3460 [hep-th].

[132] M. Lassig and G. Mussardo, "Hilbert space and structure constants of descendant fields in two-dimensional conformal theories," *Comput.Phys.Commun.* **66** (1991) 71–88.

[133] J. Maldacena and A. Zhiboedov, "Constraining Conformal Field Theories with A Higher Spin Symmetry," *J.Phys.* **A46** (2013) 214011, arXiv:1112.1016 [hep-th].

[134] S. Giombi and I. R. Klebanov, "Interpolating between a and F," *JHEP* **1503** (2015) 117, arXiv:1409.1937 [hep-th].

[135] A. Shubin, *Pseudodifferential Operators and Spectral Theory*. Springer, 2001.

[136] K. Atkinson and W. Han, *Spherical Harmonics and Approximations on the Unit Sphere: An Introduction*. Lecture Notes in Mathematics. Springer, 2012.

[137] Lüscher, M., "Volume Dependence of the Energy Spectrum in Massive Quantum Field Theories. 1. Stable Particle States," *Commun.Math.Phys.* **104** (1986) 177.

[138] A. Ludwig and J. L. Cardy, "Perturbative Evaluation of the Conformal Anomaly at New Critical Points with Applications to Random Systems," *Nucl.Phys.* **B285** (1987) 687–718.

[139] J. L. Cardy, "Operator content and modular properties of higher dimensional conformal field theories," *Nucl.Phys.* **B366** (1991) 403–419.

[140] K. Symanzik, "Continuum Limit and Improved Action in Lattice Theories. 1. Principles and ϕ^4 Theory," *Nucl.Phys.* **B226** (1983) 187.

[141] G. Z. Toth, "A Study of truncation effects in boundary flows of the Ising model on the strip," *J.Stat.Mech.* **0704** (2007) P04005, arXiv:hep-th/0612256 [hep-th].

[142] G. M. Watts, "On the renormalisation group for the boundary Truncated Conformal Space Approach," *Nucl.Phys.* **B859** (2012) 177–206, arXiv:1104.0225 [hep-th].

[143] P. Giokas and G. Watts, "The renormalisation group for the truncated conformal space approach on the cylinder," arXiv:1106.2448 [hep-th].

[144] J. C. Collins, *Renormalization*. Cambridge Univ. Press, 1984.

[145] M. Lencses and G. Takacs, "Excited state TBA and renormalized TCSA in the scaling Potts model," *JHEP* **09** (2014) 052, arXiv:1405.3157 [hep-th].

[146] A. Pelissetto and E. Vicari, "Critical phenomena and renormalization group theory," *Phys.Rept.* **368** (2002) 549–727, arXiv:cond-mat/0012164 [cond-mat].

[147] Z. Bajnok, L. Palla, G. Takacs, and F. Wagner, "The k folded sine-Gordon model in finite volume," *Nucl.Phys.* **B587** (2000) 585–618, arXiv:hep-th/0004181 [hep-th].

[148] G. Brandino, R. Konik, and G. Mussardo, "Energy Level Distribution of Perturbed Conformal Field Theories," *J.Stat.Mech.* **1007** (2010) P07013, arXiv:1004.4844 [cond-mat.stat-mech].

[149] J. Le Guillou and J. Zinn-Justin, "Accurate critical exponents for Ising like systems in noninteger dimensions," *J. Physique* **48** (1987) 19–24.

[150] Lüscher, M., "Volume Dependence of the Energy Spectrum in Massive Quantum Field Theories. 2. Scattering States," *Commun.Math.Phys.* **105** (1986) 153–188.

[151] R. Guida and J. Zinn-Justin, "Critical exponents of the N vector model," *J.Phys.* **A31** (1998) 8103–8121, arXiv:cond-mat/9803240 [cond-mat].

[152] M. Campostrini, A. Pelissetto, P. Rossi, and E. Vicari, "25th-order high-temperature expansion results for three-dimensional ising-like systems on the simple-cubic lattice," *Phys. Rev. E* **65** (2002) 066127, arXiv:cond-mat/0201180 [cond-mat].

[153] M. Hasenbusch, "Finite size scaling study of lattice models in the three-dimensional ising universality class," *Phys. Rev. B* **82** (2010) 174433, arXiv:1004.4486 [cond-mat].

[154] R. Brower, G. Fleming, and H. Neuberger, "Lattice Radial Quantization: 3D Ising," *Phys.Lett.* **B721** (2013) 299–305, arXiv:1212.6190 [hep-lat].

[155] R. C. Brower, M. Cheng, and G. T. Fleming, "Improved Lattice Radial Quantization," arXiv:1407.7597 [hep-lat].

[156] H. Neuberger, "Lattice radial quantization by cubature," *Phys.Rev.* **D90** no. 11, (2014) 114501, arXiv:1410.2820 [hep-lat].

[157] S. Weinberg, *The Quantum Theory of Fields. Vols. 1 & 2.* Cambridge University Press, 1995.

[158] M. Caselle, M. Hasenbusch, and P. Provero, "Nonperturbative states in the 3-D ϕ^4 theory," *Nucl.Phys.* **B556** (1999) 575–600, arXiv:hep-lat/9903011 [hep-lat].

[159] M. Caselle, M. Hasenbusch, P. Provero, and K. Zarembo, "Bound states in the three-dimensional ϕ^4 model," *Phys.Rev.* **D62** (2000) 017901, arXiv:hep-th/0001181 [hep-th].

[160] M. Caselle, M. Hasenbusch, P. Provero, and K. Zarembo, "Bound states and glueballs in three-dimensional Ising systems," *Nucl.Phys.* **B623** (2002) 474–492, arXiv:hep-th/0103130 [hep-th].

[161] M. F. Paulos, "JuliBootS: a hands-on guide to the conformal bootstrap," arXiv:1412.4127 [hep-th].

[162] I. Heemskerk, J. Penedones, J. Polchinski, and J. Sully, "Holography from Conformal Field Theory," *JHEP* **0910** (2009) 079, arXiv:0907.0151 [hep-th].

[163] Z. Komargodski and A. Zhiboedov, "Convexity and Liberation at Large Spin," *JHEP* **1311** (2013) 140, arXiv:1212.4103 [hep-th].

[164] P. Liendo, L. Rastelli, and B. C. van Rees, "The Bootstrap Program for Boundary CFT$_d$," *JHEP* **1307** (2013) 113, arXiv:1210.4258 [hep-th].

[165] L. F. Alday, A. Bissi, and T. Lukowski, "Lessons from crossing symmetry at large N," arXiv:1410.4717 [hep-th].

[166] M. Hogervorst, S. Rychkov, and B. C. van Rees. in preparation.

[167] M. Moshe and J. Zinn-Justin, "Quantum field theory in the large N limit: A Review," *Phys.Rept.* **385** (2003) 69–228, arXiv:hep-th/0306133 [hep-th].

[168] B. Pozsgay and G. Takacs, "Form-factors in finite volume I: Form-factor bootstrap and truncated conformal space," *Nucl.Phys.* **B788** (2008) 167–208, arXiv:0706.1445 [hep-th].

[169] I. Szécsényi, G. Takács, and G. Watts, "One-point functions in finite volume/temperature: a case study," *JHEP* **1308** (2013) 094, arXiv:1304.3275 [hep-th].

[170] S. Dalley and I. R. Klebanov, "String spectrum of (1+1)-dimensional large N QCD with adjoint matter," *Phys.Rev.* **D47** (1993) 2517–2527, arXiv:hep-th/9209049 [hep-th].

[171] G. Bhanot, K. Demeterfi, and I. R. Klebanov, "(1+1)-dimensional large N QCD coupled to adjoint fermions," *Phys.Rev.* **D48** (1993) 4980–4990, arXiv:hep-th/9307111 [hep-th].

[172] S. J. Brodsky, H.-C. Pauli, and S. S. Pinsky, "Quantum chromodynamics and other field theories on the light cone," *Phys.Rept.* **301** (1998) 299–486, arXiv:hep-ph/9705477 [hep-ph].

[173] E. Katz, G. M. Tavares, and Y. Xu, "Solving 2D QCD with an adjoint fermion analytically," *JHEP* **1405** (2014) 143, arXiv:1308.4980 [hep-th].

[174] E. Katz, G. M. Tavares, and Y. Xu, "A solution of 2D QCD at Finite N using a conformal basis," arXiv:1405.6727 [hep-th].

[175] D. Lee, "Introduction to spherical field theory," *Phys.Lett.* **B439** (1998) 85–94, arXiv:hep-th/9811117 [hep-th].

[176] D. Lee, N. Salwen, and D. Lee, "The Diagonalization of quantum field Hamiltonians," *Phys.Lett.* **B503** (2001) 223–235, arXiv:hep-th/0002251 [hep-th].

[177] V. Dobrev, V. Petkova, S. Petrova, and I. Todorov, "Dynamical Derivation of Vacuum Operator Product Expansion in Euclidean Conformal Quantum Field Theory," *Phys.Rev.* **D13** (1976) 887.

[178] V. Dobrev, G. Mack, V. Petkova, S. Petrova, and I. Todorov, *Harmonic Analysis on the n-Dimensional Lorentz Group and Its Application to Conformal Quantum Field Theory*, vol. 63 of *Lect. Notes Phys.* Springer, 1977.